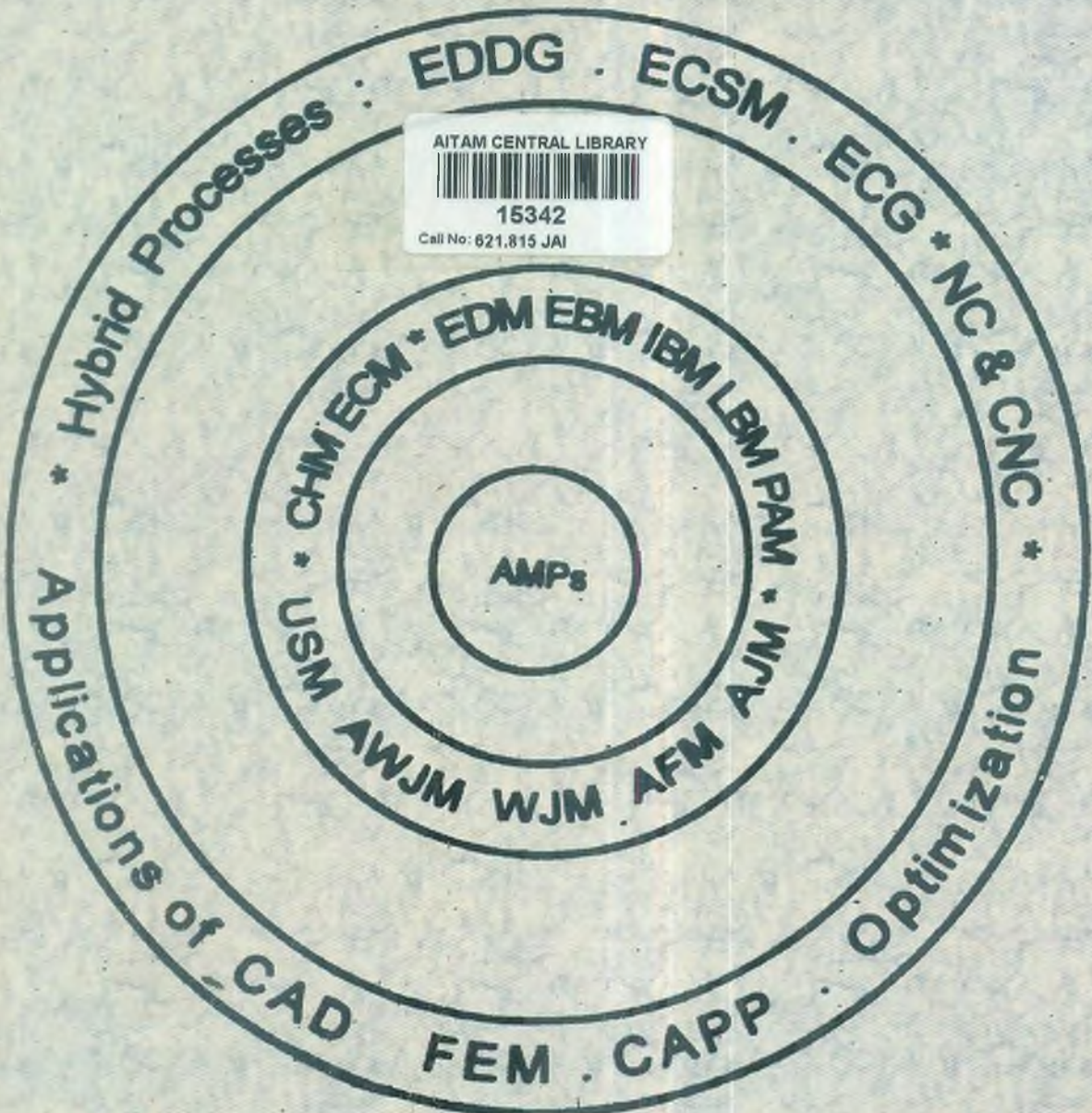


ADVANCED MACHINING PROCESSES



VIJAY K. JAIN

ALLIED PUBLISHERS PRIVATE LIMITED

Regd. Off. : 15 J.N. Heredia Marg, Ballard Estate, Mumbai-400001, Ph.: 022-22626476

E-mail: mumbai.books@alliedpublishers.com

Amber Chambers, 28-A Budhwar Peth, Appa Balwant Chowk, Pune-411002, Ph.: 020-24475743

E-mail: pune.books@alliedpublishers.com

12 Prem Nagar, Ashok Marg, Opp. Indira Bhawan, Lucknow-226001, Ph.: 0522-2614253

E-mail: appltdlk0@sify.com

Prarthna Flats (2nd Floor), Navrangpura, Ahmedabad-380009, Ph.: 079-26465916

E-mail: ahmbd.books@alliedpublishers.com

3-2-844/6 & 7 Kachiguda Station Road, Hyderabad-500027, Ph.: 040-24619079

E-mail: hyd.books@alliedpublishers.com

5th Main Road, Gandhinagar, Bangalore-560009, Ph.: 080-22262081

E-mail: bngl.books@alliedpublishers.com

1/13-14 Asaf Ali Road, New Delhi-110002, Ph.: 011-23239001

E-mail: delhi.books@alliedpublishers.com

17 Chittaranjan Avenue, Kolkata-700072, Ph.: 033-22129618

E-mail: cal.books@alliedpublishers.com

81 Hill Road, Ramnagar, Nagpur-440010, Ph.: 0712-2521122

E-mail: ngp.books@alliedpublishers.com

751 Anna Salai, Chennai-600002, Ph.: 044-28523938

E-mail: chennai.books@alliedpublishers.com



15342

Call No. 621.815 JAI

Website: www.alliedpublishers.com

© 2002, ALLIED PUBLISHERS PVT. LIMITED

No part of the material protected by this Copyright notice may be reproduced or utilized in any form or by any means, electronic or mechanical including photocopying, recording or by any information storage and retrieval system, without prior written permission from the copyright owner.

First Reprint : June, 2004

Second Reprint : August, 2004

Third Reprint : October, 2004

Fourth Reprint : September, 2005

Fifth Reprint : April, 2007

Sixth Reprint : August, 2007

ISBN 81-7764-294-4

FOREWORD

The international academic community has always respected Professor V. K. Jain for his many contributions to the subject of unconventional machining. The key to his success lies in his personal commitment to the advancement of knowledge, and his enthusiasm for research in a field that continues to give rise to new industrial applications and be driven by fresh needs of industry. These personal qualities of Professor Jain are evident in his new book. He and all of us in higher education are aware of our responsibilities towards our students. From us they have to learn how to use their "grey matter," for their own development, in order to advance the social, economic and industrial well-being of local, national and international society. Through "Advanced Machining Processes," Professor Jain has helped us all in this mission.

That industry needs unconventional machining processes is understood by colleges and universities everywhere: the subject has its own place in under- and post-graduate engineering curricula that deal with mechanical and manufacturing engineering and in research laboratories. An effective transfer of technology has already taken place with the adoption by industry of many of the processes that hitherto were a matter of academic curiosity. Professor Jain has recognised this transition. He has focussed his book on those methods that are still undergoing investigation, or are not well understood, or lack appreciation. In order to clarify the different types of processes available, the author has divided the text into: mechanical, thermo-electric and electrochemical and chemical techniques, all useful subdivisions of a highly cross-disciplinary subject. We are then provided with a treatment of the principles that govern each process, a presentation of the effects of the main process variables on engineering performance, a discussion of the capabilities and applications, and a bibliography for further reading. Every chapter carries an innovative "At-A-Glance" summary of the method discussed. A textbook on advanced machining has long been needed that properly provides for learning this subject. The acquisition of knowledge has to be tested and Professor Jain takes heed by providing three types of questions for each process: multiple-choice, 'self-test' for understanding and descriptive and numerical calculations based on working principles. Industrialists and scholars are indeed well-served.

PREFACE

Books on this subject available in the market are entitled as *non-conventional, non-traditional, or modern machining processes*. In my opinion, majority of these processes have already crossed the doors of the research labs. They are higher level machining processes than conventional ones. They are being commonly and frequently used in medium and large scale industries. This book therefore has been named as “*Advanced Machining Processes (AMPs)*.”

This book on “*Advanced Machining Processes*” is intended primarily for the undergraduate and postgraduate students who plan to take up this course as one of their majors. The objective of writing this book is to provide a thorough knowledge of the principles and applications of these processes. This book aims at bringing the readers up-to-date with the latest technological developments and research trends in the field of *AMPs*. As a result, some of the processes yet to get popularity amongst the common industrial users have been included and discussed.

The contents of the book have been broadly divided into three major parts. *Part-I* deals with the *mechanical type AMPs*, viz; ultrasonic machining (*USM*), abrasive jet machining (*AJM*), water jet machining (*WJM*), abrasive water jet machining (*AWJM*) and abrasive flow machining (*AFM*). *Part-II* describes thermoelectric type *AMPs* viz; electric discharge machining (*EDM*), laser beam machining (*LBM*), plasma arc machining (*PAM*), and electron beam machining (*EBM*). *Part-III* of the book contains details about the electrochemical and chemical type *AMPs* viz; electrochemical machining (*ECM*) and chemical machining (*ChM*). Relevant enough recent developments have been included at appropriate places in different chapters to keep the interest of the researchers alive.

Keeping in view the trends in many universities and technical institutions at home and abroad specially in large classes, three kinds of questions given at the end of each chapter. The first category includes *multiple choice questions* to test the thorough understanding of the subject. The second category of questions are *descriptive long answer type*. The third category includes the *questions based on calculations*. An attempt has been made to provide enough number of numerical problems for practice to be done by the students and a few solved problems to understand how to attack such problems.

The technology developed in research organizations can't be brought to the shop floor unless its applications are realized by the user industries. With this in view, diversified industrial applications of different *AMPs* cited in available literature have been included. This would help the readers in evolving more and more new areas of applications to make the fullest possible exploitation of capabilities of *AMPs*.

The review section given at the end of each chapter is unusually large. It is prepared to the students for quick revision of a chapter, to the teachers for preparing transparencies for teaching in a class, and 'at a glance' look for the practicing engineers to decide about the specific process to be used for machining a particular component.

I hope the readers of this book will enjoy learning *AMPs* to a great extent.

CONTENTS

FOREWORD	vii
PREFACE	ix
PART-1 MECHANICAL ADVANCED MACHINING PROCESSES	
1. INTRODUCTION	1-9
WHY DO WE NEED ADVANCED MACHINING PROCESSES (AMPs)?	1
ADVANCED MACHINING PROCESSES	3
HYBRID PROCESSES	5
REMARKS	5
PROBLEMS	5
BIBLIOGRAPHY	6
REVIEW QUESTIONS	7
AT-A-GLANCE	8
2. ABRASIVE JET MACHINING (AJM)	10-27
INTRODUCTION	10
ABRASIVE JET MACHINING SETUP	11
Gas Propulsion System	11
Abrasive Feeder	12
Machining Chamber	12
AJM Nozzle	12
Abrasives	12
PARAMETRIC ANALYSIS	13
Stand-off-Distance	13
Abrasive Flow Rate	13
Nozzle Pressure	14
Mixing Ratio	14
PROCESS CAPABILITIES	18
APPLICATIONS	19

Contents

PROBLEMS	20
BIBLIOGRAPHY	21
SELF TEST QUESTIONS	22
REVIEW QUESTIONS	23
NOMENCLATURE	23
AT-A-GLANCE	25
3. ULTRASONIC MACHINING (USM)	28–56
INTRODUCTION	28
ULTRASONIC MACHINING SYSTEM	31
MECHANICS OF CUTTING	33
MODEL PROPOSED BY SHAW	33
Grain Throwing Model	35
Grain Hammering Model	37
PARAMETRIC ANALYSIS	42
PROCESS CAPABILITIES	42
APPLICATIONS	45
PROBLEMS	45
BIBLIOGRAPHY	48
REVIEW QUESTIONS	49
NOMENCLATURE	51
AT-A-GLANCE	53
4. ABRASIVE FINISHING PROCESSES	57–94
(A) ABRASIVE FLOW FINISHING (AFF)	58
WORKING PRINCIPLE	58
ABRASIVE FLOW MACHINING SYSTEM	61
Machine	61
Tooling	61
Media	65
PROCESS VARIABLES	67
ANALYSIS AND MODELING OF ABRASIVE FLOW	
MACHINED SURFACES	69
Number of Active Grains	71
Wear of Abrasive Grains	72
PROCESS PERFORMANCE	72

APPLICATIONS	72
Aerospace	72
Dies and Molds	73
BIBLIOGRAPHY	73
REVIEW QUESTIONS	74
SELF-TEST QUESTIONS	75
NOMENCLATURE	76
(B) MAGNETIC ABRASIVE FINISHING (MAF)	77
INTRODUCTION	77
WORKING PRINCIPLE OF MAF	78
MATERIAL REMOVAL (OR STOCK REMOVAL) AND SURFACE FINISH	81
Type and Size of Grains	81
Bonded and Unbonded Magnetic Abrasives	84
Machining Fluid	85
Magnetic Flux Density	85
ANALYSIS	86
BIBLIOGRAPHY	88
SELF-TEST QUESTIONS	88
REVIEW QUESTIONS	89
NOMENCLATURE	89
AT-A-GLANCE (AFM)	91
AT-A-GLANCE (MAF)	93
5. WATER JET CUTTING (WJC)	95-102
INTRODUCTION	95
WJC MACHINE	96
PROCESS CHARACTERISTICS	96
PROCESS PERFORMANCE	97
APPLICATIONS	98
BIBLIOGRAPHY	98
SELF-TEST QUESTIONS	99
REVIEW QUESTIONS	100
ABBREVIATIONS	100
AT-A-GLANCE	101

6. ABRASIVE WATER JET MACHINING (AWJM)	103–126
WORKING PRINCIPLE	103
AWJM MACHINE	104
Pumping System	104
Abrasive Feed System	105
Abrasive Water Jet Nozzle	105
Catcher	105
PROCESS VARIABLES	106
WATER	106
Water Jet Pressure during Slotting	106
Water Flow Rate	106
ABRASIVES	109
Abrasive Flow Rate	109
Abrasive Particle Size	109
Abrasive Material	111
CUTTING PARAMETERS	112
Traverse Speed	112
Number of Passes	114
Stand-Off-Distance	115
Visual Examination	116
PROCESS CAPABILITIES	117
APPLICATIONS	117
BIBLIOGRAPHY	118
SELF-TEST QUESTIONS	118
REVIEW QUESTIONS	119
NOMENCLATURE	120
AT-A-GLANCE	121

PART-2 THERMOELECTRIC ADVANCED MACHINING PROCESSES

7. (A) ELECTRIC DISCHARGE MACHINING (EDM)	126–186
INTRODUCTION	126

WORKING PRINCIPLE OF EDM	127
RC PULSE GENERATOR	130
EDM MACHINE	131
Power Supply	131
Dielectric System	134
Electrodes	136
Servo system	139
Electrode Refeeding	139
CNC-EDM	139
ANALYSIS	141
Analysis of R-C Circuits	141
Power Delivered to the Discharging Circuit	142
Current in the Discharging Circuit	143
Material Removal Rate in RC Circuit	145
Surface Finish	146
PROCESS VARIABLES	147
Dielectric Pollution and its Effects	150
PROCESS CHARACTERISTICS	154
Gap Cleaning	156
APPLICATIONS	157
(B) ELECTRIC DISCHARGE GRINDING AND ELECTRIC DISCHARGE DIAMOND GRINDING	160
ELECTRIC DISCHARGE GRINDING	160
ELECTRIC DISCHARGE DIAMOND GRINDING	162
Working Principle	162
Capabilities and Applications	162
(C) WIRE ELECTRIC DISCHARGE MACHINING	165
WORKING PRINCIPLE	165
WIRE EDM MACHINE	165
Advances In Wirecut EDM	167
Stratified Wire	168
PROCESS VARIABLES	169
PROCESS CHARACTERISTICS	169
APPLICATIONS	169

Contents

PROBLEMS	169
BIBLIOGRAPHY	170
SELF-TEST QUESTIONS	173
REVIEW QUESTIONS	175
NOMENCLATURE	176
AT-A-GLANCE	178
8. LASER BEAM MACHINING (LBM)	186–206
PRODUCTION OF LASERS	186
WORKING PRINCIPLE OF LASER BEAM MACHINING	189
TYPES OF LASERS	190
Solid State Lasers	190
Gas Lasers	191
PROCESS CHARACTERISTICS	192
APPLICATIONS	195
Drilling	196
Cutting	198
Marking	199
Miscellaneous Applications	199
BIBLIOGRAPHY	201
SELF-TEST QUESTIONS	202
REVIEW QUESTIONS	202
NOMENCLATURE	203
ACRONYMS	203
AT-A-GLANCE	204
9. PLASMA ARC MACHINING (PAM)	207–219
WORKING PRINCIPLE	207
PLASMA ARC CUTTING SYSTEM	208
ELEMENTS OF PLASMA ARC CUTTING SYSTEM	209
PROCESS PERFORMANCE	211
APPLICATIONS	213
BIBLIOGRAPHY	214
REVIEW QUESTIONS	214
AT-A-GLANCE	215

10. ELECTRON BEAM MACHINING (EBM)	220–233
WORKING PRINCIPLE	220
ELECTRON BEAM MACHINING SYSTEM	221
Electron Beam Gun	221
Power Supply	222
Vacuum System and Machining Chamber	223
PROCESS PARAMETERS	223
CHARACTERISTICS OF THE PROCESS	224
APPLICATIONS	224
BIBLIOGRAPHY	225
PROBLEMS	225
NOMENCLATURE	226
AT-A-GLANCE	227
PART-3 ELECTROCHEMICAL AND CHEMICAL ADVANCED MACHINING PROCESSES	232–280
11. ELECTROCHEMICAL MACHINING (ECM)	232–280
INTRODUCTION	232
Electrolysis	232
Electrochemical Machining (ECM)	234
ECM MACHINE TOOL	237
Power Source	237
Electrolyte Supply and Cleaning System	240
Tool and Tool Feed System	241
Workpiece and Work Holding Device	241
ADVANTAGES AND LIMITATIONS	241
APPLICATIONS	243
MECHANICAL PROPERTIES OF ECM'd PARTS	244
THEORY OF ECM	245
Faraday's Laws of Electrolysis	245
Electrochemical Equivalent of Alloys	246
Material Removal Rate in ECM	251
Inter-electrode Gap in ECM	254
Zero Feed Rate	255
Finite Feed Rate	256

Contents

Self Regulating Feature	257
Generalized Equation for Inter-electrode Gap	258
MAXIMUM PERMISSIBLE FEED RATE IN ECM	260
ELECTROLYTE CONDUCTIVITY (K)	263
Effect of Temperature	264
Effect of Hydrogen Bubbles	267
BIBLIOGRAPHY	268
SELF-TEST QUESTIONS	270
PROBLEMS	272
NOMENCLATURE	274
Subscripts	275
Acronyms	275
AT-A-GLANCE	276
12. ELECTROCHEMICAL GRINDING (ECG)	280–290
INTRODUCTION	280
ECG MACHINE TOOL	282
PROCESS CHARACTERISTICS	285
APPLICATIONS	287
BIBLIOGRAPHY	287
REVIEW QUESTION	288
AT-A-GLANCE	289
13. ELECTROSTREAM DRILLING (ESD)	291–298
INTRODUCTION	291
PROCESS PERFORMANCE	295
BIBLIOGRAPHY	296
REVIEW QUESTIONS	296
AT-A-GLANCE	298
14. ELECTROCHEMICAL DEBURRING (ECDe)	299–315
INTRODUCTION	299
Basic Approach on Deburring	302
CLASSIFICATION OF DEBURRING PROCESSES	304
ELECTROCHEMICAL DEBURRING (ECD _e)	306

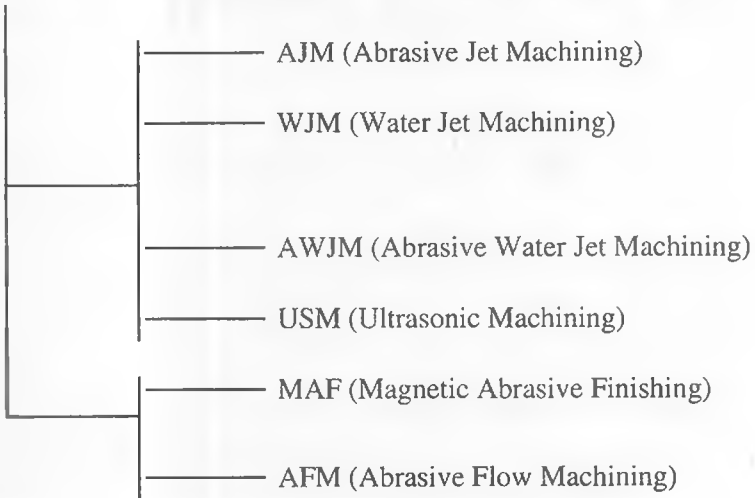
Principle of Working	306
Functions of Electrolyte and its Importance	309
APPLICATIONS	311
SPECIFIC FEATURES OF ECD _e MACHINE	311
BIBLIOGRAPHY	313
REVIEW QUESTIONS	313
ACRONYMS	314
AT-A-GLANCE	315
15. SHAPED TUBE ELECTROLYTIC MACHINING (STEM)	316–320
INTRODUCTION	316
BIBLIOGRAPHY	318
ACRONYMS	319
AT-A-GLANCE	320
16. CHEMICAL MACHINING (ChM)	321–329
INTRODUCTION	321
MASKANTS	325
Cut And Peel	325
Screen Printing	326
Photoresist Maskant	326
ETCHANT	327
ADVANTAGES AND LIMITATIONS	327
BIBLIOGRAPHY	327
REVIEW QUESTIONS	328
ACRONYMS	328
AT-A-GLANCE	329
17. ANODE SHAPE PREDICTION AND TOOL DESIGN FOR ECM PROCESSES	334–357
INTRODUCTION	334
ANODE SHAPE PREDICTION	336

Contents

Cos θ Method	339
Empirical Approach	340
Nomographic Approach	342
Numerical Methods	343
TOOL (CATHODE) DESIGN FOR ECM PROCESS	343
Cos θ Method	343
Correction Factor Method	346
BIBLIOGRAPHY	348
QUESTIONS	349
NOMENCLATURE	350
Acronyms	350
AT-A-GLANCE	351
Author Index	353
Subject Index	357

PART-I

MECHANICAL ADVANCED MACHINING PROCESSES



INTRODUCTION

WHY DO WE NEED ADVANCED MACHINING PROCESSES (AMPs)?

Technologically advanced industries like aeronautics, nuclear reactors, automobiles etc. have been demanding materials like high strength temperature resistant (HSTR) alloys having high “strength to weight” ratio. Researchers in the area of materials science are developing materials having higher strength, hardness, toughness and other diverse properties. This also needs the development of improved cutting tool materials so that the productivity is not hampered.

It is a well established fact that during conventional machining processes an increase in hardness of work material results in a decrease in economic cutting speed. It is no longer possible to find tool materials which are sufficiently hard and strong to cut (at economic cutting speeds) materials like titanium, stainless steel, nimonics and similar other high strength temperature resistant (HSTR) alloys, fiber-reinforced composites, stellites (cobalt based alloys), ceramics, and

difficult to machine alloys [DeBarr & Oliver, 1975]. Production of complex shapes in such materials by traditional methods is still more difficult. Other higher level requirements are better finish, low values of tolerances, higher production rates, complex shapes, automated data transmission, miniaturization etc. [Snoeys *et al.* 1986]. Making of holes (shallow entry angles, non-circular, micro-sized, large aspect ratio, a large number of small holes in one workpiece, contoured holes, hole without burrs, etc.) in difficult-to-machine materials is another area where appropriate processes are very much in demand. Aforesaid characteristics are commonly required in the products used in industries like aerospace, nuclear reactors, missiles, turbines, automobiles, etc. To meet such demands, a different class of machining processes (i.e. non-traditional machining processes or more correctly named as **advanced machining processes**) have been developed.

There is a need for machine tools and processes which can accurately and easily machine [Merchant, 1962; Krabacher, 1962] the most difficult-to-machine materials to intricate and accurate shapes. The machine tools should be easily adaptable for automation as well. In order to meet this challenge, a number of newer material removal processes have now been developed to the level of commercial utilization. These newer methods are also called **unconventional** in the sense that conventional tools are not employed for metal cutting. Instead the energy in its direct form is used to remove the materials from the workpiece. The range of applications of the newly developed machining process is determined by the work material properties like electrical and thermal conductivity, melting temperature, electrochemical equivalent etc. Some of these newly developed processes can also machine workpieces in the areas which are inaccessible for conventional machining methods. The use of these processes is becoming increasingly unavoidable and popular at the shop floor. These machining processes become still more important when one considers the **precision machining and ultraprecision machining**. Taniguchi [1983] has concluded that such high accuracies cannot be achieved by conventional machining methods in which material is removed in the form of chips. However, such accuracy can be achieved by some of the advanced machining techniques whereby the material is removed in the form of atoms or molecules individually or in groups.

Advanced machining processes can be **classified** into three basic categories, i.e. mechanical, thermoelectric, and electrochemical & chemical machining processes (Fig. 1.1). None of these processes is the best under all machining situations. Some of them can be used only for electrically conductive materials while

others can be used for both electrically conductive and electrically non-conductive materials. Performance of some of these processes is not very good while machining materials like aluminium having very high thermal conductivity. Also, these machining processes have their distinct characteristic features. Hence, selection of an appropriate machining process for a given situation (or product requirements) becomes very important.

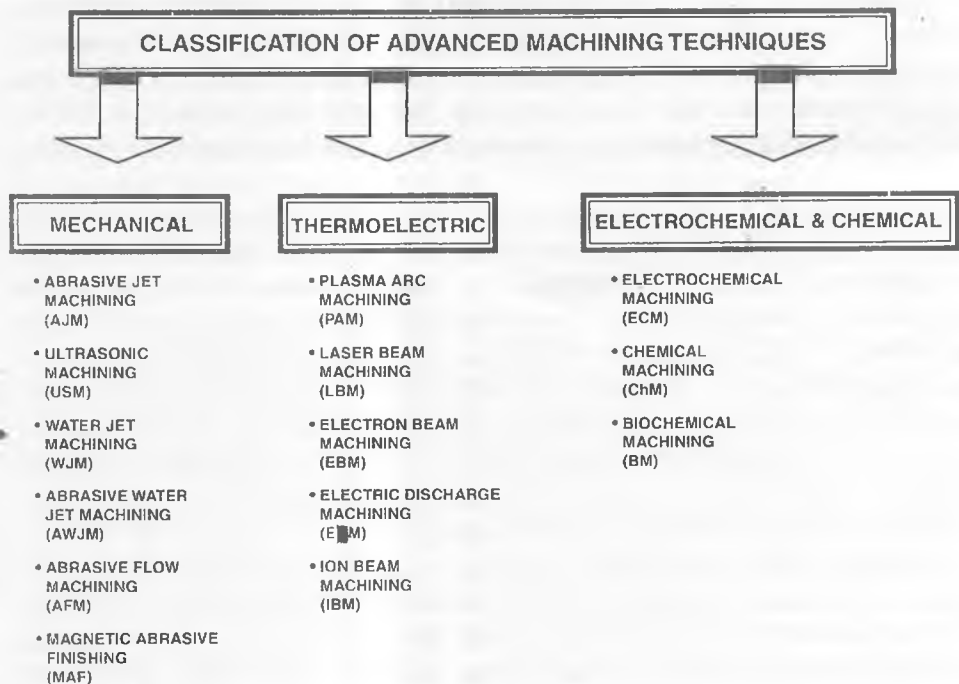


Fig. 1.1 Classification of advanced machining techniques

ADVANCED MACHINING PROCESSES

Mechanical advanced machining methods like abrasive jet machining (**AJM**), ultrasonic machining (**USM**), and water jet machining (**WJM**) have been developed but with only limited success. Here, kinetic energy (K.E.) of either abrasive particles or water jet (**WJM**) is utilized to remove material from the workpiece. Abrasive water jet machining (**AWJM**) also uses K.E. of abrasive particles flowing along with water jet. Magnetic abrasive finishing (**MAF**) is another process in which magnetic abrasive brush is utilized to reduce surface

irregularities from the premachined surfaces. A new finishing process called abrasive flow machining (**AFM**) has also been recently developed. However, performance of these processes depends upon hardness, strength, and other physical and mechanical properties of work material. What is really needed is the development of machining method(s) whose performance is unaffected by physical, metallurgical and mechanical properties of work material. Thermoelectric methods are able to overcome some of these barriers. Therefore thermoelectric processes as well as electrochemical processes are more and more deployed in metal working industries.

In **thermoelectric methods**, the energy is supplied in the form of heat (plasma arc machining-**PAM**), light (laser beam machining-**LBM**), or electron bombardment (electron beam machining-**EBM**). The energy is concentrated onto a small area of workpiece resulting in melting, or vaporization and melting both. PAM has been identified as a rough machining process. LBM and EBM are good enough for making very fine cuts and holes. However, electric discharge machining (**EDM**) is a process which is capable of machining the materials economically and accurately. This process is widely used for machining hard and tough but electrically conductive materials. It is unsuitable for many applications where very good surface finish, low damage to the machined surface, and high material removal rate (**MRR**) are the requirements. Thus, mechanical and thermo-electric methods of **AMPs** also do not offer a satisfactory solution to some of the problems of machining difficult-to-machine materials.

Chemical machining (ChM) is an etching process which has very narrow range of applications mainly because of very low **MRR** and difficulty in finding a suitable etchant for the given work material. On the other hand, **electrochemical machining (ECM)** has a very wide field of applications. It is a controlled anodic dissolution process that yields high **MRR** which is independent of any physical and mechanical properties of work material. But, work material should be electrically conductive. In this process, there is no tool wear, no residual stresses, no thermal damage caused to the workpiece material, and no burrs on the machined edges. Nevertheless, these advanced machining processes cannot fully replace the conventional machining processes. **Biochemical Machining (BM)** is a process being developed to machine biodegradable plastics. This process has very limited applications.

While selecting a process to be used, the following factors should be taken care of: process capability, physical parameters, shape to be machined, properties of

workpiece material to be cut, and economics of the process.

HYBRID PROCESSES

To further enhance the capabilities of the machining processes, two or more than two machining processes are combined to take advantage of the worthiness of the constituent processes. For example, conventional grinding produces good surface finish and low values of tolerances but the machined parts are associated with burrs, heat affected zone, and residual stresses. However, electrochemically machined components do not have such defects. Hence, a hybrid process called electrochemical grinding (ECG) has been developed. In the same way, other hybrid processes like electrochemical spark machining (ECSM), electrochemical arc machining (ECAM), electrodisscharge abrasive (EDAG), etc have been developed. Some of these processes are discussed in detail in the related chapters.

REMARKS

Most of these advanced machining processes have experienced a steady growth since their inception. In some cases, productivity as compared to conventional methods, can be increased either by reducing the total number of manufacturing operations required or by performing the operations faster. The review of recent literature has revealed the following facts:

- The trend shows that the capabilities of different advanced (or non-traditional) machining processes for higher volumetric material removal rate (MRR_v ,) are being enhanced through research efforts.
- Machine tools of some of these processes are equipped with a computer control which means higher rate of acceptance by users, higher reliability, better repeatability, and higher accuracy.
- Application of adaptive control (AC) to these processes and in-process inspection techniques being employed are helping in widening their area of use and leading towards the unmanned machining modules and automated factories.

PROBLEMS

1. How will you decide to recommend specific advanced machining processes for (A) cutting a glass plate into two pieces, (B) making a hole in a mild steel workpiece?

Solution:

(A) Cutting of a glass plate into two pieces:

- Glass is electrically non-conductive hence certain processes (**ECM**, **EDM**, **PAM**, **EBM**) are ruled out because they can't be employed for electrically non-conductive workpieces.
- LBM can be ignored being an expensive process. Chemical machining need not be considered because it is for very special applications.
- AFM and MAF are finishing processes.
- WJM is usually for comparatively softer materials.
- AJM, AWJM and USM can be applied. Which one to use will also depend on the size of the workpiece, and the kind of the accuracy required.

(B) In case of a hole in M.S., one can proceed as follows:

- Drop the finishing processes (MAF and AFM) and chemical machining.
- More suitable for comparatively harder materials, one can drop AJM, USM and AWJM.
- Being electrically conductive, ECM, EDM, LBM, EBM, and PAM can be employed. At this point, one should know the requirements of the hole in terms of dimensions, tolerances and surface integrity. If it is not a micro hole, one can easily adopt ECM or EDM. If high surface integrity is required, ECM should be used, and so on.

THUS, BY ELIMINATION PROCESS ONE SHOULD ARRIVE AT THE PARTICULAR PROCESS TO BE USED.

BIBLIOGRAPHY

1. Bellows Guy and Kohls, John B. (1982), Drilling without Drills, *Am. Machinist*, pp. 173-188.
2. Benedict G.F. (1987), *Nontraditional Manufacturing Processes*, Marcel Dekker Inc., New York.
3. Bhattacharyya A. (1973), *New Technology*, The Institution of Engineers (I), Calcutta.
4. DeBarr A.E. and Oliver, D.A. (1975) (Ed), *Electrochemical Machining*, McDonald and Co. Ltd., London.
5. Kaneeda T., Yokomizo S., Miwa A., Mitsuishi K., Uno Y., and Marjoka H. (1997), Biochemical Machining-Biochemical Removal Process of Plastic,

6. Krabacher E.J., Haggerty W.A., Allison C.R. and Davis M.F. (1962), Electrical Methods of Machining, *Proc. Int. Con. on Production Res.* (ASME), pp. 232-241.
7. McGeough J.A. (1988), *Advanced Machining Methods*, Chapman and Hall, London.
8. McGeough J.A., McCarthy W.J., and Wilson C.B. (1987), Electrical Methods of Machining, in article on Machine Tools, *Encycl. Brit.*, Vol. 28, pp. 712-736.
9. Merchant M.E. (1962), Newer Methods for the Precision Working of Metals-Research and Present Status, *Proc. Int. Con. Production Res.* (ASME), pp. 93-107.
10. Pandey P.C. and Shan H.S. (1980), *Modern Machining Processes*, Tata McGraw Hill Publishing Co. Ltd., New Delhi.
11. Snoeys R., Stallens F. and Dakeyser W. (1986), Current Trends in Non-conventional Material Removal processes, *Annls CIRP*, Vol. 35, No. 2, pp. 467-480.
12. Taniguchi N. (1983), Current Status in and Future Trends of Ultraprecision Machining and Ultrafine Materials Processing, *Annls CIRP*, Vol. 32, No. 2, pp. 1-8.

REVIEW QUESTIONS

1. How the developments in the area of materials are partly responsible for evolution of advanced machining techniques?
2. Enlist the requirements that demand the use of AMPs.
3. Write the constraints that limit the performance of different kind of AMPs. Also, write the circumstances under which individual process will have advantage over others.
4. What do you understand by the word “unconventional” in unconventional machining processes? Is it justified to use this word in the context of the utilization of these processes on the shop floor?
5. Name the important factors that should be considered during the selection of an unconventional machining process for a given job.
6. Classify modern machining processes on the basis of the type of energy employed. Also, state the mechanism of material removal, transfer media, and energy sources used.

CHAPTER I
AT-A-GLANCE
INTRODUCTION

**NEED FOR ADVANCED
MACHINING PROCESSES**

- LIMITATIONS OF CONVENTIONAL MACHINING METHODS
- RAPID IMPROVEMENTS IN THE PROPERTIES OF MATERIALS
 - METALS & NON-METALS
 - TOOL MATERIAL HARDNESS > W/P HARDNESS
- PRODUCT REQUIREMENTS
 - COMPLEX SHAPES
 - MACHINING IN INACCESSIBLE AREAS
 - LOW TOLERANCES
 - BETTER SURFACE INTEGRITY
 - HIGH SURFACE FINISH
- HIGH PRODUCTION RATE
- LOW COST OF PRODUCTION
- PRECISION & ULTRAPRECISION MACHINING (NANOMETER MACHINING)
 - ↓
REQUIRES MATERIAL REMOVAL IN THE FORM OF ATOMS OR MOLECULES

**SOME IMPORTANT
CHARACTERISTICS
OF AMPs**

- PERFORMANCE IS INDEPENDENT OF STRENGTH BARRIER
- PERFORMANCE DEPENDS ON THERMAL, ELECTRICAL OR/AND CHEMICAL PROPERTIES OF W/P
- USE DIFFERENT KINDS OF ENERGY IN DIRECT FORM
- IN GENERAL, LOW MRR BUT BETTER QUALITY PRODUCTS
- COMPARATIVELY HIGH INITIAL INVESTMENT COST

CLASSIFICATION OF ADVANCED MACHINING PROCESSES



MECHANICAL

- ABRASIVE JET MACHINING (AJM)
- ULTRASONIC MACHINING (USM)
- WATER JET MACHINING (WJM)
- ABRASIVE WATER JET MACHINING (AWJM)
- ABRASIVE FLOW MACHINING (AFM)
- MAGNETIC ABRASIVE FINISHING (MAF)

THERMOELECTRIC

- PLASMA ARC MACHINING (PAM)
- LASER BEAM MACHINING (LBM)
- ELECTRON BEAM MACHINING (EBM)
- ELECTRIC DISCHARGE MACHINING (EDM)
- ION BEAM MACHINING (IBM)

ELECTROCHEMICAL & CHEMICAL

- ELECTROCHEMICAL MACHINING (ECM)
- CHEMICAL MACHINING (CHM).
- BIOCHEMICAL MACHINING (BM)

SOME HYBRID PROCESSES



- ELECTRICAL DISCHARGE GRINDING (EDG)
- ELECTRICAL DISCHARGE ABRASIVE GRINDING (EDAG)
- ELECTROCHEMICAL GRINDING (ECG)
- ELECTROCHEMICAL SPARK MACHINING (ECSM)
- ULTRASONIC ASSISTED EDM

REMARKS

- ENHANCED VOLUMETRIC MATERIAL REMOVAL RATE
- COMPUTER CONTROL OF THE PROCESSES RESULTING IN BETTER PERFORMANCE
- APPLICATION OF ADAPTIVE CONTROL => UNMANNED MACHINING

ABRASIVE JET MACHINING (AJM)

INTRODUCTION

A jet of inert gas consisting of very fine abrasive particles strikes the work-piece at high velocity (usually between 200-400 m/s) resulting in material removal through chipping / erosive action. This erosive action has been employed for cutting, cleaning, etching, polishing and deburring. This method of material removal is quite effective on hard and / or brittle materials (viz glass, silicon, tungsten, ceramics, etc) but not so effective on soft materials like aluminum, rubber, etc. It can produce fine and complicated details on the parts made of very brittle materials [Benedict, 1987].

The essential parts of an AJM setup, developed for laboratory purposes are shown in a schematic diagram, Fig. 2.1, and the same are discussed in the following.

ABRASIVE JET MACHINING SETUP

Gas Propulsion System

The *gas propulsion system* supplies clean and dry gas (air, nitrogen, or CO₂) to propel the abrasive particles. The gas may be supplied either by a compressor or a cylinder. In case of a compressor, air filter-cum-drier should be used to avoid water or oil contamination of the abrasive powder. The gas should be nontoxic, cheap, and easily available. It should not excessively spread when discharged from nozzle into atmosphere.

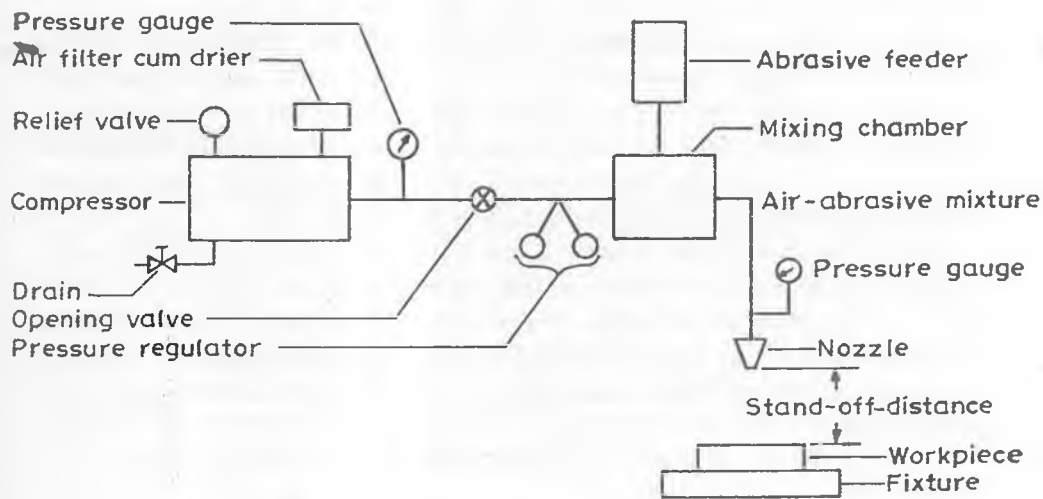


Fig. 2.1 Schematic diagram of abrasive jet machining (AJM) setup [Verma and Lal, 1984]

Abrasive Feeder

Required quantity of abrasive particles is supplied by *abrasive feeder*. In this particular setup, abrasive quantity is controlled by inducing vibration to the feeder. The particles are propelled by carrier gas to a mixing chamber. The air-abrasive mixture moves further to the nozzle. The nozzle imparts high velocity to the mixture which is directed at the workpiece surface. Material removal occurs due to the erosive action of the jet of air-abrasive mixture impinging on the work-piece surface.

Machining Chamber

The *machining chamber* is well closed so that the concentration of the abrasive particles around the working chamber does not reach to the harmful limit. Machining chamber is equipped with a **vacuum dust collector**. Special consideration should be given to the dust collection system if the toxic materials (say, beryllium) are being machined.

AJM Nozzle

The **AJM** nozzle is usually made of tungsten carbide or sapphire (usual life = 300 hr) which has high resistance to wear. The nozzle is made of either circular or rectangular cross-section. It is so designed that a loss of pressure due to bends, friction, etc is minimum possible. The nozzle pressure is generally maintained between 2-8.5 kgf/cm². Its value depends upon the material of workpiece and desired characteristics of the machined surface (accuracy, etc).

With an increase in the wear of a nozzle, the divergence of the jet stream increases resulting in more **stray cutting** and high inaccuracy. The stray cutting can be controlled by the use of masks made of soft materials like rubber (for less accurate work, or poor edge definition), or metals (for more accurate works or sharp edge definition). **Mask** covers only that part of the job where machining is not desirable.

Abrasives

Aluminium oxide (Al_2O_3), silicon carbide (SiC), glass beads, crushed glass, and sodium bicarbonate are some of the abrasives used in **AJM**. Selection of abrasive(s) depends upon the type of work material, material removal rate (MRR),

and machining accuracy desired. Al_2O_3 is good for cleaning, cutting, and deburring while SiC is also used for the similar applications but for harder work materials. For obtaining matte finish, glass beads are good while crushed glass performs better for giving sharper edges. However, cleaning, deburring, and cutting of soft materials are better performed by sodium bicarbonate. The sizes of abrasive particles available in the market range from 10 to 50 μm . Small abrasive particles are used for cleaning and polishing while large particles perform better during cutting. Fine grains are less irregular in shape, hence their cutting ability is poor. The abrasives should have sharp and irregular shape, and be fine enough to remain suspended in the carrier gas. Re-use of the abrasives is not recommended because of the two reasons. Firstly, abrasives get contaminated with metallic chips which may block the nozzle passage. Secondly, cutting ability of the used abrasive particles goes down. Further, cost of the abrasives is also low.

PARAMETRIC ANALYSIS

Important parameters that affect the material removal rate during AJM are stand-off-distance (ie. SOD, or sometimes called as nozzle tip distance - NTD), type and size of abrasive particles, flow rate of abrasive, gas pressure, work material and feed rate. The effects of these parameters on the process performance are discussed now.

Stand-Off-Distance

Effect of a change in stand-off-distance (SOD) on volumetric material removal rate (MRR_v) as well as linear material removal rate (or penetration rate- MRR_l) is shown in Fig. 2.2. Cross-sections of the actually machined profiles in Fig. 2.3 show how the shape of the machined cavity changes with a change in SOD. In a range of SOD which usually varies from 0.75 to 1.0 mm, the MRR is maximum. A decrease in SOD improves accuracy, decreases kerf width, and reduces taper in the machined groove (Fig. 2.4). However, light operations like cleaning, frosting, etc are conducted with a large SOD (say, 12.5 - 75 mm).

Abrasive Flow Rate

Ingulli [1967] has shown that MRR_g (mg/min) increases only up to a certain value of abrasive flow rate beyond which it starts decreasing (Fig. 2.5). As abrasive flow rate increases, the number of abrasive-particles cutting the workpiece

also increases thereby increasing MRR_g . However, with a further increase in abrasive flow rate (other parameters remaining unchanged), the abrasive flow velocity goes down. This decrease in abrasive flow velocity causes a reduction in MRR_g .

Nozzle Pressure

Effect of nozzle pressure on MRR_v is shown in Fig. 2.6. Kinetic energy (K. E.) of the abrasive particles is responsible for removal of material by erosion process. Abrasives must impinge on the work surface with a certain minimum velocity so that the erosion can take place. This minimum velocity for machining glass by SiC particles (size: 25 μm) is found to be around 150 m/s [Sheldon and Finnie, 1966].

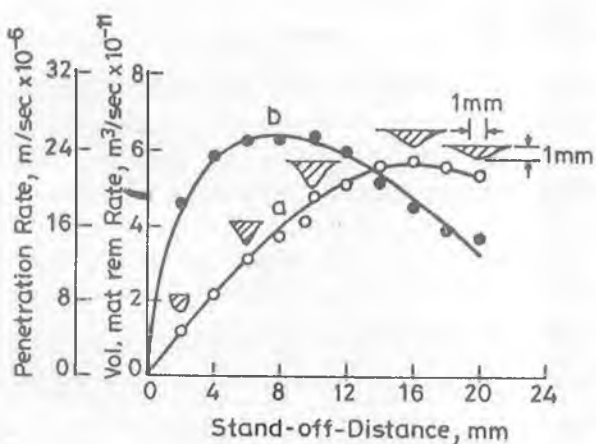


Fig. 2.2 Effects of stand-off-distance on material removal rate
(* penetration rate, ○ volumetric material removal rate)
[Verma and Lal, 1984].

Mixing Ratio

Mixing ratio (M) also influences MRR_v .

$$M = \frac{\text{volume flow rate of abrasive particles}}{\text{volume flow rate of carrier gas}} = \frac{\dot{V}_a}{\dot{V}_g} \quad \dots(2.1)$$

An increase in the value of 'M' increases MRR_v , but a large value of 'M' may decrease jet velocity and sometimes may block the nozzle. Thus, an optimum value of mixing ratio has been observed that gives maximum MRR_v . Fig. 2.7 shows the effect of SOD on MRR_v for various values of mixing ratios. In place of M, the mass ratio α , (Eq. 2.2) may be easier to determine.

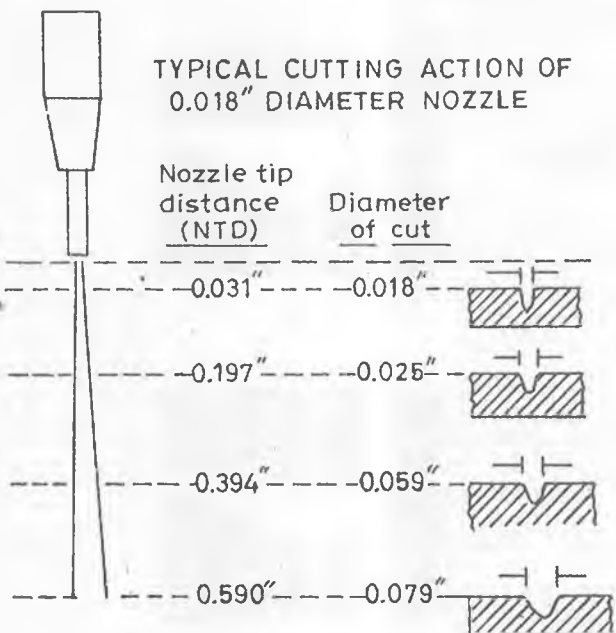
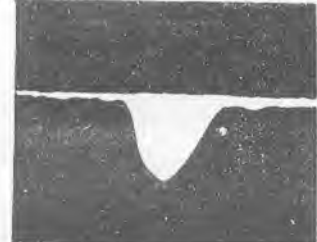


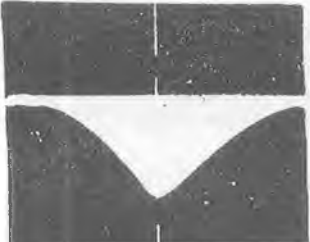
Fig. 2.3 Relationship between stand-off-distance and shape of the machined cavity.

$$\alpha = \frac{M_a}{M_{a+c}}, \quad \dots(2.2)$$

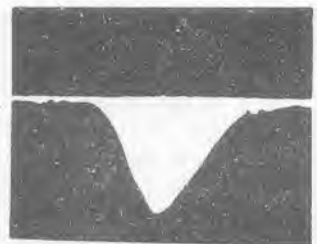
where, M_a is the abrasive mass flow rate, and M_{a+c} is abrasive and carrier gas



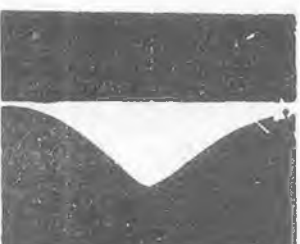
(a)



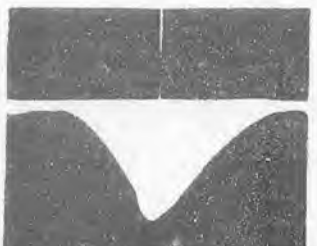
(d)



(b)



(e)



(c)



(f)

— | 1 mm —

Fig. 2.4 Photograph of the actual machined cavity profile at different stand-off-distance (a) 2 mm, (b) 6 mm, (c) 10 mm, (d) 14 mm, (e) 16 mm, (f) 20 mm. $d_p = 30 \mu\text{m}$, $\alpha = 0.148$, nozzle pressure = 147.15 kN/m^2 (gauge), and cutting time = 60 s [Verma and Lal, 1984].

combined mass flow rate. Verma and Lal [1984, 1985] have studied its effect on optimum volumetric material removal rate.

Finnie [1960] showed that the volume of material (Q) eroded by impacting particles of mass m carried in a stream of air can be calculated as

$$Q = \frac{C f(\theta) m v^n}{\sigma}, \quad \dots(2.3)$$

where, C and n are constants, σ is minimum flow stress of work material, v is velocity of impacting particles, and θ is impingement angle.

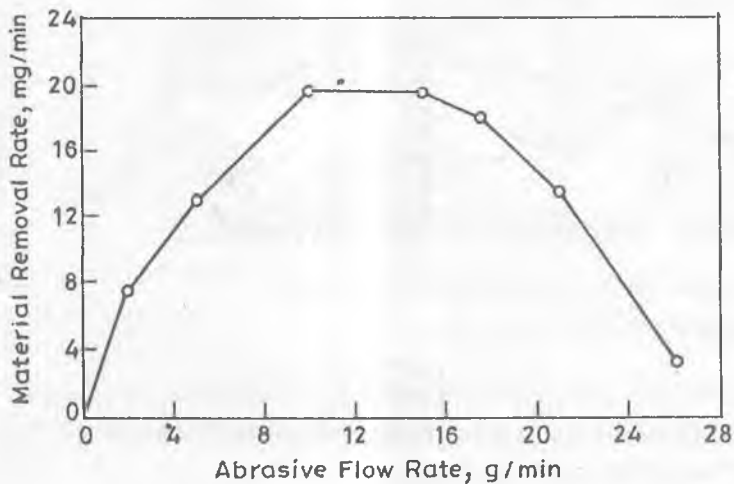


Fig. 2.5 Variation in material removal rate with a change in abrasive flow rate [Ingulli, 1967].

Sarkar and Pandey (1980) suggested a model to calculate MRR_v (Q) during AJM.

$$Q = \chi Z d^3 v^{3/2} \left(\frac{\rho}{12H_w} \right)^{3/4}, \quad \dots(2.4)$$

where, Z is no. of particles impacting per unit time, d is mean diameter of abrasive grains, v is velocity of abrasive grains, ρ is density of abrasive particles, H_w is hardness of work material (or the flow stress), and χ is a constant. There is a

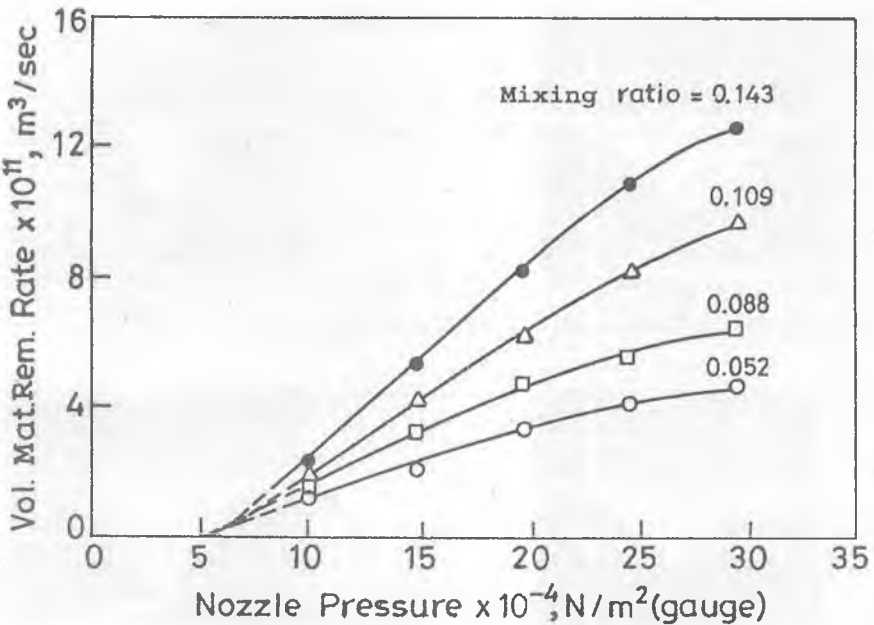


Fig. 2.6 Effect of nozzle pressure on material removal rate [Verma and Lal, 1984].

significant effect of change in mesh size (or abrasive grain diameter) and abrasive grain velocity. Eq. 2.4 also indicates that harder the work material, smaller will be MRR_v for the same machining conditions.

PROCESS CAPABILITIES

Although AJM gives low MRR_v (approx. $0.015 \text{ cm}^3/\text{min}$) but it can easily produce intricate details in hard and brittle materials. Production of narrow slots (0.12 - 0.25 mm), low tolerance ($\pm 0.12 \text{ mm}$), good surface finish (0.25 - 1.25 μm), and sharp radius (0.2 mm) on machined edge are some of the characteristics of the AJM process. Steels upto 1.5 mm thick and glass upto 6.3 mm thick have been possible to cut by AJM but at very low MRR and large taper. The process has a special application for machining thin-sectioned brittle materials, particularly in the areas which are inaccessible for conventional machining methods.

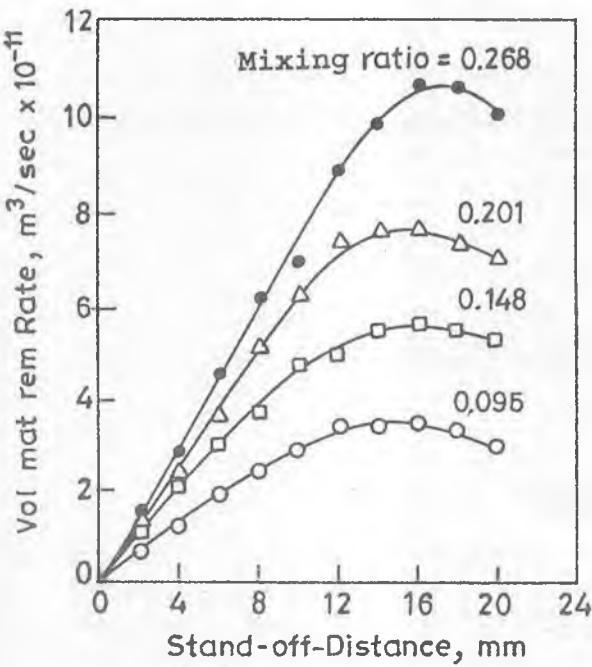


Fig. 2.7 Effect of stand-off-distance on material removal rate for various mixing ratios [Verma and Lal, 1984],

Since the heat generation is very low the resulting surface damage is also insignificant.

APPLICATIONS

AJM is useful [Butler, 1980; Dombrowski, 1983] in the manufacture of electronic devices, deburring of plastics, making of nylon and teflon parts, marking on electronic products, permanent marking on rubber stencils, deflashing small castings, cutting titanium foil, and drilling glass wafers. It is also used for engraving registration numbers, and on the toughened glass used for car windows. This process is also used for frosting glass surfaces and cutting thin-sectioned fragile components.

PROBLEMS

Problem 1

During AJM, the mixing ratio used is 0.2. Calculate mass ratio if the ratio of density of abrasive and density of carrier gas is equal to 20.

Solution:

We know, mixing ratio = $\frac{\dot{V}_a}{\dot{V}_g}$

$$\text{Mass ratio, } \alpha = \frac{\dot{M}_a}{\dot{M}_{a+g}} = \frac{\rho_a \dot{V}_a}{\rho_a \dot{V}_a + \rho_g \dot{V}_g}$$

$$\text{Or, } \frac{1}{\alpha} = \frac{\rho_a \dot{V}_a + \rho_g \dot{V}_g}{\rho_a \dot{V}_a}$$

$$= 1 + \frac{\rho_g}{\rho_a} \times \frac{\dot{V}_g}{\dot{V}_a}$$

$$= 1 + \frac{1}{20} \times \frac{1}{0.2}$$

$$= 1 + 0.25$$

$$= 1.25$$

$$\text{or, } \alpha = \frac{1}{1.25} = 0.80$$

$$\boxed{\alpha = 0.80}$$

Problem 2

Diameter of the nozzle is 1.0 mm and jet velocity is 200 m/s. Find the volumetric flow rate (cm^3/s) of the carrier gas and abrasive mixture, V_{a+g} .

Solution:

$$\text{Cross-sectional area of the nozzle} = \pi \times (0.5)^2 \times 10^{-2} \text{ cm}^2 \\ = \pi \times 25 \times 10^{-4} \text{ cm}^2$$

$$\therefore V_{a+g} = (\pi \times 25 \times 10^{-4}) \times 200 \times 10^2 \text{ cm}^3/\text{s} \\ = \pi \times 25 \times 2 \text{ cm}^3/\text{s}$$

$$V_{a+g} = 50 \pi \text{ cm}^3/\text{s}$$

BIBLIOGRAPHY

1. Benedict G.F. (1987), *Non-traditional Manufacturing Processes*, Marcel Dekker Inc., New York.
2. Bitter J.G.A. (1962-63), A Study of Erosion Phenomenon—Part I, *Wear*, Vol. 5-6, p. 5.
3. Bitter J.G.A. (1962-63), A Study of Erosion Phenomenon—Part II, *Wear*, Vol. 5-6, pp. 169-190.
4. Butler K. (Sept/Oct 1980), Blast Your Problems Away, *Tool Carbide*, pp. 12-15.
5. Dombrowski T.R. (Feb 1983), The How and Why of Abrasive Jet Machining. *Modern Machine Shop*, pp. 76-79.
6. Finnie Iain (1960), Erosion of Surface by Solid Particles, *Wear*, Vol. 3, p. 87.
7. Finnié Iain (1966), The Mechanism of Metal Removal in the Erosive Cutting of Brittle Materials, *Trans ASME. Ser. B*, Vol. 88, p. 393
8. Ingulli C.N. (1967), "Abrasive Jet Machining", *Tool and Manuf. Engrs.*, Vol. 59, p. 28.
9. McGeough J.A. (1988), *Advanced Methods of Machining*, Chapman and Hall, London, p. 211.
10. Pandey P.C. and Shan H.S. (1980), *Modern Machining Processes*, Tata McGraw Hill Publishing Co. Ltd., New Delhi, p. 39.
11. Sarkar P.K. and Pandey P.C. (1976). "Some Investigations in Abrasive Jet Machining". *J. Inst. Engrs. (I)*, Vol. 56, Pt. ME-5, p. 284.

12. Sheldon G.L. and Finnie I. (1966), The Mechanics of Material Removal in the Erosive Cutting of Brittle Materials, *Trans ASME Ser. B*, Vol. 88, p. 393.
13. Snoeys R., Stalens F., and Dekeyser W. (1986). Current Trends in Non-conventional Material Removal Processes, *Annals of the CIRP*, Vol. 35(2), p. 467.
14. Venkatesh V.C. (1984), Parametric Studies on AJM, *Annals of the CIRP*, Vol. 33, No. 1, p. 109.
15. Verma A.P. and Lal G.K. (1985), Basic Mechanics of Abrasive Jet Machining, *J. Inst. Engrs(I). Prod. Engg.*, Vol. 66, pp. 74-81.
16. Verma A.P. and Lal G.K. (1984), An Experimental Study of Abrasive Jet Machining, *Int. J. Mach. Tool Des. Res.*, Vol. 24, No. 1, pp. 19-29.

SELF TEST QUESTIONS

- (1). Examine whether the following statements are true (T) or false (F).
 - i. The surface damage during AJM is negligible.
 - ii. AJM is not a good process for cleaning metallic mould cavities.
 - iii. Glass is machined by AJM process using SiC abrasive. The minimum jet velocity required has been found to be 150 m/s.
 - iv. AJM process can be employed to machine materials irrespective of whether they are insulator or conductor of electricity.
 - v. AJM and sand blasting are similar kind of processes from application point of view.
 - vi. Carrier gas used in AJM is either air or O₂.
 - vii. Shape of the abrasive particles has no effect on MRR in AJM.
 - viii. One obtains uniform diameter hole in AJM process.
 - ix. Show (sketch only) the effect of jet pressure on MRR for different grain sizes.
- (2). Write all the correct answers.
 - i. Material used for making a nozzle employed in AJM process may be (a) copper, (b) stainless steel, (c) sapphire, (d) WC.
 - ii. In AJM, mixing ratio is governed by amplitude and frequency of vibration of sieve. The frequency of vibration of sieve is (a) 50-60 Hz, (b) 10-15 kHz, (c) above 15 kHz.

- iii. In case of AJM, higher carrier gas pressure would yield (a) higher MRR and higher nozzle-life, (b) lower MRR and lower nozzle life, (c) higher nozzle life but lower MRR, (c) None of these.
- iv. In AJM, with the increase in stand-off-distance, the width of cut (a) deceases, (b) increases, (c) remains constant.
- v. During AJM, increase of mass flow rate of abrasive particles would (a) decrease the mixing ratio, (b) increase the value of mixing ratio, (c) no definite effect on mixing ratio.
- vi. With an increase in abrasive particle size in AJM (a) MRR as well as surface finish increase, (b) MRR decreases but surface finish increases, (c) MRR increases but surface finish decreases.
- vii. The range of size of abrasive particles used in AJM is (a) 0.001-0.05 mm, (b) 0.1-0.5 mm, (c) 1-5 mm.
- viii AJM is best suited for machining (a) Aluminium, (b) Glass, (c) M.S.
- ix. In AJM, MRR increases with (a) increase in NTD, (b) decrease in NTD, (c) no effect of NTD.
- x. AJM can be recommended to machine (a) M.S., (b) C.I., (c) WC.

REVIEW QUESTIONS

1. Draw a schematic diagram of AJM system and label it.
2. Explain the working principle of AJM process.
3. With the help of sketches, show the effect of stand-off-distance on (a) width of cut, (b) material removal rate.
4. "AJM is not recommended to machine ductile materials". Comment.
5. Show the effect of carrier gas pressure on MRR during AJM.
6. Write five important variables of AJM process. Draw a sketch showing the effect of one of these variables on MRR.
7. Write the applications of different types of abrasives used in AJM.

NOMENCLATURE

AJM Abrasive Jet Machining

C_n Constants (Eq. 2.3)

d	Mean diameter of the abrasive particles
H_w	Flow stress (or hardness) of the work material
m	Impacting particle mass
M	Mixing ratio
MRR_g	Material removal rate (g/s)
MRR_t	Linear material removal rate (mm/s)
MRR_v	Volumetric material removal rate (mm^3/s)
\dot{M}_a	Mass flow rate of abrasive
\dot{M}_{a+c}	Mass flow rate of abrasive and carrier gas combined
Q	Volume of eroded material
\dot{Q}	Volumetric material removal rate
\dot{V}_a	Volume flow rate of abrasives
\dot{V}_g	Volume flow rate of carrier gas
Z	No. of particles impacting per unit time
α	Mass ratio
σ	Minimum flow stress of work material
θ	Impingement angles
v	Impacting particle (or abrasive grain) velocity
ρ_a	Density of abrasive particles
ρ_g	Density of carrier gas

CHAPTER 2
AT-A-GLANCE
ABRASIVE JET MACHINING (AJM)



HOW IT WORKS?

JET OF INERT GAS + FINE ABRASIVES → STRIKE W/P AT VERY HIGH SPEED



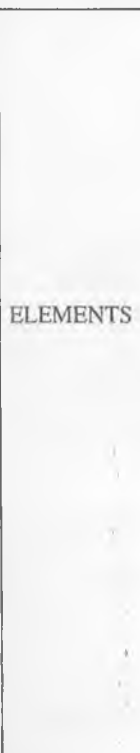
MATERIAL REMOVAL BY EROSION / CHIPPING ACTION

WHAT IT DOES?



CUTTING, CLEANING, POLISHING, DUBLURRING, ETC.

- EFFECTIVE ON HARD AND / OR BRITTLE MATERIALS
- CAN PRODUCE FINE & COMPLICATED DETAILS



GAS PROPULSION SYSTEMS

- SUPPLIES CLEAN & DRY GAS TO PROPEL ABRASIVE PARTICLES
- COMPRESSOR OR CYLINDER FILLED WITH GAS
- GAS → NON-TOXIC, CHEAP & EASILY AVAILABLE
→ NO EXCESS SPREADING

ABRASIVE FEEDER

- QUANTITY CONTROL → BY VIBRATION

MACHINING CHAMBER

- WELL CLOSED → ABRASIVE PARTICLES CONTENT SHOULD BE BELOW HARMFUL LIMIT
- VACUUM DUST COLLECTOR

AJM NOZZLES

- WC / SAPPHIRE (≈ 300 HR)
- CIRCULAR / RECTANGULAR X-SECTION
- NOZZLE PRESSURE = 2 - 8.5 kgf/cm² (W/P MATERIAL, MRR REQUIREMENTS)
- INCREASED WEAR → STRAY CUTTING & HIGHER INACCURACY





- + LESS ACCURATE - RUBBER
- + MORE ACCURATE - METAL

ABRASIVES

- ALUMINA, SiC, GLASS BEADS, SOD. BICARBONATE, ETC.
- SELECTION (W/P MATERIAL, MRR, ACCURACY)
- Al₂O₃, SOD. BICARBONATE, SiC (FOR HARDER MATERIALS) → CLEANING, CUTTING, DEBURRING, ETC.
- GLASS BEADS → GOOD FOR MATTE FINISH
- SIZE → 10 – 50 µm
 - SMALL → CLEANING & POLISHING
 - LARGE → CUTTING
- RE-USE → NOT RECOMMENDED
 - : CONTAMINATION WITH CHIPS → BLOCKS NOZZLE PASSAGE
 - : LOWER CUTTING ABILITY
 - : LOW COST

PARAMETRIC

A
N
A
L
Y
S
I
S

- | | | |
|----------------------|--|--|
| → STAND-OFF-DISTANCE | • 0.75 - 1.0 mm | → MAX MRR |
| | • LOW SOD | → HIGHER ACCURACY
→ LOW KERF WIDTH
→ LOW TAPER |
| → ABRASIVE FLOW RATE | • MAXIMA OBSERVED | |
| | • HIGHER ABRASIVE FLOW RATE →
MORE OF CUTTING → HIGHER MRR | |
| | • LOWER ABRASIVE FLOW VELOCITY
→ LOWER MRR | |
| → NOZZLE PRESSURE | • AFFECTS MRR | |
| | • MATERIAL REMOVAL-EROSIVE ACTION | |
| | • CERTAIN MINIMUM VELOCITY →
150 m/s FOR SiC → 25 µm | |
| → MIXING RATIO | • VOLUME FLOW RATE OF
ABRASIVE / VOLUME
FLOW RATE OF CARRIER GAS | |
| | • MAXIMA OBSERVED BETWEEN 'M &
MRR' | |

- $MASS\ RATIO = \dot{M}_a / \dot{M}_{a+e}$
- $MRR_p = (Q) = cf(\theta)m V''/\sigma$
- LOW MRR $\sim 15\ mm^3/min$
- INTRICATE DETAILS CAN BE PRODUCED
- NARROW SLOTS (0.12 TO 0.25 mm)
- LOW TOLERANCES (+0.12 TO -0.12 mm)
- MINIMIZATION OF TAPER \rightarrow ANGLE OF NOZZLE WRT W/P
- THIN-SECTIONED, BRITTLE MATERIAL, INACCESSIBLE AREAS
- ALMOST NO SURFACE DAMAGE

APPLICATIONS

- MANUFACTURE OF ELECTRONIC DEVICES
- DEBURRING OF PLASTICS, NYLON, AND TEFLON PARTS
- DEFLASHING SMALL CUTTINGS
- DRILLING GLASS WAFERS

ULTRASONIC MACHINING (USM)

INTRODUCTION

Ultrasonic Machining (USM) is a *mechanical type non-traditional machining process*. It is employed to machine hard and / or brittle materials (both electrically conductive and non-conductive) having hardness usually greater than 40 RC. It uses a shaped tool, high frequency mechanical motion and abrasive slurry. In USM, material is removed by the abrasive grains which are driven into the work surface by a tool oscillating normal to the work surface. To understand the working principle of USM, consider that a particle 'p' is thrown on the wax wall (Fig 3.1) with a certain force F_1 . It will penetrate into the wall to a length l_1 . If the same particle is thrown with force F_2 and F_3 ($F_3 > F_2 > F_1$) then it will penetrate deeper in the wall ($l_3 > l_2 > l_1$). USM works almost in the same way. In USM, the throw-

ing force is contributed by the tool oscillating at ultrasonic frequency. The particles are of different sizes and they are thrown many times per second. In some cases, they are hammered also through the slurry. Fig. 3.2 shows a schematic diagram of USM system.

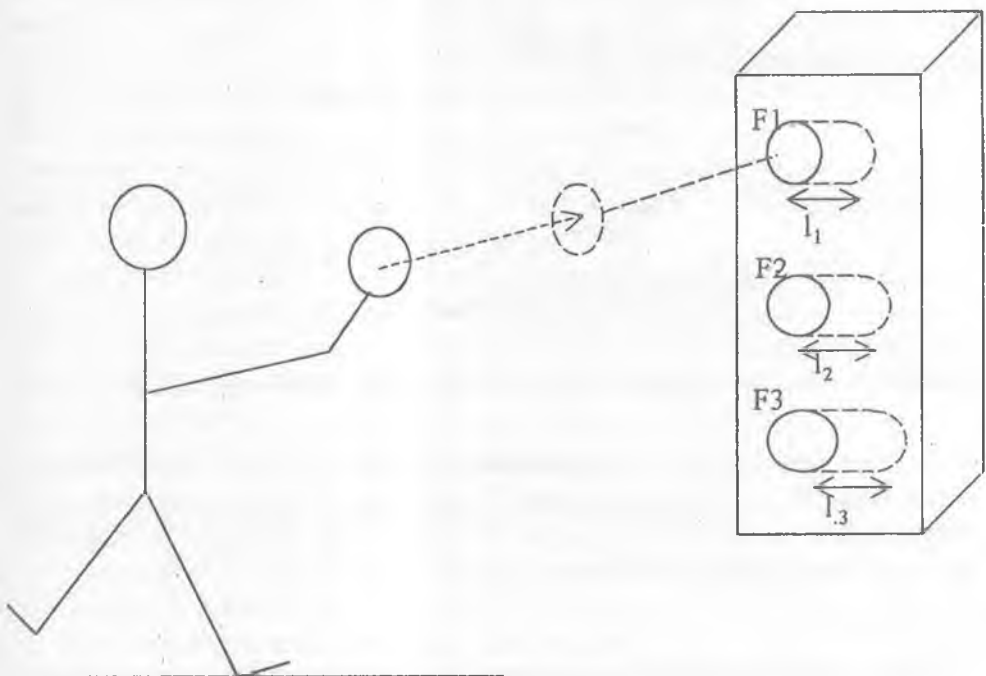


Fig. 3.1

The word **ultrasonic** describes a vibratory wave having frequency larger than upper frequency limit of human ear (usually greater than 16 kc/s). Waves are usually classified as shear waves and longitudinal waves. High velocity longitudinal waves can easily propagate in solids, liquids and gases. They are normally used in ultrasonic applications.

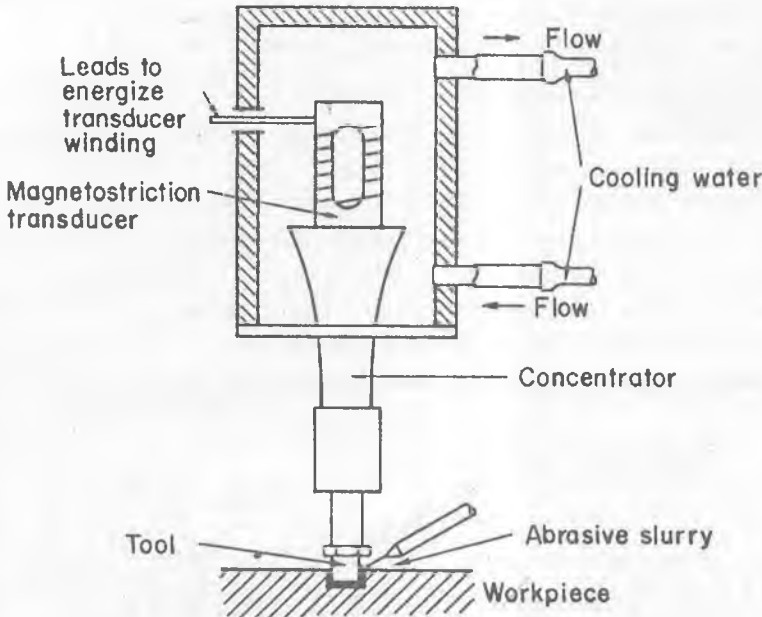


Fig. 3.2 A schematic diagram of ultrasonic machining [Kaczmarck, 1976].

In USM, the principle of **longitudinal magnetostriiction** is used. When an object made of ferromagnetic material is placed in the continuously changing magnetic field, a change in its length takes place. The coefficient of magnetostrictive elongation (E_m) is defined as

$$E_m = \Delta L / L$$

where, ΔL is the change in length and L is the length of the magnetostrictor coil. This kind of transducer is known as **magnetostriiction transducer**.

A device that converts any form of energy into ultrasonic waves is called **ultrasonic transducer**. In USM, a transducer converts high frequency electrical signal into high frequency linear mechanical motion (or vibration). These high frequency vibrations are transmitted to the tool via tool holder. For achieving optimum material removal rate (MRR), tool and tool holder are designed so that resonance can be achieved. *Resonance* (or maximum amplitude of vibration)

is achieved when the frequency of vibration matches with the *natural frequency* of tool and tool holder assembly.

The **tool shape** is made converse to the desired cavity. The tool is placed very near to the work surface, and the gap between the vibrating tool and the workpiece is flooded with abrasive slurry made up of fine abrasive particles and suspension medium (usually water). As the tool vibrates in its downward stroke, it strikes the abrasive particles. This impact from the tool propels the grains across the gap between the tool and the workpiece. These particles attain kinetic energy and strike the work surface with a force much higher than their own weight. This force is sufficient to remove material from the brittle workpiece surface and results in a crater on it. Each down stroke of the tool accelerates numerous abrasive particles resulting in the formation of thousands of tiny chips per second. A very small percentage (about 5 %) of material is also believed to be removed by a phenomenon known as **cavitation erosion**. To maintain a very low constant gap between the tool and the work, feed is usually given to the tool.

USM gives low **MRR** but it is capable to machine intricate cavities in single pass in fragile or /and hard materials. In USM, there is no direct contact between the tool and workpiece hence it is a good process for machining very thin and fragile components. A brittle material can be machined more easily than a ductile one. It is considered as a very safe process because it does not involve high voltage, chemicals, mechanical forces and heat.

ULTRASONIC MACHINING SYSTEM

USM machines are available in the range of **40 W** to **2.4 kW**. USM system has sub-systems as power supply, transducer, tool holder, tool, and abrasives.

High power sine wave generator converts low frequency (60 Hz) electrical power to high frequency (≈ 20 kHz) electrical power. This high frequency electrical signal is transmitted to the transducer which converts it into high frequency low amplitude vibration. Essentially the transducer converts electrical energy to mechanical vibration. In USM, either of the two types of transducers are used, i.e. piezoelectric or magnetostrictive type. **Piezoelectric crystals** (say, quartz) generate a small electric current when they are compressed. Also, when an electric current is passed through the crystal, it expands; when the current is removed the crystal attains its original size. This effect is known as piezoelectric effect. Such transducers are available up to a power capacity of 900 W.

Magnetostrictive transducer also changes its length when subjected to a strong magnetic field. These transducers are made of nickel, or nickel alloy sheets. Their conversion efficiency (20-35%) is much lower than the piezoelectric transducers' efficiency (up to 95%) hence their cooling is essential to remove waste heat. These magnetostrictive type transducers are available with power capacity as high as 2.4 kW. The maximum change in length (or amplitude of vibration) that can be achieved is 25 μm .

Tool holder holds and connects the tool to the transducer. It virtually transmits the energy and, in some cases, amplifies the amplitude of vibration. Material of the tool therefore, should have good acoustic properties, and high resistance to fatigue cracking. Due measures should be taken to avoid ultrasonic welding between the transducer and the tool holder. For example, attach tool holder with transducer using loose fitting screws between transducer and tool holder [Benedict, 1987].

Commonly used **materials for the tool holder** are monel, titanium and stainless steel. Because of good brazing as well as acoustic properties, monel is commonly used material for low amplitude applications. High amplitude application requires good fatigue strength of tool holder material. Further, tool holder may be **amplifying or non-amplifying**. Non-amplifying tool holders have circular cross-section and give the same amplitude at both the ends, i.e. input end and output end. Amplifying tool holders give as much as 6 times increased tool motion. It is achieved by stretching and relaxing the tool holder material. Such a tool holder yields MRR up to 10 times higher than non-amplifying tool holder. However, amplifying tool holders are more expensive, demand higher operating cost and yield poorer surface quality.

Tools are usually made of relatively ductile materials (brass, stainless steel, mild steel, etc) so that the tool wear rate (TWR) can be minimized. Value of the ratio of **TWR** and **MRR** depends upon the kind of abrasives, workpiece material, and tool material. Surface finish of the tool is important because it will affect the surface finish obtained on the workpiece. To *safeguard tool and tool holder* against their early fatigue failure, they should not have scratches or machining marks. Tools should be properly designed to account for overcut. Silver brazing of the tool with tool holder minimizes the fatigue problem associated with screw attachment method.

Hardness, particle size, usable lifetime and cost should be criteria for selecting **abrasive grains** to be used in USM. Commonly used abrasives in the order of

increasing hardness, are Al_2O_3 , SiC and B_4C (Boron carbide). In order to have high usable lifetime of abrasives, their hardness should be more than that of the workpiece material. MRR and surface finish obtained during USM are also function of abrasive size. Coarser grains result in higher MRR and poorer surface finish while reverse is true with finer grains. Mesh sizes of grits generally used range from 240 to 800. Abrasive slurry consists of water and abrasives usually in 1:1 (by weight). However, it can vary depending upon type of operations, viz. thinner (or low concentration) mixtures are used while drilling deep holes, or machining complex cavities so that the slurry flow is more efficient. The slurry stored in a reservoir, is pumped to the gap formed by the tool and the work (Fig. 3.2). In case of heavy duty machines, a cooling system may be required to remove heat from the abrasive slurry.

MECHANICS OF CUTTING

Various mechanisms of material removal have been proposed by different researchers (*Miller, 1957; Shaw, 1956; Kazantsev and Rosenberg, 1965; Kainth, et al, 1979*). Theory proposed by *M.C. Shaw (1956)* is briefly explained in the following.

Model Proposed by Shaw

Material removal during USM due to cavitation under the tool and chemical corrosion due to slurry media are considered insignificant. Hence, material removal due to these two factors has been ignored. Contributions to the material removal by abrasive particles due to '*throwing*' and '*hammering*' actions have been analyzed.

Abrasive particles are assumed to be spherical in shape having diameter as ' d ' units. Abrasive particles (suspended in carrier) move under the high frequency vibrating tool. There are two possibilities when the tool hits an abrasive particle. If the size of the particle is small and the gap between the bottom of the tool and work surface is large enough, then the particle will be thrown by the tool, to hit the work surface (*throwing model*). Under the reverse conditions, the particle will be hammered over the work surface. In the both cases, a particle after hitting the work surface generates a crater of depth ' h ' and radius ' r '. It is also assumed that the volume of the particle removed is approximately proportional to the diameter of indentation ($2r$). The volume of material (V_g) removed (shown by dashed lines

in Fig. 3.3a and 3.3b, assuming hemi-spherical crater) due to fracture per grit per cycle is given by

$$V_g = \frac{1}{2} \left(\frac{4}{3} \pi r^3 \right). \quad \dots(3.1)$$

From the geometry of Fig. 3.3b, it can be shown that

$$\begin{aligned} r^2 &= \left(\frac{d}{2} \right)^2 - \left(\frac{d}{2} - h \right)^2 \\ &\approx dh \text{ (neglecting } h^2 \text{ terms as } h \ll d). \end{aligned} \quad \dots(3.2)$$

From Eqs. (3.1) and (3.2), we can write

$$V_g = K_1 (hd)^{3/2} \quad \dots(3.3)$$

where, K_1 is a constant.

Number of impacts (N) on the workpiece by the grits in each cycle will depend upon the number of grits beneath the tool at any time. This is inversely proportional to the diameter of the grit (assumed spherical) as given below.

$$N = K_2 \frac{1}{d^2} \quad \dots(3.4)$$

where, K_2 is a constant of proportionality.

All abrasive particles under the tool need not be necessarily effective. Let K_3 be the probability of an abrasive particle under the tool being effective. Then volume (V) of material removed per second will be equal to the frequency (f) times the amount of material removed per cycle (V_g).

$$V = V_g \times f = K_1 K_2 K_3 \sqrt{\frac{h^3}{d}} \cdot f$$

...(3.5)

To evaluate the depth of penetration ' h ' of an abrasive particle, *Shaw* [1956] proposed two models. Model 1 considers that when a particle is hit by the tool it is thrown (Fig. 3.3a) on the workpiece surface. Model 2 assumes that a particle is hammered (Fig. 3.3b) by the tool into the workpiece. Both these models are discussed below.

Model 1 (Grain Throwing Model)

It is assumed that a particle is hit and thrown by the tool onto the workpiece surface. Assuming sinusoidal vibration, the displacement (Y) of the tool is given by Eq. (3.6) in which 't' is time period and $a/2$ is amplitude of oscillation.

$$Y = \frac{a}{2} \sin(2\pi ft). \quad \dots(3.6)$$

From Eq. (3.6), velocity of the tool is evaluated as follows

$$\dot{Y} = \pi af \cos(2\pi ft). \quad \dots(3.7)$$

The maximum velocity of the tool \dot{Y}_{max} is derived as follows:

$$\dot{Y}_{max} = \pi af \quad (\text{for } \cos(2\pi ft) = 1). \quad \dots(3.8)$$

Let us assume that the grits also leave the tool with the same maximum velocity, i.e. \dot{Y}_{max} . Then kinetic energy (KE) of a grit is given by

$$\begin{aligned} KE &= \frac{1}{2} m \pi^2 a^2 f^2 \\ &= \frac{1}{2} \left(\frac{\pi}{6} d^3 \rho_a \right) \pi^2 a^2 f^2. \end{aligned} \quad \dots(3.9)$$

A grit penetrates to the depth equal to 'h' into the workpiece. It is assumed that full KE of the grit is absorbed by the workpiece before it comes to rest. Then the work done by a grit (assuming triangular variation of force (F) with the depth of penetration) is given by

$$\text{Work done, } W_g = \frac{1}{2} F h_{th} \quad (\text{From Fig. 3.3c}). \quad \dots(3.10)$$

Work done by the grit (W_g) should be equal to the KE of the particle.

$$\frac{1}{2} F h_{th} = \frac{1}{2} \left(\frac{\pi}{6} d^3 \rho_a \right) \pi^2 a^2 f^2,$$

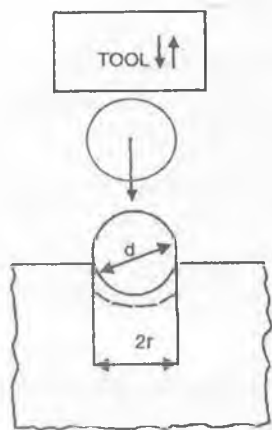


Fig. 3.3 (a) Throwing

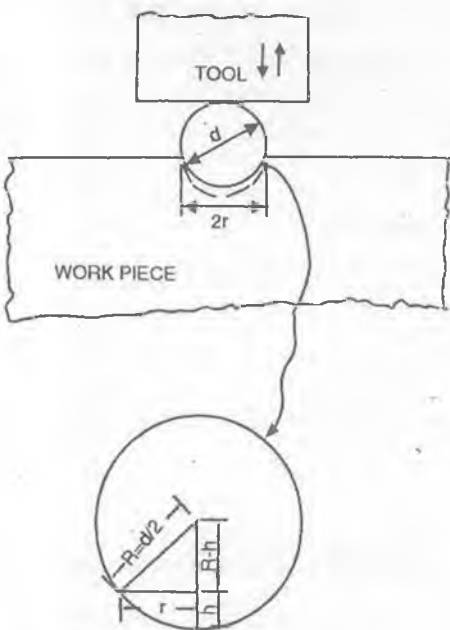


Fig. 3.3 (b) Hammering

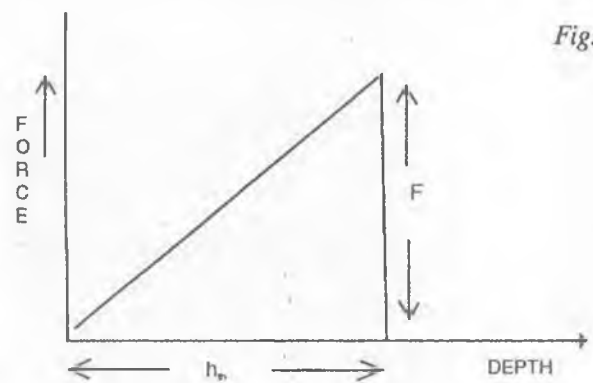


Fig. 3.3 (c)

Fig. 3.3 Development of fracture in the workpiece due to hitting by a grain, (a) by throwing, (b) by hammering, (c) variation of force (F) with a change in depth of penetration.

or,

$$h_{th} = \frac{\pi^3 a^2 f^2 d^3 \rho_a}{6 F}. \quad \dots(3.11)$$

'F' can be written in terms of workpiece property that can be known beforehand. Mean stress acting on the workpiece surface (σ_w) is given by

$$\sigma_w = \frac{F}{A} = \frac{F}{\pi h_{th} d} \quad (\text{Using Eq. (3.2), and taking } h = h_{th})$$

$$F = \pi \sigma_w h_{th} d. \quad \dots(3.12)$$

From Eqs. (3.11) and (3.12),

$$h_{th} = \frac{\pi^3 a^2 f^2 d^3 \rho_a}{6 \pi \sigma_w h_{th} d},$$

$$h_{th}^2 = \pi^2 a^2 f^2 d^2 \cdot \frac{\rho_a}{6 \sigma_w}.$$

$$\text{or, } h_{th} = \pi a f d \sqrt{\frac{\rho_a}{6 \sigma_w}}. \quad \dots(3.13)$$

Volumetric material removal rate due to throwing mechanism (V_{th}) can be obtained using Eqs. (3.5) and (3.13).

$$V_{th} = K_1 K_2 K_3 \left[\frac{\pi^2 a^2 \rho_a}{6 \sigma_w} \right]^{3/4} d f^{5/2}.$$

...3.14

Model 2 (Grain Hammering Model)

When the gap between the tool and the workpiece is smaller than the diameter of the grit it will result into partial penetration in the tool (h_u) as well as in the workpiece (h_w) (Fig. 3.4a). The values of h_w and h_u will depend on the hardness of the tool and workpiece material, respectively. Force 'F' acts on the abrasive particle only for a short time (ΔT) during the cycle time 'T' (Fig. 3.4b). During this

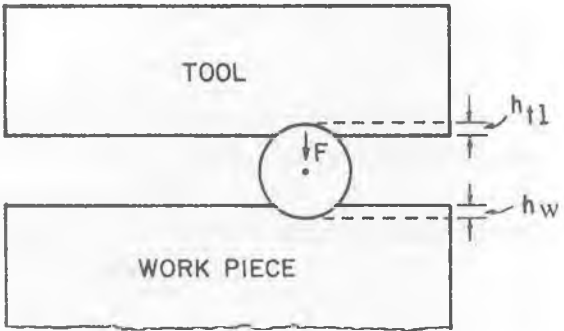
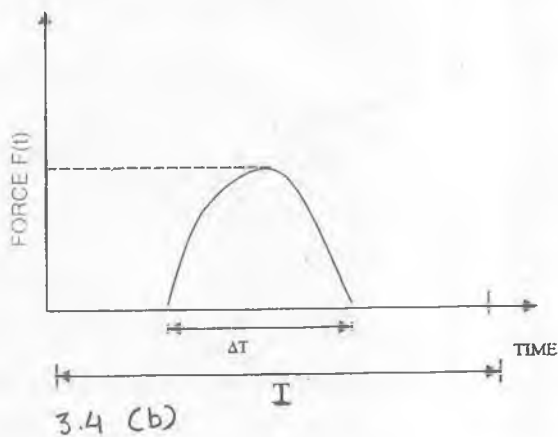


Fig. 3.4 (a)



3.4 (b)

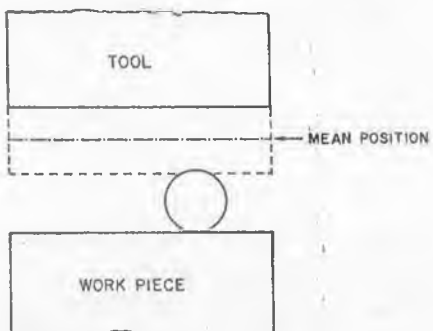


Fig. 3.4 (c)

Fig. 3.4 (a) Partial penetration of a grit in the tool and workpiece, (b) Variation of force (F) with time (T), (c) Schematic diagram of a grain hammering model.

time period, the abrasive particle is in contact with the tool and workpiece both (Fig. 3.4c). The mean force (F_{avg}) on the grit can be expressed by Eq. (3.15),

$$F_{avg} = \frac{1}{T} \int_0^T F(t) dt. \quad \dots(3.15)$$

Here, $F(t)$ is the force at any instant of time 't'. Force on the grit by the tool starts increasing as soon as the grit gets in contact with both the tool and the workpiece at the same time. It attains maximum value and then starts decreasing until attains zero value. Hence, the momentum equation can be written as

$$\int_0^T F(t) dt \approx \left(\frac{F}{2}\right) \Delta T. \quad \dots(3.16)$$

Total penetration due to hammering (h_h) (Fig. 3.4a) is given as

$$h_h = h_w + h_d \quad \dots(3.17)$$

$a/2$ is amplitude of oscillation of the tool. The mean velocity of the tool during the quarter cycle (from O to B in Fig. 3.5a) is given by $(a/2) / (T/4)$. Therefore, time (ΔT) required to travel from A to B is given by the following equation:

$$\begin{aligned} \Delta T &\equiv \frac{h_h}{(a/2)} \cdot (T/4) \\ &= \frac{h_h}{a} \left(\frac{T}{2}\right). \end{aligned} \quad \dots(3.18)$$

From Eqs. (3.15), (3.16), and (3.18)

$$F = F_{avg} \frac{4a}{h_h}. \quad \dots(3.19)$$

Let 'N' be the number of grains under the tool. Stress acting on the tool (σ_d) and the workpiece (σ_w) can be found as follows:

$$\sigma_w = \frac{F}{N(\pi h_w d)} \quad \dots(3.20)$$

$$\sigma_{\text{tl}} = \frac{F}{N(\pi h_{\text{tl}} d)}$$

$$= \sigma_w \frac{h_w}{h_{\text{tl}}} \quad (\text{from Eq. 3.20}) \quad \dots(3.21)$$

From Eqs. (3.4), (3.19) and (3.20),

$$\begin{aligned} \sigma_w &= F_{\text{avg}} \frac{4a d^2}{h_{\text{tl}} K_2(\pi h_w d)} \\ &= \frac{4F_{\text{avg}} ad}{\pi K_2 h_w (h_w + h_{\text{tl}})} \\ &= \frac{4F_{\text{avg}} ad}{\pi K_2 h_w^2 \left(\frac{h_{\text{tl}}}{h_w} + 1 \right)}. \end{aligned} \quad \dots(3.22)$$

From Eq. (3.21),

$$h_{\text{tl}}/h_w = \sigma_w/\sigma_{\text{tl}} = j \quad \dots(3.23)$$

j can be taken as the ratio of hardness of workpiece material to the hardness of tool material. From Eqs. (3.22) and (3.23),

$$h_w = \sqrt{\frac{4F_{\text{avg}} a d}{\sigma_w \pi K_2 (j + 1)}}.$$

...(3.24)

Volumetric material removal rate from the workpiece due to hammering mechanism (V_h), can be evaluated using Eqs. (3.5) and (3.24) as follows:

$$V_h = K_1 K_2 K_3 \left[\frac{4a F_{\text{avg}}}{\sigma_w \pi K_2 (j + 1)} \right]^{3/4} d f$$

...(3.25)

From computational results obtained using Eqs. (3.14) and (3.25), it is observed that $V_h \gg V_{\text{th}}$.

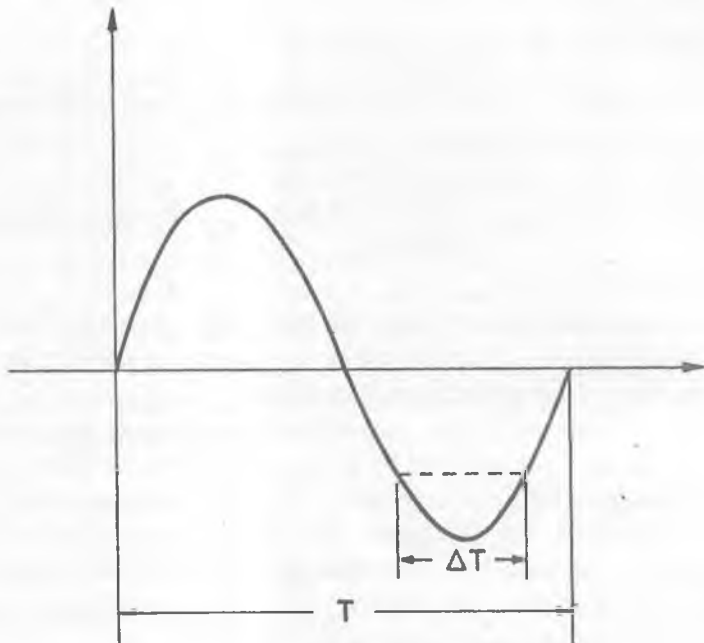


Fig. 3.5 (a)

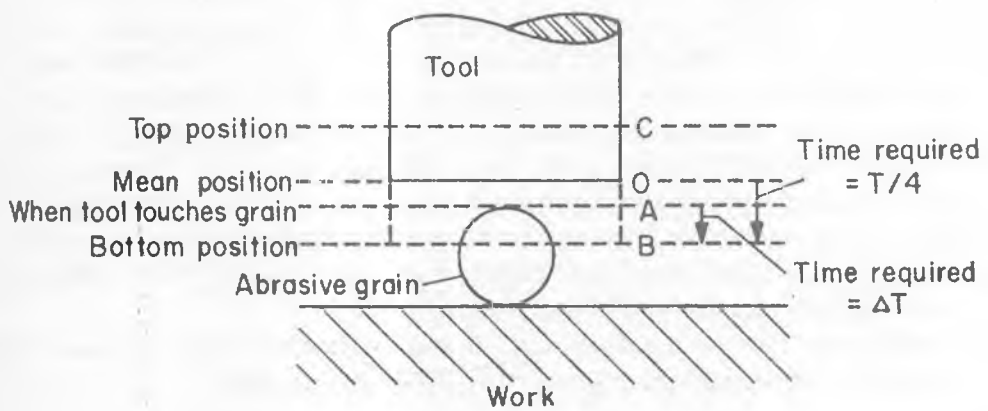


Fig. 3.5 (b)

- Fig. 3.5 (a) Assumed mode of tool vibration.
 (b) Various positions of tool while hitting workpiece via a grit.

PARAMETRIC ANALYSIS

Performance (MRR, accuracy and surface finish) of the USM process depends upon the following parameters:

- *Abrasives* : size, shape, and concentration.
- *Tool and tool holder* : material, frequency of vibration, and amplitude of vibration.
- *Workpiece* : hardness.

Depending upon the mass of tool and tool holder, the power rating is determined. **Trepanning** type of tool should be used to reduce power requirements in the operations like drilling of large diameter holes.

The elongation obtained from a magnetostrictor operating at resonance ranges from 0.001 to 0.1 μm . It is achieved by using a "concentrator" at the output end of the tool. To maximize the amplitude of vibration, the concentrator should operate at resonance condition. Fig. 3.6 shows the effect of amplitude of vibration on MRR_i. Increase in the **amplitude of vibration** increases MRR_i. This is the most significant process parameter that affects MRR_i. Under certain circumstances, this also limits the maximum size of the abrasives to be used.

The effect of **abrasive grain size** is illustrated in Fig. 3.7. An increase in abrasive grain size results in higher MRR_i but poorer surface finish. Surface finish is also influenced by the parameters like amplitude of vibration, properties of the workpiece material, finish of the tool surface, and viscosity of the liquid carrier for the abrasives. Maximum MRR_i is achieved when abrasive grain size is comparable with the amplitude of vibration of the tool. Hardness of the abrasives and method of introducing slurry in the machining zone also affect the machining rates. **Frequency of vibration** also has a significant effect on MRR_i (Fig. 3.8). Efficient cutting is obtained at resonance frequency. Tool and tool holder combination having higher resonance frequency will yield higher MRR_i provided machining is done at the resonance frequency.

MRR_i goes down as the depth of the hole increases. It happens so because of inefficient flow of slurry through the cutting zone at high depth.

PROCESS CAPABILITIES

USM works satisfactorily only when workpiece hardness is greater than HRC 40 (hardness on Rockwell scale 'C'). It works very well if workpiece hardness is

greater than HRC 60. Materials (carbides, ceramics, tungsten, glass, etc.) that can't be easily machined by conventional methods can be easily machined by this technique.

Tolerances that can be achieved by this process range between $7\mu\text{m}$ and $25\mu\text{m}$. Holes as small as $76\mu\text{m}$ have been drilled. Hole depths up to 51 mm have been easily achieved while 152 mm deep holes have also been drilled by using special flushing technique. The aspect ratio of 40:1 has been achieved.

Linear material removal rate, MRR, (also known as penetration rate) achieved during USM ranges from 0.025 to 25.0 mm/min, and it depends upon various parameters. Surface finish achieved during the process varies from $0.25\mu\text{m}$ to $0.75\mu\text{m}$, and it is mainly governed by abrasive particle size. USM results in a **non-directional surface texture** compared to conventional grinding process.

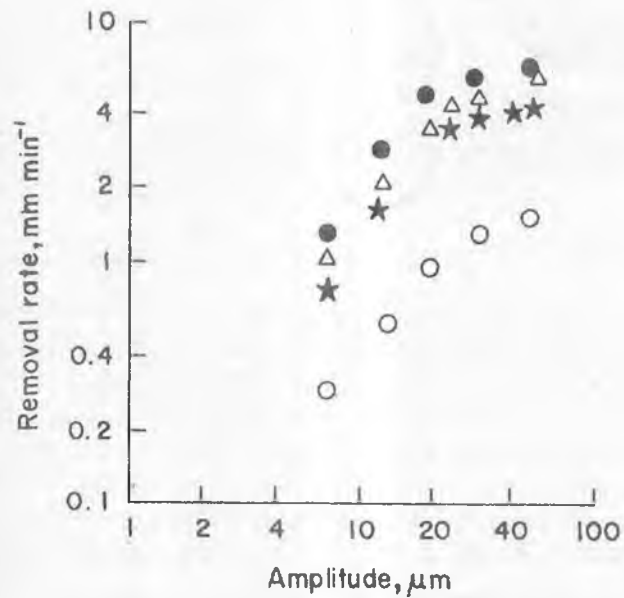


Fig. 3.6 Effects of amplitude of vibration on material removal rate during USM. Workpiece: glass; tool: steel; abrasive: B_4C (120 mesh size); pressure:
• 0.20 MPa; Δ 0.16 MPa; * 0.10 MPa; \circ 0.04 MPa. [Kremer et al., 1981].

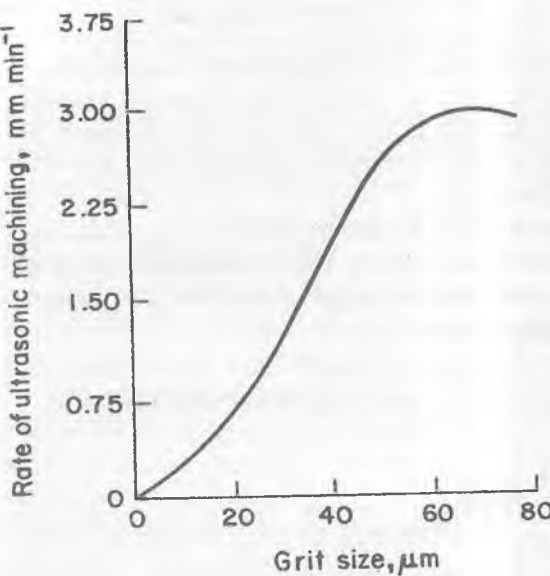


Fig. 3.7 Relationship between penetration rate and abrasive grain size [Kazantsev, 1956].

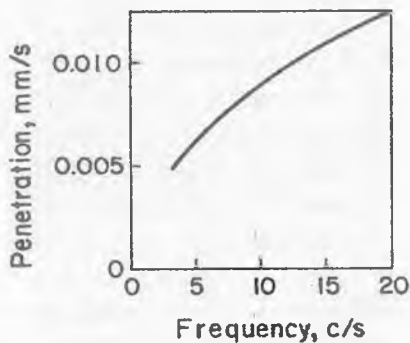


Fig. 3.8 Relationship between penetration rate and frequency of vibration of tool [Neppiras and Foskett, 1956].

Accuracy of the machined surface is governed by the size of the abrasive grains, tool wear, transverse vibration and machined depth. Usually overcut (the clearance between the tool and the workpiece) is used as a measure of accuracy.

Radial overcut may be as low as 1.5 to 4.0 times the mean abrasive grain size. Overcut also depends on the other parameters like workpiece material and method of tool feed. The overcut is not uniform along the machined depth and it results in the *conicity* in the machined cavity. Various means are suggested to reduce the conicity, viz. use of higher static load, direct injection of slurry into the machining zone, and use of a tool having negative taper.

Out-of-roundness is another criterion used to measure the accuracy of drilling cylindrical holes. Inaccurate setting of the tool during USM is the main source of lateral vibration which results in out-of-roundness in the cavity. Out-of-roundness depends on the type of workpiece material also.

APPLICATIONS

Most successful USM application is machining of cavities (or holes) in electrically non-conductive ceramics. It is quite successful in case of fragile components in which otherwise scrap rate is quite high. To increase productivity it is used to drill multiple number of holes at a time, viz. 930 holes each of radius equal to 0.32 mm [Benedict, 1987]. For this purpose hypodermic needles have been used as tools. USM has also been employed for multistep processing for fabricating silicon nitride (Si_3N_4) turbine blades.

PROBLEM

Find out the approximate time required to machine a hole of diameter equal to 6.0 mm in a tungsten carbide plate (fracture hardness = $6900 \text{ N/mm}^2 = 6.9 \times 10^9 \text{ N/m}^2$) of thickness equal to one and half times of hole diameter. The mean abrasive grain size is 0.015 mm diameter. The feed force is equal to 3.5 N. The amplitude of tool oscillation is 25 μm and the frequency is equal to 25 kHz. The tool material used is copper having fracture hardness equal to $1.5 \times 10^3 \text{ N/mm}^2$. The slurry contains one part abrasive to one part of water. Take the values of different constants as $K_1 = 0.3$, $K_2 = 1.8 \text{ mm}^2$, $K_3 = 0.6$, and abrasive density = 3.8 g/cm^3 .

Also calculate the ratio of the volume removed by throwing mechanism to the volume removed by hammering mechanism.

Solution

Following data are given:

Hole diam. = $6 \times 10^{-3} \text{ m}$, plate thickness = $1.5 \times \text{hole diam.} = 9 \times 10^{-3} \text{ m}$, mean abrasive grain size (d) = $1.5 \times 10^{-5} \text{ m}$, feed force (F) = 3.5 N, amplitude of tool

oscillation ($a/2$) = 25×10^{-6} m, frequency of oscillation (f) = 25000 cps, fracture hardness of workpiece material, σ_w (=H_w) = 6.9×10^9 N/m², fracture hardness of tool material (=H_t) = 1.5×10^9 N/m², abrasive grain density (ρ_a) = 3.8×10^3 kg/m³, $j = H_w/H_t = 4.6$, K₁ = 0.3, K₂ = $1.8 \text{ mm}^2 = 1.8 \times 10^{-6} \text{ m}^2$, K₃ = 0.6, C = 1.

The following procedure should be followed to solve the given problem:

What is the time required to machine the hole?

We know that the volume (V) of material removed during USM can be calculated using the following relationship:

$$V = K_1 K_2 K_3 \sqrt{\frac{h^3}{d}} \cdot f \quad \dots(3.5)$$

Step 1.

Calculate the value of "h" which is different for throwing model (h_{th}) and for hammering model (h_w).

Step 2.

After knowing the values of h_{th} and h_w, calculate V_{th} and V_w by substituting these values in above Eq. (3.5). Find total volume of material removed per unit time (V_s) by adding V_{th} and V_w.

Step 3.

Calculate the total amount of material to be removed to make the required hole. Divide it by V_s to find the total time required to make the hole.

Step 4.

Find the ratio of V_{th}/V_w.

Following the above steps, all calculations are made as follows.

Step 1.

In Eq. (3.5), except "h" all other parameters are known.

Let us calculate h_{th} as

$$h_{th} = \pi a f d \sqrt{\frac{\rho_a}{6\sigma_w}}$$

$$= \pi \times (50 \times 10^{-6}) \times (2.5 \times 10^4) \times (1.5 \times 10^{-5}) \times \sqrt{\frac{3.8 \times 10^3}{6 \times (6.9 \times 10^9)}}$$

$$h_{th} = 1.78 \times 10^{-5} \text{ mm}$$

Penetration (h_w) in the workpiece due to hammering is given as

$$h_w = \sqrt{\frac{4 F_{avg} ad}{\pi K_2 \sigma_w (j+1)}}$$

$$= \sqrt{\frac{4 \times 3.5 \times (2 \times 25 \times 10^{-6}) \times (1.5 \times 10^{-5})}{\pi \times (1.8 \times 10^{-6}) \times (6.9 \times 10^9) (1 + 4.6)}}$$

$$h_w = 2.192 \times 10^{-4} \text{ mm}$$

Step 2.

Now, volume removed by throwing (V_{th}) is given as

$$V_{th} = K_1 K_2 K_3 \sqrt{\frac{h_{th}^3}{d}} \cdot f$$

$$= 0.3 \times 1.8 \times 0.6 \sqrt{\frac{(1.78 \times 10^{-5})^3}{1.5 \times 10^{-2}}} \times 2.5 \times 10^4$$

$$V_{th} = 4.97 \times 10^{-3} \text{ mm}^3/\text{s}$$

Volume removed by hammering is given by

$$V_h = K_1 K_2 K_3 \sqrt{\frac{h_w^3}{d}} \cdot f$$

$$= 0.3 \times 1.8 \times 0.6 \sqrt{\frac{(2.192 \times 10^{-4})^3}{1.5 \times 10^{-2}}} \times 2.5 \times 10^4$$

$$V_h = 0.2146 \text{ mm}^3/\text{s}$$

Step 3.

$$\begin{aligned}\text{Time required to drill a hole} &= \frac{\text{Volume of the hole to be drilled}}{\text{Volumetric MRR } (= V_h + V_{th})} \\ &= \frac{(\pi/4) \times 6^2 \times 9}{0.21987}\end{aligned}$$

$$= 19.289 \text{ min}$$

Step 4.

$$\text{Ratio, } \frac{V_{th}}{V_h} = \frac{0.00497}{0.2146}$$

$$= 0.023$$

Thus, it is evident that the material removed by hammering is much more than by throwing (approximately 43 times). Hence, for approximate calculations, V_{th} can be ignored as compared to V_h .

BIBLIOGRAPHY

1. Bellows G. and Kohls, J.B. (1982), Drilling Without Drills, *American Special Report*, 743, p. 187.
2. Benedict G.F. (1987), *Nontraditional Manufacturing Processes*, Marcel Dekker Inc., New York.
3. Bhattacharyya A. (1973), *New Technology*, The Institution of Engineers (I), Calcutta.

4. Kainth G.S., Nandy A. and Singh K. (1979), On the Mechanics of Material Removal in Ultrasonic Machining, *Int. J. Mach. Tool Des. Res.*, Vol. 19, pp. 33-41.
5. Kaczmarek J. (1976), Principles of Machining by Cutting Abrasion and Erosion, Peter Peregrinus Ltd., Stevenage, pp. 448–462.
6. Kazantsev V.F. and Rosenberg L.D. (1965), The Mechanism of Ultrasonic Cutting, *Ultrasonics*, Vol. 3, p. 166.
7. Kennedy D.C. and Grieve R.J. (Sept. 1975), Ultrasonic Machining: A Review, *Prod. Eng.*, Vol. 54, pp. 481-486.
8. Kremer D. *et al.* (1981), The State of the Art of Ultrasonic Machining, *Annls CIRP*, Vol. 30(1), pp. 107-110.
9. Markov A.I. *et al.* (1977), Ultrasonic Drilling and Milling of Hard Non-Metallic Materials with Diamond Tools, *Mach. Tooling*, Vol. 48(9), pp. 33-35.
10. McGeough J.A. (1988), *Advanced Methods of Machining*, Chapman & Hall, London.
11. Miller G.E. (1957), Special Theory of Ultrasonic Machining, *J. Appl. Phys.*, Vol. 28(2), p. 149.
12. Neppiras E.A. and Foskett R.D. (1956-57), Ultrasonic Machining, Philips Technical Review, Vol. 18, pp. 325, 368.
13. Pandey P.C. and Shan H.S. (1980), *Modern Machining Processes*, Tata McGraw Hill, New Delhi.
14. Shaw M.C. (1956), Ultrasonic Grinding, *Microtecnic*, Vol. 10, p. 257.
15. Soundararajan V. and Radhakrishnan V. (1986), An Experimental Investigation on Basic Mechanism Involved in Ultrasonic Machining, *Int J. Mach. Tool Des. Res.*, Vol. 26(3), pp. 307-332.

REVIEW QUESTIONS

Q1. Write True (T) or False (F)

- (i) In USM, for the same static load but higher tool diameter penetration rate is higher.
- (ii) Audible frequency would give higher MRR than ultrasonic frequency.
- (iii) Magnetostrictive transducers are made up of laminated construction.
- (iv) The ratio of MRR to tool wear rate can be as low as 0.5 in case of USM using WC as work material and alumina as abrasive material.

Q2. Multiple Choice Questions:

- (i) During calculation of MRR for USM (using Shaw's throwing model), the abrasive density by mistake has been used as 2 units in place of 3 units. Calculate the ratio of MRR with actual density and wrong density.
(a) 1.71; (b) 1.36; (c) 0.74; (d) none.
- (ii) In USM, the frequency of oscillation is
(a) 10-15 kHz; (b) below 10 kHz; (c) above 15 kHz; (d) none of these.
- (iii) Lowering the temperature of the workpiece during USM would result in:
(a) increased MRR_v ; (b) decreased MRR_v ; (c) no effect on MRR_v ; (d) unpredictable.
- (iv) Performance of USM process is better in case of:
(a) electrically conductive work material; (b) work material having high thermal conductivity; (c) soft material; (d) no such constraint.
- (v) The number of impacts (in USM) on the workpiece is
(a) directly proportional to the square of the diameter of the grit; (b) inversely proportional to the grit diameter; (c) inversely proportional to the square of the grit diameter; (d) none of these.
- (vi) Volume of material removal in USM is
(a) directly proportional to frequency 'f'; (b) inversely proportional to 'f'; (c) none of these two.
- (vii) Relationship between MRR_v and grain size shows
(a) monotonously increasing trend; (b) monotonously decreasing trend; (c) a maxima; (d) a minima.
- (viii) During USM, abrasive mean diameter size is increased from 2 units to 3 units while workpiece hardness is increased to 2.25 times. What will be the ratio of new depth of penetration to the old depth of penetration?
(a) 0.33; (b) 3.00; (c) 1.00; (d) none of these.

Q3. Write short notes on the following

- (i) Transducers used in USM machine.
- (ii) Effect of amplitude of vibration, frequency of vibration, grain size, and % of abrasive concentration, on MRR in USM.
- (iii) Possible effects of use of audible frequency in USM.
- (iv) Functions of slurry, horn, transducer, and oscillator in USM.
- (v) Types of abrasives used in USM.

- (vi) Conventional grinding and USM.
- (vii) Working principle of USM (show the necessary sketch)
- Q4. (i) What do you understand by “transducer” and “magnetostriction effects”?
- (ii) Explain the functions of a “horn” in USM.
- (iii) Draw the relationship observed during USM for the following cases:
 (a) frequency vs penetration rate; (b) grain size vs machining rate; (c) concentration vs machining rate; (d) ratio of workpiece hardness to tool material hardness vs MRR.
- (iv) A cylindrical impression of 10 mm diameter and 1 mm deep is to be made on a WC specimen. Feed force is constant, and is equal to 5 N. Average diameter of grains in the slurry is 10 μm . Tool oscillates with the amplitude of 30 μm at 20 kHz. Abrasive and water ratio in the slurry is 1. Fracture hardness of WC workpiece may be taken as 7000 N/mm² and that of copper tool as 1500 N/mm². Calculate the time required to complete the job if only 20% of pulses are effective. Assume $K_1 = 0.3$, $K_2 = 1.8 = \text{mm}^2$ and $K_3 = 0.6$. Make the assumptions if necessary.
- (v) Write the four basic mechanisms by which material removal in USM can take place.
- (vi) Derive an equation suggested by Shaw to obtain volumetric material removal rate (consider both throwing and hammering mechanisms).
- (vii) USM is used for drilling a hole (under the same machining conditions) in aluminium and C.I. Which one will have higher depth of the drilled hole?

NOMENCLATURE

$a/2$	Amplitude of vibration
A	Area
$d (=2R)$	Abrasive diameter
E_m	Coefficient of magnetostriktor elongation
f	Frequency of vibration of tool
F	Force
h	Crater height
h_d	Abrasive penetration depth in the tool
h_w	Abrasive penetration depth in the workpiece
j	Ratio of hardness of workpiece material to that of the tool material

KE	Kinetic energy
K_1, K_2	Constants
K_3	Probability of an abrasive particle under the tool being effective
L	Length of the magnetostrictor coil
ΔL	Change in length of the magnetostrictor coil
m	Mass of a grit
N	Number of impacts on the workpiece by the grits in each cycle
r	Crater radius
t	Time
T	Cycle time
ΔT	Small time period
USM	Ultrasonic machining
V_c	Amount of material removed per cycle
V_s	Volume of material removed per second
V_g	Volume of material removed per grit per cycle
V_h	Volumetric MRR from the workpiece due to hammering mechanism
V_{th}	Volumetric MRR from the workpiece due to throwing mechanism
W_g	Work done by the grit
Y	Displacement of the tool
\dot{Y}_{max}	Maximum velocity of the tool
ρ_a	Density of abrasive particles
σ_w	Mean stress acting on the workpiece surface
σ_{tl}	Mean stress acting on the tool surface

Suffix

a	abrasive
avg	average
h	hammering
max	maximum
t	total
th	throwing
tl	tool
w	workpiece

CHAPTER 3
AT-A-GLANCE
ULTRASONIC MACHINING
(USM)

WHAT IS ULTRASONIC ?

- * VIBRATORY WAVES HAVING FREQUENCY GREATER THAN THE UPPER FREQUENCY LIMIT (~ 16 kHz) OF THE HUMAN EAR

WAVES

- * LONGITUDINAL WAVES
 - USED IN ULTRASONICS
 - EASILY PROPAGATE IN SOLIDS, LIQUIDS, & GASES
- * SHEAR WAVES

LONGITUDINAL
MAGNETOSTRICTION

- * IF A FERROMAGNETIC MATERIAL IS PLACED IN CONTINUOUSLY CHANGING MAGNETIC FIELD



IT RESULTS IN A CHANGE IN LENGTH OF TRANSDUCER



MAGNETOSTRICTION TYPE TRANSDUCER

ULTRASONIC
TRANSDUCER

- * CONVERTS ANY FORM OF ENERGY INTO ULTRASONIC WAVES

WORKING OF USM SYSTEM



AC POWER
SUPPLY



US WAVES
GENERATOR



US
TRANSDUCER



TOOL
CONNECTOR



K E AND / OR HAMMERING
ACTION ERODES W/P



THOUSANDS OF
CRATERS ON W/P

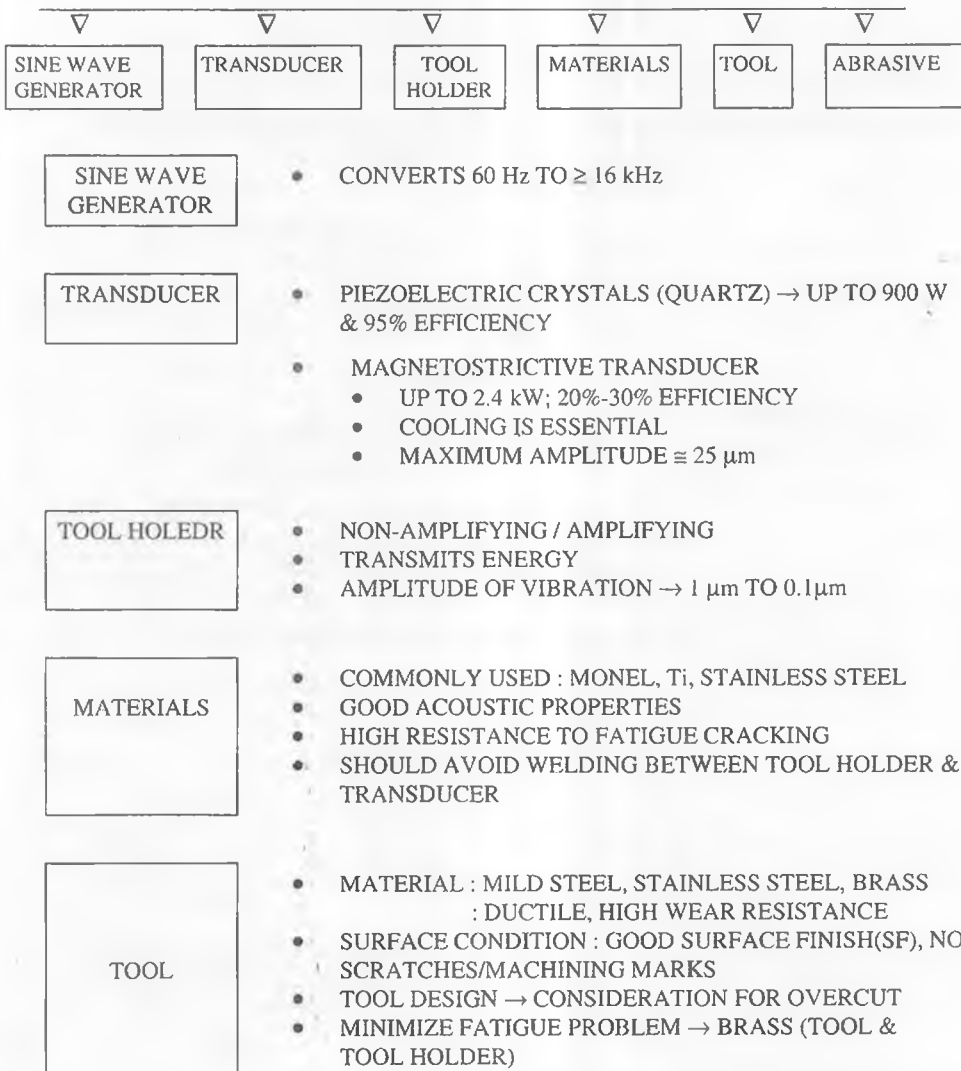


FINISHED
COMPONENT



TOOL

SOME ELEMENTS OF USM SYSTEMS



ABRASIVE

- Al_2O_3 , SiC, BORON CARBIDE
- ABRASIVE HARDNESS > W/P HARDNESS
- SELECTION CRITERIA : HARDNESS, SIZE, LIFE & COST
- LOW CONCENTRATION : DEEP HOLE DRILLING,
COMPLEX CAVITIES, ETC.
- PROCESS PERFORMANCE (MRR & SF) → GRAIN MESH
SIZE (240 - 800)

PARAMETRIC ANALYSIS

- AMPLITUDE OF VIBRATION & PENETRATION RATE
- FREQUENCY OF VIBRATION & PENETRATION RATE
- ABRASIVE GRAIN SIZE & PENETRATION RATE

PROCESS CAPABILITIES

WORK MATERIAL

- WORKS BETTER FOR HARDNESS > HRC 40
- CARBIDE, CERAMICS, W, GLASS, ETC

SURFACE FINISH

- 0.25 TO 0.75 μm

ACCURACY

- CONICITY IN THE DRILLED HOLE
 - TO REDUCE CONICITY → NEGATIVE TAPER AND HIGHER STATIC LOAD
- OUT-OF-ROUNDNESS CRITERION (IN HOLES)
- TOLERANCE : 7-25 μm
 - DEPTH 51 mm. EVEN UP TO 152 mm.
 - ASPECT RATIO (DEPTH TO DIAMETER) = 40 : 1

PROCESS APPLICATIONS

- BOTH ELECTRICALLY NON-CONDUCTIVE & CONDUCTIVE
- FRAGILE COMPONENTS
- ALSO FOR MULTIPLE HOLES
- PROCESSING OF SILICON NITRIDE TURBINE BLADES
- GLASS, CERAMICS, TITANIUM, TUNGSTEN, ETC
- DRILLING (DENTIST DRILLING HOLE IN TEETH), GRINDING, PROFILING
- USM ALSO USED IN CONJUNCTION WITH ECM, EDM.

ABRASIVE FINISHING PROCESSES

The need for high accuracy and high efficiency machining of difficult-to-machine materials is making the application of abrasive finishing technologies increasingly important. The most labour intensive, uncontrollable area in the manufacture of precision parts involves final machining (or finishing) operations. The cost of surface finish increases sharply for a roughness value of less than one micron. The result of high quality finish on the parts is improved performance, and considerable increase in the length of life of the component.

The basic idea of abrasive fine finishing processes is to use a large number of random cutting edges with indefinite orientation and geometry for effective removal of material with chip sizes smaller than those obtained during machining using cutting tools with defined edges. Because of extremely thin chips produced

in abrasive machining, it allows better surface finish, closer tolerances, generation of more intricate surface features, and machining of harder and difficult-to-machine materials [Subramanian, 1994]. The capabilities of four important fine finishing process, are compared in Table-4.1 [Jain and Jain, 1998]. Lapping and honing are the two important but well known processes while the other two—magnetic abrasive finishing (MAF) and abrasive flow machining (AFM)—are the new ones. This chapter deals with AFM and MAF processes only.

Table-4.1 Comparison of four finishing processes [Jain and Jain, 1998]

Sl.No.	Process features	Lapping	Honing	MAF	AFM
1.	Surface finish ($\mu\text{ m}$)	0.025–0.1	0.025–0.5	0.04–1.0	0.05–1.0
2.	Dimensional tolerance ($\mu\text{ m}$)	0.5	0.5–1.25	0.5	5.0
3.	Material removal (mm)	< 0.0025	0.061–0.183	0.002–0.007	0.008–0.010
4.	Pressure	0.01–0.2 N/sq. mm	1–3 N/sq.mm	0–0.007 kPa	0.69–22.0 MPa
5.	Abrasive product type	Abrasive grain entrained in a liquid vehicle	Bonded abrasives	Magnetic abrasives composed of ferromagnetic particles and conventional abrasive grits	Semisolid abrasive media composed of viscoelastic carrier and abrasive grits
6.	Work surface configuration	Flat, cylindrical, and spherical surfaces	Cylindrical surfaces	Flat and cylindrical surface	Inaccessible areas and complex internal passages

(A) ABRASIVE FLOW FINISHING (AFF)

WORKING PRINCIPLE

Developments in the area of materials science are taking place at a fast rate; at

the same time demand for better quality and lower cost products is also increasing. There is a consistent demand for a decreased lead time from design to production. Further, finishing operations usually cost approximately 15% of the total machining cost [Rhoades, 1988] in a production cycle. In view of this, a need of automated finishing operations to substitute manual finishing operations is felt. To meet such requirements a non-traditional finishing process named as **abrasive flow machining (AFM)** has been developed. It seems to have a potential to offer better accuracy, and higher efficiency, economy and consistency.

Abrasives flow machining is a kind of finishing process in which a small quantity of material is removed by flowing a semisolid abrasive laden putty over the surface to be finished. The media has such a high viscosity that it can be held between fingers (Fig. 4.1) like a rubber ball which can be deformed by applying a little pressure. Two vertically opposed cylinders (Fig. 4.2) extrude abrasive media back and forth through passage(s) formed either by workpiece and tooling, or by

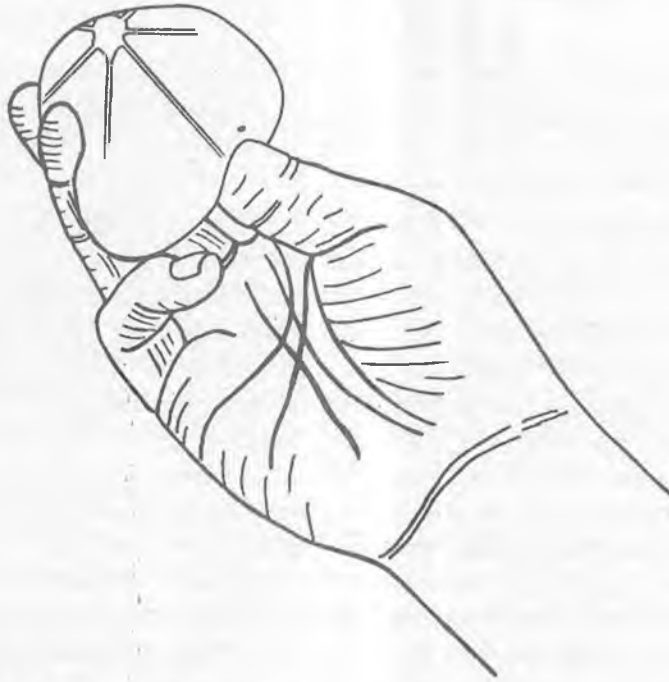


Fig. 4.1 Media held between fingers.

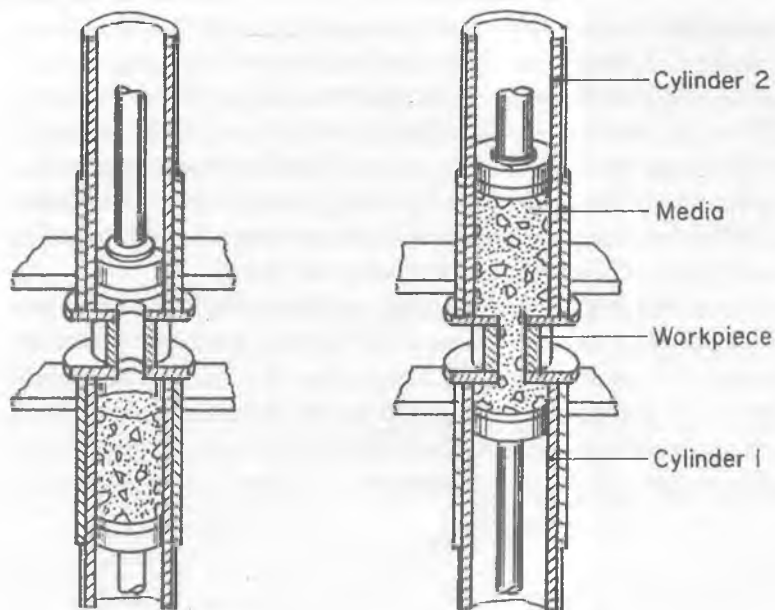


Fig. 4.2 Schematic diagram of abrasive flow machining of a hole to explain its working principle

workpiece alone. This process is good for operations like deburring, radiusing, polishing, removing recast layer, producing compressive residual stresses, etc. The process can be employed to machine tens of parts at the same time to enhance productivity. This has a high flexibility, i.e., the same machine can be used to do a variety of jobs by changing toolings, machining parameters, media and abrasives.

The semisolid abrasive media is forced through the workpiece or through the restrictive passage formed by workpiece and tooling together. Force may be applied hydraulically or mechanically. Velocity of media is governed by cross-sectional area of passageways. More the restriction offered by the passageway, larger is the force required. Abrasive particles act as cutting tools; hence it is a **multi-point cutting process** giving very low MRR. It is employed both for metals and non-metals. It is equally suitable for workpieces which contain passageways that are *not accessible* (Fig. 4.3) for conventional deburring and polishing tools.

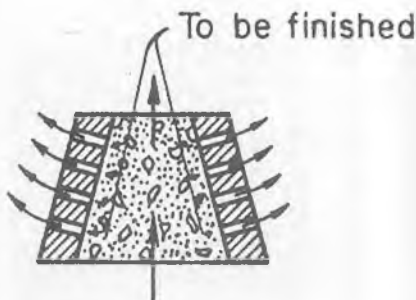


Fig. 4.3 Deburring/finishing of inaccessible holes using AFM process.

ABRASIVE FLOW MACHINING (AFM) SYSTEM

It consists of three elements, viz., machine, tooling, and media.

(i) Machine

Machine having two cylinders and abrasive media controls the *extrusion pressure* and flow volume. The media is extruded (or forced) back and forth from one cylinder to another with the help of a hydraulic ram. These cylinders/chambers are clamped together with the workpiece sandwiched between them. The enclosed workpiece area through which the media is forced, is called the **extrusion passage**. The media extruding pressure ranges from 0.70 to 22 MPa. To maintain a constant media viscosity, in some applications, coolers for lowering the temperature of the media are also used. Manual or computer control machines are available [*Extrude Hone*]. The controllable variables are volume of media, no. of stroke, number of cycles and pressure. Fig. 4.4 shows a schematic diagram and labelled photograph of an AFM system [Sunil Jha, 1998].

(ii) Tooling

Tooling is that element of an AFM system which is used to confine and direct the flow of media to the appropriate areas (Fig. 4.5(d)). Basic principle of tooling design in AFM system is to selectively permit or block the flow of media into or out of workpiece passages where deburring, radiusing, and surface improvements are desired. *Tooling* for AFM machine is designed with two aims:

- to hold the parts in position, and
- to contain the media and direct its flow.

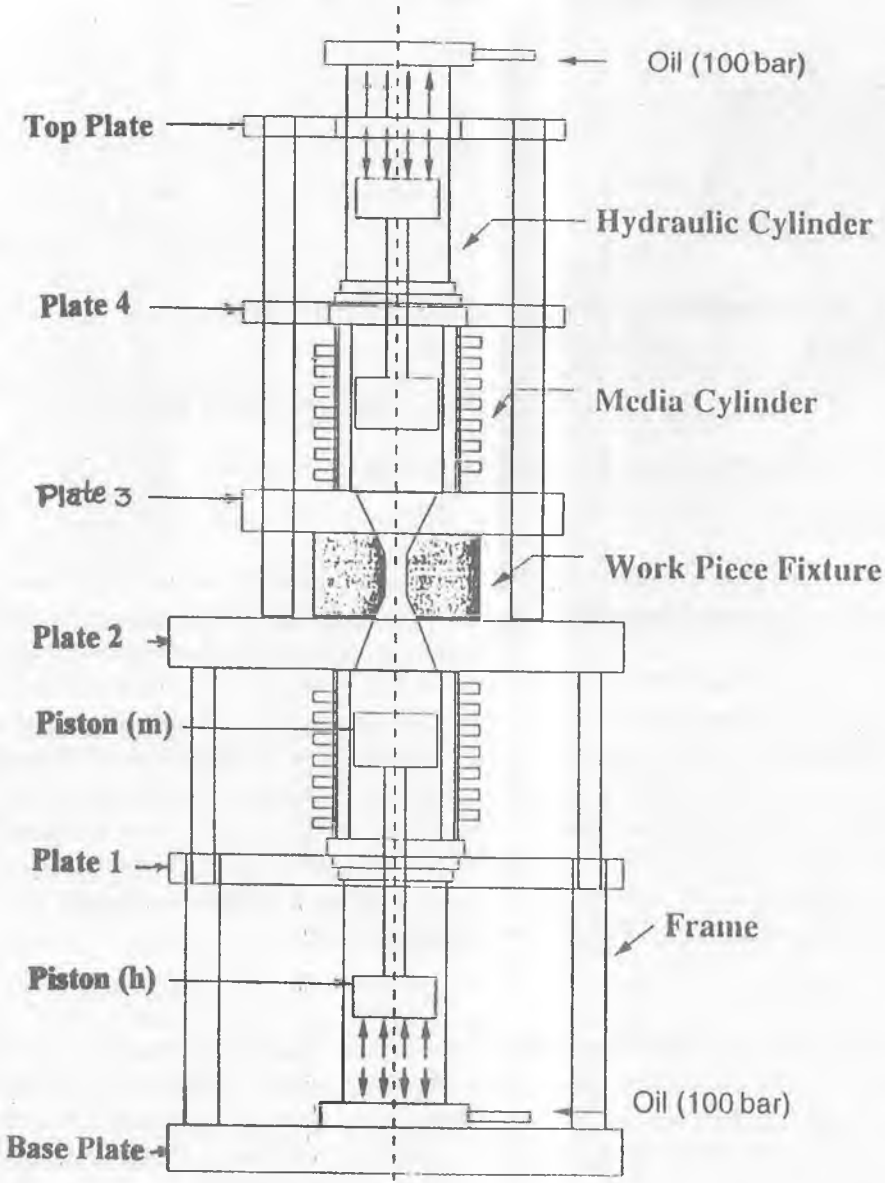


Fig. 4.4a Schematic diagram of abrasive flow machining setup [Sunil Jha, 1998].

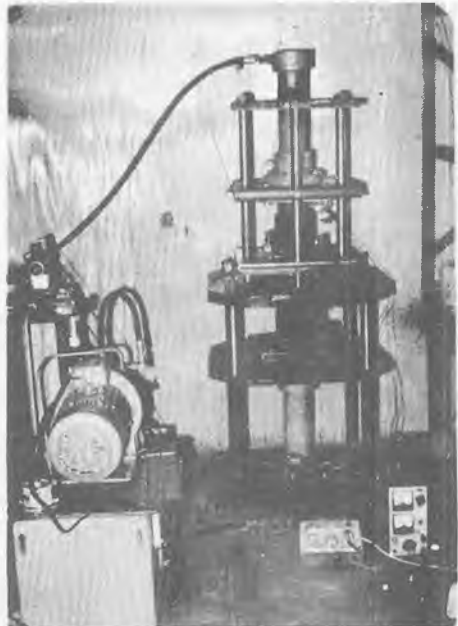
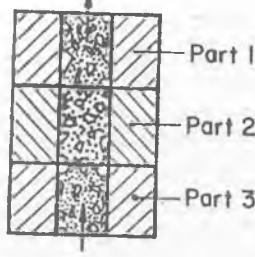


Fig. 4.4b Photograph showing abrasive flow machining setup [Sunil Jha, 1998].

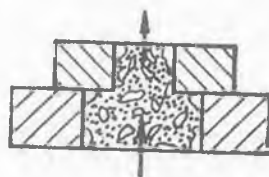
Maximum machining takes place wherever there is a maximum restriction to the flow of abrasive. While machining **internal surfaces** like bore of a shaft, configuration of the bore itself decides the extent of restriction present to the flow of media. Figs. 4.5a, 4.5b and 4.5c show finishing of internal surfaces. In case of **external surfaces**, the designer of tooling decides the extent of restriction to be imposed (Figs. 4.5d and 4.5e). In case of polishing of spur gear teeth, diameter of a cylinder placed around the gear teeth determines the **extent of restriction** present for the flow of media (Fig. 4.5d).

Passages of similar nature can be *processed in parallel* (Fig. 4.5a). In case of a non-uniform cross-section, MRR of narrowest section will be maximum and that of widest section will be minimum (Fig. 4.5b). Replaceable inserts made of nylon, teflon, or similar other materials are used for restricting flow of media to induce abrasive action. Once these inserts are worn out, they are replaced by new ones. Life of such inserts may be in terms of thousands of parts if they are properly designed.



(a)

Fig. 4.5a Finishing of multiple parts having the same configuration.



(b)

Fig. 4.5b Finishing of two parts but with different configurations.

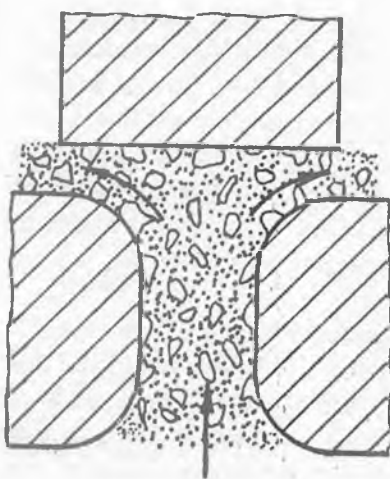


Fig. 4.5c Finishing and radiusing of an internal hole.

(iii) Media

Characteristics of media determine aggressiveness of action of abrasives during AFM process. AFM media is pliable (easily moulded, Fig. 4.1) material which is resilient enough to act as a self *deforming grinding stone* (Fig. 4.6) when forced through a passageway [Rhoades, 1988]. It consists of base material and abrasive grits. The base material (**viscoplastic/viscoelastic material**) is made up of an organic polymer, and hydrocarbon gel. Composition of the base material determines its degree of stiffness. The *stiffest media* is used for largest hole, while *soft media* is used for small holes. High stiffness of the media results in a kind of pure extrusion while soft media will lead to a faster flow in the centre than along walls. It is reported that a more stiff media finishes a passageway more uniformly while a less stiff media results in a greater radius at the passage opening [Williams, 1989].

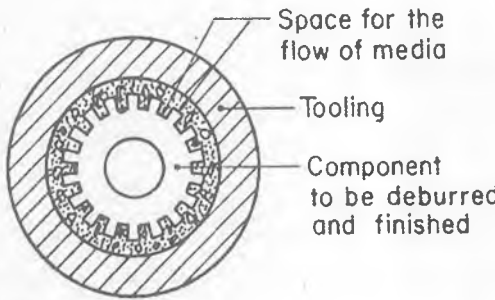


Fig. 4.5d Tooling for deburring and finishing of a gear using AFM process.

When the abrasive grains laden media comes in contact with the workpiece surface to be machined, the abrasive grains are held tightly in place and the media acts as a **deformable grinding stone**. Fig. 4.6 shows that how the same media takes different shapes depending upon configuration of the workpiece to be finished. Hundreds of holes in a combustion liner can be sized to a tolerance of hundredth of a millimetre. **Types of abrasives** used are Al_2O_3 , SiC , cubic boron nitride (CBN) and diamond (written in the order of their increasing hardness and cost). These abrasives are available in different grit sizes. The abrasives have limited life. As a thumb rule, when the media has machined an amount equal to 10% of its weight, it must be discarded. To assure a *proper mixing* of a new batch

of media and abrasive, it should be cycled 20-50 times through a scrap part. Machined parts should be properly cleaned before use, by air or vacuum.

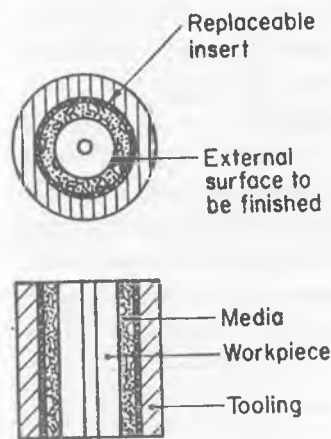


Fig. 4.5e Tooling for external surface to be finished.

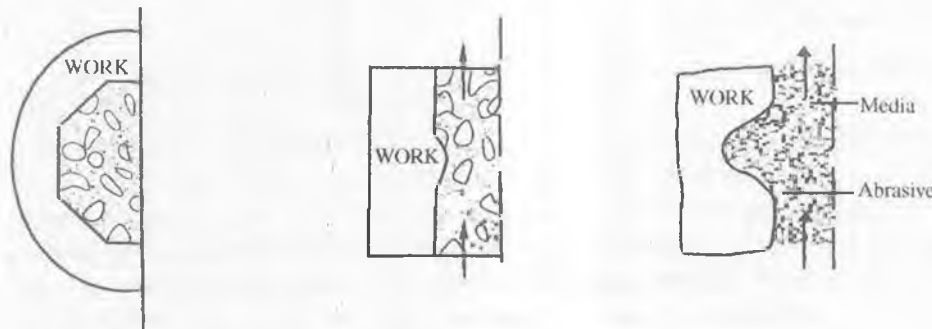


Fig. 4.6 Media acting as a 'self-deformable stone'.

PROCESS VARIABLES

Abrasive flow machining process is in its *infancy*. Mechanism of the process, parametric relationships, surface integrity, and other related issues are yet to be effectively addressed. The discussion under this section is based on very limited experimental results reported by researchers [Williams, (1989); Williams and Rajurkar (1989); and Williams, Rajurkar and Rhoades (1989)].

Important factors that affect performance of the process and the product quality (viz, accuracy, MRR, and surface integrity), are shown in Fig. 4.7. They are workpiece material (hardness and composition), machine and tooling (fixture design, cylinder size, clamping pressure, etc), adjustable parameters (pressure, number of cycles, etc), geometry of the component(s) (passage shape, length to diameter ratio, length of flow path, etc), and media (viscosity and its change during the process, volume flow rate, and abrasive-type, -size, and -concentration).

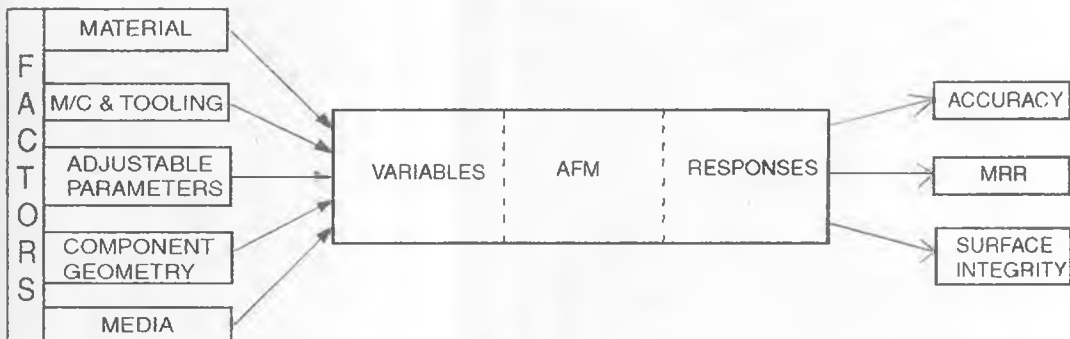


Fig. 4.7 Variables and responses of AFM process.

Williams and others [1989] have conducted experiments to evaluate the effects of viscosity, pressure and flow rate of media on MRR, surface finish, and surface integrity. They have also attempted to stochastically model and analyze the machined surface profile for understanding the mechanics of surface generation during AFM. Experiments were carried out on sleeve type parts made of AISI 4140. Some experiments were planned based on *full factorial design* while others were done as *one variable at a time* approach.

In the absence of actual values of viscosity, three viscosity levels were chosen

[Williams and co-workers, 1989] as low (LV), medium (MV), and medium high (MHV) viscosity. Pressure levels chosen were 500, 1000 and 1500 psi. Work-pieces were run for 10 cycles with a media flow volume of 70 in³/stroke. Concentration of abrasives in the media was 66%. Linear **material removal** was measured. To minimize the effect of time error variability, the trials were randomized. Fig. 4.8a shows the *effect of workpiece material* on material removal. Fig. 4.8b shows the effect of viscosity on linear material removal (in inches). It was concluded based on statistical tests that there was a significant difference between LV, and MV as well as LV, and MHV but insignificant difference between MV and MHV. Fig. 4.8c shows the *effect of pressure* on mean metal removal (in inches). At 1500 psi, there is hardly any improvement in MR as compared to 1000 psi.

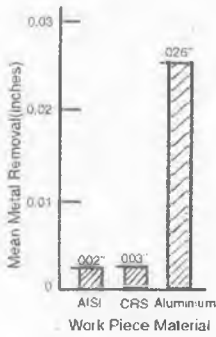


Fig. 4.8(a)

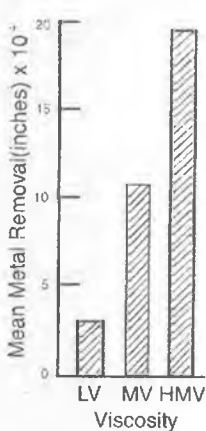


Fig. 4.8(b)

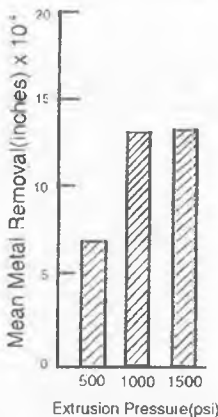


Fig. 4.8(c)

Fig. 4.8 Effect of (a) workpiece material, (b) viscosity, (c) pressure, on mean material removal during AFM. [Williams and others, 1989].

Figs. 4.9a and 4.9b show the *effect of viscosity and pressure*, respectively on mean final **surface roughness**. It was also concluded that the *effect of flow rate* on material removal is insignificant.

Scanning electron micrographs (SEM) of some specimens after abrasive flow

finishing were taken. Some of the photographs taken during experimentation at $1600 \times$ magnification are shown in Fig. 4.10. Fig. 4.10a shows the photograph of original specimen having rough surface with many tears present. It is evident from Figs. 4.10b-4.10d [Williams and others, 1989] that major changes in surface finish take place just after a few cycles. Number of cycles required to achieve the desired surface finish depends on the values of the variables set, and the difference between the initial and final surface finish.

ANALYSIS AND MODELLING OF ABRASIVE FLOW MACHINED (AFM'd) SURFACES

Profiles of AFM'd surfaces are unidirectional and random in nature, and have been modeled by stochastic modeling and analysis technique (called data dependent system - DDS) [Williams and Rajurkar, 1992; Pandit and Wu, 1983]. It gives differential/difference equation model using the raw data. This fits ARMA (n, n-1) models using non-linear least square method till the residual sum of squares of random disturbances is significantly reduced as determined by F-test criterion. Surface roughness profiles of AFM'd surfaces are digitized and analyzed using data acquisition software. A typical ARMA (2,1) model for the surface profiles generated during AFM (Fig. 4.11), is as follows:

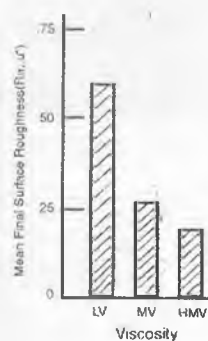


Fig. 4.9(a)

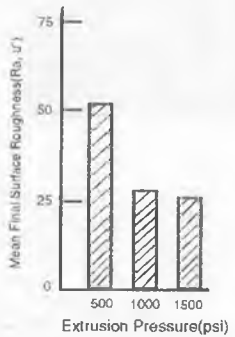
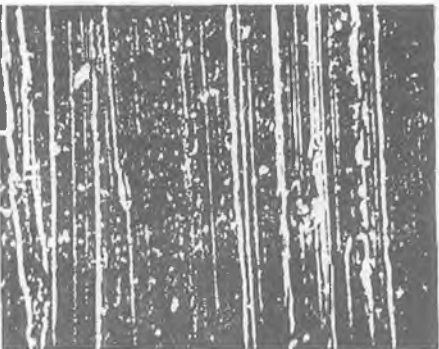


Fig. 4.9(b)

Fig. 4.9 Effect of (a) viscosity, (b) pressure, on mean final surface roughness [Williams and others, 1989].



(a) Bored Part Before AFM



(b) AFM for 5 Cycles



(c) AFM for 10 Cycles



(d) AFM for 15 Cycles

Fig. 4.10 Scanning electron micrographs showing the effect of number of cycles (media: MV-36, pressure: 1000 psi) [Williams and others, 1989].

$$X_t - 1.883 X_{t-1} + 0.911 X_{t-2} = a_t + 0.045 a_{t-1} \quad \dots(4.1)$$

where X_t , X_{t-1} and X_{t-2} are heights of the machined surface profiles, a_t and a_{t-1} are random disturbances (or noise), and t , $t-1$ and $t-2$ (subscripts) indicate distances.

This technique has also been used to compare peak to valley profile height (R_{\max}) with center line average (CLA) roughness (R_a). The computed and experimentally obtained values from profilometer are found to compare favourably.

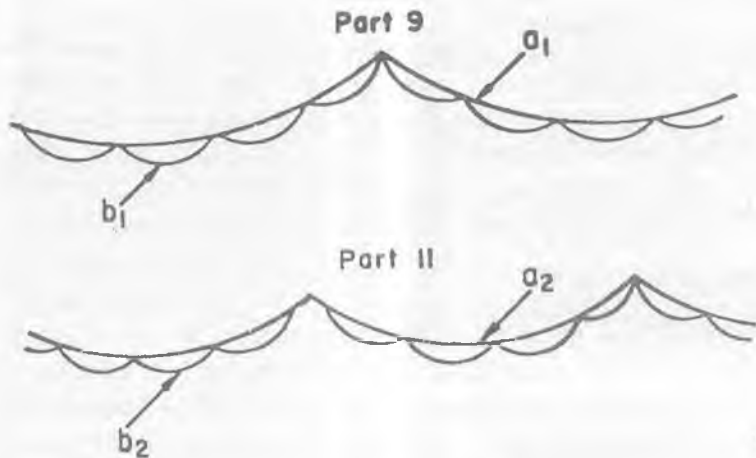


Fig. 4.11 A typical ARMA model (2, 1) for the surface profiles generated during AFM [Williams and Rajurkar, 1992].

Wavelength decomposition results have been explained based on the viscosity of the media. Higher viscosity restricts the freedom of movement and orientation of the grains. As a result, even the dull grains continue to cut the material and hence lower surface roughness. On the other hand, lower viscosity allows a continuous rapid change of position and orientation. It results in higher pseudo frequency and higher surface roughness.

Number of Active Grains

For consistency and accuracy of the process, number of dynamically active grains (C_d) is required. Using the frequency decomposition data, C_d can be evaluated as

$$C_d = \frac{\text{Frequency} \times \text{Time for one stroke}}{\text{Cross-sectional area of extrusion passage}} \quad \dots(4.2)$$

With the passage of time more number of grains would fracture resulting in larger number of grains but smaller in size. It is conjectured that after the critical number of strokes, the value of C_d will go down sharply. It is analogous to wheel loading in grinding process demanding dressing.

Wear of Abrasive Grains

As the time for the use of abrasives increases they undergo wear due to attritious wear phenomenon resulting in dull cutting edges. This yields increased wavelength (primary) of the surface profile. This would also tell about the extent of wear of grains [Pandit and Sathyaranayanan, 1981, 1985]. Decision regarding when to replace the media is usually based either on the operator's experience, or at the instant when it is found that the parts are being machined out of tolerance.

PROCESS PERFORMANCE

AFM has produced surface finish as good as $0.05 \mu\text{m}$ ($= 50 \text{ nm}$). Surface irregularities like deep scratches, large bumps, out-of-roundness, and taper can't be corrected by this process because it machines all surfaces almost equally. A minimum limit on the hole size that can be machined / deburred properly is 0.22 mm and the largest size (or diameter) that has been machined is around 1000 mm. It can produce dimensional tolerance as good as $\pm 0.005 \text{ mm}$ ($\pm 5 \mu\text{m}$).

APPLICATIONS

AFM is *suitable to automate* finishing operations that ask for high cost and which are labour intensive, and can be performed manually. It is very useful for finishing of extrusion dies, nozzle of flame cutting torch, and airfoil surfaces of impellers; deburring of aircraft valve bodies and spools; removing recast layer after EDM, etc. It is also employed for finishing operations, specially in the industries related to the manufacture of aerospace, automotive, semiconductor, and medical components. Some of the specific examples are given in the following:

Aerospace:

1. Conditions of the airfoil surface (compressors and turbines) are improved. Such surfaces are made by ECM, EDM, casting (say, investment castings), or milling. For finishing of such surfaces, this process *easily works even in inaccessible areas*.
2. Removal of thermal recast layers left by EDM, or laser beam machining.
3. Accessory parts like fuel spray nozzles, fuel control bodies, and bearing components are finished.

4. Resistance offered to the flow of air by blades, nozzles, diffusers, etc can be adjusted or tuned accurately by modifying surface using AFM process.
5. AFM improves the mechanical *fatigue* strength of blades, disks, hubs, shafts, etc.
6. AFM is also employed for removing coke and carbon deposits, and to improve surface integrity.
7. It can also be employed to remove left out light machining marks. The surface finish can be improved from say $1.75 \mu\text{m}$ to $0.4 \mu\text{m}$.
8. Both radiusing and deburring of cooling turbine blades are done in one pass by AFM.

Dies and Moulds:

1. Multiple passages can be processed at one time.
2. Surface finish can be improved to a large extent with least change in dimension.
3. It saves considerable time when compared with finishing by skilled hands. Jobs demanding hours for polishing can be completed in minutes automatically.
4. Finishing of two-stroke cylinders and four-stroke engine heads is done using AFM for improved air flow and better performance. Stainless steel impeller made by investment casting is polished to $0.37 \mu\text{m}$ using this process.

Precise edge finishing of gears, and deburring, radiusing and polishing of fuel injector components at the rate as high as 30 components per minute in a single fixture can be done by AFM. Uniform finishing of threaded holes is also one of the common applications of this process.

BIBLIOGRAPHY

1. Benedict G.F. (1987), *Nontraditional Manufacturing Processes*, Marcel Dekker Inc., New York, pp. 53-65.
2. Extrude Hone Technical Pamphlet, U.S.A.
3. Jha Sunil (1998), *On the Abrasive Flow Machining Process Performance*, M. Tech. Thesis, I.I.T. Kanpur, India.

4. Kohut T. (1984), Automatic Die Polishing: Extrusion Productivity Through Automation, *The Aluminium Association*, Washington D.C., Vol. 1, pp. 193-202.
5. Kohut T. (1988), Surface Finishing with Abrasive Flow Machining, Proc. 4th Int. Aluminium Extrusion Technology Seminar, Vol. 2, The Aluminium Association, Washington D.C.
6. Przyklen K. (1986), Abrasive Flow Machining—A Process for Surface Finishing and Deburring of Workpieces, with a Complicated Shape by Means of Abrasive Laden Medium, In '*Advances in Nontraditional Machining*', PED, Vol. 22., ASME, New York, pp. 101–110 (Ed.: Rajurkar K.P.).
7. Pandit S.M. and Sathyaranarayanan G. (1981), A New Approach to the Analysis of Wheel Workpiece Interaction in Surface Grinding, Proc. 9th North American Manufacturing Research Conference, pp. 311–320.
8. Pandit S.M. and Wu S.M. (1983). *Time Series and System Analysis with Applications*, John Wiley, New York.
9. Rhoades L.J. (1988), Abrasive Flow Machining, *Manuf. Eng.*, pp. 75-78.
10. Sathyaranarayanan G. and Pandit S.M. (1985), Fracture and Attritious Wear Rates in Grinding by Data Dependent System, Proc. 13th North American Manufacturing Research Conference, pp. 314–320.
11. Williams R.E. (1989), *Metal Removal and Surface Finish Characteristics in Abrasive Flow Machining*, M.S. Thesis, University of Nebraska at Lincoln. Nebraska, (U.S.A.).
12. Williams R.E. and Rajurkar K.P. (1989), Mechanics of Deburring and Surface Finishing Processes, paper presented at Winter Annual Meeting of ASME, held at San Francisco, Dec. 10–15, 1989, PED, Vol. 38, pp. 93–106.
13. Williams R.E., Rajurkar K.P. and Rhoades L.J. (1989), Performance Characteristics of Abrasive Flow Machining, SME Technical Paper, FC 8980-610 to F8980-616.
14. Williams R.E. and Rajurkar K.P. (1992), Stochastic Modeling and Analysis of Abrasive Flow Machining, *Trans ASME, J. Engg. for Industry*, Vol. 114, pp. 74-80.

REVIEW QUESTIONS

1. With the help of a neat diagram, explain the working principle of abrasive flow machining process.

2. Justify the statement: "AFM has high flexibility".
3. How the restriction offered by passageway governs MRR? Make necessary sketches.
4. Write independent and dependent variables of AFM process.
5. What is the basic principle of tooling design for AFM process? Suggest the tooling for finishing of 200 gears of one type made of the same material. Would you consider parallel processing? Justify your answer.
6. Write the salient features of AFM system.
7. Detail the important process variables and responses.
8. Write five applications (component names) of AFM process.
9. In which cases of the following, you will recommend the use of AFM process:
 - (a) A component has been machined by EDM process. It is found that the top layer ($\approx 7 \mu\text{m}$) has to be removed before it can be put to use.
 - (b) ECM'd component is found weak in fatigue strength. It is decided to remove a layer of material ($\approx 1 \times 10^{-5} \text{ m}$) to improve its fatigue strength.
 - (c) During gear cutting, burrs are formed. Gears can be used only after removing these burrs.
 - (d) A cylinder has 100 small sized (0.5 mm diam.) holes to be finished. Every day 50 such cylinders are to be finished.
10. A hollow cylinder (inner diam. = 4 mm, outer diam. = 14 mm) requires improved surface finish on its outer and inner curved surfaces. Would you recommend AFM? Note that workpiece material is hardened steel and permissible dimensional change in its diameter is 20 μm . Draw the suggested tooling, if any.
11. Comment on the re-use of abrasives in AFM process.

SELF-TEST QUESTIONS

12. (A) Write true (T) or false (F).
 - i. AFM can be used to reduce the diameter of a mild steel rod from 14 mm to 12 mm.
 - ii. Stiff media is used for radiusing.
 - iii. At the intersection of two holes drilled at an angle ($< 90^\circ$), burrs are produced. Can you use AFM for deburring?

- iv. After AFM, you obtain HAZ of approximately $0.5 \mu\text{m}$.
- v. Workpiece material has no effect on the time required for AFM.
- vi. Major improvement in surface finish takes place in the initial five cycles or so.
- vii. Centre line average roughness value (R_a) changes from 3 to 1. The surface roughness has deteriorated.
- viii. Self deformable stone means the workpiece deforms to suit the media.
- ix. The life of media in AFM is very high (approaches infinity).
- x AFM process gives good dimensional tolerances.

NOMENCLATURE

- X Height of the machined surface profile.
- a Random disturbance (or noise)
- t Distance
- C_d Number of dynamically active grains

(B) MAGNETIC ABRASIVE FINISHING (MAF)

INTRODUCTION

Although the magnetic abrasive finishing (MAF) process was originated in U.S., it was in the former U.S.S.R and Bulgaria that much of the developments took place. The researchers have shown that the technique can be applied to a wide range of products. Japanese researchers followed this work and conducted research for finish polishing applications. Mainly two configurations of the MAF system have been in use, viz. one for cylindrical workpieces (Fig. 4.12a for external surfaces and Fig. 4.12b for internal surfaces), and another for flat workpieces (Fig. 4.12c). *Shinmura et al.* [1984–1985, 1990] and *Fox et al.* [1994] proposed designs for various equipments to study internal finishing of tubes, external

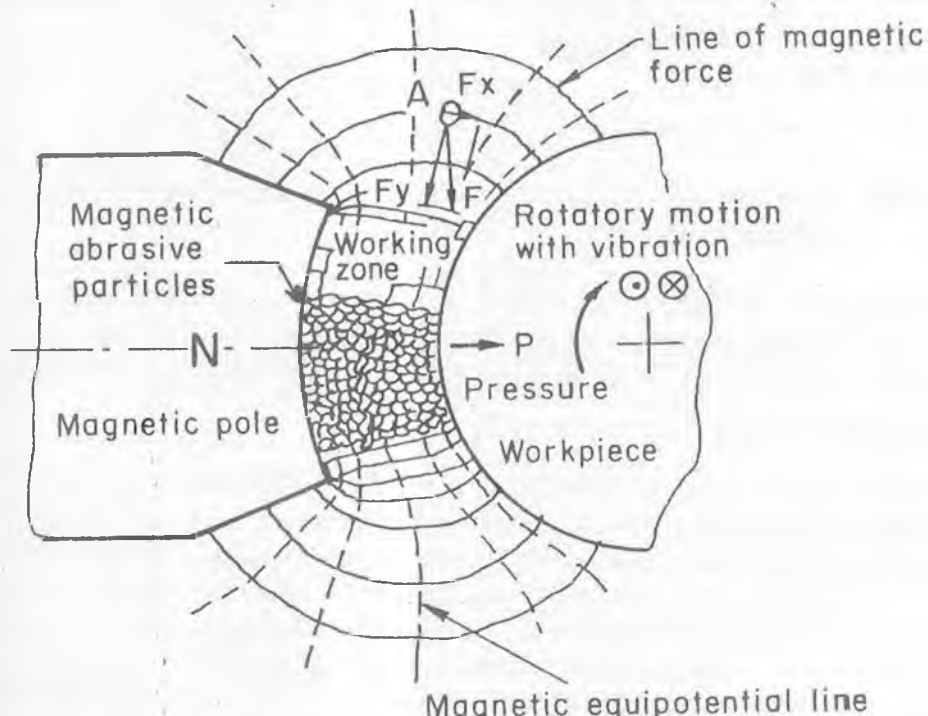


Fig. 4.12a Magnetic field distribution and magnetic force acting on a magnetic abrasive particle [*Shinmura et al.*, 1993].

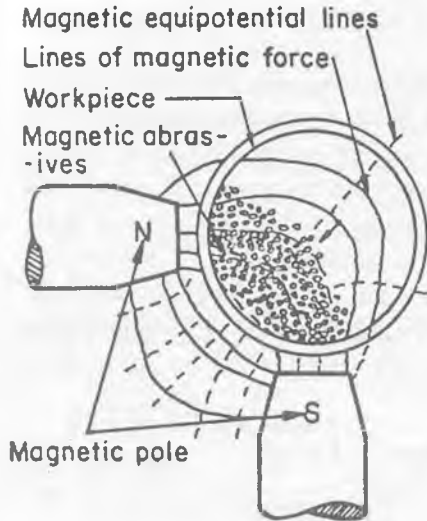


Fig. 4.12b Schematic view of internal finishing by magnetic abrasives [Kim and Choi, 1995].

finishing of rods, finishing of flat surfaces, etc. The workpiece may be made of either ferromagnetic materials, or non-ferromagnetic materials. Deburring and chamfering applications of MAF have also been reported [Shinnura *et al.*, 1990].

WORKING PRINCIPLE OF MAF

In MAF process, granular magnetic abrasive (Fig. 4.12d) composed of ferromagnetic material (as iron particles) and abrasive grains (say, Al_2O_3 , SiC, or diamond) are used as cutting tools and the necessary finishing pressure is applied by electro-magnetically generated field. The principle of working of MAF process is explained with the help of Fig. 4.12a. The magnetic particles are joined to each other magnetically between magnetic poles S and N along the lines of magnetic force forming **flexible magnetic abrasive brushes** (FMAB). When a cylindrical workpiece with rotatory, vibratory, and axial movement (Fig. 4.12a) is inserted in such a magnetic field, surface and edge finishing is performed by the magnetic abrasive brush [Shinnura *et al.*, 1990]. The finishing efficiency and quality are

greatly influenced by the rigidity of the magnetic abrasive brush. If the workpiece is of non-magnetic material, the lines of magnetic field go around it (i.e. through the magnetic abrasives), and if it is of magnetic material then they pass through the workpiece.

Magnitude of *magnetic force* prevailing between the two poles is also affected by the material, shape, and size of the workpiece, and shape and size of the

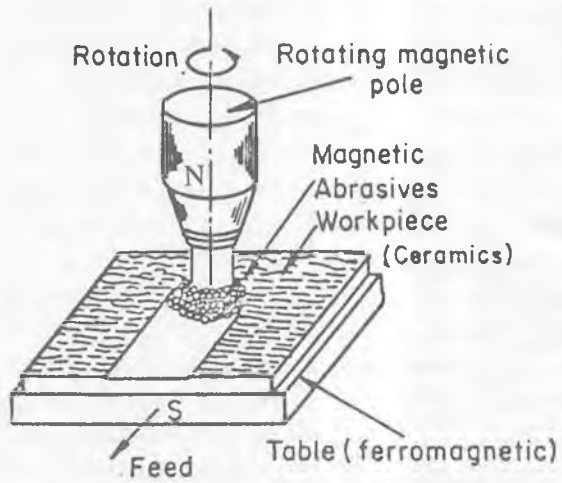


Fig. 4.12c Schematic view of plane (flat surface) magnetic abrasive finishing [Shinmura *et al.*, 1984].

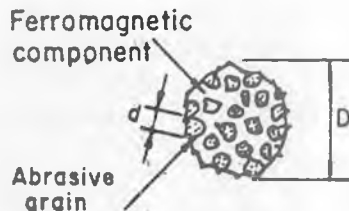


Fig. 4.12d Magnetic abrasive particle [Shinmura *et al.*, 1990].

magnetic poles. These factors therefore, should be considered during the design of the system [Shinmura *et al.*, 1985]. It is experimentally observed that the pressure exerted by the magnetic abrasives is decreased as the clearance (i.e., gap between the magnetic pole and the workpiece) is increased provided the filling density, ρ (g/cm^3) of the abrasive grains in the gap remains constant. Fig. 4.13 indicates that the magnetic abrasive pressure P acting on the work surface increases as the flux density on the magnetic abrasive grains increases for a given value of clearance.

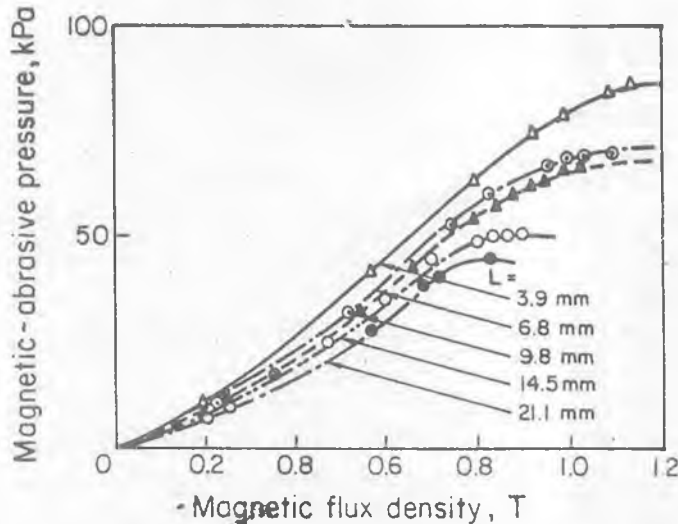


Fig. 4.13 Relationship between magnetic abrasive pressure and magnetic flux density for various values of clearance [Shinmura *et al.*, 1985].

Consider a diamond magnetic abrasive particle 'A' (Fig. 4.12a) on which two forces F_x (along the lines of magnetic force) and F_y (along the equipotential magnetic lines) act simultaneously, and F shows their resultant. These forces can be evaluated using Eqs. (4.3) and (4.4),

$$F_x = (\pi D^3 / 6) k H (\partial H / \partial x). \quad \dots(4.3)$$

$$F_y = (\pi D^3 / 6) k H (\partial H / \partial y). \quad \dots(4.4)$$

where, D and k are diameter (Fig. 4.12d) and susceptibility of magnetic abrasive particle, respectively and H is the magnetic field strength.

The **magnetic force F_y** is responsible for actuating the abrasive particles such that they take part in finishing the workpiece. The force F_x acts on the abrasive grains along the line of magnetic force, and it is mainly responsible for cutting action (or penetration in the workpiece). Any change in the strength of the magnetic field in the direction of the line of magnetic force near the workpiece surface, will actuate the magnetic abrasive particles. In addition to improving the surface finish, it also enhances the surface integrity by introducing residual compressive stresses.

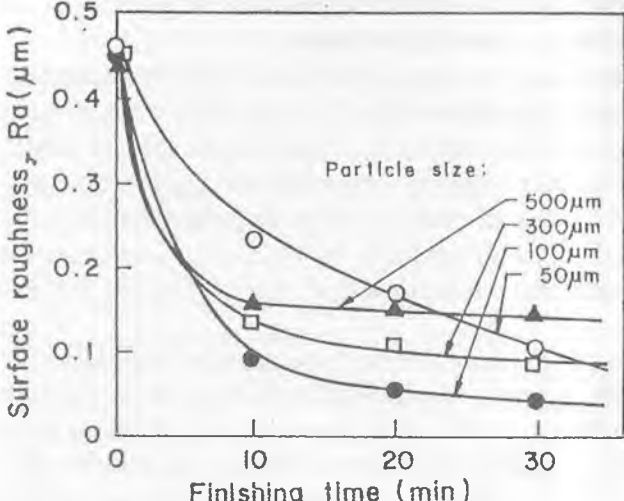
The effective way of changing the force (or finishing pressure) and rigidity of the **magnetic abrasive brush** is through the change in diameter D of magnetic abrasive particle. Hence, ferromagnetic particles of several times the diameter of diamond abrasive (d) are mixed to form the magnetic abrasive brush. This configuration results [Shinmura et al, 1984] in higher rigidity of the brush and permits to use only one kind of small diameter (d) diamond abrasives (which are responsible for actual finishing/material removal) with the different sized ferromagnetic particles. A ‘trade-off’ between ‘d’ and ‘D’ is required because the two have opposing effects on surface finish and material removal rate, as discussed later. Further, the mixing proportion of these two basic constituents determines the number of cutting edges.

Some **variables** of the MAF process are type and size of magnetic abrasives, mixing ratio of abrasive grains with ferromagnetic particles, working clearance, rotational speed, vibration (amplitude and frequency both), properties of work-piece material, magnetic flux density and relative speed of magnetic abrasive to the workpiece surface. The effects of these variables on the various responses (viz material (or stock) removal, machined depth, surface finish, out of roundness, and surface integrity) have been studied by various researchers. Some of them are discussed in what follows.

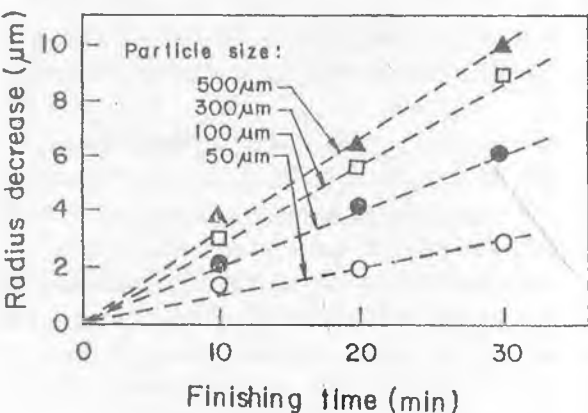
MATERIAL REMOVAL (OR STOCK REMOVAL) AND SURFACE FINISH

Type and Size of Grains

In the plane finishing process, magnetic force on the surface and rigidity of the magnetic abrasive brush are governed mainly by the grain size of magnetic abra-



(a)



(b)

Fig. 4.14 Change in (a) surface roughness, and (b) radius decrease with finishing time during finishing fine ceramics (Workpiece: Si_3N_4 ; diamond grain size: 2/4 μm) [Shinmura et al., 1990]

sives. Finishing tests were carried out using silicon nitride fine ceramic bar as workpiece. As shown in Fig. 4.14a, surface roughness rapidly improves in the beginning, then it levels off to a constant value. Larger is the particle size, poorer is the finished surface (except for the case of 50 μm particles) but higher is the stock removal (or radius decrease), which increases linearly with finishing time (Fig. 4.14b) [Shinmura *et al.*, 1990]. The process performance further improves if irregular shaped iron particles are used.

Finishing efficiency can be remarkably improved by mixing small sized diamond abrasive with irregular shaped large sized ferromagnetic particles (iron particles) [Shinmura *et al.*, 1984]. Both the size and mixing proportion of ferromagnetic particles influence characteristics of the finished surface. In some cases, there is an optimum value of mixing weight percentage of ferromagnetic particles for obtaining the best finish and the largest machined depth (Fig. 4.15). Diamond magnetic abrasives, composed of cast iron balls (diameter $\approx 100 \mu\text{m}$)

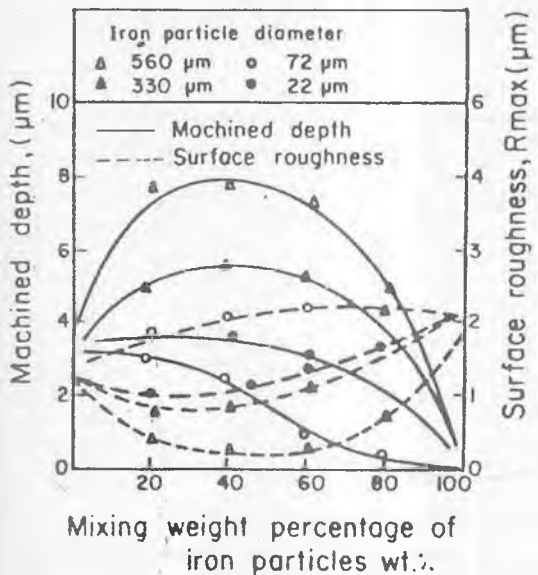


Fig. 4.15 Change in machined depth and surface roughness with mixing weight percentage of iron particles [Shinmura *et al.*, 1984].

and diamond micron sized powders (diameter $\approx 2/4 \mu\text{m}$) were used for finishing Si_3N_4 fine ceramics. Surface roughness of $0.45 \mu\text{m}$ was efficiently reduced to $0.04 \mu\text{m}$ [Shinmura *et al.*, 1990]. Using Cr_2O_3 and Fe (Chromium oxide abrasives of $3 \mu\text{m}$ size and iron particles of $75, 330$ and $510 \mu\text{m}$ size) mixing type magnetic abrasives, the surface finish of silicon nitride fine ceramic plate could be improved from $0.8 \mu\text{m}$ to $0.05 \mu\text{m}$ [Shinmura *et al.*, 1994]. Use of iron particles alone is not recommended because it is not capable to improve the surface finish appreciably.

Bonded and Unbonded Magnetic Abrasives

Magnetic abrasives have been used in the form of either a mixture (unbonded) of abrasive and ferromagnetic particles, or as magnetic abrasive conglomerate, i.e., abrasives held in a ferromagnetic matrix (bonded) formed by sintering or other techniques. Fox *et al.* [1994] conducted experiments with bonded as well as unbonded magnetic abrasive particles for finishing stainless steel rollers. It was found that unbonded magnetic abrasives yield higher removal rates whereas bonded magnetic abrasives are found to give better surface finish (Fig. 4.16).

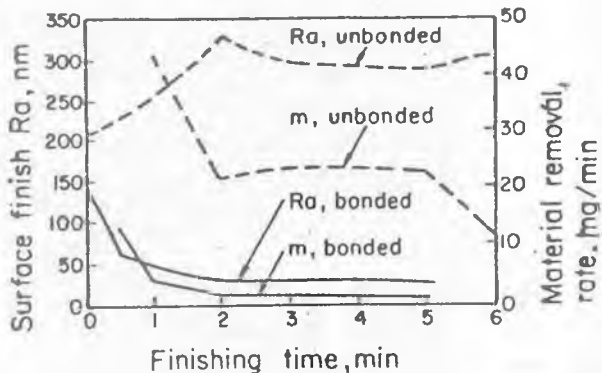


Fig. 4.16 Variation in surface finish and material removal rate with finishing time for bonded and unbonded magnetic abrasive particles (Surface speed: 1.3 m/s ; flux density: 0.37 T ; lubricant: oil (SAE 30)) [Fox *et al.*, 1994].

Machining Fluid

Addition of machining fluid with magnetic abrasives during MAF can be recommended [Shinmura, 1986], because it has revealed improvements in stock removal by the use of various types of commonly used grinding fluids. The best surface finish that could be achieved was $0.5 \mu\text{m}$ (R_{\max}). However, a better surface finish has been reported in the absence of cutting fluid.

Magnetic Flux Density

An increase in the magnetic flux density increases the tangential finishing force for various % of grinding fluid [Shinmura, 1986]. Machined depth increases with increase in magnetic flux density (T) and iron particle size (Fig. 4.17a), and decreases with increase in working clearance, (Fig. 4.17b). It has been reported [Shinmura et al., 1985], in plane finishing operations, that surface roughness improves with the increased magnetic flux density, and finishing time (Fig. 4.18). Further, the grinding burrs are more efficiently removed than turning burrs [Shinmura et al., 1985]. This is attributed to the fact that magnetic flux concentrates on the edges of ferromagnetic substance.

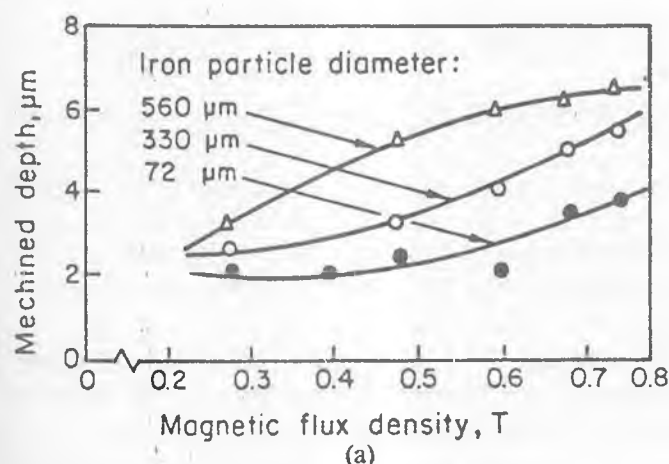


Fig. 4.17a Change in machined depth with magnetic flux density [Shinmura et al., 1984].

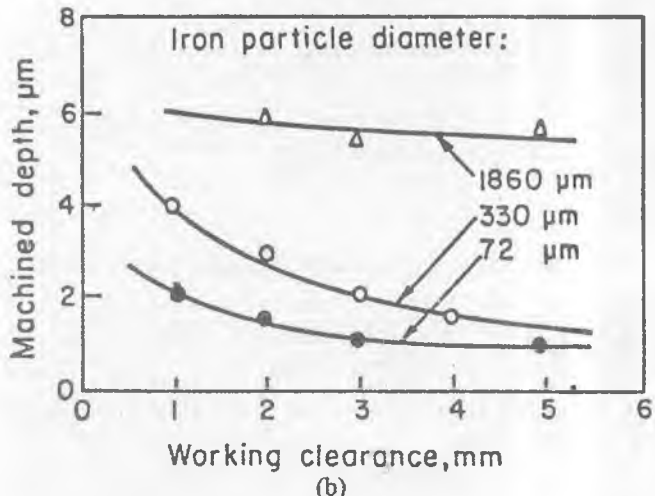


Fig. 4.17b Change in machined depth with working clearance (Magnetic flux density: 0.6 T) [Shinmura et al., 1984].

ANALYSIS

The machining pressure (P) between the abrasives and the workpiece is expressed [Kim and Choi, 1995] as:

$$P = \mu_0 (H_a^2/4) \cdot [3\pi(\mu_r - 1) W] / [3(2 + \mu_r) + (\mu_r - 1) W] \quad \dots(4.5)$$

where, μ_0 is magnetic permeability in vacuum, μ_r is relative permeability of pure iron, H_a is magnetic field strength in the air gap, and W is volume ratio of iron in a magnetic abrasive particle.

Based on the simplified assumptions like no porosity between the magnetic abrasive particles, all the particles are actively participating etc, the following equation for stock removal (m) in machining time ' t ' has been proposed.

$$m = \Delta m n N \quad \dots(4.6)$$

where, n = number of edges of a magnetic abrasive particle simultaneously acting on the surface, N = number of active magnetic abrasive particles, and Δm = volume of material removed by an edge in time ' t ', and

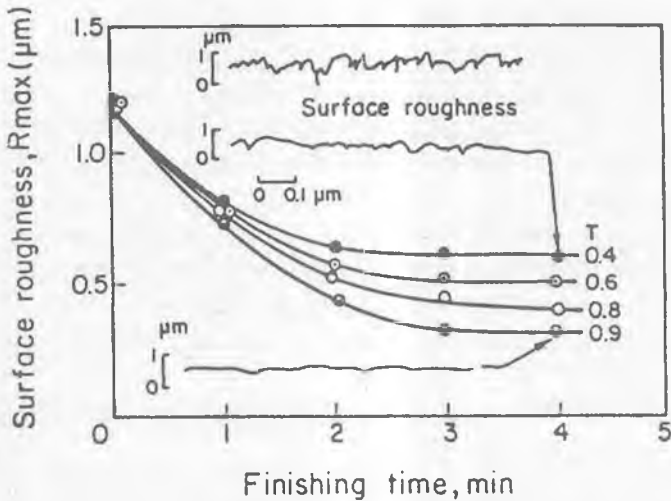


Fig. 4.18 Relationship between surface roughness and finishing time for various magnetic flux densities (Working clearance: 3 mm; peripheral speed of rotating pole: 166 m/min) [Shinmura et al, 1985].

$$\Delta m = C (\Delta f / H_w \pi \tan \theta) (1 - R_a / R_{ao}) v t \quad \dots(4.7)$$

where, Δf is force acting on a grain edge, H_w is workpiece hardness, θ is mean angle of asperity of abrasive cutting edges, R_a is final surface roughness, R_{ao} is initial surface roughness, v is speed of magnetic abrasives, and t is machining time.

Using the relationship between the surface roughness and stock removal, the following equation for evaluation of surface roughness is derived.

$$R_a = R_{ao} - C^1 (R_{ao})^{-1/8} (l_w)^{-5/4} (n N \Delta f v t / H_w \pi l_w \tan \theta)^{1/4} \quad \dots(4.8)$$

where, l_w is machined length and C^1 is a constant.

Using above models, surface roughness and stock removal in internal surfaces have been computed [Kim and Choi, 1995; Keremen et al, 1995], and comparison of computed and experimental results are found satisfactory.

BIBLIOGRAPHY

1. Fox M., Agrawal K., Shinmura T. and Komanduri R. (1994), Magnetic Abrasive Finishing of Rollers, *Annls CIRP*, Vol. 43, pp. 181-184.
2. Jain R.K. and Jain V.K. (1999), Abrasive Fine Finishing Process—A Review, *The Int. J. Mfg. Sc. Prod.*, Vol. 2, No. 1, pp. 55-68.
3. Kim Jeong-Du and Choi Min-Seog (1995), Simulation for the Prediction of Surface Accuracy in Magnetic Abrasive Machining, *J. Mater. Processing Technol.*, Vol. 53, pp. 630-642.
4. Kermen G.Z., Elysyed E.A. and Rafalovich V.I. (1995), Mechanism of Material Removal in the Magnetic Abrasive Process and the Accuracy of Machining, *J. Mater. Processing Technol.*, Vol. 53, pp. 630-640.
5. Shinmura T. (1986), Study on Magnetic Abrasive Finishing, *Bull. Japan Soc. Precision Engg.*, Vol. 20, No. 1, pp. 52-54.
6. Shinmura T., Takazawa K., and Hatano E. (1990), Study on Magnetic Abrasive Finishing, *Annls CIRP*, Vol. 39, pp. 325-328.
7. Shinmura T., Takazawa K., Hatano E. and Aizawa T. (1985), Study on Magnetic Abrasive Process—Process Principle and Finishing Possibility, *Bull. Japan Soc. Precision Engg.*, Vol. 19, No. 1, pp. 54-55.
8. Shinmura T., Wang F.H. and Aizawa T. (1984), Study on a New Finishing Process of Fine Ceramics by Magnetic Abrasive Machining, *Int. J. Japan Soc. Precision Engg.*, Vol. 28, pp. 99-104.
9. Shinmura T. and Wang F.H. (1994), A New Process for Precision Finishing of Silicon Nitride Fine Ceramics by the Application of Magnetic Abrasive Machining Using Chromium Oxide Abrasives Mixed with Iron Particles, *Int. J. Japan Soc. Precision Engg.*, Vol. 28, pp. 229-230.
10. Subramanian K. (1994), Finishing Methods Using Multipoint or Random Cutting Edges, *Surf. Engg.*, ASM, Vol. 5, pp. 91-109.

SELF-TEST QUESTIONS

1. Write true (T) or false (F).
 - i. MAF is suitable for finishing fine holes.
 - ii. Stainless steel powder and Al_2O_3 abrasive particles will form a strong magnetic abrasive brush during MAF.

- iii. Brass rod cannot be finished by MAF because it is non-magnetic in nature.
- iv. Due to low magnetic abrasive filling density, strength of the magnetic abrasive brush is low, hence MRR is also low.
- v. Diamond particles are smaller in size but material removal is done by them, and not by ferromagnetic particles.
- vi. Unbonded abrasives give better surface finish compared to bonded abrasives.
- vii. With a change in iron particle size, machined depth during MAF is not affected.
- viii. During MAF, major % improvement in surface finish takes place during first few minutes only.

REVIEW QUESTIONS

1. Explain the working principle of MAF with the help of a neat sketch. Clearly show lines of magnetic force, magnetic equipotential lines, direction of pressure acting on the workpiece, direction of rotatory motion, and a semi-magnetic abrasive particle.
2. Make a schematic diagram of MAF of internal surface of a cylinder showing the details mentioned in Q1.
3. Can you use MAF process to finish a ceramic thin plate (3 mm thick)? If yes, sketch a schematic diagram for the same, else justify your answer.
4. During experimentation, it is found that material removal decreases with the increase in clearance (ie., gap between the w/p and the magnet). Explain the reason(s) for the observation.
5. What is gap filling density? Explain with the help of a figure.
6. Write the type (material type) and size of the abrasive and magnetic particles used in MAF.

NOMENCLATURE

C' Constant

D Mean diameter of the magnetic abrasive particle

FMAB_s Flexible magnetic abrasive brushes

F_x	Magnetic force acting on a magnetic abrasive particle along the magnetic lines of force
F_y	Magnetic force acting on a magnetic abrasive particle along the equipotential magnetic lines
H	Magnetic field strengthd
H_a	Magnetic field strength in the air gap
H_w	Workpiece hardness
k	Susceptibility of the magnetic abrasive particle
l_w	Machined length
m	Stock removal (volumetric)
MAF	Magnetic abrasive finishing
N	Number of active magnetic abrasive particles
n	Number of edges of a magnetic abrasive particle simultaneously acting
P	Machining pressure
R_a	Final surface roughness
R_{ao}	Initial surface roughness
t	Machining time
v	Speed of magnetic abrasives
W	Volume ratio of iron in a magnetic abrasive particle
Δf	Force acting on a grain edge
μ_0	Magnetic permeability in vacuum
μ_r	Relative permeability of pure iron
Δm	Volume of material removed by a grain edge
θ	Mean angle of asperity of abrasive cutting edges

CHAPTER 4A
AT-A-GLANCE
ABRASIVE FLOW MACHINING (AFM)

ABRASIVE
FLOW
MACHINING

- FINISHING PROCESS : DEBURRING, RADIusing, POLISHING, PRODUCING COMPRESSIVE RESIDUAL STRESSES, ETC.
- SEMISOLID ABRASIVE LADEN PUTTY → DEFORMABLE GRINDING WHEEL → REMOVES SMALL AMOUNT OF MATERIAL
- FORCE: HYDRAULIC OR MECHANICAL
- MORE RESTRICTION → LARGER FORCE & VELOCITY
- FOR BOTH METALS & NON-METALS
- AREAS NOT ACCESSIBLE FOR CONVENTIONAL METHODS → MAY BE FINISHED

ELEMENTS OF ABRASIVE FLOW MACHINING



MACHINE

HOW AFM WORKS?

- MEDIA CONTAINING TOOLS (ABRASIVE PARTICLES) MOVES OVER THE W/P SURFACE AND REMOVES MATERIAL → JUST LIKE GRINDING
- PRESSURE → 0.70 TO 22 MPa
- FOR MAINTAINING CONSTANT VISCOSITY → COOLERS TO LOWER TEMPERATURE OF MEDIA
- CONTROLLABLE VARIABLES : VOLUME / STROKE, NO. OF CYCLES AND PRESSURE

TOOLING

- HOLDS MEDIA
- DIRECTS THE FLOW OF MEDIA
- MACHINING RATE → FUNCTION OF THE RESTRICTION TO THE FLOW OF MEDIA

- > INTERNAL SURFACES → ITSELF DECIDE THE EXTENT OF RESTRICTION
-----> EXTERNAL SURFACES → DESIGNER DECIDES THE EXTENT OF RESTRICTION
-----> NARROWEST SECTION : MAXIMUM MRR
-----> WIDEST SECTION : MINIMUM MRR

• INSERTS FOR RESTRICTING AREAS → RESIST ABRASIVE ACTION

→ NYLON, TEFLON, ETC.

- * CHARACTERISTICS : PLIABLE (EASILY MOULDED) MATERIAL ACTS AS A SELF-DEFORMING GRINDING STONE
- * CONSTITUENTS : BASE (ORGANIC POLYMER & HYDROCARBON GEL) + ABRASIVE GRITS
- * DEGREE OF STIFFNESS : DETERMINED BY COMPOSITION
 - : FOR LARGE HOLE - STIFF MEDIA
 - : FOR SMALL HOLE - SOFT MEDIA
- * ABRASIVES : Al_2O_3 , SiC, CBN, DIAMOND
 - : REPLACE MEDIA IF MACHINED AMOUNT = 10% OF ITS WEIGHT
- * MIXING OF A NEW MEDIA : CYCLE 20-25 TIMES THROUGH A SCRAP PART
- * CLEANING OF A MACHINED PART : AIR / VACUUM / CHEMICAL

PROCESS VARIABLES

- * NO. OF CYCLES
- * PRESSURE
- * MEDIA
- * WORKPIECE CONFIGURATION

PROCESS PERFORMANCE

- * SURFACE FINISH → $0.05 \mu\text{m}$
- * DIMENSIONAL TOLERANCE → $\pm 0.05 \mu\text{m}$
- * SURFACE IRREGULARITY (SCRATCHES, BUMPS, OUT-OF-ROUNDNESS) CANNOT BE CORRECTED

WHY?

⇒ MACHINES ALL SURFACES ALMOST EQUALLY

- * FINISHING AIRFOIL SURFACES OF IMPELLERS & EXTRUSION DIES
- * NOZZLE OF TORCH FLAME, ETC.

APPLICATIONS

CHAPTER 4B
AT-A-GLANCE
MAGNETIC ABRASIVE FINISHING (MAF)

INTRODUCTION

HISTORY : US / USSR / BULGARIA / JAPAN <- DEVELOPMENTS

SETUP CONFIGURATIONS:

- FOR FLAT SURFACES
- FOR CYLINDRICAL SURFACES
 - + EXTERNAL
 - INTERNAL

W/P MATERIAL : FERROMAGNETIC / NON-FERROMAGNETIC

TYPES OF OPERATIONS : FINISHING, RADIusing, DEBURRING, INTRODUCING RESIDUAL COMPRESSIVE STRESSES, ETC

WORKING PRINCIPLE

MAGNETIC ABRASIVE PARTICLES (MAPs) → • FERROMAGNETIC PARTICLES + ABRASIVE PARTICLES (FIG.4.12d)
• ACT AS CUTTING TOOLS

FLEXIBLE MAGNETIC ABRASIVE BRUSH (FMAB) → • MAPs JOIN EACH OTHER UNDER THE INFLUENCE OF MAGNETIC FIELD

WORKPIECE → • ROTATES, VIBRATES AND MOVES AXIALLY
• FMAB DOES FINISHING BY SHEARING PEAKS ON W/P SURFACE

FACTORS → MAGNETIC FLUX DENSITY → ϕ (W/P MATERIAL (TYPE, SHAPE, AND SIZE), MAGNETIC POLE <- SHAPE & SIZE)

MAGNETIC ABRASIVE PRESSURE ON W/P → ϕ (FLUX DENSITY, CLEARANCE)

FORCES ACTING ON A PARTICLE → F_x, F_y (Eqs. 4.3, 4.4)

HOW TO CHANGE RIGIDITY OF MAB → EASY WAY → CHANGE 'D' OF MAPs AND FINISHING PRESSURE

'TRADE OFF' BETWEEN 'D' & 'd' → HAVE OPPOSING EFFECT ON MRR & SF

VARIABLES

- MAGNETIC ABRASIVES → + TYPE & SIZE + MIXING RATIO
- WORKING CLEARANCE
- ROTATIONAL SPEED, VIBRATION (FREQUENCY & AMPLITUDE), AND AXIAL MOVEMENT
- PROPERTIES OF W/P MATERIAL
- MAGNETIC FLUX DENSITY

RESPONSES

- MATERIAL REMOVAL
- MACHINED DEPTH
- SURFACE FINISH

- OUT-OF-ROUNDNESS
- SURFACE INTEGRITY

MATERIAL REMOVAL AND SURFACE FINISH

TYPE AND SIZE OF GRAINS

- WITH FINISHING TIME, SURFACE ROUGHNESS RAPIDLY IMPROVES; LATER ON LEVELS OFF TO A CONSTANT VALUE
- LARGER PARTICLE SIZE → POOR SURFACE FINISH (FIG.4.14a)
 - HIGHER STOCK REMOVAL
 - ↓
 - INCREASES LINEARLY WITH FINISHING TIME (FIG 4.14b)
- IRREGULAR SHAPED IRON PARTICLES → BETTER PERFORMANCE
- MIXING WEIGHT PERCENTAGE → OPTIMUM MACHINED DEPTH (FIG 4.15a)
 - OPTIMUM SURFACE ROUGHNESS (FIG 4.15b)
- ONLY FERROMAGNETIC PARTICLES → NOT RECOMMENDED. DOES NOT IMPROVE SURFACE FINISH APPRECIABLY

BONDED AND UNBONDED MAGNETIC ABRASIVES

BONDED MAGNETIC ABRASIVES → BETTER SURFACE FINISH
 UNBONDED MAGNETIC ABRASIVES → HIGHER MRR

MACHINING FLUID

- USE OF MACHINING FLUID → HIGHER STOCK REMOVAL
 - POORER SURFACE FINISH

MAGNETIC FLUX DENSITY

- MACHINED DEPTH INCREASES BY → INCREASED MAGNETIC FLUX DENSITY
 → INCREASED PARTICLE SIZE
 → DECREASED WORKING CLEARANCE
- SURFACE FINISH IMPROVED BY → INCREASED FLUX DENSITY
 → INCREASED FINISHING TIME
 → HIGHER RELATIVE SPEED
 → SMALLER WORKING CLEARANCE

ANALYSIS

STOCK REMOVAL 'm' IN MACHINING TIME 't', $m = \Delta m \cdot n \times t$

$$\Delta m = C \times (\Delta f / (H_w \pi \tan \theta)) \times (1 - R_a / R_{ao}) \times Vt$$

$$\text{SURFACE ROUGHNESS, } R_a = R_{ao} - C^1 (R_{ao})^{-1/8} (1_w)^{-5/4} \left(\frac{n N \Delta f v t}{H_w \pi \tan \theta l_w} \right)^{1/4}$$

WATER JET CUTTING

INTRODUCTION

This process is good for cutting and slitting of porous non-metals like wood, leather, foam, etc. It is also used for cutting composites, wire stripping, and deburring. This process works on the principle of erosion effects of a high velocity, small diameter jet of water. Quality of the machined edge obtained during this process is usually superior to the other conventional cutting processes. In water jet machining (WJM), water jet is a cutting tool which never dulls or breaks. This process does not generate airborne dust; hence hazards during machining of fibre composites and asbestos, are minimum. The jet velocity may be as high as 900 m/s. Basic cutting action is performed by tight water jet core. Interaction with air diverges the shroud around the core.

WJC MACHINE

Fig. 5.1 shows a schematic diagram of WJC system. The **pumping unit** (i.e. oil pump) is driven by an electric motor. The oil drawn from a reservoir, is pumped to an intensifier which uses low pressure oil to produce very high pressure water. The intensifier that acts as a high pressure pump, produces water pressure as high as 40 times that of the oil. Water pressure (P_w) can be determined from the following equation:

$$P_w = (p_o \times A_o) / A_w \quad \dots(5.1)$$

where, p_o is oil pressure, A_o is oil piston area, and A_w is water piston area.

To minimize pulsation in water flow, a high pressure **accumulator** (i.e., a pressure vessel to store high-pressure water to give smooth outflow) is used. High pressure water is transported to nozzle through the rigid high pressure tubing and rigid connectors (not shown in figure). Off/on control valve of water flow can be operated manually or electronically.

Proper **design of nozzles** has made it possible to discontinue the use of *long-chain polymers* to lower down friction in fluid flow. Internal diameter of nozzle usually ranges from 0.07 to 0.50 mm. These nozzles are made of synthetic sapphire which is wear resistant but easily machinable. Presence of foreign particles (say, dirt) in water results in failure of nozzle by chipping. Sometimes, constriction of nozzle by mineral deposits also results in nozzle failure. Life of a sapphire nozzle is usually 250-500 hr.

Water jet outside the nozzle, travels at a very high speed (usually more than sound velocity). To minimize the exposed length of a jet, from safety point of view and also to minimize the process noise, a **catcher** (a slot type or tube type) is used. It is attached to a draining hose. The catcher uses hard and replaceable inserts to break the jet quickly and completely before it reaches bottom of the tube. Slot type catcher is less efficient in reducing noise level.

PROCESS CHARACTERISTICS

Pressure, diameter of nozzle, traverse rate, and stand-off-distance are four important **variables** that affect the performance of WJC process. Stand-off-distance is less effective variable and its value normally lies between 3–25 mm.

Cutting at higher water jet pressure is faster. Thick materials can be machined without difficulty at high jet pressure and / or low traverse rate.

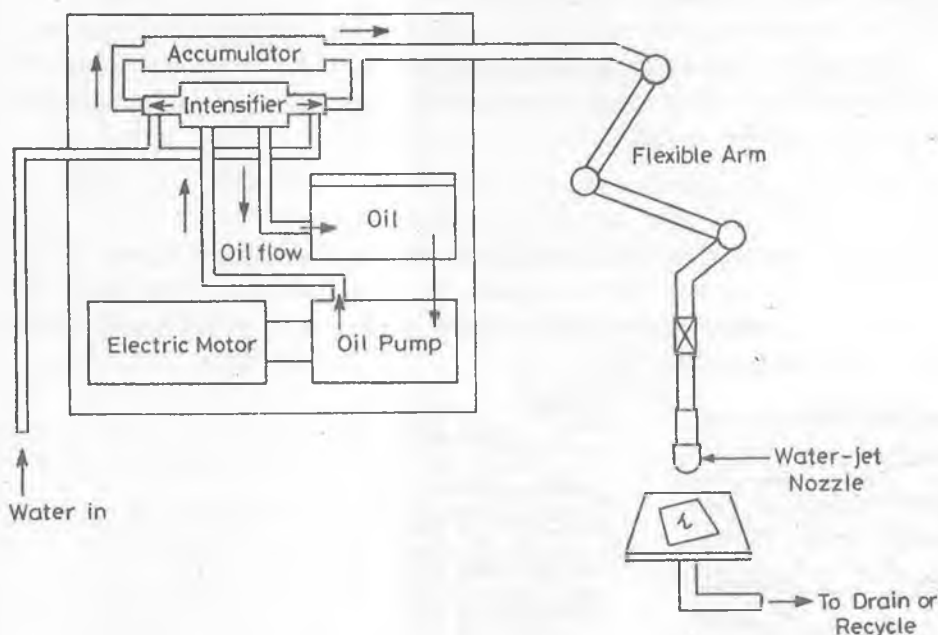


Fig. 5.1 Schematic diagram of water jet machining system
[Source: Norwood and Johnston, 1984].

PROCESS PERFORMANCE

This process is useful for **cutting materials** which are porous, fibrous, granular, or soft. It includes the materials like corrugated board (cutting speed (relative speed between water jet and the w/p surface normal to the jet axis) = 3 m/s), granite (0.25 m/s), rubber (0.13 m/s), plywood (0.025 m/s), glass (0.025 m/s), aluminium (0.0025 m/s), etc. This process *does not require predrilled hole* to start cutting in any direction and location provided the location is accessible for the water jet. Too thick materials can be cut in *more than one pass*. Second and subsequent passes are used to make the cut deeper rather than wider. Energy consumption per unit length in **multi pass cutting** is less than single pass cutting of the same workpiece material but with a more powerful jet. *Machined surfaces*

have no burrs, no thermal damage, and a good surface finish. Surface finish, tolerance, and straightness of the cut edges also depend on material thickness, cutting speed, and other machining parameters.

Water jet at lower pressure (69–200 MPa) has been used to cut *insulation of the cables* without damaging the underlying metallic cable. The water jet nozzle rotates around the cable to cut all around. It takes about 5-10 s / cable depending upon thickness of the insulation.

APPLICATIONS

In aerospace and other similar industries, cutting of asbestos is done by WJ to minimize airborne dust in the atmosphere. It is also used to cut fiber glass and polyethylene automotive parts. This technique is also used for high speed cutting of the corrugated box (Fig. 5.2).

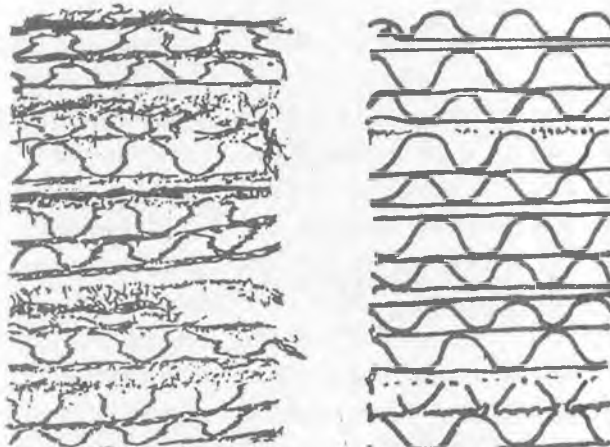


Fig. 5.2 Mechanically slit (left) and water jet slit (right) corrugated cardboard [Source: *Flow System, Inc., Kent, Wash.*].

BIBLIOGRAPHY

1. Atkey M. (1983), Water Jet Cutting: A Production Tool, *Mach. Prod. Eng.* Vol. 141(3631), pp. 18-19.
2. Benedict G.F. (1987), *Nontraditional Manufacturing Processes*, Marcel Dekker Inc., New York.

3. De Meis R. (1986), Cutting Metal with Water, *Aerospace Am*, Vol. 24(3), pp. 22-23.
4. Engemann B.K. (1981), Water Jet Cutting of Fibre Reinforced Composite Materials, *Ind. Prod. Engg.*, Vol. 3, pp. 162-164.
5. Konig W., Wulf Ch., Groß P., and Willerscheid H. (1985), Machining of Fiber Reinforced Plastics, *Annals CIRP*, Vol. 34(2), pp. 537-548.
6. Labus T.J. (1978), Cutting and Drilling of Composites using High Pressure Water Jets, Paper G2 of the 4th Int. Symp. on Jet Cutting Technology, Univ. of Kent, Canterbury, pp. G2 9-18.
7. McGeough J.A. (1988), *Advanced Methods of Machining*, Chapman & Hall, New York.
8. Pandey P.C. and Shan H.S. (1980) *Modern Machining Processes*, Tata McGraw Hill, New Delhi.

SELF-TEST QUESTIONS

Q1. Write the most appropriate answer

- i. Best suited cutting process under explosive environment is
(a) ECM, (b) WJC, (c) AJM, (d) EDM.
- ii. Polymers are added in water jet in WJC to
(a) increase MRR, (b) improve surface finish, (c) improve dimensional accuracy, (d) none of these.
- iii. WJC can be applied only for
(a) metals having high thermal and high electrical conductivity,
(b) non-metals, (c) metals as well as non-metals, (d) none of these.
- iv. The source of pulsation in water flow is
(a) intensifier, (b) type of pump, (c) nozzle design, (d) long chain polymers.
- v. When a thick material is to be cut by WJC, one should prefer
(a) very powerful jet and single pass cutting, (b) multipass cutting,
(c) low stand-off-distance, (d) all of these.
- vi. Water used in WJM
(a) can be reused directly, (b) cannot be reused, (c) can be reused after post process treatment.

REVIEW QUESTIONS

Q2.

- i. Give four applications of WJC process.
- ii. What do you mean by pulsation? How do you minimize pulsation in water flow?
- iii. What is the basic function of a catcher? What problems do you expect in the absence of a catcher during WJC?
- iv. Explain the way you will cut the insulation of a large diameter underground electric power supply cable.

Q3. Write the factors that affect the performance of WJM process. Discuss their effects in brief.

Q4.

- i. "Cutting tool" never dulls or breaks in WJM. Explain.
- ii. What are the functions of a catcher used in WJM system?
- iii. Write the unique applications of WJM process (other than those given in Q2(i)).

ABBREVIATIONS

A_o Oil piston area

A_w Water piston area

P_o Oil pressure

P_w Water pressure

CHAPTER 5
AT-A-GLANCE
WATER JET CUTTING (WJC)

- UTILIZES EROSION EFFECTS OF A HIGH VELOCITY SMALL DIAMETER JET OF WATER
- WATER JET → CUTTING TOOL → UPPER LIMIT OF VELOCITY \approx 900 m/s
- CUTTING BY TIGHT WATER JET CORE
- SHROUD AROUND THE CORE → DIVERGES DUE TO INTERACTION WITH AIR
- CUTTING AND SLITTING → BASICALLY POROUS NON-METALS, COMPOSITES, ETC
- WIRE STRIPPING AND DEBURRING ALSO

WJC MACHINE

INTENSIFIER INCREASES WATER PRESSURE

$$P(w) = P(O) A(o) / A(w)$$

- TO MINIMIZE PULSATION IN WATER FLOW → A HIGH PRESSURE ACCUMULATOR

NOZZLE

- INTERNAL DIAMETER OF NOZZLE → 0.07 mm TO 0.5 mm
- MATERIAL : SYNTHETIC SAPPHIRE → WEAR RESISTANT AND EASILY MACHINEABLE
- FAILURE → PRESENCE OF FOREIGN PARTICLES IN WATER → CONSTRICTION BY MINERAL DEPOSITS
- LIFE → 250 – 500 hr

CATCHER

- JET SPEED → AROUND SOUND VELOCITY
- TO MINIMIZE NOISE AND EXPOSED LENGTH OF THE JET → A CATCHER IS USED
- COMPLETELY BREAKS THE JET BEFORE IT REACHES THE BOTTOM OF THE TUBE
- USES A HARD, REPLACEABLE INSERT TO BREAK THE JET QUICKLY.

**PROCESS
CHARACTERISTICS**

=> VARIABLES



- PRESSURE → HIGHER VALUE → CAN CUT THICKER MATERIALS
- NOZZLE DIAMETER
- TRAVERSE RATE → DECREASED VALUE FOR THICKER PARTS
- STAND-OFF-DISTANCE : 3 mm–25 mm

- MATERIAL CUT
 - POROUS, FIBROUS, GRANULAR, SOFT
 - CORRUGATED BOARD (3 m/s), RUBBER (0.13 m/s), PLYWOOD (0.025 m/s), GLASS (0.025 m/s), ALUMINIUM (0.0025 m/s) etc.
- NO PREDRILLED HOLE IS REQUIRED → ANY DIRECTION & LOCATION BUT ACCESSIBLE FOR THE WATER JET
- TOO THICK PARTS → CUT IN MORE THAN ONE PASS → ENERGY CONSUMPTION / UNIT LENGTH IS LESS
- MACHINED SURFACE: NO BURRS, NO THERMAL DAMAGE, & GOOD SURFACE FINISH
: TOLERANCE, STRAIGHTNESS OF CUT EDGES & FINISH = \varnothing (WORKPIECE THICKNESS & CUTTING SPEED)
- TO CUT INSULATION OF CABLES → 69-200 MPa → 5-10 s/ CABLE

APPLICATIONS

- CUTTING OF ASBESTOS (MINIMIZES AIRBORNE DUST)
- CARBIDE GRIT SAFETY WALKS
- FIBRE GLASS & POLYETHYLENE AUTOMOTIVE PARTS
- HIGH SPEED CUTTING OF CORRUGATED BOX

ABRASIVE WATER JET MACHINING (AWJM)

WORKING PRINCIPLE

Abrasive jet machining (AJM), abrasive flow machining (AFM), and ultrasonic machining (USM) are the processes which use abrasives for machining of materials. In AJM, air driven abrasive jet strikes the workpiece and removes the material while in USM, abrasive grains in liquid slurry strike the workpiece surface at ultrasonic frequency and cut the material at low material removal rate (MRR). Recent developments have witnessed improvements in jet cutting technology by using abrasive water jets where water is used as carrier fluid. In principle, this process is similar to abrasive jet machining except that in this case water is used

as a carrier fluid in place of gas. These processes offer advantage of cutting electrically non-conductive as well as difficult-to-machine materials comparatively more rapidly and efficiently than other processes. Other advantages claimed for this process may be listed as: practically no dust, high cutting speed, multidirectional cutting capacity, no fire hazards, no thermal or deformation stresses, high quality of machined edge, easy adaptation for remote control, recycling of abrasive particles, low power requirements, almost no delamination, and reduced striations.

A water jet and a stream of abrasives coming from two different directions, mix up and pass through the abrasive jet nozzle. Here, a part of the momentum of water jet is transferred to the abrasives. As a result, velocity of the abrasives rises rapidly. Thus, a high velocity stream of mixture of abrasives and water impinges on the workpiece (W/P) and removes material. Depending upon the type of the W/P material being cut, material removal may occur due to erosion, shear, or failure under rapidly changing localized stress fields.

In abrasive water jet cutting (AWJC), an erosive action of an abrasive laden water jet is employed for cutting, drilling, and cleaning of hard materials [Benedict, 1987]. The pressure at which water jet operates is about 400 MPa which is sufficient to produce a jet speed as high as about 900 m/s. Water-abrasive mixture jet exiting from the nozzle at such a high velocity is fully capable to cut ceramics, composites, rocks, metals, etc. Removal of material from upper most position of a kerf is governed by erosive action while that at depth it is governed by deformation wear [Hashish, April 1989].

AWJM MACHINE

Abrasive water jet machining (AWJM) set-up is made up of four important elements, viz. pumping system, abrasive feed system, abrasive jet nozzle, and catcher.

Pumping System

It produces a high velocity water jet by pressurizing water to as high as 415 MPa by means of an intensifier. To acquire such a high pressure, 75 HP motor may be required. Water flow requirements up to 3 gpm are quite common.

Abrasive Feed System

It must deliver a controlled flow of abrasive particles to the jet nozzle. Present abrasive feed system delivers a stream of dry abrasives to the nozzle. Flow of water jet in a mixing tube is responsible to create enough suction for the flow of the abrasives. Flow rate of abrasives can be controlled by changing the diameter of the control orifice. Such systems have the limitation that they cannot supply the abrasives over a long distance. To overcome this drawback, researchers are developing a system in which it is possible to directly use slurry (mixture of abrasives and water) instead of mixing them in a nozzle. This System would make it possible to feed slurry over a long distance. However, it would require more power than the power required by the dry abrasive feed system.

Highly pressurized water is passed through a nozzle of diameter ranging from 0.075 to 0.635 mm to obtain the desired velocity (about 700 m/s) of a jet of abrasive water mixture. For longer life (say, 250-500 hr) of the nozzle, it should be made of sapphire.

Abrasive Water Jet Nozzle

It performs two functions: (i) mixing of abrasive jet and water, and (ii) to form a high velocity water abrasive jet. It should give a coherent, and focussed abrasive stream at exit from the nozzle which is made of sapphire, tungsten carbide (WC), or boron carbide. Internal details and two **kinds of abrasive jet nozzles** (viz. Single jet side feed nozzle and multiple jet central feed nozzle) are shown in (Fig. 6.1). In a single jet side feed nozzle, abrasives fed from the side mix with water jet in the mixing chamber. This nozzle is less expensive, simple to make but does not provide an optimal mixing efficiency, and experiences a rapid wear at the exit part of the nozzle. The multiple jets central feed nozzle consists of a centrally located abrasive feed system surrounded by multiple water jets which are disposed such as a converging annulus of water is produced. It gives higher nozzle life and better mixing of abrasives into the *water jet*. However, it is difficult and costly to fabricate such nozzles because of the angle of convergence.

Catcher

Another element of the system is a catcher which is used when the nozzle remains stationary and the workpiece moves. Catcher is a long narrow tube placed under the point of cut to capture the used jet. In case when the workpiece remains

stationary and the nozzle moves, a water filled settling tank is placed directly underneath the workpiece. The used jet dies out in this tank. High pressure water from the pump is transmitted to the nozzle by high pressure flexible hose (if pressure \leq 124 MPa) or rigid tubing (if pressure $>$ 124 MPa).

PROCESS VARIABLES

Parameters which affect performance of AWJM process are water (flow rate, and pressure), abrasives (type, size, and flow rate), water nozzle and abrasive jet nozzle (design), cutting parameters (feed rate, and stand-off-distance), and work material. Other cutting parameters can be listed as mixing tube diameter and its length, angle of cutting and traverse speed. Number of passes is also identified as one of the important variables that affects cutting performance during AWJC. Some of these variables and their effects on the performance of the process are now discussed as follows.

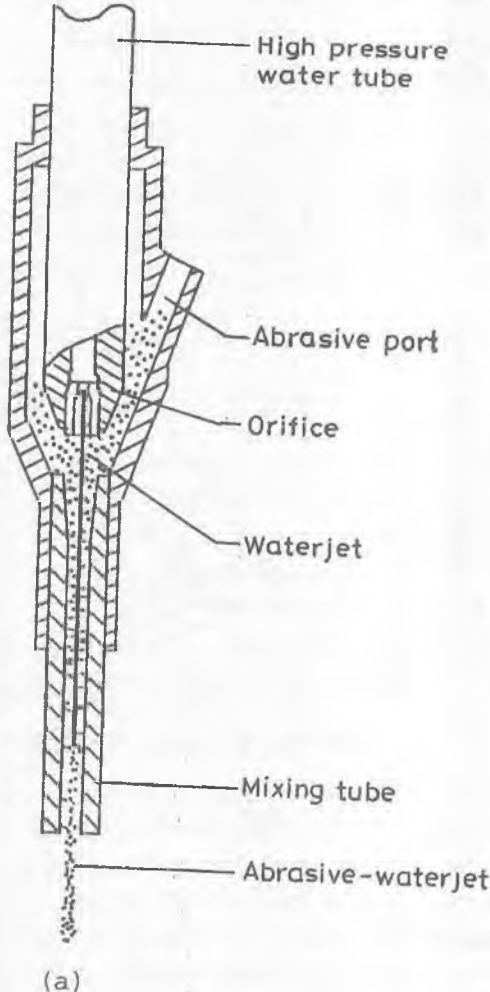
WATER

Water Jet Pressure during Slotting

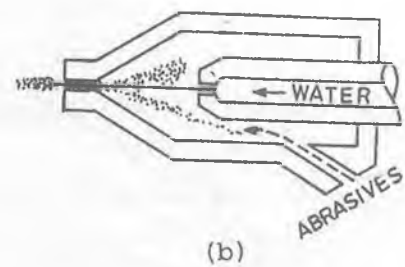
Relationships between pressure and depth of cut for different abrasive flow rates (kg/min) and nozzle diameters are shown in Fig. 6.2. Fig. 6.2a shows the effect of water jet pressure *on the depth of cut* for various abrasive flow rates. Fig. 6.2b shows the relationship between depth of cut and water jet pressure for two nozzle diameters. There is a minimum pressure (i.e. critical pressure or threshold pressure, P_c) below which no machining would take place [Hashish, 1983]. This **critical pressure** (P_c) exists because a minimum abrasive particle velocity (or K_E) is required to cut a particular material. P_c is obviously different for different workpiece materials. The machined depth tends to stabilize, beyond a certain value of water jet pressure. The machined depth versus pressure relationship becomes steeper as the abrasive flow rate increases. An increase in pressure also increases rate of nozzle wear and cost of pump maintenance, and lowers volumetric efficiency.

Water Flow Rate

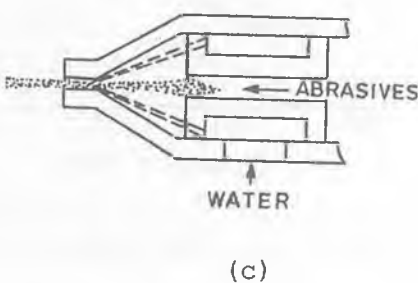
In abrasive jet machining where gas (usually air) is used as a propelling fluid, only small mass flow rates of abrasives (up to 100 g/min) can be achieved. In



(a)



(b)



(c)

Fig. 6.1 Abrasive water jet nozzle, (a) details of construction, (b) single jet side feed nozzle, (c) multiple jets central feed nozzle [Hashish, 1982].

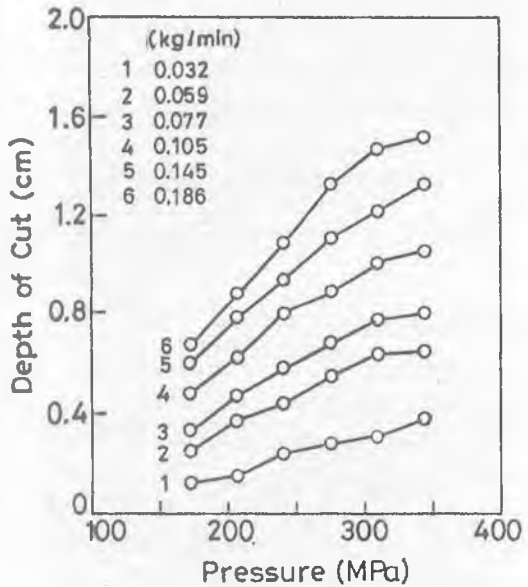


Fig. 6.2(a)

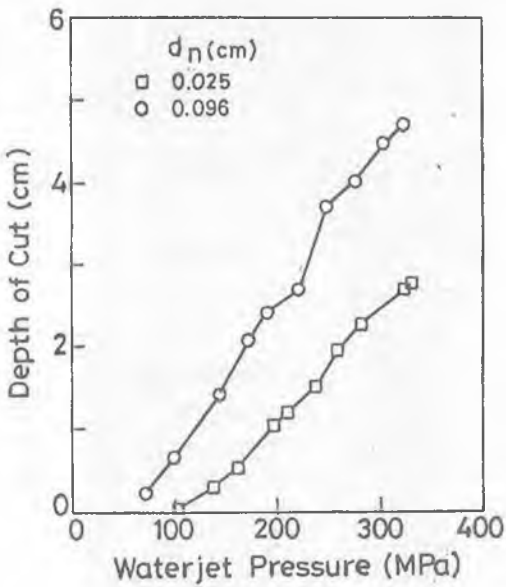


Fig. 6.2 (b)

Fig. 6.2 Effect of water jet pressure on machined depth (a) in mild steel workpiece for various abrasive flow rates, (Garnet # 80, nozzle diameters (d_n) = 0.025 cm, u = 15 cm / min), (b) for various nozzle diameters (d_n), using Aluminium 6061-T6 as workpiece (Garnet, # 80, m_a = 0.93 kg/min; u = 20 cm/min) [Hashish, 1986].

AWJM, water is used as a propelling fluid which enables high abrasive flow rates (0.1–5 kg/min) to be achieved, and makes it possible to accelerate abrasives to high velocities (over 300 m/s). AWJs are more suitable for cutting as compared to gas abrasive jets because earlier ones are more coherent.

Water flow rate (Q) is proportional to square root of pressure ($Q \propto \sqrt{P}$) and square of diameter of the nozzle ($Q \propto d_n^2$). It is concluded from the experimental study that a percentage increase in depth of cut is always lower than a percentage increase in water flow rate. Increase in water flow rate beyond a certain value may result in insignificant gain in particle velocity, higher pressure losses in supply lines, unacceptable environmental conditions (in mining or constructional applications), and in some cases with reduced machined depth.

ABRASIVES

Abrasive Flow Rate

Machined depth (depth of cut) is proportional to the abrasive flow rate (\dot{m}) and square of particle velocity (V_p). However, an increase in abrasive flow rate beyond the critical value (\dot{m}_c) would reduce machined depth. Increase in abrasive flow rate enhances wear rate of mixing nozzles and reduces mixing efficiency inside AWJ nozzle. Relationships between abrasive flow rate and depth of cut for various work materials (Fig. 6.3a), and for various nozzle diameters (Fig. 6.3b) are shown.

Abrasive Particle Size

Commonly used abrasive particle size ranges from 100-150 grit. There is an optimum particle size for a particular workpiece material and also for a particular nozzle mixing chamber configuration.

Recently efforts have been made to quantify the effect of abrasive particle size on depth of cut. Results have shown that an optimum particle size range exists for cutting different types of materials. Mesh size 60 is more effective for relatively shallow depth of cut obtained with two passes (Fig. 6.4) during machining of stainless steel [Hashish, 1986]. Approximate diameter (in mm) of abrasive grit of mesh size 's' can be obtained from [Malkin, 1989] the following equation [Hashish, 1982; Hashish, 1986]

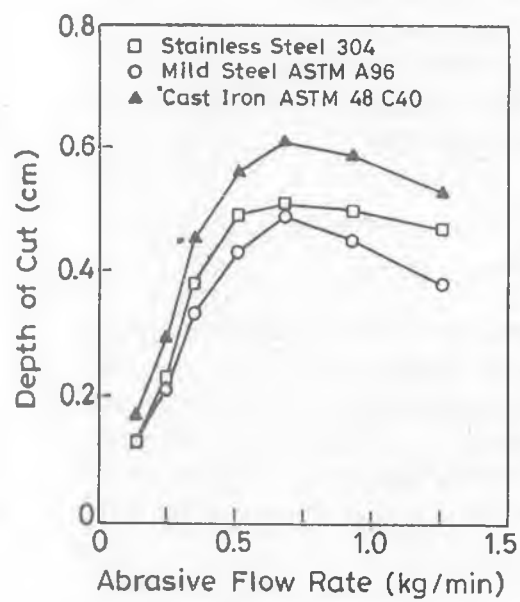


Fig. 6.3 (a)

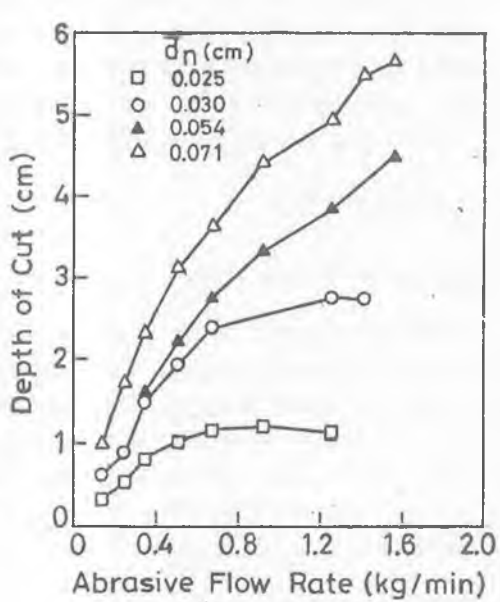


Fig. 6.3 (b)

Fig. 6.3 Relations between abrasive flow rate and depth of cut for
 (a) various work materials using Garnet as abrasive material;
 $u = 15 \text{ cm/min}$; $d_n = 0.025 \text{ cm}$, and $P = 207 \text{ MPa}$, (b) for various nozzle diameters using aluminium as work material (Garnet #60; $P = 207 \text{ MPa}$;
 $u = 20 \text{ cm/min}$) [Hashish, 1986].

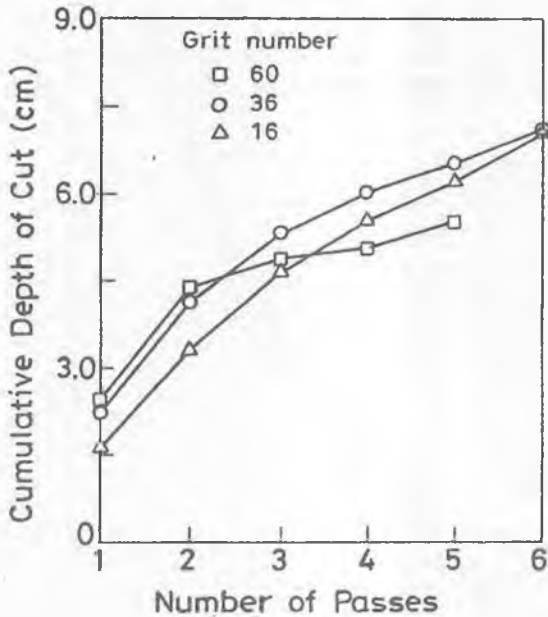


Fig. 6.4 Effect of particle size for multipass cutting in stainless steel 17-4PH (Garnet; $P = 276$ MPa; $d_n = 0.071$ cm; $u = 20$ cm/min; $m = 1.8$ kg/min) [Hashish, 1986].

$$d_n = \frac{(0.6) \times 25.4 \text{ mm}}{s} \quad \dots(6.1)$$

Ignoring the practical difficulties, the strategy recommended [Hashish, 1986] for deep cutting is to use different abrasive sizes with different number of passes to maximize the effect of abrasive particle size on machined depth. However, the effect of particle size on nozzle wear should also be considered as one of the important selection criteria.

Abrasive Material

Garnet, silica and silicon carbide are commonly used abrasives in AWJC. Type of abrasive to be used is determined after knowing hardness of the workpiece material. Higher the hardness of the workpiece material, harder should be the abrasives to be used. Complete recycling of the abrasives is not possible.

Machined depth is also affected by the type of the abrasives used (Fig. 6.5). While selecting a type of abrasive for a particular application, one should consider cost, nozzle wear rate, environment constraints, machining rate, and strength of the particles.

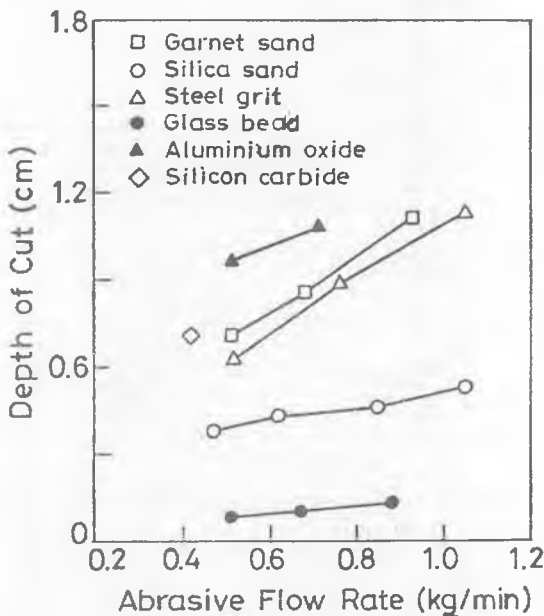
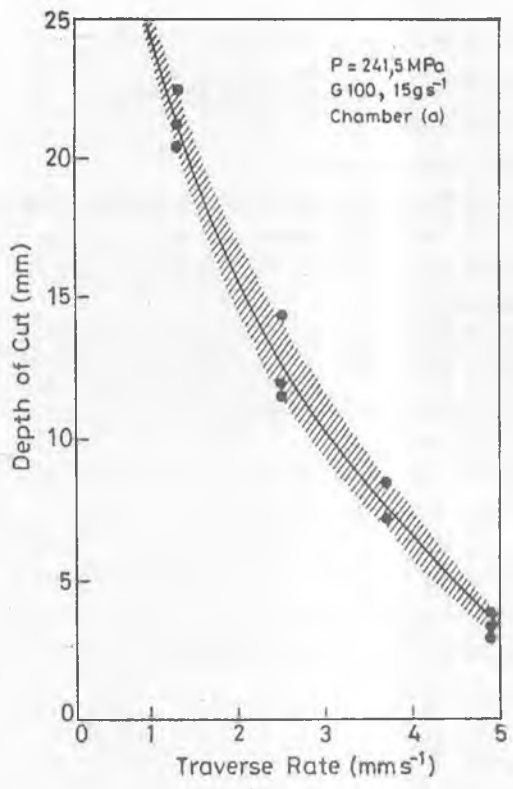


Fig. 6.5 Variation in depth of cut with a change in abrasive flow rate for various abrasive materials while using tool steel A2 as work material ($P = 207 \text{ MPa}$; $d_n = 0.051 \text{ cm}$; $u = 25 \text{ cm/min}$) [Hashish, 1986].

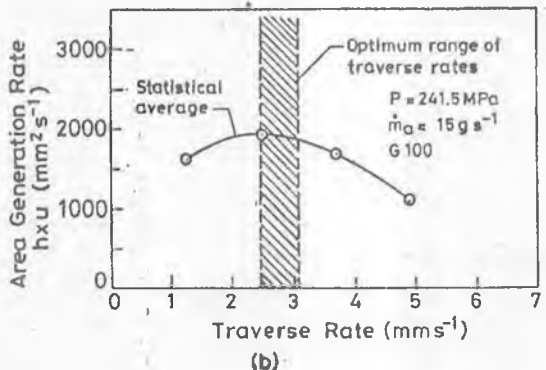
CUTTING PARAMETERS

Traverse Speed

A decrease in traverse rate (u) increases the depth of cut (Fig. 6.6a). However, if one goes below a minimum critical traverse rate there would be hardly any increase in the depth of cut. Fig. 6.6b shows an optimum traverse rate that exists for generation of a maximum kerf area (Traverse rate \times depth of cut). However, in case of mild steel, the rate of kerf (slot) area generation decreases with an increase in traverse speed beyond the optimum value.



(a)



(b)

Fig. 6.6 Effect of traverse rate on (a) depth of cut, (b) area generation rate [Hashish, 1982].

Number of Passes

Multiple passes can be employed in the following two different ways:

- (i) a single water jet with multiple passes, and
- (ii) multiple tandem AWJs with a single traverse (pass).

In case of a single water jet, whole power and quantity of abrasives are used by a single jet while in second case both the available power and the abrasives are divided among multiple jets. The distribution of power and abrasives among them are considerations for overall optimization.

Multiple pass cutting requires special catching and containment precautions because the initial pass cutting results in jet back flow and rebounding. Fig. 6.7 shows a relationship between number of passes and cumulative depth of cut.

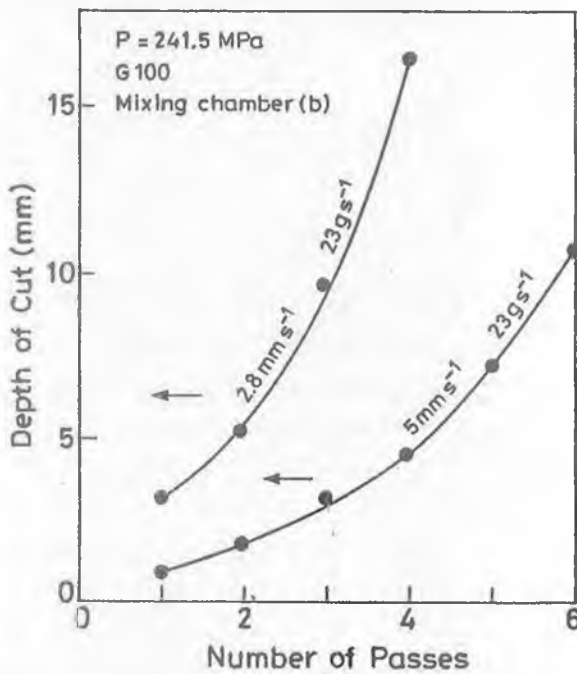


Fig. 6.7 Variation in depth of cut with a change in no. of passes (at high traverse rates) [Hashish, 1982].

It is also evident that as the number of passes increases, the slope of the curve also increases. This increase in slope has been attributed to the fact that the kerf

acts as a local mixing chamber that tends to focus the abrasive jet stream for more effective cutting. However, this effect is nullified in case of a greater cumulative depth at lower traverse rate by the effects of '*stand-off-distance*' (SOD) and kerf friction drag.

Stand-Off-Distance (SOD)

An increase in stand-off-distance rapidly decreases machined depth (Fig. 6.8). This has been explained by arguing that the liquid phase of the jet breaks up into droplets resulting in free abrasive particles. These free abrasive particles rebound upon impact that leads to a shallower penetration. There is an upper value of SOD beyond which the process will no longer do the cutting. However, in case of multi pass cutting the kerf made in the earlier passes helps the jet to remain intact. It is concluded that the smaller the stand-off-distance the deeper is the cut.

Hashish [1989] has developed a model to predict the depth of machining. It has been reported that the correlation coefficient between the predicted and experimental values for different materials is greater than 0.9. Two properties, viz. flow stress and critical velocity are found to be most significant (note that the flow stress has strong dependence on the modulus of elasticity) parameters.

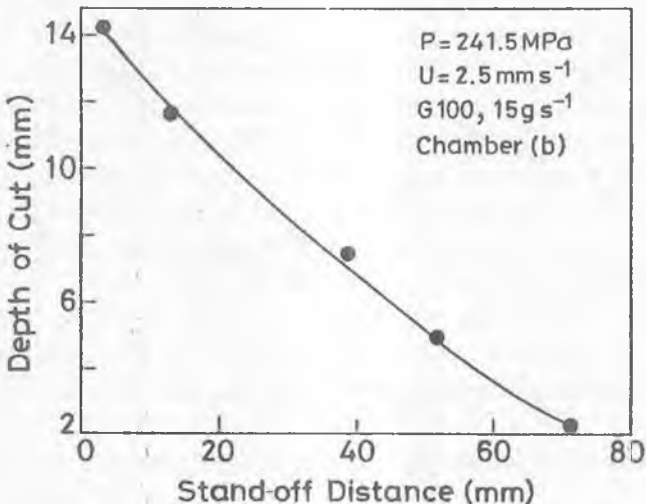


Fig. 6.8 Effect of stand-off-distance on depth of cut [Hashish, 1982].

Visual Examination

Visual examination of the process was conducted on lexan, lucite and glass as work materials with the help of a movie camera. The mechanism of material removal has been attributed to two modes: cutting wear mode that occurs at shallow angles of impact, and deformation wear mode which occurs at lower part of the cut at larger angles of impact. Nature of actual penetration of abrasive water jet in solids has been reported by Hashish [June 1988].

Fig. 6.9 shows a relationship between penetration rate and depth of cut as a function of machining time estimated from the sequence of photographs. It is found that a number of steps are formed below the steady state interface at the top. The step formation takes place as the jet traverses over the workpiece. Size of the step increases with the increase in the machined depth.

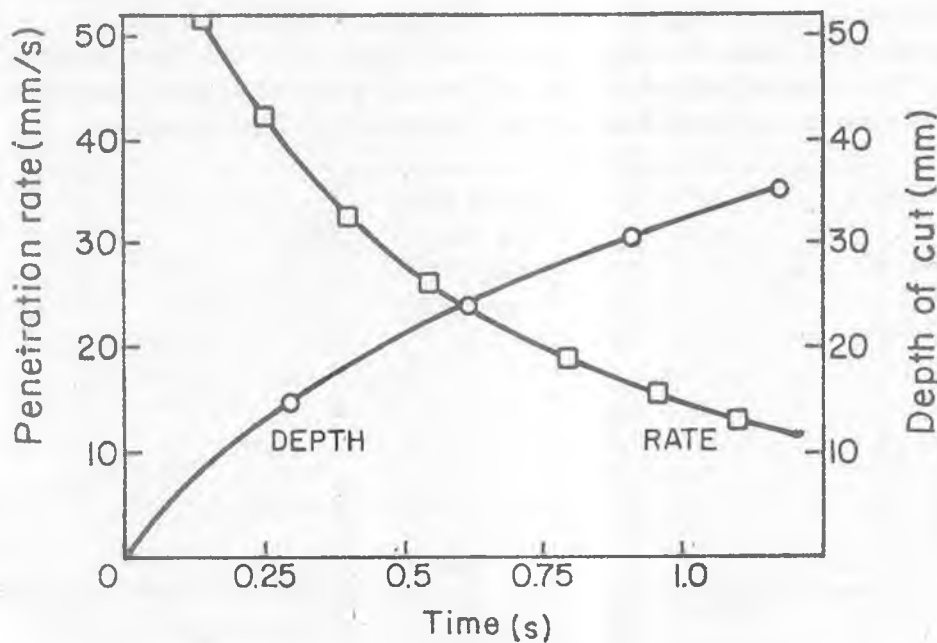


Fig. 6.9 Variation in depth of cut and penetration rate with machining time [Hashish, 1989].

PROCESS CAPABILITIES

AWJM process has been used to cut even thick materials (200 mm) with a narrow kerf. Width of the kerf depends upon the workpiece hardness. For hard materials, the kerf narrows down towards the bottom while the reverse is true in case of a soft material. Machined surfaces have not revealed [Benedict, 1987] the presence of any thermal or mechanical damage to them. In case of machining of glass, stray cutting may result in frosting.

APPLICATIONS

This process has been employed to cut a wide range of **materials** including both metals (copper and its alloys, lead, tungsten carbide, aluminium, etc), and non-metals (graphite, silica, glass, acrylic, concrete, etc). The process has been applied to machine the sandwiched honeycomb structural materials currently used in the aerospace industries. Its advantage is the capability of omnidirectional cutting having no burrs. The edges of structural aluminium plate have also been successfully cut. This technique is getting acceptance as a standard tool for cutting materials in a number of **industries** like aerospace, nuclear, oil, foundry, automotive, construction and glass. The specific advantages claimed by promoters of this technique are economic and environmental.

AWJ cutting has been employed for decommissioning **nuclear facilities**. The optimum performance has been reported with 0.38 mm jet at 200 MPa with an abrasive flow rate of 0.54 kg/min. In some cases, this technique has proved to be economical as compared to conventional bulk material removal methods.

Slotting is one of the common applications of AWJC. Various steels (stainless steel, mild steel, special alloy steel, etc) have been cut into different shapes like plate, tube, corrugated structure, etc. Kerf (slot) widths observed are in the range 0.75–2.25 mm. Roughness of the cut surfaces varies with the machined depth and abrasive water jet cutting parameters. It is also reported [Hashish, Oct-Sept. 1984] that no embedded abrasives were seen while examining the machined surfaces under Scanning Electron Microscope (SEM). Being a cold machining process, thermal stresses are not witnessed in the machined surfaces. Aluminium has also been cut successfully.

BIBLIOGRAPHY

1. Benedict G.F. (1987), *Nontraditional Manufacturing Processes*, Marcel Dekker Inc., New York.
2. Hashish M. (1982), The Application of Abrasive Jets to Steel Cutting, *Proc. 6th Int. Symp. Jet Cutting Technol.*, Guildford, England, pp. 447-464.
3. Hashish M. (1982), Steel Cutting with Abrasive Water Jets, *Proc. 6th Int. Symp. Jet Cutting Technol.*, Guildford England, pp. 465-487.
4. Hashish M. (1983), Experimental Studies of Cutting with Abrasive Water Jets, *Second U.S. Water Jet Symposium*, Rolla MO.
5. Hashish M. (1984), Cutting with Abrasive Water Jets, *Carbide Tool J.*, pp. 16-23.
6. Hashish M. (Sept., 1986), Aspects of Abrasive Water Jet Performance Optimization, *Proc. 8th Int. Symp. Jet Cutting Technology*, Durham (U.K.), pp. 297-308.
7. Hashish M. (June, 1988), Visualization of the Abrasive Water Jet Cutting Process, *Exptl. Mech.*, pp. 159-170.
8. Hashish M. (April, 1989), A Model for Abrasive Water Jet (AWJ) Machining, *Trans. ASME, J. Engg. Mater. Technol.*, Vol. 111, pp. 154-162.
9. Hashish M., Halter M. and McDonald M. (May, 1985), Abrasive Water Jet Deep Kerfing in Concrete for Nuclear Facility Decommissioning, *Proc. 3rd U.S. Water Jet Conf.*, held at Univ. of Pittsburgh (Ed. Dr. N. Styler), pp. 123-143.
10. Malkin S. (1989), *Grinding Technology: Theory and Applications of Machining With Abrasives*, Ellis Horwood, U.K.
11. Momber A.W. and Kovacevic R. (1998), *Principles of Abrasive Water Jet Machining*, Springer-Verlag London.

SELF-TEST QUESTIONS

- Q1. Write true (T) or false (F)
- (i) AWJM can't be applied to cut composite materials.
 - (ii) Physical and mechanical properties of workpiece material do not affect performance of AWJM process.
 - (iii) MRR obtained during AJM is higher than AWJM.
 - (iv) Life of a nozzle made of sapphire is as high as 400 hr.

(v) It is difficult to fabricate multiple jets central feed nozzle as compared to single jet side feed nozzle.

Q2. Choose correct answer from the given choices

- (i) In AWJM, process intensifier is used to
 - (a) increase the pressure of water,
 - (b) increase the flow rate of abrasives,
 - (c) increase the velocity of water jet,
 - (d) none of these.
- (ii) It is a finish machining process
 - (a) AWJM,
 - (b) AJM,
 - (c) USM,
 - (d) AFM.

REVIEW QUESTIONS

Q3. Write the names of various elements of AWJC machine and explain them, in brief.

Q4. Why a need is being felt to develop a system which can directly use slurry instead of mixing abrasives and water?

Q5. Answer the following questions, in brief.

(a) Some parts in an aerospace industry are made of asbestos. Because of high level of asbestos in the air (harmful to the health of workers) at cutting station, Osha shuts down Lockheed Georgia Company's mechanical cutting operation section.

You as incharge of the section, are asked to suggest two of the suitable advanced machining techniques so that the work can be resumed in this section.

(b) Composite plates are to be cut down into smaller pieces on large scale. Good finish is required. Which process(es) will you recommend?

(c) 5 mm diameter hole is to be drilled in a concrete block of a machine tool foundation. Which advanced machining process(es) would you recommend?

Q6. Write the differences (in table form) between WJM, AJM, AFM, and AWJM processes (working principles, applications, limitations, and merits of the processes).

NOMENCLATURE

d_g	grit size
d_n	nozzle diameter
K E	kinetic energy
m_a	abrasive mass flow rate
P	water jet pressure
P_c	critical water jet pressure
Q	water flow rate
s	mesh size
SOD	stand-off-distance
u	traverse rate
V_p	particle velocity

CHAPTER 6
AT-A-GLANCE
ABRASIVE WATER JET MACHINING
(AWJM)

INTRODUCTION

- JET OF MIXTURE OF WATER AND ABRASIVE PARTICLES REMOVES MATERIAL
- PRESSURE → 100 MPa. UPPER LIMIT OF VELOCITY → 900 m/s
- CUTTING IN UPPER PART OF KERF : EROSION ACTION
- CUTTING IN LOWER PART OF KERF : DEFORMATION
- USED TO MACHINE :
 - NON-METALS : CERAMICS, COMPOSITES, ROCKS, ETC
 - METALS : COPPER, ALUMINIUM, WC, LEAD, ETC
- OPERATIONS : DRILLING, CUTTING, DEBURRING, ETC
- CAN CUT ANY KIND OF MATERIAL, HIGH EDGE QUALITY, ADAPTABLE FOR REMOTE CONTROL, RECYCLING OF ABRASIVES, ETC

ELEMENTS OF AWJM SYSTEM

- PUMPING SYSTEM
- ABRASIVE FEED SYSTEM
- ABRASIVE WATER JET NOZZLE
- CATCHER

PUMPING SYSTEM

- INTENSIFIER → 415 M Pa, 75 HP MOTOR
- HIGH VELOCITY JET

ABRASIVE FEED SYSTEM

- DELIVERS DRY ABRASIVES
- TO CONTROL FLOW RATE → CONTROL ORIFICE DIAM.
- CANNOT SUPPLY ABRASIVES OVER LONG DISTANCES → USE DIRECTLY SLURRY → TO FEED OVER A LONG DISTANCE → MORE POWER REQUIRED
- WATER JET NOZZLE DIAM. → 75 TO 635 µm
- FOR LONG LIFE OF A NOZZLE → SAPPHIRE

ABRASIVE JET NOZZLE

- FUNCTIONS :
 - MIXING OF ABRASIVES & WATER
 - FORMING HIGH VELOCITY JET
- MATERIALS:
 - WC, BORON CARBIDE, SAPPHIRE
- TYPE:
 - SINGLE JET SIDE FEED NOZZLE
 - SIMPLE TO MAKE
 - RAPID WEAR OF EXIT PART
 - NON-OPTIMAL MIXING EFFICIENCY
 - MULTIPLE JETS CENTRAL FEED NOZZLE
 - CENTRALLY LOCATED ABRASIVE FEED SYSTEM
 - SURROUNDED BY MULTIPLE WATER JETS → CONVERGING ANNULUS
 - HIGHER NOZZLE LIFE & BETTER MIXING
 - DIFFICULT & COSTLY TO FABRICATE

CATCHER

- STATIONARY NOZZLE & MOVING WORKPIECE
 - + LONG NARROW TUBE PLACED UNDER THE POINT OF CUT
- MOVING NOZZLE & STATIONARY W/P
 - + A WATER FILLED SETTLING TANK UNDERNEATH THE W/P
 - + TRANSFER OF HIGH PRESSURE WATER
 - FLEXIBLE HOSE (PRESS. < 24 MPa)
 - RIGID TUBING (PRESS. > 24 MPa)

PROCESS PARAMETERS

- WATER → FLOW RATE AND PRESSURE
- ABRASIVES → TYPE, SIZE, AND FLOW RATE
- WATER NOZZLE AND ABRASIVE JET NOZZLE
- CUTTING PARAMETERS → FEED RATE AND STAND-OFF-DISTANCE
- W/P MATERIAL
- MIXING TUBE → DIAMETER & LENGTH
- ANGLE OF CUTTING
- TRAVERSE SPEED
- NUMBER OF PASSES

WATER JET PRESSURE

- CRITICAL PRESSURE (P_c) → BELOW THIS PRESSURE NO CUTTING
→ DIFFERENT FOR DIFFERENT WORKPIECE MATERIALS
- ABOVE A DEFINITE JET PRESSURE → MACHINED DEPTH TENDS TO STABILIZE
- RELATIONSHIP BETWEEN JET PRESSURE AND MACHINED DEPTH → STEEPER WITH HIGHER ABRASIVE FLOW RATE
- INCREASED PRESSURE → HIGHER NOZZLE WEAR RATE
- INCREASED PRESSURE → HIGHER COST OF PUMP MAINTENANCE
- INCREASED PRESSURE → LOWER EFFICIENCY

WATER FLOW RATE

- WATER → PROPELLING FLUID ENABLES HIGH ABRASIVE FLOW RATE (UP TO 5 kg/min)
- ABRASIVE VELOCITY → UP TO 300 m/s
- AWJs → COHERENT HENCE MORE SUITABLE FOR CUTTING

$$\bullet \quad Q\alpha\sqrt{p} \quad \bullet \quad Q\alpha d_n^2$$

ABRASIVE FLOW RATE

- MACHINED DEPTH $\propto (V_p^2 m)$
- ABOVE m_c → REDUCED MACHINED DEPTH
- INCREASE IN m → ↑ WEAR OF MIXING NOZZLE
↓ MIXING EFFICIENCY

ABRASIVE PARTICLE SIZE

- OPTIMUM PARTICLE SIZE
- FINER PARTICLES → FOR SHALLOW DEPTH OF CUT
COARSE PARTICLES → FOR HIGH DEPTH OF CUT
- DIFFERENT ABRASIVE SIZES FOR DIFFERENT DEPTHS OF CUT

ABRASIVE MATERIALS

MACHINED DEPTH → ϕ (TYPE OF ABRASIVE)

TRAVERSE SPEED

- OVERCUT DECREASES WITH AN INCREASE IN TRAVERSE SPEED
- TRAVERSE SPEED vs AREA GENERATION RATE HAS AN OPTIMUM

NUMBER OF PASSES

- MULTIPLE PASSES →
 - SINGLE WATER JET WITH MULTIPLE PASSES
 - MULTIPLE TANDEM JETS WITH SINGLE PASS
 - + INCREASE IN NUMBER OF PASSES → ↑ CUMULATIVE DEPTH
 - + KERF ACTS AS A LOCAL MIXING CHAMBER

STAND-OFF-DISTANCE

- ↑ STAND-OFF-DISTANCE → ↓ MACHINED DEPTH

↓

REBOUND OF PARTICLES

- BEYOND UPPER VALUE OF SOD → NO CUTTING
- SMALLER SOD → DEEPER CUT

VISUAL EXAMINATION

VISUAL EXAMINATION USING MOVIE CAMERA

↓

TWO MODES OF MATERIAL REMOVAL

- i) CUTTING MODE → SHALLOW ANGLE OF IMPACT
- ii) DEFORMATION MODE → LARGER ANGLE OF IMPACTS.

PENETRATION RATE AND DEPTH OF CUT → FUNCTION OF TIME

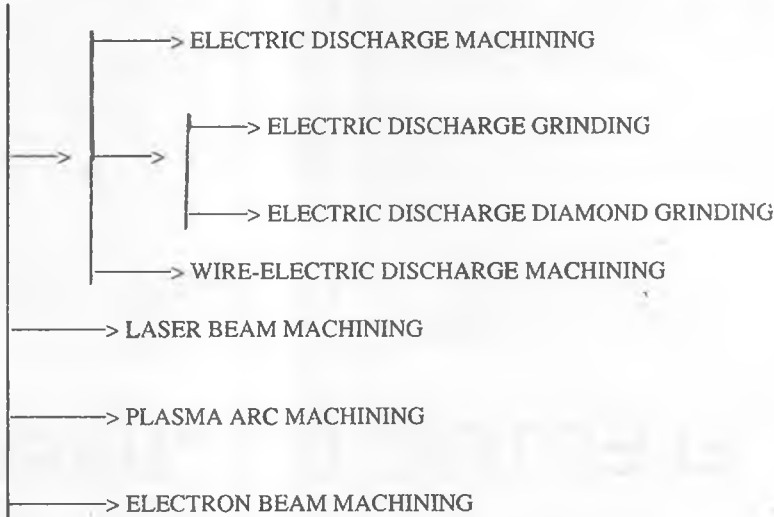
PROCESS PERFORMANCE

- CAN CUT THICK MATERIALS → UPTO 200 mm
- KERF WIDTH DECREASES AS W/P HARDNESS INCREASES
- MACHINED SURFACES → NO THERMAL / MECHANICAL DAMAGE
- MACHINING OF GLASS → STRAY CUTTING LEADS TO FROST SURFACE

APPLICATIONS

- METALS & NON-METALS BOTH
- OMNI-DIRECTIONAL CUTTING WITH NO BURRS
- INDUSTRIES → AEROSPACE, NUCLEAR, FOUNDRIES, CONSTRUCTION, ETC
- STEEL COMPONENTS CUT → PLATES, TUBES, CORRUGATED STRUCTURES, ETC

THERMOELECTRIC ADVANCED MACHINING PROCESSES



ELECTRIC DISCHARGE MACHINING (EDM)

INTRODUCTION

Whenever sparking takes place between two electrical contacts a small amount of material is removed from each of the contacts. This fact was realized and the attempts were made to harness and control the *spark energy* to employ it for useful purpose, say, for machining of metals. It was found that the sparks of short duration and high frequency are needed for efficient machining. Further, it was also observed that if the discharge is submerged in dielectric, the energy can be concentrated into a small area. A **relaxation circuit** (known as RC circuit) was

proposed in which electrodes (tool and workpiece) are immersed in the dielectric like kerosene, and are connected to the capacitor.

The capacitor is charged from a direct current (DC) source. Fig. 7.1a shows RC circuit and Fig. 7.1b shows voltage (V_{cl}) vs time, and current (i_{cl}) vs time relationships for a capacitor. As soon as the potential across the electrodes crosses the breakdown voltage (V_b), the **sparking** takes place at a point of least electrical resistance. It usually occurs at the smallest inter-electrode gap (IEG). After each discharge, capacitor recharges and spark appears at the next narrowest gap. Occurrence of each spark generates heat energy which is shared in different modes by workpiece, tool, dielectric, debris and other parts of the system, as shown in Fig. 7.2.

The dielectric serves some important functions, viz, cools down the tool and workpiece, cleans (or flushes away) the IEG, and localizes the spark energy into a small cross-sectional area. Energy content in each spark and frequency of sparking are governed by the conditions in the IEG.

WORKING PRINCIPLE OF EDM

EDM is a **thermoelectric process** in which heat energy of a spark is used to remove material from the workpiece. The workpiece and tool should be made of electrically conductive materials. A spark is produced between the two electrodes (tool and workpiece) and its location is determined by the narrowest gap between the two. Duration of each spark is very short. The entire cycle time is usually few micro-seconds (μs). The frequency of sparking may be as high as thousands of sparks per second. The area over which a spark is effective (or spark radius) is also very small. However, temperature of the area under the spark is very high. As a result, the spark energy is capable of partly melting and partly vaporizing material from localized area on both the electrodes, i.e. workpiece and tool. The material is removed in the form of *craters* which spread over the entire surface of the workpiece. Finally, the cavity produced in the workpiece is approximately the replica of the tool. To have machined cavity as replica of the tool, the tool wear should be zero. To minimize wear of the tool the operating parameters and polarity should be selected carefully.

Particles eroded from the electrodes are known as **debris**. Analysis of the debris has revealed that it is the mixture of irregular shaped particles (resulting from resolidification from the molten state) as well as hollow spherical particles

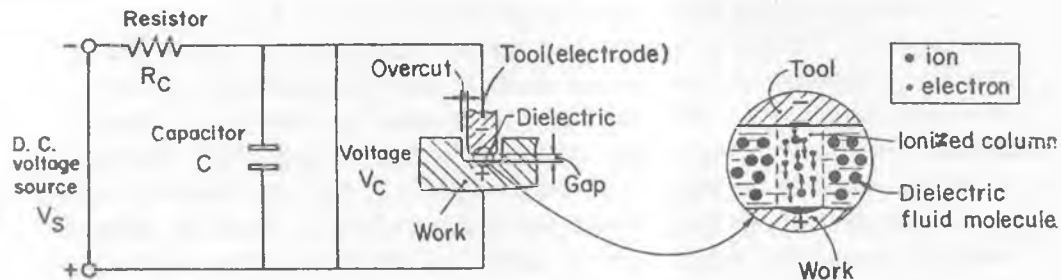
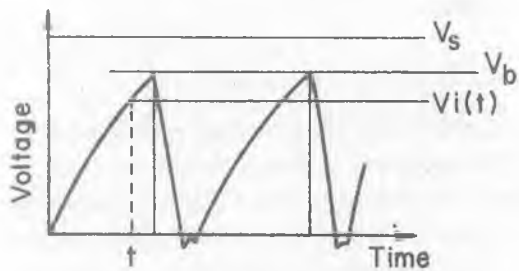
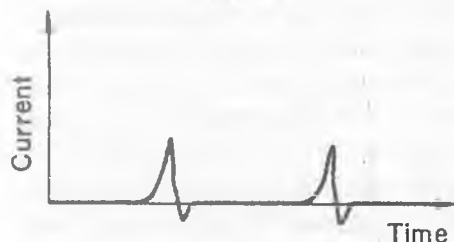


Fig. 7.1a A schematic diagram of electric discharge machining using relaxation circuit.



(b) (i)



(b) (ii)

Fig. 7.1b (i) Voltage vs time relationship, (ii) Current vs time relationship in EDM using relaxation circuit.

(resulting from the vapour condensation). Usually the amount of material eroded from the tool surface is much smaller than that from the workpiece surface. A very small gap (even lesser than hundredth of a millimetre) between the two electrodes is to be maintained to have the spark to occur. For this purpose, a tool driven by the servo system is continuously moved towards the workpiece.

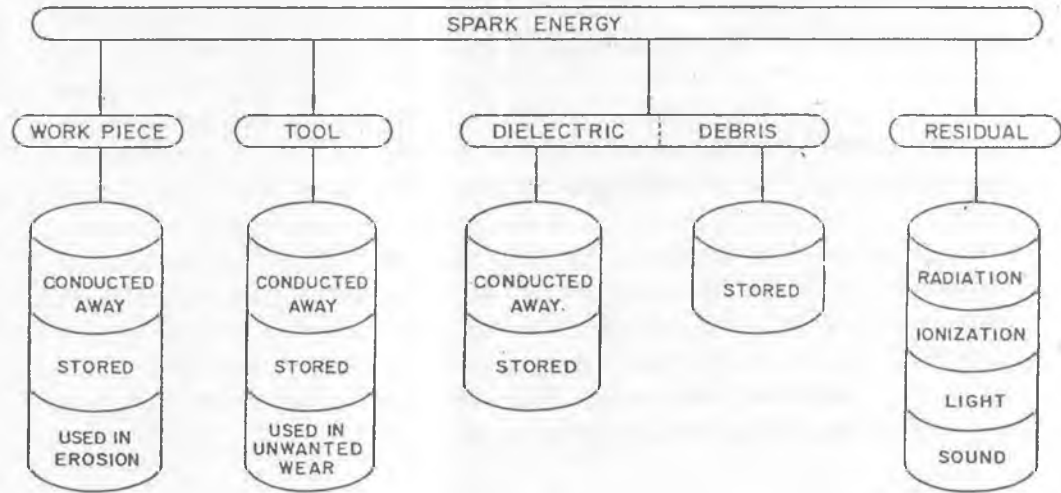


Fig. 7.2 Distribution of spark energy evolved during EDM.

During EDM, pulsed DC of 80–100 V at approximately 5 kHz is passed through the electrodes. It results in the intense electrical field at the location where surface irregularity provides the narrowest gap. Negatively charged particles (electrons) break loose from the cathode surface and move towards the anode surface under the influence of the electric field forces. During this movement in the IEG, the electrons collide with the neutral molecules of the dielectric (kerosene, water, or some other appropriate dielectric). In this process, electrons are also detached from these neutral molecules of the dielectric resulting in still more ionization. The **ionization** soon becomes so intense that a very narrow channel of

continuous conductivity is established. In this channel, there is a continuous flow of considerable number of electrons towards the anode and that of ions towards the cathode. Their K E is converted into heat energy, hence heating of anode due to the bombardment of electrons and heating of cathode due to the bombardment of ions, take place. Thus, it ends up in a momentary current impulse resulting in a **discharge** which may be an arc or a spark. The spark energy raises the localized temperature of the tool and workpiece to such a high value that it results either in melting, or melting as well as vaporization of a small amount of material from the surface of both electrodes at the point of spark contact. In fact, due to evaporation of dielectric the pressure in the plasma channel rises to a very high value (say, 200 atm.) and it prevents the evaporation of superheated metal. As soon as the off-time of a pulse starts, the pressure drops instantaneously allowing the superheated metal to evaporate. The amount of material eroded from the workpiece and the tool will depend upon the contributions (in the form of K E) of electrons and ions, respectively. The **polarity** normally used is straight (or normal polarity) in which the tool is -ve and workpiece is +ve, while in reverse polarity the tool is +ve and workpiece is negative (Fig. 7.3). Movement of the tool towards the workpiece is controlled by a servomechanism. The sparking takes place over the entire surface of the workpiece hence the replica of the tool is produced on the workpiece. Usually, a component made by EDM process is machined in two stages, viz *rough machining* at high MRR with poor surface finish, and *finish machining* at low MRR with high surface finish.

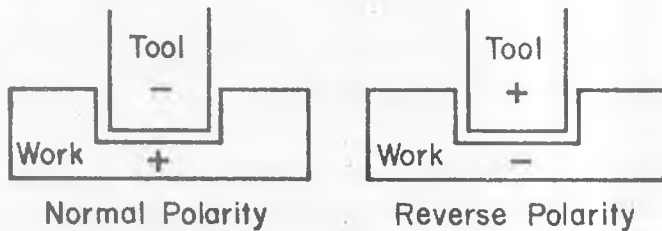


Fig. 7.3 Normal and reverse polarity in EDM.

RC PULSE GENERATOR

RC pulse generator is shown in Fig. 7.1. This generator has the following characteristics:

- Low material removal rate (MRR) because of long idle time (or charging time) and very short spark time.
- Improved surface finish, achieved during finish machining, is associated with further reduction in MRR.
- High tool wear rate (TWR).

From Fig. 7.4a, it is evident that the peak current attained in RC circuit is very high. This high value of peak current results in a very high temperature which is not required and it may also result in thermal damage to both the workpiece and the tool. **Controlled pulse generator** overcomes these problems [Bhattacharyya, 1971; and Pandey and Shan, 1980]. As shown in Fig. 7.4b, such generators can give low peak current, short idle time, and desired length of pulse, enabling us to select either rough machining conditions (high energy and low frequency of sparking), or finish machining conditions (low energy and high frequency).

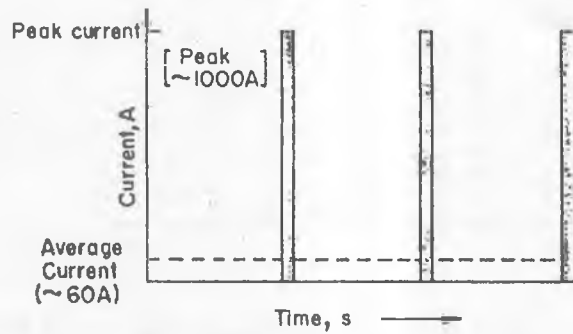


Fig. 7.4a Peak current attained and its rapid decline on spark initiation in RC circuit.

EDM MACHINE

EDM is one of the most popular non-traditional machining process used in various industries. Any EDM machine tool (m/t) has four major components, viz power supply, dielectric system, tool (electrode) and workpiece, and servosystem. Fig. 7.5 shows a schematic diagram of EDM system.

Power Supply

Power supply converts alternating current (AC) into pulsed direct current (DC)

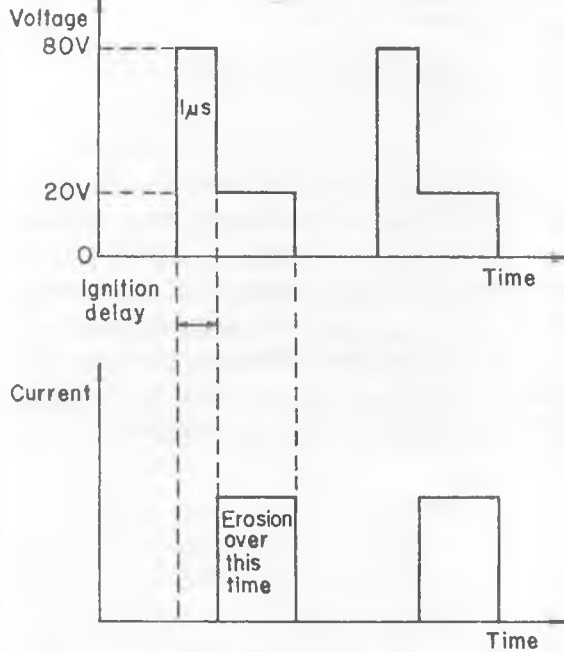


Fig. 7.4b Typical voltage and current characteristic for a controlled pulse generator.

used to produce sparks between tool and workpiece. Solid state **rectifier** is used to convert AC into DC. A fraction of DC power is used to generate a square wave signal with the help of a digital multi-vibrator oscillator. This signal triggers a bank of power transistors that act as high speed switches to control the flow of remaining DC power. It creates high power pulsed output responsible for generating sparks between the electrodes.

For a given input voltage, a spark can be generated only at or below a certain gap between the tool and workpiece. EDM power supply senses the voltage between the electrodes and then sends the relevant signals to the **servosystem**, which maintains the desired gap value between the electrodes.

Power supply should also be able to control the **parameters** like voltage, current, duration and frequency of a pulse, duty cycle (the ratio of on-time to pulse-time), and electrode polarity. Duty cycle (or duty factor) controls the amount of

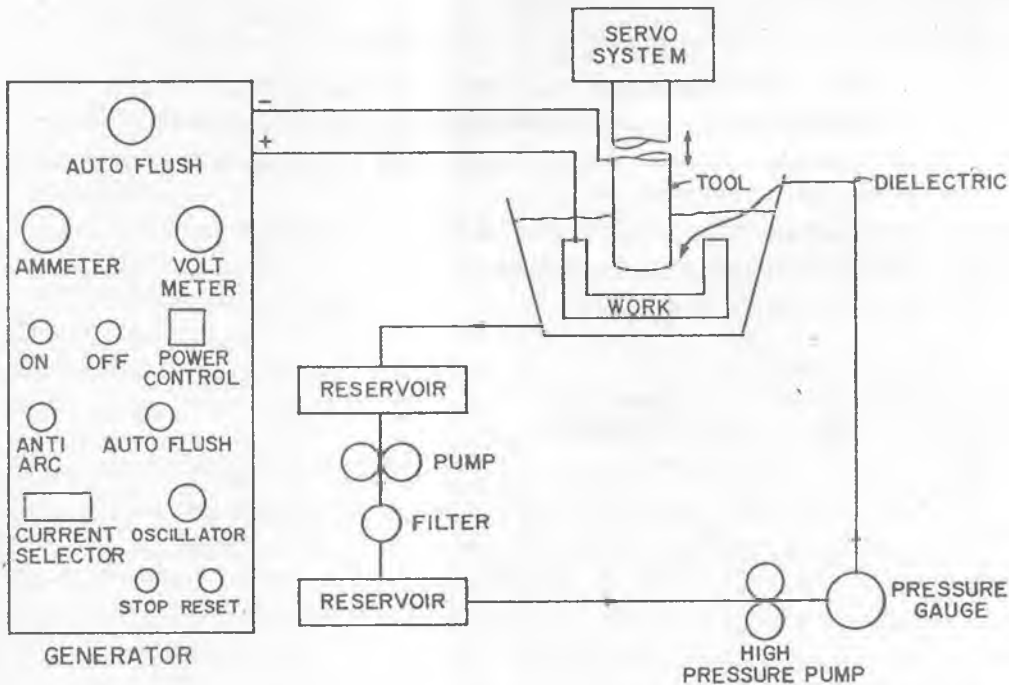


Fig. 7.5 Schematic diagram of EDM system.

time the energy is on during each pulse (Fig. 7.6). EDM power supplies are also equipped with cut-off protection circuit. As soon as an arc, due to a short circuit between the electrodes, occurs the cut-off circuit terminates the power. The power is also cut-off due to overvoltage and overcurrent.

During EDM, one of the four states can occur, i.e. normal discharge, free discharge (arc), short circuit and open circuit. The pulse detection and discrimination have been treated as a "pattern recognition" problem [Dauw *et al.*, 1983]. EDM-pulse discriminator (EDM-PD) has been developed for this purpose. Variation in voltage with time has been used as a basis to identify the type of the discharge that occurs at a particular moment.

Dielectric System

It consists of dielectric fluid, reservoir, filters, pump, and delivery devices. A good **dielectric fluid** should possess certain properties, viz , it should:

- (i) have high dielectric strength (i e remain electrically non-conductive until the required breakdown voltage between the electrodes is attained),
- (ii) take minimum possible time to breakdown (i e ignition delay time) once the breakdown voltage is reached,
- (iii) deionize the gap immediately after the spark has occurred,
- (iv) serve as an effective cooling medium, and
- (v) have high degree of fluidity.

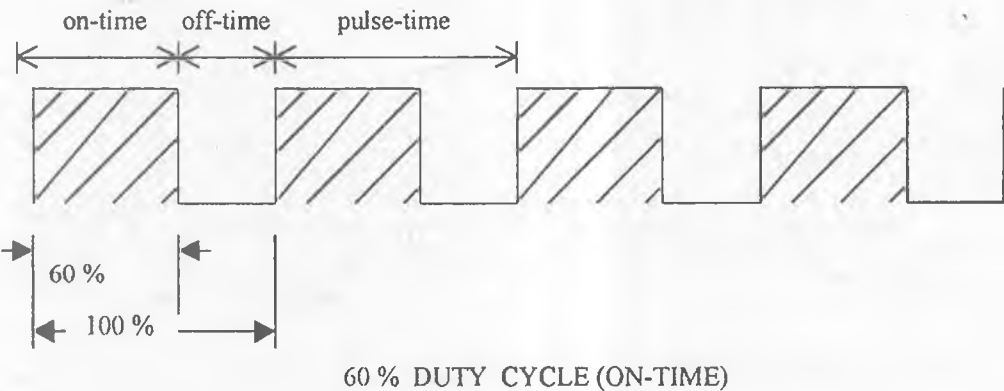


Fig. 7.6 An illustration of on-time, off-time, pulse time and duty cycle.

The fluids commonly used as dielectric are transformer oil, paraffin oil, kerosene, lubricating oils, and deionized water. **Deionized water** gives high MRR and functions as more effective cooling medium but also causes high electrode wear rates. Further, it suffers from the drawback of causing corrosion. To overcome this problem inhibitors are used but they result in increased electrical conductivity to an unacceptable level.

Deionized water is commonly used as dielectric in wire-EDM and drilling of small diameter holes. **Filtration** of dielectric fluid before re-circulation is highly essential so that a change in its insulation qualities during the process is minimal. Dielectric is filtered to remove debris as fine as $2\mu\text{m}$ [Albert, 1981].

The concentration of the debris particles in the gap increases rapidly as the machining progresses. These wear particles should be removed from the gap so that fresh dielectric enters the IEG for spark discharges. Increase in the pollution of dielectric results in decrease in the breakdown intensity of the field [Bruyn, 1970]. Hence, IEG at the entrance of the clean fluid is much narrower than at the exit of the flow. This significantly affects the reproduction accuracy of the process. It is possible to correct such errors only if it could be feasible to predict quantitatively the error of shape. However, complex shaped electrodes with sharp edges or protruding points further add for poor reproduction accuracy. Hence, the flushing is decisive for process efficiency and product quality.

Effective flushing of dielectric removes by-products from the gap. Ineffective flushing results in low MRR and poor surface finish. The effective flushing may increase MRR as much as by a factor of 10 or so [Koshy et al, 1993]. Poor flushing ends up with stagnation of dielectric and build-up of machining residues which apart from low MRR also lead to short circuits and arcs. A good flushing system is the one that shoots the dielectric to the place where the sparking occurs. It is felt that adequate flushing in case of blind cavities is difficult.

Various methods have been proposed by different researchers [Masuzawa et al, 1983; Erden, 1982; Kremer et al, 1985; Bruyn, 1970 and deBryun, 1978] to ensure proper and adequate **flushing** of the gap and thereby obtain a better process output. Suction through electrodes, pressure through electrodes, jet flushing, alternating forced flushing, ultrasonic vibration of electrodes, and rotating electrode flushing [Koshy et al, 1993] are some of the dielectric flushing techniques (Fig. 7.7) reported in the literature. It is also reported [Albert, 1981] that more than one mode of flushing may be used for effective cleaning of the gap. In some cases, hypodermic needles have been used as nozzles for flushing in tight quarters.

In case of **machining of blind cavities**, flushing through a hole in the tool is most effective but it gives rise to protruding bump (or spike). This is the situation similar to the one faced during ECM [Sreejith et al, 1994]. To avoid this problem, a rotating tool with an eccentric hole (off-centred holes) for dielectric supply can be used. Jet flushing is less effective hence it should be used only when none of the other methods can be used due to tool or workpiece configuration. In case of inflammable dielectric fluids, the workpiece should always be immersed in the dielectric fluid to minimize any chance of accidental fire. As machining continues, the dielectric gets contaminated with more and more amount of debris. Pres-

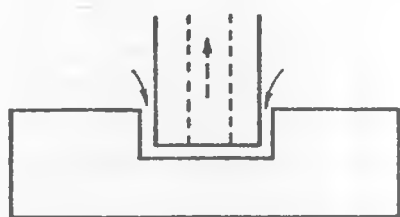
ence of such debris in the IEG, results in bridging the gap. It yields more number of arcs. Arcs are undesirable in EDM because they damage both tool and workpiece. Occurrence of such arcs can be eliminated by proper filtration of the dielectric as well as appropriate flushing of the IEG.

Electrodes

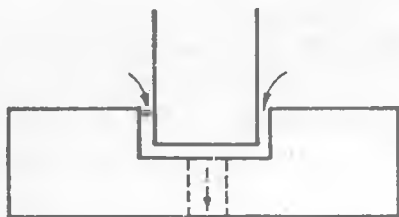
Both tool and workpiece are electrodes in EDM. However, in general, the word 'electrode' is used only for tool. The **material** to be used as tool electrode should possess desirable properties like easily machinable, low wear rate, good conductor of electricity and heat, cheap, and readily available. Graphite (easily machinable, low wear rate, and high conductivity), copper, brass (highly stable and relatively low wear rate), copper tungsten (low wear rate, expensive, and cannot be easily shaped), cast aluminium, copper boron, and silver tungsten are some of the materials that are used for making the tools for EDM. However, copper and graphite are more commonly used because they can be easily machined. A graphite electrode with finer grains results in lower TWR (Tool Wear Rate), better surface finish, and higher MRR. However, its brittleness is an undesirable characteristic because of which it is prone to breakage.

During electro-spark sinking operation, overcut is unavoidable. Electrode **shape degeneration** due to uncontrolled wear of tool is a serious problem encountered during EDM. The problem is difficult due to unequal degeneration of geometrical form of the tool. This deterioration in electrode shape cannot be compensated by overfeeding the roughing electrode as is true in case of electrode with shorter length. As a result, higher '*finishing allowance*' (volume) will be provided leading to the higher time required for finishing cut during EDM.

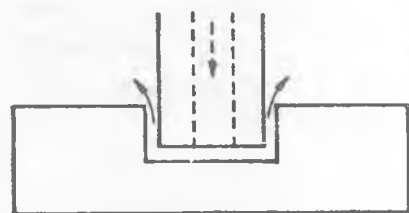
As discussed above, *erosion of tool electrode is inevitable*. Recent developments in pulse shape and tool material, and selection of proper machining conditions have led to very low electrode wear rate. Hence, it is a normal practice to have the tool electrode, for finish electro-discharge machining, conferring closer to the required shape and size of the workpiece. The tool gets tapered and its corners rounded off due to shape degeneration during EDM. Fig. 7.8a shows **overcut** obtained during electro-discharge drilling (EDD) operation. Its value is governed by machining parameters, work material, and also tool material. Overcut should be taken care of at the stage of tool design.



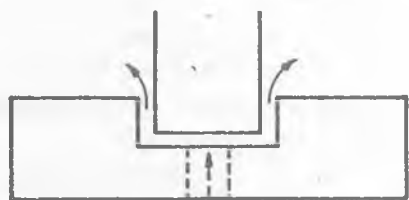
(a)



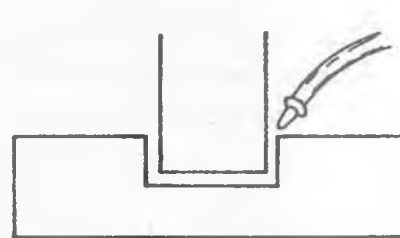
(b)



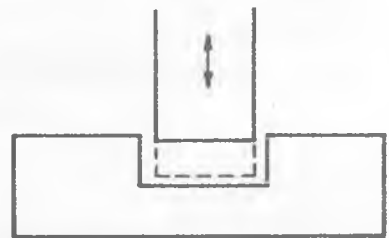
(c)



(d)



(e)

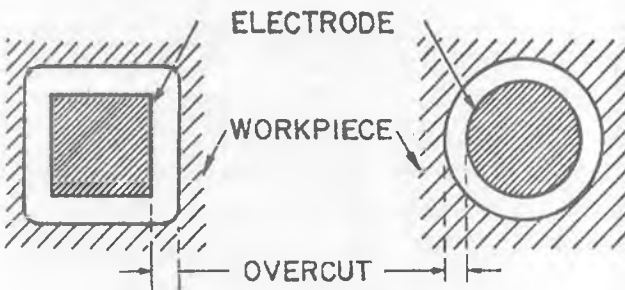


(f)

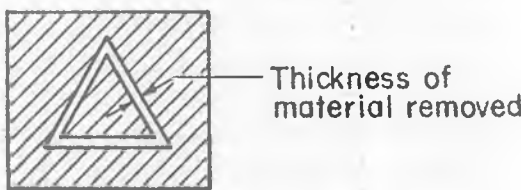
Fig. 7.7 Various methods for dielectric flushing: (a) suction through electrode, (b) suction through workpiece, (c) pressure through electrode, (d) pressure through workpiece, (e) jet flushing, (f) periodic cycling of electrode [HMT, Bangalore, Catalogue].

The model developed [Jain, 1989] for the prediction of tool electrode wear lacks in generality mainly because of involvement of so many variables. As the electric field density is highest at the corners, they wear (or round off) faster than the remaining part.

The tool wear is usually quantified by ‘wear ratio’ (ratio of the volume of tool material removed to the workpiece material worn out during the same period). Electrode wear is more at the corners/edges than the rest of the tool. Depending upon the tool and workpiece materials, machining conditions, and type of operation, the wear ratio may vary in the range of 0.05:1 to 100:1. Under certain situations, a through hole may be produced by employing trepanning operation (Fig. 7.8b) rather than drilling because it is very fast compared to the drilling. In electro spark trepanning operation, only a small thickness of material around periphery of the cavity is removed by machining in place of removing the material equal to the volume of through hole during electric discharge drilling (EDD).



(a)



(b)

Fig. 7.8 (a) Schematic diagram for overcut obtained during electric discharge drilling (EDD), (b) trepanning operation.

Servo system

A servo system is used to maintain a predetermined gap between tool and workpiece. There is a gap voltage sensor in power supply, which sends signals to the servo system. As soon as it senses that the gap between the electrodes has been bridged by some electrically conductive material, a signal will be sent to the servo system to reverse its direction. The servo system will keep the tool reciprocating towards the workpiece until the dielectric fluid flushes the gap, and clears it off the electrically conductive material. If the dielectric flushing system is inefficient in cleaning the cutting gap, the machining cycle time will be long and vice versa. Two of the requirements of the servo system are sensitivity for small movements, and enough power to overcome weight of ram, electrode, and flushing forces.

Electrode Refeeding

Tool wear during EDD also reduces length of the tool. For accurate machining, the reduced length must be compensated; otherwise the length of each successive hole to be drilled will be shorter than the desired one. Simple way to overcome this problem is to estimate the amount by which the electrode length is reduced after drilling each hole and, in turn, to increase the infeed by this amount each time. However, even a small error will finally compound into a large error after drilling a large number of holes using the same tool. Another method used is electrode refeeding in which the tool, after drilling a hole, is brought back every time to the reference point wherefrom the depth of drilling is measured. The electrode refeeding can be done manually or automatically.

CNC-EDM

Computer numerical control (CNC) of EDM m/t has made it very efficient and versatile. Tolerance up to $25 \mu\text{m}$ are easily achieved [Albert, 1982]. It offers the provision of fine finish settings which flatten the microscopic peaks on the EDM'd surface. It eliminates the bench-work by proper selection of EDM parameters. Helical gears have been made [Albert, 1982] with relative ease by using the canned cycles. With CNC-EDM, it is possible to run jobs unattended overnight or several days together. It is also possible to minimize the setting up time. Operator needs not to babysit the EDM m/c and hence can use his/her time elsewhere in a

more productivity way, viz planning of another job. This is possible because of **adaptive control (AC)** of CNC-EDM. It monitors power supply parameters, as well as does sampling of electrical conditions versus time for each pulse so that the m/t can be protected against arcing. By the use of CNC, mechanical orbiters have been replaced by software orbiters by which orbiting pattern of any shape can be programmed. Orbiting electrodes agitate the dielectric fluid which results in a better flushing. Exploiting CNC-EDM with AC facility, the m/t can be programmed to retract electrode from the workpiece periodically so that the flow of clean fluid takes place into the gap. Thus, improved flushing works hand-in-hand with adaptive control. By the use of CNC-adaptive control, it is possible to monitor and control the discharge energy which will permit to machine at '**no-wear setting**', which improves the repeatability of the process.

Automatic tool changer (ATC) is the most recent innovation in which many tools are mounted on the tool holder and stored in a carousel (or a magazine) until called for by the CNC program. The ATC employed on EDM machines makes it possible to change electrodes automatically in any programmed sequence, and with minimum loss of production time. Hence, one can load the tools for rough, semifinish, or finish cuts. EDM with CNC can employ a DC servo drive for quill (or tool) rotation, which is fourth axis (c-axis) rotation. **CNC-EDM** [*Quinlan, 1983; Albert, 1983*] has a 16-station automatic tool changer. CNC feature is utilized to run the machines unattended for days together. Whenever a specific tool is required, automatic tool changer (or a lever arm) exchanges the used tool with the new tool to be used. This helps in reducing the tool change time even for different hole shapes or cavities to be machined. Nowadays, CNC-EDM machines, in advanced industries, are more popular than conventional type of EDM machines.

Recent systems have automatic **electrode-zeroing** feature [*Anon, 1981*]. Sensors automatically determine the correct starting point, i.e zero point. All the time, the cutting starts from zero. This facility permits for compensation for the wear of electrode so that the depth is controlled accurately on the successive batches of production. Further, with today's CNC-EDM systems, programming is easier and faster because they are **menu driven** and utilize English language, prompts and commands. Some of the systems have graphic display facility as well. Some other program-controlled features associated with CNC-EDM are *centering, edge finding, flushing and slope compensation*.

ANALYSIS

Analysis of R-C Circuits

Charging voltage and charging current

The relaxation type circuit (Fig. 7.9) consists charging, and discharging circuits. The charging current (i_{ct}) flowing in charging circuit at time 't' is given by

$$i_{ct} = \frac{V_o - V_{ct}}{R_c}, \quad \dots(7.1)$$

Also,

$$i_{ct} = C \frac{d V_{ct}}{d t}, \quad \dots(7.2)$$

where, V_o is the supply voltage, and V_{ct} is the charged voltage of the condenser at time 't'. R_c is charging resistance and C is capacitance of the condenser.

From the above,

$$\frac{d V_{ct}}{V_o - V_{ct}} = \frac{1}{R_c C} d t. \quad \dots(7.3)$$

Now, integrate both sides,

$$\ln(V_o - V_{ct}) = -\frac{t}{R_c C} + K_1, \quad \dots(7.4)$$

where, K_1 is a constant of integration. Use the boundary condition ($V_{ct} = 0$ at $t = 0$) to evaluate K_1 . It gives

$$K_1 = \ln V_o. \quad \dots(7.5)$$

Substitute the value of K_1 in Eq. (7.4) and simplify to get

$$V_{ct} = V_o \left(1 - e^{-t/R_c C}\right) \quad \dots(7.6)$$

The time required by the condenser to attain 0.638 times of its charging voltage ($= 0.638 V_o$) is called "time constant" ($\tau = R_c C$).

Substitute the value V_{ct} from Eq. (7.6) in Eq. (7.1) and simplify to get Eq. (7.7).

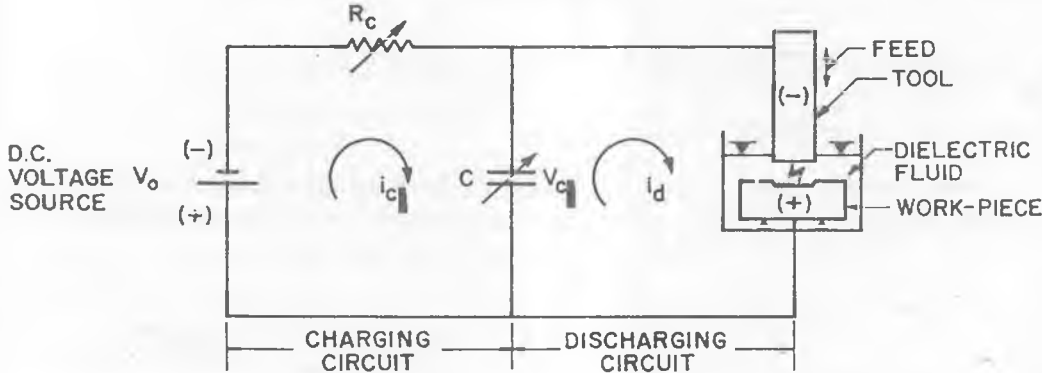


Fig. 7.9 Various parts of a relaxation circuit.

$$i_{cl} = \frac{V_o}{R_c} \left(e^{-t/R_c C} \right) \quad \dots(7.7)$$

Power Delivered to the Discharging Circuit

The energy delivered to the discharging circuit at any time t is given by

$$d E_n = i_{cl} V_{cl} d t.$$

Substituting the values of V_{cl} and i_{cl} from Eqs. (7.6) and (7.7) respectively in the above equation, we get

$$d E_n = \frac{V_o}{R_c} \left(e^{-t/R_c C} \right) \cdot V_o \left(1 - \left(e^{-t/R_c C} \right) \right) dt. \quad \dots(7.8)$$

Integrate Eq. (7.8) to get

$$E_n = \frac{V_o^2}{R_c} \left[-t e^{-t/\tau} + \frac{\tau}{2} e^{-2t/\tau} \right] + K_2 \quad \dots(7.9)$$

where, $\tau = R_c C$. K_2 is a constant, and can be evaluated by using the boundary condition ($E_n = 0$ at $t = 0$). Substitute the value of K_2 in (7.9) to get

$$E_n = \frac{V_o^2 \tau}{R_c} \left[\frac{1}{2} + \frac{1}{2} e^{-2\tau/\tau} - e^{-\tau/\tau} \right]. \quad (7.10)$$

Suppose the energy E_n is delivered to the discharging circuit for time $\tau_c (= t)$ then the average power delivered (P_{avg}) is given by

$$P_{avg} = \frac{E_n}{\tau_c} = \frac{V_o^2}{R_c x} \left[\frac{1}{2} + \frac{1}{2} e^{-2x} - e^x \right], \quad ... (7.11)$$

where, $x = \tau_c/\tau$. The condition for the maximum power to be delivered to the discharging circuit is given by

$$\frac{dP_{avg}}{dx} = 0. \quad ... (7.12)$$

After solving Eq. (7.12), we get $x = 1.26$. Substitute this value of x in Eq. (7.6).

$$V_{ct} = V_o(1 - e^{-1.26}) \approx 0.72 V_o. \quad ... (7.13)$$

Thus, the discharging voltage for the maximum power delivery is about 72% of the supply voltage (Fig. 7.10). In other words, for maximum power delivery through the gap, the breakdown voltage and the supply voltage should follow the following relationship:

$$V_b \approx 0.72 V_o.$$

Current in the Discharging Circuit

Let R_s represent the sparking resistance (other resistances are assumed to be negligible hence neglected). Then the current i_d at any time 't' is given

$$i_d = -\frac{dq}{dt} = -C \frac{dV_{ct}}{dt}. \quad ... (7.14)$$

$$i_d = \frac{V_{ct}}{R_s}. \quad ... (7.15)$$

Also,

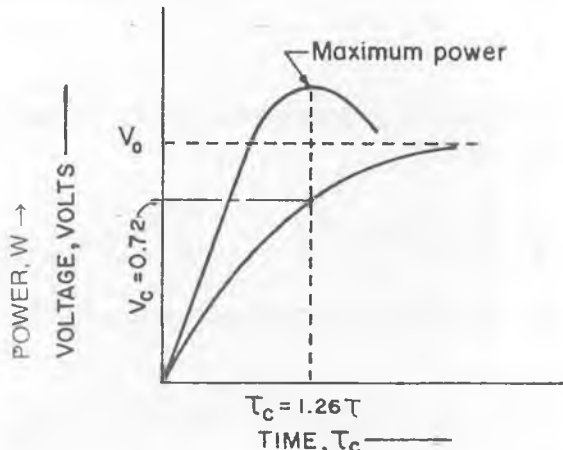


Fig. 7.10 Schematic diagram showing the condition for maximum power delivery for the RC circuit.

Therefore,

$$\frac{V_{ct}}{R_s} = -C \frac{dV_{ct}}{dt},$$

or,

$$\frac{dV_{ct}}{V_{ct}} = -\frac{dt}{R_s C}.$$

After integration of the above equation,

$$\ln V_{ct} = -\frac{t}{R_s C} + K_3.$$

Constant K_3 is evaluated using the boundary condition, $V_{ct} = V_{co}$ at $t = 0$.

$$K_3 = \ln V_{co}.$$

Therefore,

$$V_{ct} = V_{co} e^{-t/R_s C}.$$

Hence,

$$i_d = \frac{V_{ct}}{R_s} = \frac{V_{co}}{R_s} e^{-tR_s C}$$

...(7.16)

Energy dissipated across the IEG is given by

$$W_d = \frac{1}{2} C V_b^2$$

...(7.17)

where, V_b is breakdown voltage.

Material Removal Rate in RC Circuit

Eq. (7.6) can be rewritten as

$$t = R_c C \ln \left(\frac{1}{1 - V_{ct}/V_o} \right).$$

Frequency of charging (f_c) is given by

$$f_c = \frac{1}{t} = \frac{1}{R_c C} \left[\frac{1}{\ln \frac{1}{(1 - V_b/V_o)}} \right].$$

Material removal rate should be proportional to the total energy delivered in the sparking per second.

$$MRR \propto \frac{1}{2} C V_b^2 f_c$$

Substitute the value of V_b and f_c , and let K_4 be a constant of proportionality. Then,

$$MRR = K_4 C V_b^2 \cdot \frac{1}{R_c C} \left[\frac{1}{\ln \frac{1}{(1 - V_b/V_o)}} \right].$$

Thus, $MRR \propto 1/R_c$, i.e. R_c should be decreased to increase MRR, however, at very low value of R_c , it will result in arcing. The minimum value of the resistance (R_c) that will prevent arcing is known as **critical resistance**.

Value of the critical resistance can be proved [Bhattacharyya, 1973] to be equal to

$$R_{\min} = \sqrt{\frac{L}{C}}.$$

Above equation is not obeyed during experiments. Based on the experimental results, it is found that

$$R_{\min} \geq 30 \sqrt{\frac{L}{C}}.$$

Surface Finish

In EDM, each spark results in approximately spherical crater formation on the surface of the workpiece. Hence, the centre line average (H) value of surface finish will be a function of crater depth (h) and frequency of sparking (f_c).

$$H \propto \frac{h}{f_c}.$$

The volume of the material removed ($\propto h^3$) per discharge will be proportional to the energy delivered during sparking ($= CV_b^2 / 2$). Hence,

$$h^3 \propto \frac{1}{2} C V_b^2$$

or,
$$h \propto C^{1/3} V_b^{2/3}.$$

Therefore,

$$H \propto \frac{V_b^{2/3} C^{1/3}}{f_c},$$

$$H = \frac{K_5 V_b^{2/3} C^{1/3}}{f_c}.$$

But, $f_c \propto R^{-m} C^{-n}$ (for RC type circuit).

Therefore,

$$H = K_6 V_b^{2/3} C^{n+1/3} R^m.$$

However, from different experimental results it is concluded that

$$H = K_7 V_b^{0.5} C^{0.31 \sim 0.36}$$

PROCESS VARIABLES

An increase in current results in increased MRR as well as increased value of surface roughness (Figs. 7.11a and 7.11b). Similar effect is also observed when spark voltage (or breakdown voltage) is increased. However, an increase in spark frequency results in an improved surface finish (Fig. 7.11c). Since the energy available for material removal during a given period of time is shared by a larger number of sparks, the size of the crater is reduced. The inter-electrode gap (12-50 μm) is determined by the gap current and gap voltage. A decrease in the gap results in lower MRR, better surface finish, and higher accuracy. Further, an increase in pulse duration (ranging from few μs to several ms) decreases MRR (Fig. 7.12a) as well as deteriorates surface finish (Fig. 7.12 b). Increase in pulse duration decreases the **relative electrode wear (REW)** (7.12c)

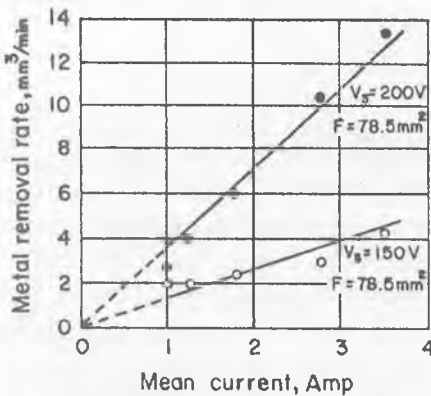
$$\left(\text{REW} = \frac{\text{vol. of tool eroded over the test duration}}{\text{vol. of work eroded over the test duration}} \times 100 \right).$$

Fig. 7.12a shows the relationship between MRR and pulse duration for different current values and electrode material with different polarities. A decrease in MRR with increase in pulse duration is attributed to unsteady machining conditions observed for pulses greater than 20 μs .

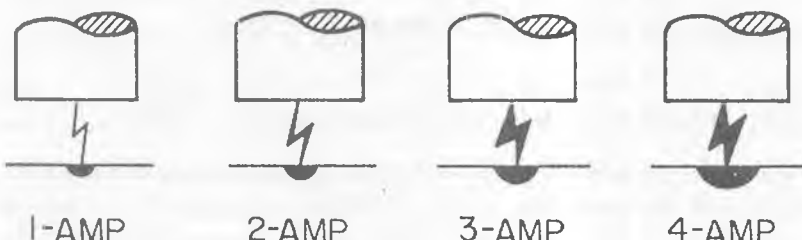
Fig. 7.12b shows that copper tools, in general, yield better surface finish as compared to brass. Experiments have also been conducted using tap water and the mixture of tap and distilled water as dielectric during EDM. Fig. 7.12c shows the relationship between REW and pulse duration. In case of copper electrode with negative polarity for the specified conditions, there seems to be a pulse duration for which REW is negative due to metal deposition. However, no appropriate explanation exists for this.

The plasma channel diameter in EDM varies along the gap with time [Shankar et al., 1997] (Fig. 7.13). It has been reported [deBruyn, 1978] that major part of the tool erosion occurs during first few microseconds of the pulse. Hence, use of a pulse with low initial current could reduce tool wear.

Pulsed power for EDM can be obtained either by using relaxation circuit or high power transistor circuit. In the first case, the spark energy is directly related to the inter-electrode gap characteristics during charging period (pause/off



(a)



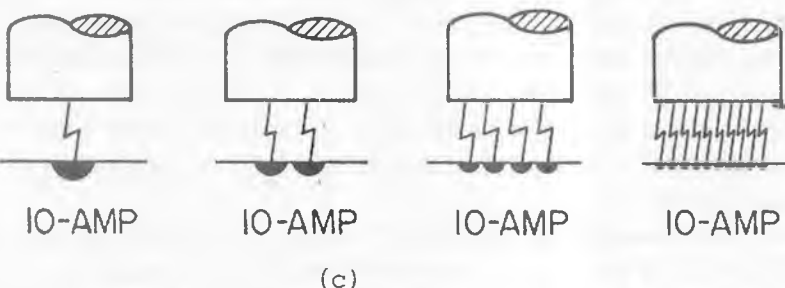
1-AMP

2-AMP

3-AMP

4-AMP

(b)



10-AMP

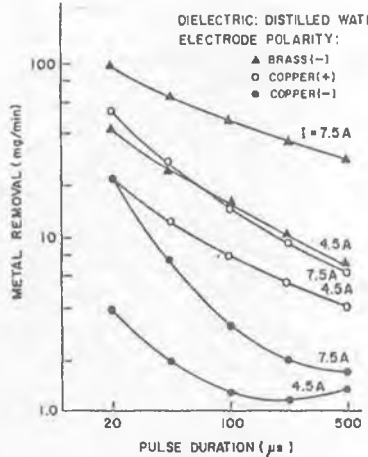
10-AMP

10-AMP

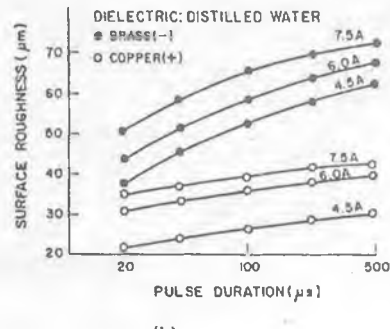
10-AMP

(c)

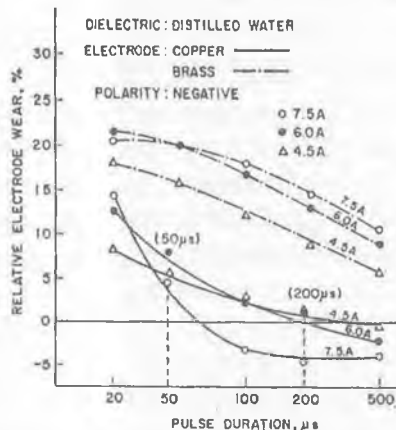
Fig. 7.11 (a) Effect of mean current on MRR; dielectric = Kerosene, tool = brass, work = low carbon steel, F = tool electrode area [Pandey and Shan, 1980], (b) Effect of current during sparking on surface finish. (or crater size), (c) Effect of frequency of sparking on surface finish.



(a)



(b)



(c)

Fig. 7.12 Effect of pulse duration on (a) material removal rate (mg/min), (b) surface finish, (c) relative electrode wear [Jilani and Pandey, 1984].

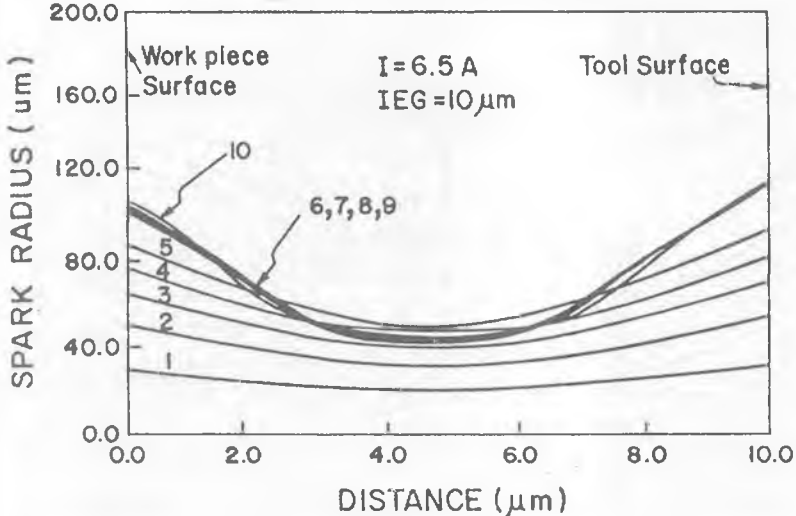


Fig. 7.13 Theoretical plasma channel radius variation in the gap with time (1 μ s to 10 μ s) [Shankar *et al.*, 1997]

period). Dielectric (say, tap water) which would give low breakdown potential will give low energy stored in the condenser hence low energy per spark.

In case of **EDM generators** with high power transistor circuits, the use of tap water and deionized water as dielectric has been made [Godinho and Noble]. Use of water as dielectric makes the EDM process more safe (i.e. without any risk of fire or explosion). Specially in case of deep electric discharge machining, the use of water as dielectric in place of mineral oil has shown improved results (Fig. 7.14).

Dielectric Pollution and its Effects

Dielectric during EDM may get polluted due to erosion of tool and workpiece, and decomposition of the dielectric itself. **Dielectric contamination** has been reported [Erden and Bilgin, 1980] to influence breakdown, time lag (or ignition delay), short circuit, machined surface characteristics, spark gap and machining rate (or machining performance in general).

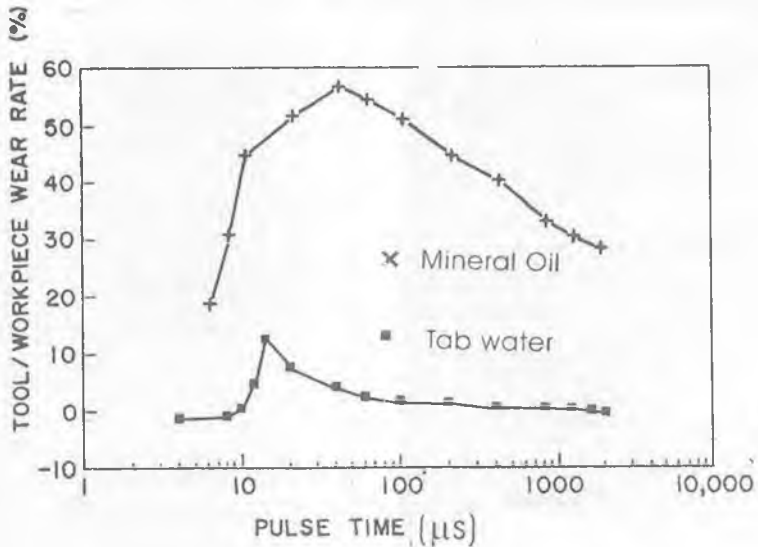


Fig. 7.14 Comparison of EDM performance while using water and mineral oil as dielectric. Dielectric pressure = 70 psi (tap water); = 50 psi (mineral oil); Tool polarity -ve (tap water) and +ve (mineral oil) [Godinho and Noble].

The impurity particles tend to gather around surface irregularities due to **electric field concentration** around such points (Fig. 7.15). It has theoretically been shown [Erdin and Bilgin, 1980] that the larger impurity particle size results in shorter time lag and vice versa. Experiments have also been conducted to investigate the effects of dielectric impurity on the performance of the EDM process. For this purpose, commercially pure metal powders (market grade) of Cu, Al, Fe and C were used. Electrodes are ground and polished prior to machining to minimize possible **surface effects**. Presence of above impurities decreases the time-lag and some of the open circuit pulses are replaced by the effective discharges, thus improving the EDM performance. However, such effects are not observed when copper is used as electrode material because copper, by its own virtue, gives short time lag, and absence of short circuit and open circuit pulses.

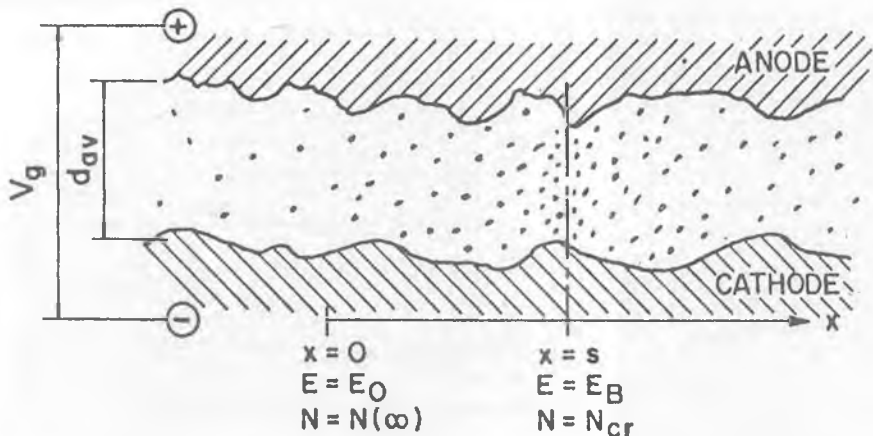


Fig. 7.15 Schematic diagram of concentration of impurity particles (Cu, Al, Fe, or C) around surface irregularities [Erdin and Bilgin, 1980].

Fig. 7.16a shows the effect of impurity concentration on workpiece erosion rate (or machining rate) for different types of impurities in powder form, and Fig. 7.16b shows the same effect for different pulse times (t_s). The particles suspended in the dielectric liquid aid in the breakdown because the total time spent in erosion is increased due to decrease in the time-lag. This fact is further supported by the results shown in Fig. 7.16b where the effect of impurity concentration on machining rate is more pronounced at longer pulse times. In case of short pulses the voltage pulse applied across the IEG ends before the breakdown conditions are satisfied. It is reverse in case of long pulses that is why the number of pulses with effective discharges is significantly increased leading to higher MRR. Further, IEG is reported to increase by an increase in concentration of the impurity in dielectric liquid. Machining rate is appreciably increased at low concentration of impure particles but remained almost constant for higher values of impurity concentration.

As explained above, tool wear rate is also influenced by the kind and concentration of impurity in the dielectric, Fig. 7.16c.

Microcrack length has been found to depend on the discharge power in general, and on the pulse duration in particular. Longer pulse durations ($\geq 800 \mu\text{s}$) result in abnormally long cracks which may extend into the HAZ.

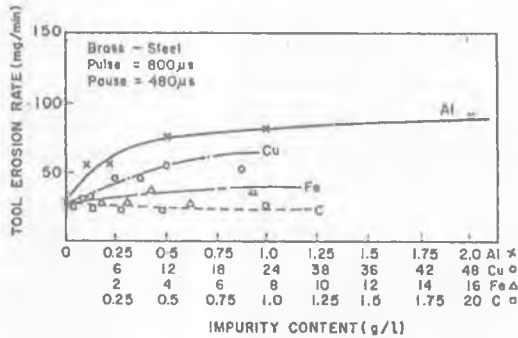
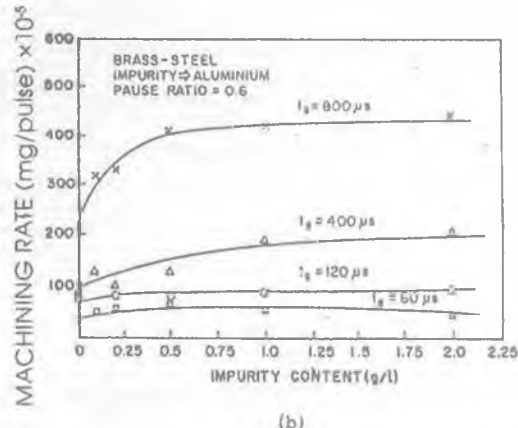
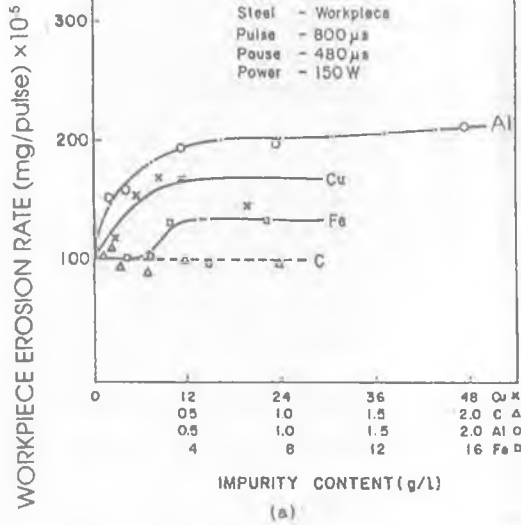


Fig. 7.16 Effect of impurity concentration on (a) workpiece erosion rate for various kinds of impurities, (b) change in workpiece erosion rate for different pulse times, (c) tool erosion rate for various kinds of impurities [Erdin and Bilgin, 1980].

PROCESS CHARACTERISTICS

Physical, mechanical and metallurgical properties of the workpiece do not significantly influence the performance of the process. EDM can be employed for machining any electrically conductive material irrespective of its hardness and other mechanical and physical properties. It can perform different kinds of operations, viz drilling, slotting, multiple hole drilling, etc. It gives high degree of **repeatability** and high **accuracy** of the order of ± 0.025 to ± 0.127 mm. It can give tolerances as good as $\pm 2.5\mu\text{m}$. When deep and accurate holes are to be drilled, use of separate tools for roughing and finishing passes is recommended so that the taper can be minimized. **Taper** ranges from 0.005 to 0.050 mm/cm depending upon the values of machining parameters employed. **Aspect ratio** of 100:1 during drilling of small holes can be achieved if special care about flushing of gap is observed.

Volumetric material removal rate (**MRR_v**) achieved during EDM is quite low (0.1 to 10 mm³/min-A). Actual value of MRR_v depends upon the machining conditions employed.

Surface integrity deals basically with two issues, e.g. surface topography and surface metallurgy (i.e. possible alterations in the surface layers after machining). Surface integrity greatly affects the performance, life and reliability of the component.

Microscopic study of the machined components reveals three kinds of layers, e.g. recast layer, heat affected zone (HAZ), and converted layer (Fig. 7.17). If molten material from the workpiece is not flushed out quickly, it will resolidify and harden (as a martensite) due to cooling effect of the dielectric, and gets adhered to the machined surface. This thin layer (say, about 2.5 to 50 μm or so) is known as “**re-cast layer**”. It is extremely hard (65 HRC) and brittle. The surface is porous and may contain microcracks. Such surfaces should be removed before using these products. The layer next to the recast layer is called “**heat affected zone**” (HAZ which is approximately 25 μm thick). Heating, cooling and diffused material are responsible for the presence of this zone. Thermal residual stresses, grain boundary weaknesses, and grain boundary cracks are some of the characteristics of this zone. **Conversion zone** (or converted layer) is identified below the HAZ and is characterized by a change in grain structure from the original structure.

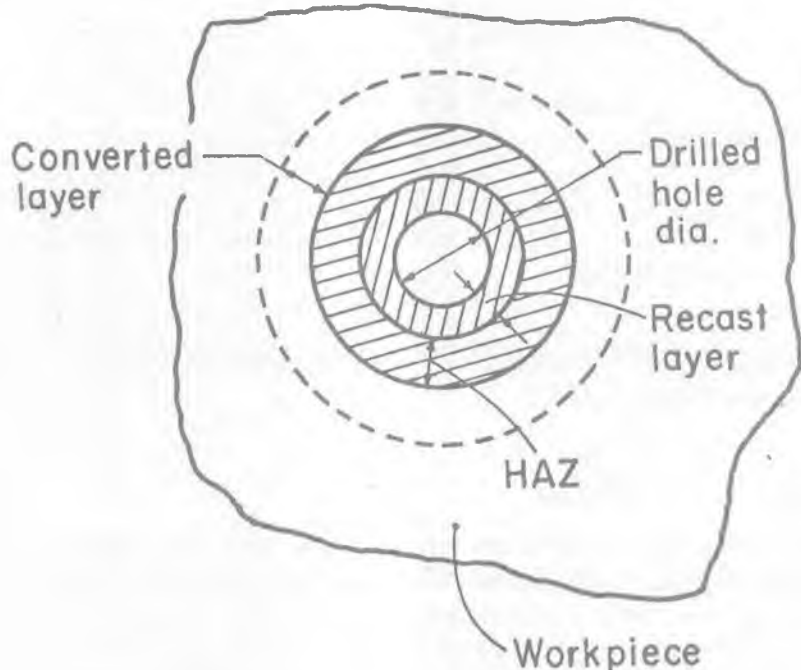


Fig. 7.17 Schematic diagram of three kinds of layers on an EDM'd component.

Excessive local thermal expansion and subsequent contraction may result in **residual tensile stresses** in the eroded layer. Such experiments were conducted [Barash, 1959] on mild steel and hard rolled brass. It was found that the thickness of the affected layer was less than $25\mu\text{m}$.

The “**surface finish**” achieved ($0.8\text{--}3.1\mu\text{m}$) during EDM is also influenced by the chosen machining conditions. New generation EDM machines are capable to produce surface finish as good as $0.18\text{--}0.25\mu\text{m}$. Surface finish is mainly governed by pulse frequency and energy per spark. The texture of eroded surface has been analyzed by *Kahng and Rajurkar* [1977], and a schematic illustration of roughing and subsequent finishing is given in Fig. 7.18. It is observed that the application of higher discharge energy results in deeper HAZ and subsequently deeper cracks. Spark eroded surfaces have been examined [Barash, 1959] to study after-machining characteristics.

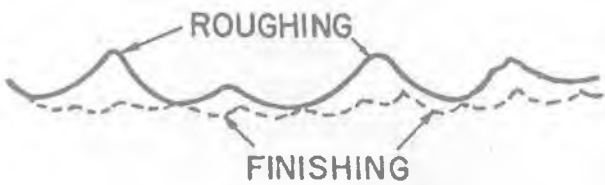


Fig. 7.18 Schematic diagram of roughing and subsequent finishing operation [Kahng and Rajurkar, 1977].

Gap Cleaning

Gap cleaning is one of the crucial factors for good EDM. At the termination of a spark, cooling starts and the spark, plasma channel and vapour bubbles collapse. As a result, relatively cool dielectric fluid rushes into this zone of a spark. This leads to the explosive expulsion of the melted material from the electrodes. This process of removal of molten material is greatly assisted by **forced flushing** of a gap by dielectric.

EDM usually gives machined workpiece surface of **matte appearance**. Such surface is achieved because of removal of material from the workpiece in the form of craters. Craters produced during EDM are roughly spherical in shape having the depth of the crater as 0.10 to 0.02 times of its diameter. The typical values of diameter and depth of craters are $12.50\text{ }\mu\text{m}$ and $1.25\text{--}0.25\text{ }\mu\text{m}$, respectively. The EDM'd surface is fully covered with such craters resulting in non-directional surface, which is different from the surface obtained by a conventional machining method.

Normalized steel was turned to a surface finish of $1.5\text{--}2.0\text{ }\mu\text{m}$ while another specimen made of the same steel was spark eroded to a surface finish of $6\text{--}8\text{ }\mu\text{m}$. It has also been found [Barash, 1959] that the **endurance limit** of the spark eroded specimens was about 15% less than that of the turned one (Fig. 7.19). In some cases this decrease in endurance limit may be more than 15%. With decrease in pulse duration, the roughness of the machined surface and the length

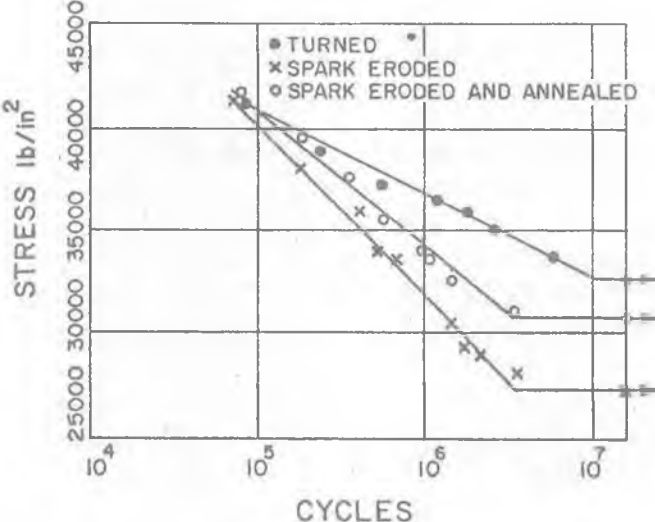


Fig. 7.19 Effect of type of machining operation on the endurance limit [Barash, 1959]

of the microcracks also decreased. Hence, transverse rupture strength [Heuvelman, 1980] and endurance limits are found to decrease with increase in pulse duration specially while machining WC. However, below $3\mu\text{s}$ pulse duration microcracks are hardly observed. Further, post-machining operations like '*shot peening*' [Neema and Pandey, 1980] also help to improve the quality of surface integrity. This operation also enhances fatigue strength and stress corrosion resistance of the machined component.

APPLICATIONS

EDM can be employed to machine any material (hard, tough, brittle, exotic, etc.) provided it has some minimum electrical conductivity (Fig. 7.20). The manufacture of hardened steel dies is the field of application other than aerospace, automobile, tools, and machine tool components. It is used for making through cavities, and miniature holes. Application of EDM in die and mould engineering is exemplary. It is used in making components for plastic injection moulding m/c [Albert, 1981]. EDM can be used for making dies for moulding, casting, forging, stamping, coining, forming, etc. It is also used to make dies for extruding, wire drawing, etc., which require through holes. It is employed for tiny holes, orifices

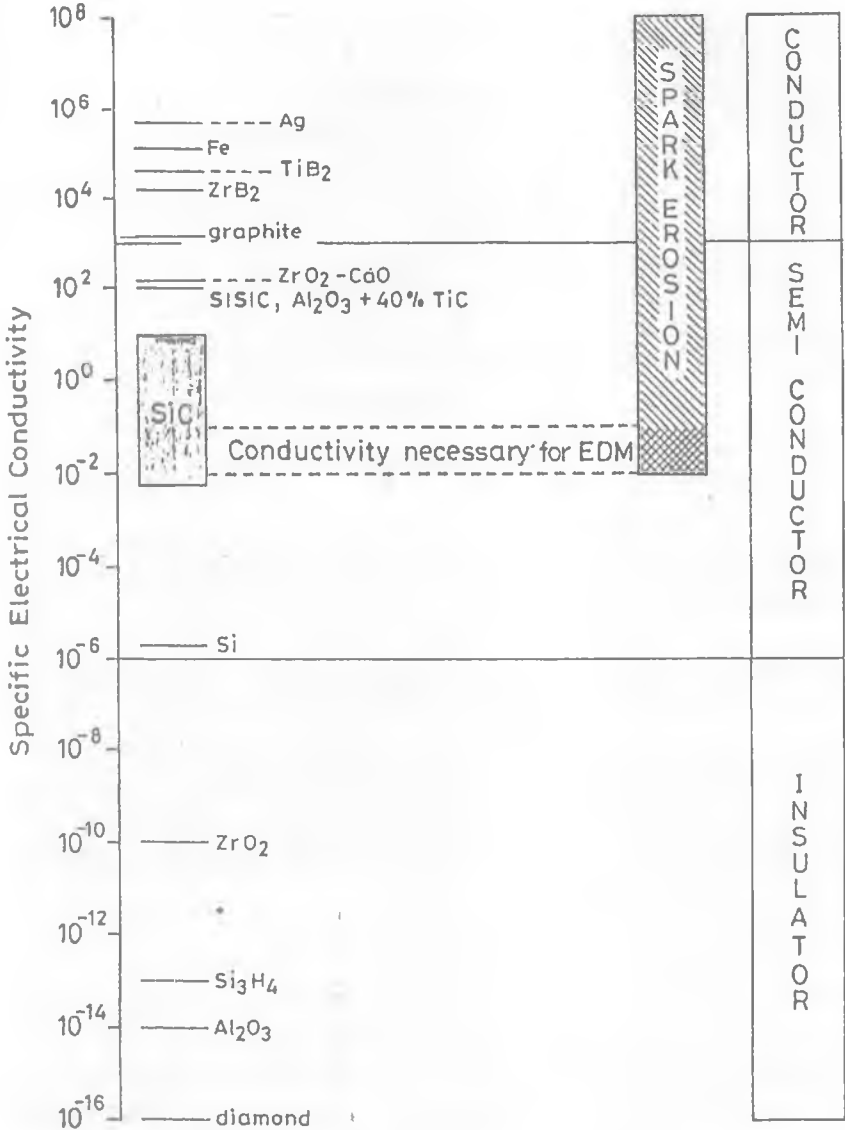


Fig. 7.20 Specific electrical conductivity of various materials [Konig and Dauw, 1988].

(say, 50 µm) and fragile features (micro sized slots). In case of making of intricate shaped dies, the machining time has come down to 50% or even less. Some of the industries claim that because of EDM technology die changes are faster. EDM'd dies are free of burrs and have higher life as compared to the dies made by using conventional methods. It permits the use of more durable die materials, viz carbide, hardened steel, exotic, etc. Matte finish obtained during EDM minimizes polishing time required.

One of the common applications of EDM is the removal of broken taps, drills, studs, reamers, pins, etc. By using EDM, one can eliminate handwork (sharp details); we can do EDM (including rework) after heat treatment and can choose better die material without worrying about its machining problems. It can be used to produce shapes which are extremely difficult to make otherwise, viz squares, 'D' holes, splines, narrow slots and grooves, blended features, etc.

In EDM, no mechanical forces act as in conventional machining; hence the process can be employed to machine thin and fragile components without any danger of a damage due to such forces.

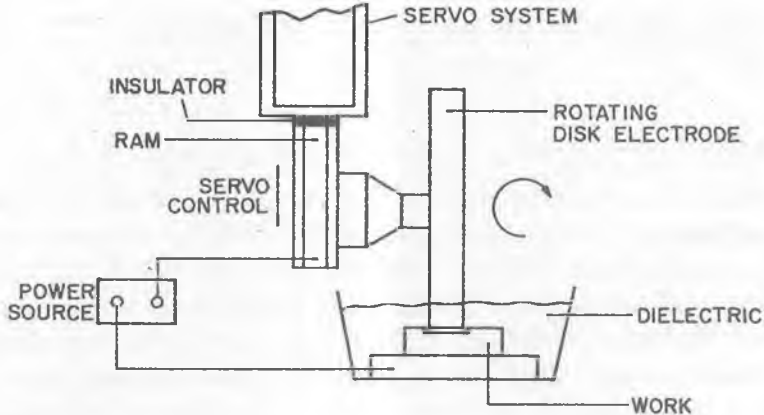
ELECTRIC DISCHARGE GRINDING (EDG) AND ELECTRIC DISCHARGE DIAMOND GRINDING (EDDG)

ELECTRIC DISCHARGE GRINDING

Grinding can be classified into two categories, viz., conventional (or mechanical) grinding and hybrid grinding. **Hybrid grinding** includes those processes in which mechanical grinding is assisted by one or more (advanced) machining techniques. Some of the hybrid grinding processes are electrochemical grinding (ECG), ultrasonic grinding (USG), electric discharge grinding (EDG), electric discharge diamond grinding (EDDG), etc.

Electric discharge grinding (EDG) is the process which works on the same principle as EDM. A rotating wheel, made of electrically conductive material (usually graphite), is used as a tool. A part of the grinding wheel (cathode) and workpiece (anode) both are immersed in the dielectric, and are connected to pulsed DC supply (Fig. 7.21). The rotating motion of the wheel ensures the effective flow of dielectric in the IEG, and hence flushing of the gap with dielectric can be eliminated. Mechanism of material removal is exactly same as in EDM except that rotary motion of the tool (i.e. wheel) helps in effective ejection of the molten material. Contrary to conventional grinding, there is no direct physical contact (except during short circuit, if so) between the tool and the workpiece, hence, fragile and thin sectioned specimens can be easily machined. EDG is considered to be economical compared to the conventional diamond grinding. During EDG, the material removal takes place due to melting and/or vaporization but not by mechanical action like shearing.

EDG is also used for **dressing** of the metal bonded diamond grit grinding wheels [Polvani and Evans, 1994]. It removes the bond material by melting rather than mechanical shear as in conventional dressing.



ROTATING DISK ELECTRODE FOR EDM

Fig. 7.21 Schematic diagram of electric discharge grinding process [Koshy et al, 1996].

EDG machine tool is very similar to EDM m/t. In EDG, grinding wheel having no abrasive is made up of electrically conductive material like graphite which is inexpensive and easy to machine. Because of a small IEG maintained between the tool and workpiece, the compensation for the overcut on the workpiece should be taken care of while designing the wheel. **EDG m/t** may have current in the range of 0.5–200A, voltage in the range of 40–80V, and pulse frequency in the range of 50–250 kHz. To achieve the desired MRR and surface integrity, optimum machining parameters should be chosen. Upper limit for wheel surface speed is about 180 m/min. Peak (1982) has suggested an empirical relationship to find the process cycle time.

The **servo-system** of EDG m/t maintains a constant inter-electrode gap by feeding workpiece into the wheel. If debris somehow blocks the gap, the workpiece is retracted to allow the debris to be flushed out of the gap.

EDG is **capable to machine** extremely hard materials, say, carbides at 2 to 3 times faster than conventional diamond grinding. Good surface finish (0.2 to 0.3 μm) and high accuracy ($\pm 2.5 \mu\text{m}$) are achieved by this process.

ELECTRIC DISCHARGE DIAMOND GRINDING (EDDG)

Working Principle

Electric discharge diamond grinding is a hybrid process which involves machining of hard materials using advantages of EDM as well as conventional grinding. EDDG process permits the use of water or water-based cutting fluid as dielectric. In this process, **metal bonded diamond grit wheel** is used in place of a simple electrically conductive wheel (graphite) used in EDG. Sparking takes place between metallic bonding material and workpiece. Heat generated during sparking softens the work material and hence machining by diamond abrasive particles becomes easier. Sparking in the IEG during EDDG, results in continuous dressing of the grinding wheel and hence the wheel does not clog also. As a result, cutting properties of the grinding wheel are stabilized. Authors have therefore, suggested the use of EDDG for precise **trueing/dressing** of the metal bonded grinding wheels employing numerically controlled (NC) grinding m/t, Fig. 7.22a. They have been able to employ wire EDM m/t, as well as die sinking EDM m/t having NC movement of the table, for trueing/dressing.

Fig. 7.22b shows the schematic illustration of on-machine electro-discharge (ED) trueing/dressing method. Precise trueing, dressing and profile generation on grinding wheels of various grain sizes are possible just by changing electro-discharge conditions. The dressing of the diamond wheels using tubular and solid electrodes has also been done. Rotary speed of diamond wheel and amount of the swarf (very fine chips) generated during EDDG also influence the process performance.

The EDDG has also been named as electro-contact abrasion finishing (ECAF) and has been employed for cutting blanks of various materials, profiles and dimensions.

Capabilities and Applications

This process is also being used for machining of cermates, super alloys, and other metal matrix composites. EDDG has been employed to machine tungsten free carbides with reverse polarity using fixed plunged feed rate. It has been reported that EDDG gave MRR_v as 270 mm³/min, **wheel life** as more than 120 min, and good **surface finish** (Ra value as 10.32 to 0.15 µm) without cracking.

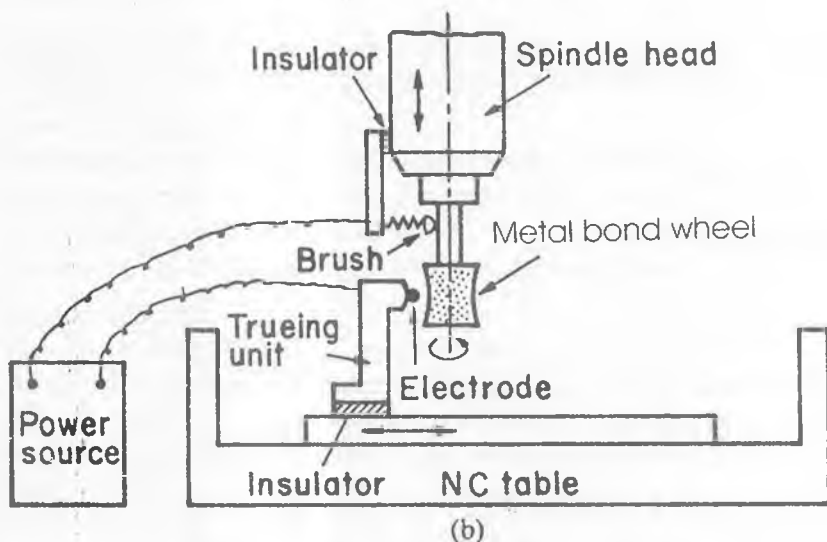
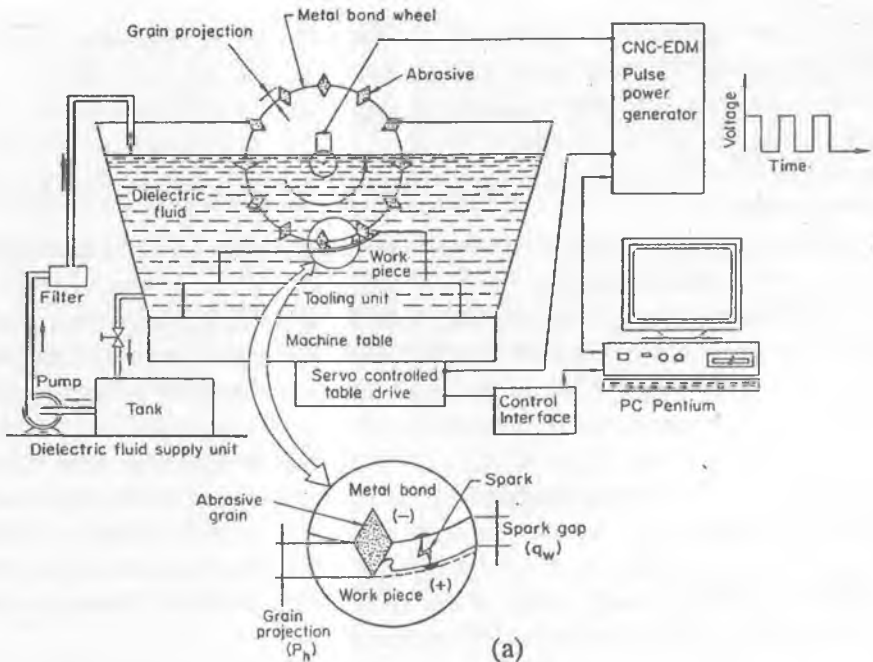


Fig. 7.22 (a) NC EDDG set up, (b) Schematic diagram of on-machine electric discharge trueing/dressing operation [Suzuki et al, 1987].

EDDG is recommended in preference to electrochemical discharge grinding (ECDG) because of its much less corrosive effects.

It has been concluded that while electrodiamond grinding of cemented carbide drilling bits, diamond wheel has about 25% higher wheel life as compared to conventional diamond grinding. It also gave higher MRR, and lower operating costs.

Another application of EDDG process is dressing/trueing of metal bonded diamond (or other abrasive) wheels.

The efficiency of metallic bond diamond wheels after electro-contact erosion dressing, has been compared with the efficiency of the same wheels after traditional abrasive dressing. It has been found that the wheel life in terms of the period between two dressings is increased by a factor ranging from 5-10 in case of contact erosion dressing, than after traditional abrasive dressing. It is recommended that rough dressing of grinding wheels with high voltage and current should be followed by finish dressing with lower voltage and current in order to obtain uniformly exposed working surface on the diamond wheel. It has been concluded that the accuracy achieved during electrical discharge diamond grinding is better than that in conventional diamond grinding.

WIRE ELECTRIC DISCHARGE MACHINING (WIRE EDM)

WORKING PRINCIPLE

In wire electric discharge machining (wire EDM), a wire (about 0.05–0.30 mm diameter) is used as an electrode and deionized water as dielectric. A nozzle is employed to inject the dielectric in the machining area in wire EDM. Electrodes (wire and workpiece) are connected to a pulsed DC supply. Heat generated due to sparking results in the melting of workpiece and wire material, and sometimes part of the material may even vaporize like in conventional EDM. A constant gap between tool (wire) and workpiece is maintained with the help of a computer-controlled positioning system. This system is used to cut through complicated contours specially in difficult-to-machine materials. This process gives a high degree of accuracy and a good surface finish. Fig. 7.23 shows details of the wire EDM system.

WIRE EDM MACHINE

There are four basic elements of this machine tool, e.g. the power supply system, the dielectric system, the positioning system, and the drive system.

(i) Power Supply System

Wire EDM power supply system differs from conventional EDM power supply system basically in pulse frequency which is about 1 MHz. It results in reduced crater size or better surface finish. However, because of very small wire size, it usually cannot carry current more than 20A.

(ii) Dielectric System

Water is a likely substitute for kerosene as dielectric in EDM. It is an attractive proposition because of its availability, desirable thermal properties, low viscosity and pollution-free working. It gives higher MRR and better surface finish under the identical machining conditions.

Deionized water has low viscosity, no fire hazard, high cooling rate and high MRR. That is why water is used as dielectric in most of the wire EDM systems. Low viscosity helps in efficient flow while high cooling rate yields very thin recast layer. Water gives high MRR and high TWR. However, wire is not reused

hence high TWR does not adversely affect the process performance. More efficient way of dielectric delivery is to provide a stream of deionized water along the axis of the wire.

Cost of the dielectric can be lowered down by reusing it after proper filtration. About 5 μm size disposable paper filters are used. To minimize rust formation on the machined part, special additives are mixed with it.

(iii) Positioning System

Usually positioning system is a computerized numerical control (CNC) **two-axes table**. However, it operates in an adaptive control mode so that in case wire approaches very near to the workpiece, or the gap is bridged by debris and causes a short circuit, the positioning system should be capable to sense it. Instantaneously, it should move back to re-establish proper cutting conditions in the gap.

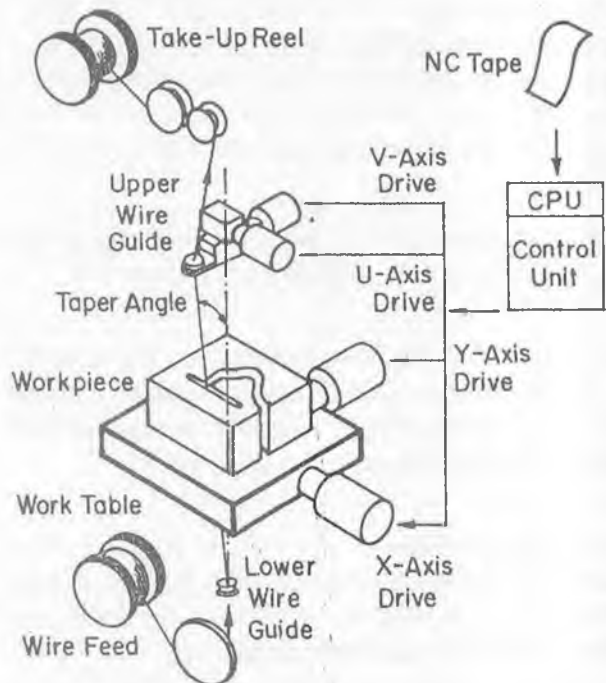


Fig. 7.23 Schematic illustration of wire electric discharge machining.

(iv) Wire Drive System

This system serves two purposes, viz continuously delivers fresh wire, and always keeps the wire under appropriate tension so that it moves in the machining zone as a straight wire. The latter requirement is important from the point of view of quality of the machined surface. For example, it helps to minimize taper, streaks as well as vibration marks. It also minimizes the "wire breaks" during machining. On the way while moving to the machining zone, wire is guided by sapphire or diamond "wire guides". As it moves towards the take up spool, the wire passes through a series of tensioning rollers.

To enhance the productivity as well as to make the machine to **run unattended**, modern wire EDM machines are equipped with the devices which permit *automatic reloading* of wire after it has broken up during its use [Anon, Feb. 1981]. Large diameter (0.15–0.30 mm) wires, used in wire EDM, are made of copper or brass while small diameter wires are usually made of molybdenum steel. Wire is discarded after it has been used once because the sparking takes place at its leading surface, hence, it no longer remains round.

Advances in Wirecut EDM

Other features of wirecut EDM system are automatic wire threading, self restarting and improved tensioning devices. CNC features have been incorporated with wirecut EDM too. An operator can input for wire compensation at the machine. It is easier to interrupt the process and change the machining parameters (**V**, **I**, etc) and other settings more easily with CNC than that with tape control.

In today's wire EDM m/t, it is possible to program wire to follow a complex path in two axes. Hence, it is possible to use this m/t for making dies for stamping fine blanking and extrusion as well as 2-D through holes. It is possible to tilt the wire in positions other than perpendicular to X and Y axes. Such machines also have the facility for speedy automatic realignment of wire.

It is possible to perform 3-D cutting using wire EDM in which two additional axes (**U** and **V**) have been introduced. The drive motors which tilt the wire towards front or back (**V** axis) and left or right (**U** axis) are controlled by the programmed commands in CNC wire EDM. The extent to which the wire can be tilted (say, $\pm 10^{\circ}$ or so) tells about the limitation of the m/t. In a versatile m/t, all the four axes (**X**, **Y**, **U** and **V**) can be controlled simultaneously. Such machines

usually have closed loop control arrangement for work table and wire guide positions. This facility has been used to make, in one stroke, a draft or relief in the mould, and constant radius corners along the tapered walls [Albert, 1983] of molds and dies.

Stratified Wire

Properties of the wire used in this process have an impact on MRR and quality of the cut surface. Nowadays, stratified wires are used as electrodes. These wires are made of copper core with a thin layer of zinc over it (Fig. 7.24). Such a wire can carry more current hence gives higher MRR. A stratified wire for wire EDM has been developed by Charmiles Corporation of Switzerland. This wire has a layer of zinc / zinc alloy on the outside and a core of drawn copper wire on the inside just like electrical wire is clad with vinyl plastic for insulation. The wire is used only once and then scrapped because it is not very expensive, and also because it gets eroded during the process.

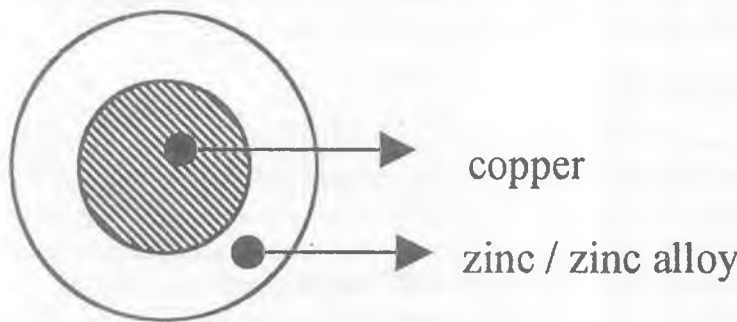


Fig. 7.24 Stratified wire used in wire EDM.

A wire can carry **heavier load** if it can absorb more amount of heat without breaking. A heavier load also means a spark with more energy hence higher MRR resulting in higher cutting speed. Zinc melts and even evaporates at a temperature lower than the melting temperature of copper. In other words, core of the stratified wire gets no hotter than the temperature at which the outer layer of the zinc will vaporize. Hence, more **powerful sparks** can be discharged. MRR is related to current density which, in turn, is related to the surface area of the wire engaged in the cut.

In the tiny space (0.025 mm or so), workpiece is eroded by a violent, extremely localised and momentary action of the spark. Gas bubbles are rapidly formed during this process; and on the way to escape out, these bubbles press against wire in the gap. This pressure results in **bowing of wire** which tends to drag on bends and sharp corners as it advances. As a remedy, wire guiding and feeding mechanism should be designed such that the wire can withstand higher tension. Therefore, the effect of gap condition on the quality of the product will be minimized. Huge sized spools are used which can supply wire for machining for a long period of time, say 60 hr or so [Albert, 1981].

PROCESS VARIABLES

Most of the variables that control the process are common in case of EDM die sinking as well as wire EDM. The linear cutting rate in wire EDM is dependent on the thickness of the workpiece but not on the complexity of the cut. Wire speed may be as high as 40 mm/s.

PROCESS CHARACTERISTICS

This process produces accurate **matte finish**. Thousands of tiny craters on the machined surface help in retaining the lubricating oil and result in increased *die life*. *Surface finish* of the order of $0.1 \mu\text{m}$ can be achieved in finish pass. Accuracies of the magnitude of $\pm 7 \mu\text{m}$ or even lower, in some cases, can be achieved. However, uniformity of wire diameter, temperature as well as resistivity of the dielectric should be closely controlled. With today's systems, machining rate for definite materials has gone up from $12.50 \text{ cm}^2/\text{hr}$ to about $40 \text{ cm}^2/\text{hr}$.

APPLICATIONS

Wire EDM has been employed for making dies of various types. It is possible to control tolerances very effectively. The process is also used for fabrication of press tools and electrodes for use in other areas of EDM.

PROBLEMS

Problem 1

EDM is used to machine a metallic sheet. Calculate surface finish value if $C = 15 \mu\text{F}$, $V_b = 130 \text{ V}$, $K_6 = 4.0$. Use the equation based on experimental results.

Solution:

Surface finish equation based on experimental results:

$$H_{CLA} = K_6 V_b^{0.5} C^{0.33}$$

Substituting the values of different variables.

$$H_{CLA} = 4.0 \times (130)^{0.5} \times (15 \times 10^{-6})^{0.33}$$

$$H_{CLA} = 1.17 \mu m$$

BIBLIOGRAPHY

1. Albert M. (1981), EDM: Close Control for a Closer Shave, *Modern Mach. Shop*, pp. 79-87.
2. Albert M. (1982), How CNC has Changed EDM, *Modern Mach. Shop*, pp. 1-11.
3. Albert M. (1982), Stratified Wire for TWEDM, *Modern Mach. Shop*, pp. 97-102.
4. Albert M. (1983), Taper Cutting: Value Added TWEDM, *Modern Mach. Shop*, pp. 75-79.
5. Anon (Feb 1981), Wirecut EDM Can Cut it, *Production*, pp. 72-75.
6. Bakhtiarov Sh. A. (1987), Improvement of Contact Erosion Dressing of Diamond Wheels with an End Working Surface, *Sov. Eng. Res.*, Vol. 58, No. 12, pp. 19-20.
7. Bakhtiarov Sh. A. (1989), Efficiency of Diamond Wheels After Contact Erosion Dressing, *Stanki Instrum.*, Vol. 60, No. 1, pp. 18-19.
8. Barash M. (Feb. 1959), Some Properties of Spark Eroded Surfaces, *Micro-technique*, pp. 51-54.
9. Benedict G.F. (1987), *Nontraditional Manufacturing Processes*, Marcel Dekker, New York.
10. Bhattacharyya A. (1973), *New Technology*, The Institution of Engineers (India), Calcutta.
11. CIRP Scientific Technical Committee E (1979), *Summary Specifications of Pulse Analysers for Spark Erosion Machining*, Vol. 2, No. 2.

12. Dauw D.F., Snoeys R. and Dekeyser W. (1983), Advanced Pulse Discriminating System for EDM Process Analysis and Control, *Annls CIRP*, Vol. 32, pp. 541-549.
13. de Bruyn H.E. (1970), Some Aspects of the Influence of Gap Flushing on the Accuracy in Finishing by Spark Erosion, *Annls CIRP*, Vol. 18, pp. 147-151.
14. de Bruyn H.E. (1978), Effect of a Magnetic Field on the Gap Cleaning in EDM, *Annls CIRP*, Vol. 27, pp. 93-95
15. Erden A. and Bilgin S. (1980), Role of Impurities in EDM, *Proc. 21st Int. Machine Tool Design and Research Conference*, Swansea, pp. 345-350.
16. Erden A. (1982), Role of Dielectric Flushing on EDM Performance, *Proceedings of the 23rd Int. Machine Tool Design and Res. Conference*, pp. 283-289.
17. Gnusarev V.F. *et al* (1987), Electrical Discharge Diamond Grinding of Drilling Bits, *Sov. Engg. Res.*, Vol. 58, No. 9, pp. 29-30.
18. Godinho L.H. and Noble C.F., The Use of Water as Inter electrode Medium in Pulsed EDM (personal communication).
19. Golubev I.V., Grodzinskii E. Ya. and Krapivko A.T. (1988), Accuracy in Electrical Discharge Diamond Grinding, *Stanki Instrum.*, Vol. 59, No. 2, pp. 34-35.
20. Grodzinskii E. Ya. and Zubatova L.S. (1982), Electrochemical and Electrical Discharge Abrasive Machining, *Sov. Engg. Res.*, Vol. 53, No. 3, pp. 28-29.
21. Grodzinskii E. Ya. *et al.* (1983), Electrical Discharge Diamond Grinding of Tungsten-free Carbides, *Sov. Engg. Res.*, Vol. 54, No. 2, pp. 22-23.
22. Grodzinskii E. Ya. Golubev I.V., and Krapivko A.T. (1989), Selecting a Supply Source for Electrical Discharge Diamond Grinding, *Stanki Instrum.*, Vol. 60, No. 2, pp. 34-35.
23. Hewuvelman C. J. (1980), CIRP Technical Reports, *Annls CIRP*, Vol. 29, No. 2, pp. 541-544.
24. Jain V.K. (1989), Analysis of Electro Discharge Drilling of a Blind Hole in HSS Using Bit Type of Tools, *Microtecnica*, No. 2, p. 34.
25. Jilani S.T. and Pandey P.C. (1984), An Analysis of Surface Errors in Electrical Discharge Machining, *Wear*, Vol. 84, pp. 275-284.
26. Jilani S.T. and Pandey P.C. (1984), Experimental Investigations into the Performance of Water as Dielectric in EDM, *Int. Mach. Tool Design & Res.*, Vol. 24, No. 1, pp. 31-43.

27. Kahng C.H. and Rajurkar K.P. (1977), Surface Characteristic Behaviour Due to Rough and Fine Cutting by EDM, *Annls CIRP*, Vol. 25, No. 1, pp. 77-82.
28. Konig W. and Dauw D.F. (1988), EDM—Future Step Towards the Machining of Ceramics, *Annls CIRP*, Vol. 37, No. 2, pp. 623-631.
29. Koshy Philip (1996), Electrical Discharge Diamond Grinding: Mechanism of Material Removal and Modeling, Ph. D. Thesis, I.I.T. Kanpur (India).
30. Koshy Philip, Jain V.K. and Lal G.K. (1993), Experimental Investigations into Electric Discharge Machining With Rotating Disk Electrode, *Precision Engg.*, Vol. 15, No. 1, pp. 6-15.
31. Kremer D., Lebrun, J.L., Hosori, B. and Moisan, A. (1989), Effects of Ultrasonic Vibrations on the Performance in EDM, *Annls CIRP*, Vol. 38, pp. 199-202.
32. Masuzawa T. and Heuvelman C. J. (1983), A Self Flushing Method with Spark Erosion Machining, *Annls CIRP*, Vol. 32, pp. 109-111.
33. McGeough J.A. (1988), *Advanced Machining Methods*, Chapman and Hall, London.
34. Neema M.L. and Pandey P.C. (1980), Investigation of the Performance Characteristics of Cold-worked Machined Surfaces, *Wear*, Vol. 60, pp. 157-166.
35. Pandey P.C. and Shan H.S. (1980), *Modern Machining Processes*, Tata-McGrawHill, New Delhi (India).
36. Polvani R.S. and Evans C.J. (1994), Electrically Assisted Grinding of Advanced Ceramic Materials, (Personal correspondence).
37. Shankar Prem, Jain V.K. and Sundararajan T. (1997), Analysis of Spark Profiles During EDM Process, *Machng. Sci. Technol.*, Vol. 1, No. 2, pp. 195-217.
38. Sreejith P.S., Jain V.K. and Lal G.K. (1994), Investigations into the Characteristics of Spike Obtained during EC Drilling of Blind Holes in HSS, *Processing of Advanced Materials*, Vol. 4, pp. 67-79.
39. Quinlan J.C. (1983), Harnessing the Spark—the Evolution in EDM, *Tooling & Prod.*, pp. 37-42.
40. Snoeys R. and Van Dijck F. (1972), Plasma Channel Diameter Growth Affects Stock Removal in EDM, *Annls CIRP*, Vol. 21, pp. 39-40.

41. Suzuki K., Uematsu T. and Nakagawa T. (1987), On Machine Trueing Dressing of Metal Bond Grinding Wheels by Electro Discharge Machining, *Annls CIRP*, Vol. 36, No. 1, pp. 115-118.
42. Vitlin V.B. (1977), Electro-contact Abrasion as a Finishing Metal Cutting Process, *Machines and Tooling*, Vol. 48, No. 4, pp. 32-34.

SELF-TEST QUESTIONS

1. Write True (T) or False (F)
 - (i) Usually the life of a die made using EDM process is higher than the die made using ECM process.
 - (ii) To provide the controlled electrical resistance in the inter-electrode gap during EDM, an appropriate insulating fluid is flooded between the tool and workpiece.
 - (iii) Tool life in EDM is infinite.
 - (iv) Dielectric fluid is reused during EDM.
 - (v) EDM cannot be used to drill a slanted hole in the aluminium alloy workpiece.
 - (vi) Flash point of the dielectric used in EDM should be high enough.
2. Make the most appropriate choice:
 - (i) Surface damage to the machined component is insignificant in case of (a) EDM, (b) ECM, (c) Grinding, (d) PAM.
 - (ii) During calculation of MRR in EDM, supply voltage was used as 60V in place of the actual supply voltage of 40V. What is the ratio of actual and calculated MRR? Assume that the condition for maximum power delivery to the discharging circuit is satisfied. (a) 1.5, (b) 0.44, (c) 2.25, (d) none.
 - (iii) The current used during EDM is (a) AC, (b) DC, (c) pulsed AC, (d) Pulsed DC.
 - (iv) Location of spark generated during EDM is (a) random, (b) governed by dielectric strength, (c) governed by surface finish of tool and workpiece both, (d) none of these.
 - (v) Stratified wires are used so that they can (a) withstand more mechanical forces, (b) carry more heat energy, (c) both of these, (d) none of these.

- (vi) For maximum power delivery through the circuit during EDM, ratio of the breakdown voltage to supply voltage is (a) 0.72, (b) 1.0, (c) 0.75, (d) 0.65.
- (vii) Feed to the electrode during EDM is given (a) to maintain constant velocity of dielectric flow in the IEG, (b) to maintain constant IEG, (c) to maintain constant current density, (d) none of these.
- (viii) Relative electrode wear (REW) during EDM is (a) <100%, (b) >100%, (c) 100%, (d) none of these.
- (ix) Value of surface roughness with the increase in breakdown voltage: (a) increases, (b) decreases, (c) remains unchanged.
- (x) Discharging time (in RC circuits) as compared to charging time is (a) more, (b) less, (c) equal, (d) no definite relationship.
- (xi) Servomechanism operates when there is (a) short circuit, (b) high IEG, (c) low IEG, (d) all of these.
- (xii) Poor flushing during EDM results in (a) low MRR, (b) short circuit, (c) both, (d) none.
- (xiii) A graphite electrode composed of very fine grains results in surface finish of the machined component as (a) improved, (b) deteriorated, (c) no effect.
- (xiv) If the flushing system of EDM m/c is inefficient the machining cycle time will be: (a) longer, (b) shorter, (c) no effect, (d) no definite trend.
- (xv) Wear of tool during EDD process would result in (a) deeper hole, (b) lesser diameter hole, (c) both, (d) none.
- (xvi) Electrode refeed system in EDM is used to compensate for wear in (a) length, (b) diameter, (c) both, (d) none.
- (xvii) During EDM, the charged voltage of the condenser is increased from V_1 to V_2 ($V_2 = 4V_1$). What will be surface roughness at V_2 if its value at V_1 is equal to R_{a1} . (a) $2R_{a1}$, (b) $2.5R_{a1}$, (c) $4R_{a1}$, (d) $0.25R_{a1}$.
- (xviii) In the above question, in place of changing the charged voltage the frequency is changed from f_1 to f_2 ($f_2 = 0.5 f_1$). The new surface roughness is (a) $2R_{a1}$, (b) $0.5R_{a1}$, (c) $4R_{a1}$, (d) $0.25R_{a1}$.
- (xix) Which process would you recommend to make cooling holes (diam. = 0.5 mm, and depth to diameter ratio may be as high as 75) in a turbine blade. (a) EDM, (b) AJM, (c) USM, (d) PAM.

- (xx) Dielectric to be used in EDM should have dielectric strength (a) high, (b) low, (c) moderate, (d) any of these.

REVIEW QUESTIONS

3. Explain the following terms:
(a) duty factor, (b) ignition delay, (c) flash point, (d) relative electrode wear or wear ratio, (e) heat affected zone (HAZ), (f) dielectric strength, (g) 'time constant', (h) critical resistance in RC circuit.
4. What are the functions of an 'adaptive control system' used for EDM?
5. With the help of a neat sketch, explain the mechanism of material removal in EDM.
6. Find the condition for maximum power delivery to the discharging circuit in EDM.
7. Explain the working principle of wire EDM. Also explain how the stratified wire works?
8. Sketch different feasible dielectric flushing techniques applicable in case of EDD.
9. Derive the relationship for surface roughness in EDM.
10. Write short notes on the following: (a) resolidification of molten metal in EDM, (b) minimization of bowing of wire in wire EDM.
11. When using water as dielectric during machining of high speed steel (HSS) by EDM process, which specific problem do you expect?
12. Sketch the effects of following parameters on MRR during EDM: (a) resistance, (b) current density, (c) pulse energy, (d) capacitance.
13. Illustrate the effect of (a) magnitude of current, and (b) frequency, on the shape and size of the craters formed during EDM.
14. A through hole (diam. = 10 mm) in a plate (5 mm thick) is to be drilled using EDM. Estimate the time required for the process. Assume $R = 50 \Omega$, $C = 10 \text{ mF}$, $V_s = 200 \text{ V}$, $V_b = 150 \text{ V}$, $K_l = 0.18$ to obtain MRR in mm^3/min .
15. (i) For RC circuit, adjusted for maximum power delivery condition, the following data are available:
 $R = 250 \Omega$, $C = 25 \text{ mF}$ and supply voltage = 75 V. Calculate charging current and frequency of discharge when the circuit is closed.

- (ii) A 10 mm diameter hole is to be drilled in a 5 mm HSS plate by EDM using RC circuit. The required surface finish is $20 \mu\text{m}$. Determine specifications of a capacitor to be used when supply and discharge voltages are 220 V and 150 V, respectively. Use resistance as 50Ω and value of the constant as 0.4. Also estimate time required to complete the job.

NOMENCLATURE

C	Capacitance
E	Energy
f	Frequency
h	Crater depth
H	Centre line average value of surface finish
i	Current
K, K ₁ , ..., K ₇	Constants
m, n	Constants
L	Inductance
P	Power
R	Resistance
t	Time
V	Voltage

Acronyms

AC	Adaptive control, Alternating current
ATC	Automatic tool changer
CNC	Computer numerical control
DC	Direct current
EDD	Electric discharge drilling
Hz	Hertz
IEG	Inter electrate gap
K E	Kinetic energy
MRR	Material removal rate
m/t	Machine tool
NC	Numerically controlled (Numerical control)
REW	Relative electrode wear

TWR Tool wear rate
W/P Workpiece

Subscripts

avg Average
b Breakdown condition
c Charging (circuit)
ct Charging at time 't'
d Discharging (circuit)
min Minimum
o Supply condition
s Sparking (zone)

CHAPTER 7
AT-A-GLANCE
ELECTRIC DISCHARGE MACHINING
(EDM)

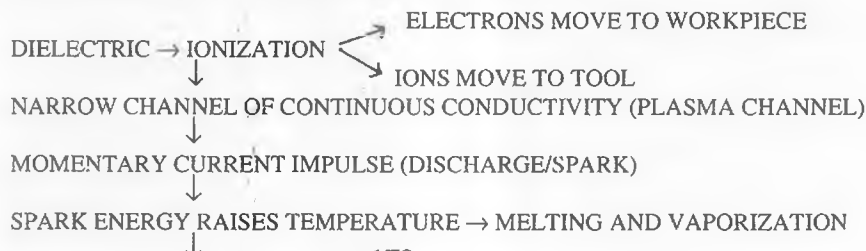
- SPARKING BETWEEN TWO ELECTRICAL CONTACTS → LOSS OF MATERIAL
↓
HARNESS → CONTROL THE SPARK ENERGY TO EMPLOY FOR MACHINING
- IF DISCHARGE SUBMERGED IN DIELECTRIC → ENERGY IS CONCENTRATED INTO A SMALL AREA.
- BREAKDOWN VOLTAGE IS REACHED → SPARKING OCCURS AT A POINT OF LEAST ELECTRICAL RESISTANCE
↑
AT NARROWEST GAP
- RECHARGING / SPARKING FREQUENCY → MANY THOUSANDS PER SECOND
- FUNCTIONS OF THE DIELECTRIC → COOLING OF ELECTRODES
→ CONCENTRATION OF SPARK ENERGY

WORKING PRINCIPLE

- LOCALISED SPARK ENERGY → VERY HIGH TEMPERATURE → MELTING AND VAPORIZATION OF TOOL AND WORKPIECE
- MATERIAL REMOVAL → BY CRATER FORMATION OVER ENTIRE W/P SURFACE
- SERVOSYSTEM TO MAINTAIN GAP → MOVES TOOL TOWARDS WORKPIECE

HOW SPARKING TAKES PLACE?

- INTENSE ELECTRICAL FIELD AT THE NARROWEST GAP
- NEGATIVELY CHARGED PARTICLES (ELECTRONS) DETACH FROM CATHODE → MOVE TO THE ANODE
- ELECTRONS COLLIDE WITH NEUTRAL MOLECULES OF



METAL IS REMOVED FROM TOOL AND WORKPIECE → CRATERS

⇒ FREQUENCY OF SPARKING → MANY THOUSANDS / SECOND

⇒ TO MINIMISE WEAR OF TOOL → MACHINING CONDITIONS AND POLARITY ARE SELECTED CAREFULLY

RC PULSE GENERATOR

- LOW MRR ← LONG IDLE TIME, SHORT SPARK TIME
- IMPROVED SF
- HIGH TWR
- ATTAINS HIGH PEAK CURRENT AND THEN HIGH RATE OF DECLINE



VERY HIGH TEMPERATURE ← NOT NEEDED



THERMAL DAMAGE

- CONTROLLED PULSE GENERATOR OVERCOMES THIS PROBLEM
- ENABLES TO SELECT ROUGH MACHINING (HIGH ENERGY AND LOW FREQUENCY) OR FINISH MACHINING (LOW ENERGY AND HIGH FREQUENCY)

EDM MACHINE

→ POWER SUPPLY

ELEMENTS

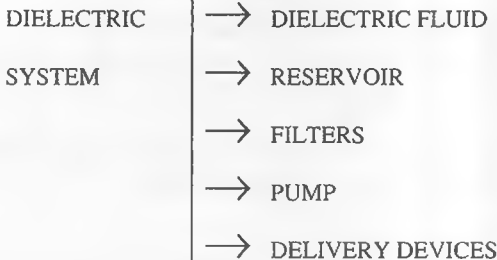
→ DIELECTRIC SYSTEM

→ ELECTRODES: WORKPIECE AND TOOL

→ SERVO SYSTEM

POWER SUPPLY

- SOLID STATE RECTIFIER → AC TO DC
- HIGH POWER PULSED OUTPUT → SPARKING
- FOR A GIVEN VOLTAGE → SPARKING AT OR BELOW A MINIMUM GAP
- EDM POWER SUPPLY CONTROLS SERVO SYSTEM → DESIRED GAP VALUE
- ALSO CONTROLS PARAMETERS → V,I,PULSE DURATION, DUTY FACTOR, FREQUENCY, AND POLARITY
- EQUIPPED WITH CUT-OFF-PROTECTION CIRCUIT → IN CASE OF OVER-VOLTAGE OR OVER-CURRENT → POWER CUTS OFF



- * GOOD DIELECTRIC FLUID
 - HIGH DIELECTRIC STRENGTH
 - MINIMUM IGNITION DELAY TIME
 - MINIMUM DEIONIZATION TIME
 - EFFECTIVE COOLANT
 - HIGH DEGREE OF FLUIDITY
- * DIELECTRIC FLUIDS
 - TRANSFORMER OIL
 - PARAFFIN OIL
 - LUBRICATING OIL
 - KEROSENE OIL
 - DEIONIZED WATER → HIGH MRR, HIGH TWR, CORROSIVE, GOOD COOLANT → USED IN WIRE EDM
- * EFFECTIVE FLUSHING
 - REMOVES "BY PRODUCTS" FROM GAP
 - HIGH MRR AND GOOD SF
 - AVOIDS SHORT CIRCUITS ← ABSENCE OF RESIDUES
- * TECHNIQUES FOR PROPER FLUSHING
 - SUCTION THROUGH TOOL / WORKPIECE
 - PRESSURE THROUGH TOOL / WORKPIECE
 - JET FLUSHING
 - ROTATING DISK ELECTRODE
 - ALTERNATING FORCED FLUSHING

- FLUSHING THROUGH A HOLE IN THE TOOL → SPIKE FORMATION
- ↓
- CAN BE AVOIDED BY ROTATING A TOOL WITH ECCENTRIC HOLE(S)
 - JET FLUSHING LESS EFFECTIVE
 - INFLAMMABLE DIELECTRIC → WORKPIECE IMMERSED IN DIELECTRIC → MINIMIZES CHANCE OF FIRE
 - ARCS ARE UNDESIRABLE → CAUSED DUE TO CONCENTRATION OF DEBRIS IN IEG
- ↑

REQUIRES PROPER FILTRATION/FLUSHING

- * ELECTRODES → TOOL & WORKPIECE → BOTH ELECTRICALLY CONDUCTIVE
 - TOOL MATERIAL REQUIREMENTS
 - ⇒ EASILY MACHINABLE
 - ⇒ LOW WEAR RATE
 - ⇒ GOOD CONDUCTOR OF ELECTRICITY AND HEAT
 - ⇒ CHEAP AND READILY AVAILABLE
- * TOOL MATERIALS → GRAPHITE, COPPER, BRASS, COPPER TUNGSTEN, ETC
 - GRAPHITE
 - ⇒ LOWER TWR
 - ⇒ HIGHER MRR
 - ⇒ BETTER SF
 - ⇒ BRITTLENESS → PRONE TO BREAKAGE
- * OVERCUT

OVERCUT DURING EDD IS FUNCTION OF

 - ⇒ MACHINING CONDITIONS
 - ⇒ WORKPIECE MATERIAL
 - ⇒ TOOL MATERIAL
 - TAKE CARE AT DESIGN STAGE
- * THROUGH HOLE
 - ⇒ ONLY VERY SMALL THICKNESS OF MATERIAL
- * SERVO SYSTEM
 - TO MAINTAIN PRE-DETERMINED GAP BETWEEN ELECTRODES
 - GAP BRIDGED BY ELECTRICALLY CONDUCTIVE MATERIAL → SIGNAL TO SERVO SYSTEM → REVERSED DIRECTION
 - RECIPROCATES TOWARDS WORKPIECE UNTIL DIELECTRIC FLUSHES GAP
 - IF INEFFICIENT FLUSHING → VERY LONG CYCLE TIME

* TOOL WEAR

- COMPENSATION FOR REDUCED TOOL LENGTH → TOOL WEAR



INCREASE INFEED AFTER EACH HOLE

- ELECTRODE REFEEDING → BRING TOOL TO A REFERENCE POINT

* AUTOMATIC TOOL CHANGER (ATC)

- RECENT INNOVATION
- MANY TOOLS MOUNTED ON A MAGAZINE → CALLED BY CNC PROGRAM
- REDUCES TOOL-CHANGE TIME
- CNC - EDM MORE POPULAR

PROCESS VARIABLES

- INCREASE IN CURRENT OR SPARK VOLTAGE → INCREASED MRR, HIGHER SURFACE ROUGHNESS
- INCREASE IN SPARK FREQUENCY → IMPROVED SF ← ENERGY SHARED BY MORE # OF SPARKS → DECREASED CRATER SIZE
- LOW IEG → LOW MRR, HIGH SF, BETTER ACCURACY
- DECREASED PULSE DURATION → LOW VALUE OF MRR AND SF, HIGH ELECTRODE WEAR

PROCESS CHARACTERISTICS

- WORKPIECE MATERIAL → ELECTRICALLY CONDUCTIVE
- OPERATIONS → DRILLING, SLOTTING, DIE SINKING, ETC
- ACCURACY → ± 0.025 TO ± 0.127 mm
- DEEP ACCURATE HOLES → ROUGHING / FINISHING PASSES ← MINIMIZE TAPER (0.005 TO 0.050 mm/cm)
- ASPECT RATIO → 100 : 1 ← SPECIAL CARE OF FLUSHING
- MRR, → LOW
- MATTE SURFACE
- KINDS OF SURFACE LAYERS
 - ⇒ RECAST LAYER → 2 TO 50 μm → EXTREMELY HARD AND BRITTLE
← SHOULD BE REMOVED
 - ⇒ HEAT AFFECTED ZONE → ~ 25 μm . RESIDUAL STRESSES, GRAIN BOUNDARY CRACKS, ETC
 - ⇒ CONVERTED LAYER → CHANGE IN GRAIN STRUCTURE
 - ⇒ PARENT MATERIAL

APPLICATIONS

- ANY MATERIAL → ELECTRICALLY CONDUCTIVE
- AEROSPACE, AUTOMOBILES, TOOLS AND DIE MAKING INDUSTRIES
- THIN FRAGILE COMPONENTS ← NO DANGER OF DAMAGE

ELECTRIC DISCHARGE GRINDING (EDG)

- SAME PRINCIPLE AS THAT OF EDM
- ELECTRICALLY CONDUCTIVE GRINDING WHEEL (NO ABRASIVE PARTICLES)
- ROTATING WHEEL → PROPER CIRCULATION OF DIELECTRIC IN IEG
- MATERIAL REMOVAL → MELTING AND VAPORIZATION

ELECTRIC DISCHARGE DIAMOND GRINDING

* WORKING PRINCIPLE

- HYBRID PROCESS → EDM + GRINDING
- WATER/WATER BASED CUTTING FLUID → DIELECTRIC
- METAL BONDED DIAMOND GRIT WHEEL
- SPARKING → BETWEEN BONDING MATERIAL AND W/P
- MATERIAL REMOVAL BY BOTH → EDM + GRINDING ← EASIER
- SELF DRESSING OF GRINDING WHEEL

* CAPABILITIES AND APPLICATIONS

- MACHINING OF CERMATES, SUPER ALLOYS, METAL MATRIX COMPOSITES
- HIGH MRR_v, HIGH WHEEL LIFE, GOOD SF, BETTER SURFACE INTEGRITY

WIRE ELECTRIC DISCHARGE MACHINING (WIRE EDM)

- WORKPIECE MATERIAL → ELECTRICALLY CONDUCTIVE
- TOOL → 0.05 - 0.30 mm DIA. WIRE
- STRATIFIED WIRES
- DIELECTRIC → DEIONIZED WATER
- MATERIAL REMOVAL → MELTING, VAPORIZATION
- CONSTANT IEG → COMPUTER-CONTROLLED POSITIONING SYSTEM



CAN CUT COMPLICATED CONTOURS

- HIGH DEGREE OF ACCURACY AND GOOD SF

WIRE EDM MACHINE

- POWER SUPPLY SYSTEM
- DIELECTRIC SYSTEM
- POSITIONING SYSTEM
- DRIVE SYSTEM

POWER SUPPLY SYSTEM

- PULSE FREQUENCY → 1 MHz → REDUCED CRATER SIZE → BETTER SF
- SMALL WIRE SIZE → CURRENT CARRYING CAPACITY < 20 A

DIELECTRIC SYSTEM

- WATER AS DIELECTRIC

↓

- ⇒ LOW VISCOSITY → EFFICIENT FLOW
- ⇒ NO FIRE HAZARD
- ⇒ HIGH COOLING RATE
- ⇒ HIGH MRR AND HIGH TWR

↓

DOES NOT AFFECT PERFORMANCE

- REUSED AFTER FILTRATION
- 5 µm SIZE DISPOSABLE FILTER
- ADDITIVES TO MINIMIZE RUSTING

POSITIONING SYSTEM

- CNC 2-AXES TABLE ← ADAPTIVE CONTROL MODE
- IN CASE OF SHORT CIRCUITING (← GRINDING GAP → TOO SMALL → WIRE AND WORKPIECE TOO CLOSE) → SENSES AND MOVES BACK TO RE-ESTABLISH PROPER CUTTING GAP CONDITIONS

WIRE DRIVE SYSTEM

- FUNCTIONS
- DELIVERS FRESH WIRE
 - KEEPS WIRE ALWAYS UNDER TENSION

- FOR HIGH QUALITY → AVOID TAPER, STREAKS ETC
- MINIMIZES WIRE BREAKAGE FREQUENCY
 - WIRE GUIDED BY WIRE GUIDES
 - SAPPHIRE
 - DIAMOND
 - WIRE MOVEMENT TOWARDS TAKE UP SPOOL → SERIES OF TENSIONING ROLLERS
 - AUTOMATIC RELOADING OF BROKEN WIRE
 - + TO ENHANCE PRODUCTIVITY
 - + TO RUN THE M/C UNATTENDED
 - WIRE MATERIAL
 - SMALL DIAM (< 0.15 mm) MOLYBDENUM
 - LARGE DIAM (0.15-0.3mm) → COPPER OR BRASS
 - WIRE DISCARDED AFTER USED ONCE. → AFTER WEAR AT LEADING SURFACE IT NO LONGER REMAINS STRAIGHT

PROCESS VARIABLES

- LINEAR CUTTING RATE → THICKNESS OF WORKPIECE BUT NOT THE COMPLEXITY OF CUT
- HIGHEST WIRE SPEED → 40 mm/s

PROCESS CHARACTERISTICS

- MATTE SURFACE
- CRATERS HELP IN RETAINING LUBRICATING OIL → INCREASED DIE LIFE
- SF IN FINISH PASS → $0.1 \mu\text{m}$
- TOLERANCE → $\pm 7 \mu\text{m}$

APPLICATIONS

- DIES
- PRESS TOOLS
- ELECTRODES, ETC

LASER BEAM MACHINING (LBM)

PRODUCTION OF LASERS

Most of us are familiar with a common experiment performed for fun during the school days, in which sun rays are focussed by a lens to burn a piece of paper. The energy density achieved in this experiment is about 1W/mm^2 . In the same way, let a laser beam be focussed at the diamond surface. The energy density at the diamond surface may be achieved so high (about 1000 W/mm^2) that it can melt and even vaporize the diamond.

Such a tremendous amount of energy release is achieved due to collision of oscillating, high energy-level atoms with electromagnetic waves having resonant frequency. These waves absorb energy from the atoms and become highly powerful, and are called **MASER** (Microwave Amplification by

Stimulated Emission of Radiation). Later, LASER (Light Amplification by Stimulated Emission of Radiation) was invented by amplifying ordinary light waves based on similar principle (ie to transmit light waves with constant frequency and wavelength without interference).

Einstein hypothesized that under appropriate conditions, light energy of a particular frequency can be used to stimulate the electrons in an atom to emit additional light with exactly the same characteristics as the original stimulating light source. An atom, initially in any of the excited states, does not remain forever in that state (or energy level). Einstein proposed that when an atom at 'q' energy level has light of right frequency *acting* on it, it absorbs photons of that light and the transition takes place from lower energy level 'q' to higher energy level 'p'. This phenomenon of the movement of an atom to the higher energy level is called **absorption** (Fig. 8.1). On the other hand, transition of an atom from the higher energy level 'p' back to the lower energy level 'q' is known as **emission**. The emission could be one of the two kinds, viz spontaneous emission (independent of light intensity) and stimulated emission (influenced by the intensity of light).

Suppose each horizontal line in Fig. 8.2 indicates the allowed value of energy of an atom at that energy level. Let an atom (or molecule) be brought to high energy level (say, E_3 in Fig. 8.2) by an outside energy source (say, heat, light, chemical, etc). Now, if it is allowed to decay back to its ground state energy level (E_0), a photon (unit of light) is released (Fig. 8.2). If this photon comes in contact with another molecule or atom at high energy level (E_3) then this atom will also decay back to ground state releasing another 'photon'. This chain of events would produce photons having same characteristics (viz wavelength, phase, direction and energy). This sequence of triggering clone photons from stimulated atoms (or molecules) is known as **stimulated emission**. Stimulated emission forms the basis of laser operation. This process is reverse of the one in which photons (or electromagnetic waves) are absorbed by atomic system. Further, to produce a working laser, the energy source should be so powerful that most of the atoms (or molecules) of the lasing material are at their higher energy level. It is known as *population inversion* and refers to the population of atoms/molecules in the lasing material.

Feedback mechanism is an essential element of the laser producing system. It captures and redirects a part of the coherent photons back into the

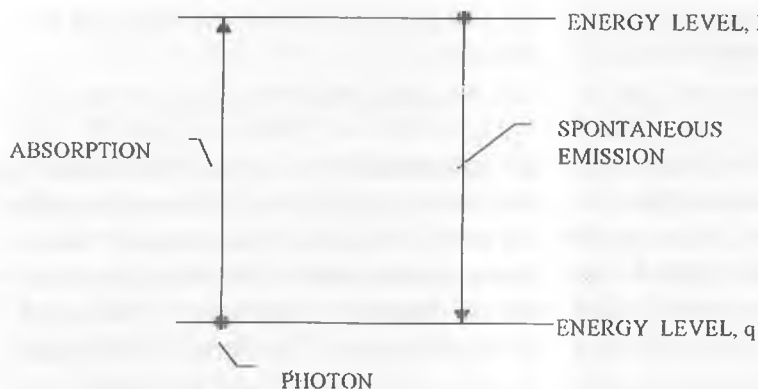


Fig. 8.1 Transition by absorption and spontaneous emission between two given energy levels of an atom [Bhattacharyya, 1973].

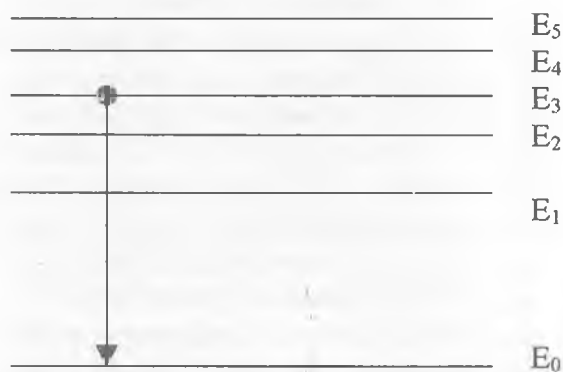


Fig. 8.2 Energy diagram for an atom showing level to level transition [Bhattacharyya, 1973].

active medium. These photons further stimulate the emission of some more photons of the same frequency and phase. This mechanism also permits a small percentage of coherent photons to exit the system in the form of laser

light. This laser light is utilized for various useful purposes as discussed in the following sections. Rest of the photons remain in the system and are responsible to maintain the amplification process through stimulated emission.

WORKING PRINCIPLE OF LASER BEAM MACHINING

Laser light is monochromatic, i.e. its wavelength occupies a very narrow portion of the spectrum. Hence, a simple lens is able to focus and concentrate laser light to a spot of much smaller diameter and much higher intensity than that obtained by other types of light. Laser light is coherent in nature (it travels in phase). Hence, it gives higher focussed intensities than normal light which is incoherent in nature. The low divergence rate of lasers is also responsible for high intensity of light.

Thus, laser beam is a light source having unique properties like high monochromaticity, high degree of coherence, high brightness, high peak power, high energy per pulse, and very small size of the focussed spot. Wavelength of commonly used lasers lies between $0.21\text{ }\mu\text{m} - 11\text{ }\mu\text{m}$ (Ruby = $0.7\text{ }\mu\text{m}$, Nd : YAG $\approx 1.0\text{ }\mu\text{m}$, CO $\approx 2.7\text{ }\mu\text{m}$ and CO₂ $\approx 10.6\text{ }\mu\text{m}$).

Fig. 8.3 shows three important elements of any laser device, viz. a laser medium (a collection of atoms, molecules, or ions), a pumping energy source required to excite these atoms to higher energy level, and optical feedback system. Consider a *gas laser* consisting of a thin tube filled with gas at low pressure. There are electrodes placed at both ends of the tube. Electric current when passed through provides sufficient energy to stimulate the atoms/molecules of the gas in the tube. As shown in Fig. 8.4, the *feedback mechanism* for laser resonator consists of parallel mirrors kept at the ends of the tube. One of these mirrors is fully reflective (HR mirror in Fig. 8.4) while the other one is partially transparent to provide the laser output (output mirror). It allows a beam of radiation to either pass through, or bounce back and forth repeatedly through the laser medium.

To make the laser beam useful for **processing of materials**, its power density should be increased by focusing. The power density of laser beam and its interaction with the workpiece will determine whether the beam will be able to perform the function of welding, cutting, heat treatment or marking. To perform a machining operation, laser beam power density should lie between 1.5×10^6 to $1.5 \times 10^8\text{ W/cm}^2$, and the workpiece should be kept very close to prime focus. However, for welding, lower power densities of the order of 1.5×10^4 to $1.5 \times 10^5\text{ W/cm}^2$ are adequate.

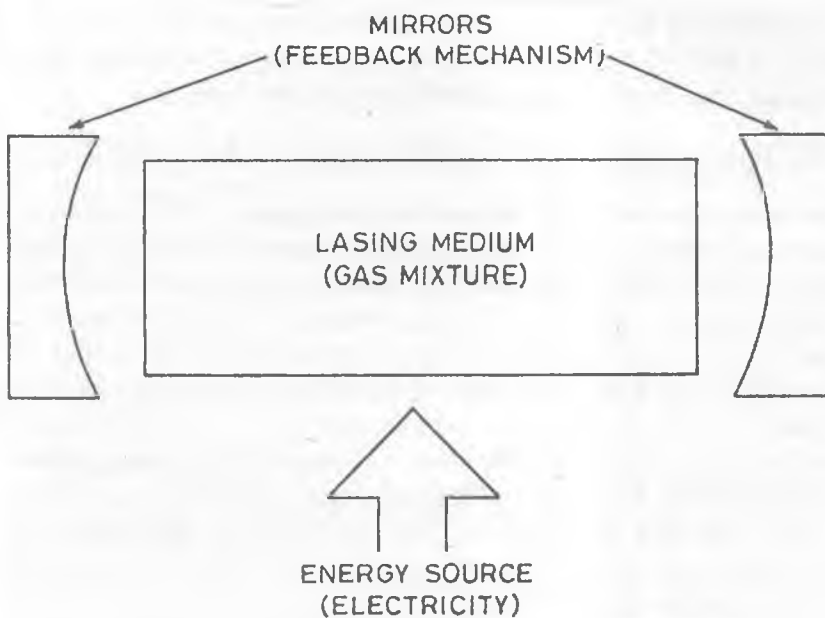


Fig. 8.3 Components of a gas laser [Benedict, 1987].

As the laser beam falls on the workpiece surface, reflection and transmission of electromagnetic waves at the interface of air-workpiece material takes place. Reflection and transmission of electromagnetic waves of given wavelength depend on its reflectivity and absorption coefficient. Depending upon the intensity of the beam, one of the following events may take place:

- (i) in case of low intensity beam, there may be no phase change of the irradiated work material;
- (ii) in case of high intensity beam, the work surface temperature would rise up to or above its boiling point and vaporization would take place.

TYPE OF LASERS

Basically lasers are of two types, i.e. solid state laser and gas laser.

Solid State Lasers

Because of poor *thermal properties of solid state* lasers (viz ruby and Nd: glass), they can't be used for heavy duty work. Such lasers do not operate faster

than 1 or 2 Hz. They are used only for low pulse applications like spot welding, drilling, etc. However, Nd: YAG laser, most powerful in solid state lasers, is also used for operations like cutting. Its mean power (< 1000 W) is much lower than CO₂ laser. Hence, it is usually employed for light works.

Many materials with laser action have been developed, viz calcium fluoride crystals doped with neodymium (Ca + F₂ Nd). The round crystal rods with reflective ends are used. Crystalline ruby is another material used for laser action. It is aluminium oxide with chromium ion impurities distributed through the aluminium lattice sites (Al₂O₃ + Cr₂ (0.05%)). Flash lamp surrounding the ruby rod produces light. Flash lamp and ruby rod are enclosed in the cylinder. This cylinder has highly reflective internal surfaces. These surfaces direct light from the flash lamp into the rod. This light excites the chromium ions of ruby crystal to high energy levels. While on return journey to the normal state, these excited ions at high energy levels release the photons (or energy). Thus, desired energy is obtained in the form of short duration pulses.

Gas Lasers

In this type of laser, CO₂, He, or N₂ act as a lasing medium. These gases are recirculated and replenished to reduce the operating cost. Direct electrical energy is used to provide energy for stimulating lasing medium.

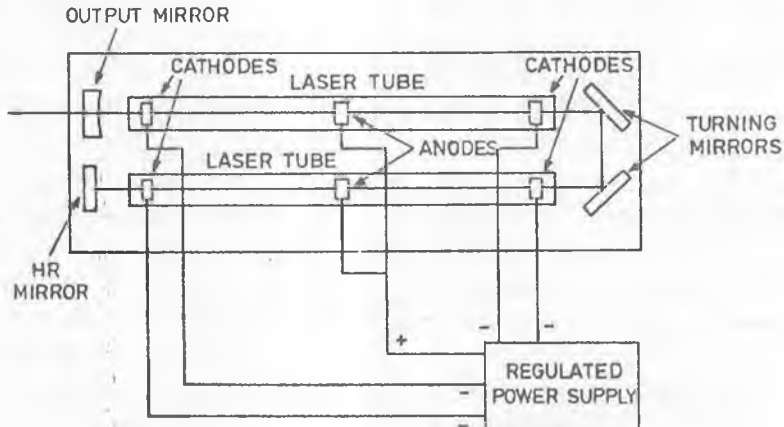


Fig. 8.4 Folded resonator axial flow carbon dioxide laser [Benedict, 1987].

Axial flow CO_2 laser is shown in Fig. 8.4, and its power giving capacity is usually 100 W each meter length of the tube. For higher powers up to 1500 W and reduced floor space, folded resonator axial flow CO_2 lasers are used. For very high power (several thousand watts) and still very compact CO_2 laser is known as transverse flow, or *gas transport laser*. Some of the details of the gas laser set-up are as follows:

Large amount of gas volume is used. The resonator mirrors are positioned to reflect the beam several times before it escapes through the output mirror. Most of the lasers are *computer controlled* to take advantage of their high speed processing. During the processing of materials, motion can be given to either workpiece or the beam or both depending upon the design.

PROCESS CHARACTERISTICS

Fig. 8.5 shows the various processes in which the laser power is utilized during LBM [Yeo *et al.*, 1994]. The relative magnitudes of heat consumption as losses and absorption by workpiece depend upon thermal and optical properties of the work material, and intensity and pulse duration of the laser beam. It is also to be noted that a part of the material being expelled from the work surface stays in the path of the beam in the form of small droplets and continues to absorb energy.

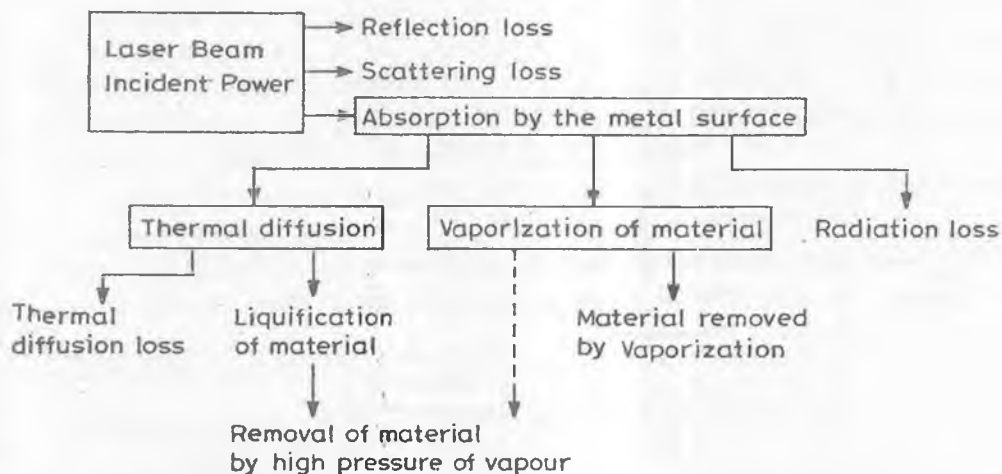


Fig. 8.5 A laser beam power balance diagram for LBM [Yeo *et al.*, 1994].

High capital and operating cost, and low machining efficiency (usually less than 1%) prevent LBM from being competitive with conventional machining techniques. **Industrial lasers** operate either in continuous wave mode (CW) or impulsed mode. CW lasers are used for processes like welding, laser chemical vapour deposition (LCVD), surface hardening, etc which require uninterrupted supply of energy for melting and phase transformation. Controlled pulse energy is desirable for the processes like cutting, drilling, marking, etc, so that HAZ is minimum possible. It has also been found [Huber and Marx, 1979] that machining by LBM technique also reduces fatigue strength of the machined component as compared to the fatigue strength of the component when machined by conventional processes.

LBM results in a **heat affected zone (HAZ)**. It has also been found that as the feed rate in LBM increases, the thickness of the HAZ goes down. The thickness of the HAZ is also governed by the type of assisting gas and its pressure (in case of gas assisted laser cutting), gas nozzle diameter, and the distance between the nozzle tip and the workpiece.

In LBM, there are no *mechanical forces* exerted on the workpiece. LBM process is capable of easily machining refractory, brittle, hard, metallic, and non-metallic materials, viz cast-alloy, tungsten, titanium, alumina, and diamond. It can machine through any optically transparent material (say, glass). As long as the beam path is not obstructed, it can be used to machine in otherwise **inaccessible areas**. The laser beam can operate through transparent environment like air, gas, vacuum, and in some cases even liquids. However, LBM cannot be applied to highly conductive and reflective materials *which have high heat conductivity and or high reflectivity* (viz aluminium, copper, and their alloys). Because of this property, table made of aluminium is used to hold the workpiece while machining it by LBM process. It should also be noted that LBM systems are quite inefficient.

The least diameter to which a laser beam can be focussed depends upon the laser beam divergence, which is a function of the quality of the laser material and depth at which machining is being done. Using LBM, holes of large aspect ratio (= hole depth/diameter of hole) and of a very small diameter can be drilled. Fig. 8.6 shows a schematic diagram of the cross-section of a **hole drilled** using LBM process. The taper angle of a drilled hole reduces with an increase in the depth of the hole [Scott, 1976]. Geometry of Fig. 8.6 can be used to evaluate taper angle, α (= $(e-c)/d$). **Recast layer** (ie any molten or vaporized material that resolidifies

and deposits on the machined surface) has microcracks and is loose enough to be scraped off easily. It is also easy to drill holes at an angle other than 90° to the surface (no less than approximately 10°).

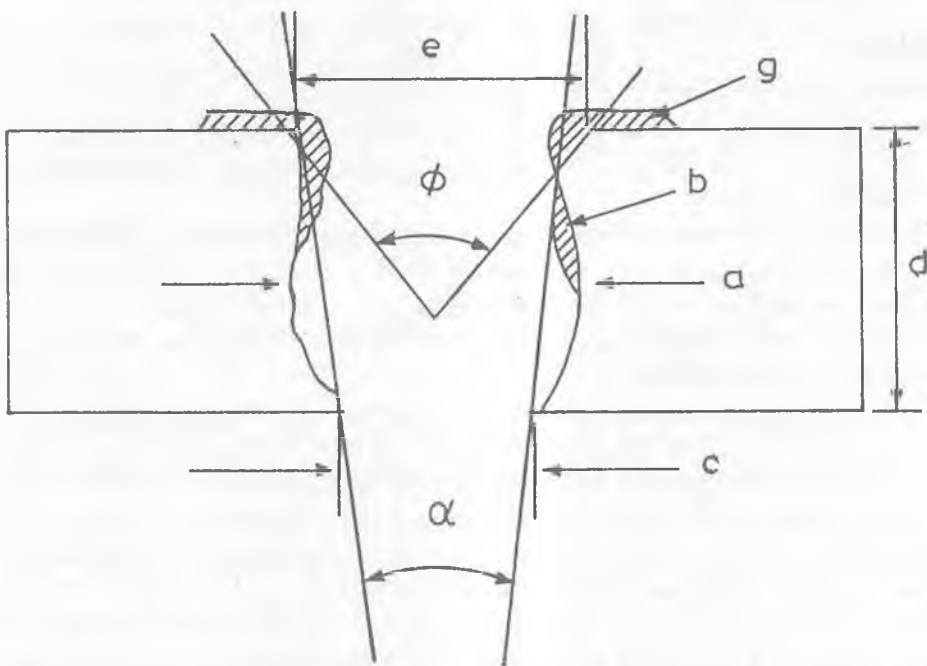


Fig. 8.6 Geometry of a hole drilled using LBM process, **a**-the diameter of the mid span, **b**-the thickness of the recast layer, **c**-the exit diameter, **d**-the hole depth, **e**-the inlet diameter, **g**-the thickness of the surface debris, ϕ - the inlet cone angle, α -the taper angle
[Garcia de Vicuna et al, 1989].

For a good quality **drilled hole**, high peak power (or ratio of high pulse energy and short pulse duration) and high power density are recommended. The recommended range of pulse duration suitable for deep hole drilling is 0.1 to 2.5 ms. It is reported [James and Mike, 1989] that the time required to drill a given size hole is inversely proportional to the amount of energy delivered per pulse (Fig. 8.7).

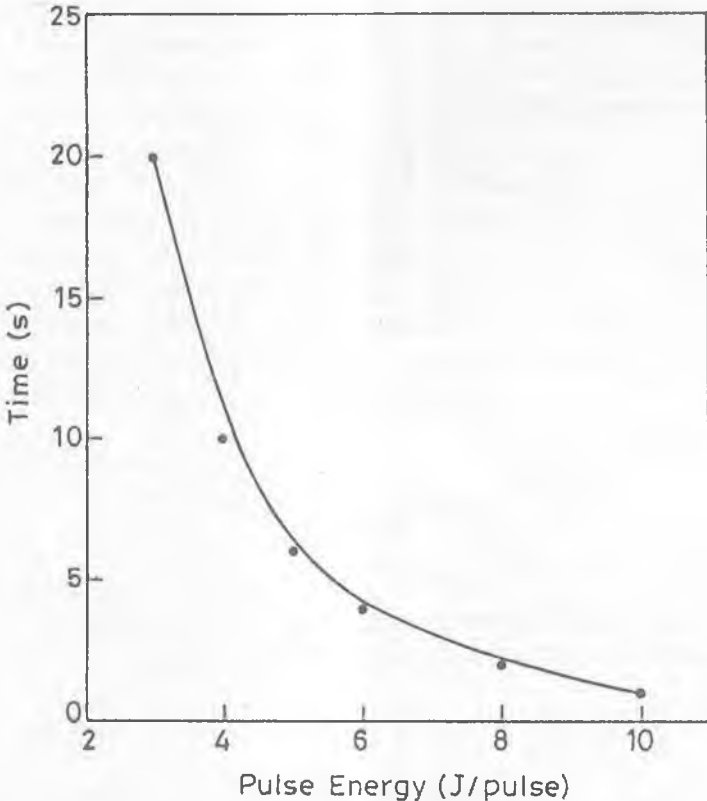


Fig. 8.7 Effect of pulse energy on time required for drilling a hole of constant depth ($= 6.355$ mm) in steel alloy [James and Mike, 1989].

The process is quite efficient for the first few seconds and afterwards its penetration rate goes down as shown in Fig. 8.8.

APPLICATIONS

Laser beam energy has been favourably employed for cutting difficult-to-machine materials such as hardened steels, composites, ceramics, etc. However, the process is employed to those materials which have favourable thermal and optical properties.

Laser beam energy has been utilized for operations like drilling, cutting,

micromachining, trepanning, trimming, marking, welding, soldering, brazing, etc. [Kobayashi, 1984].

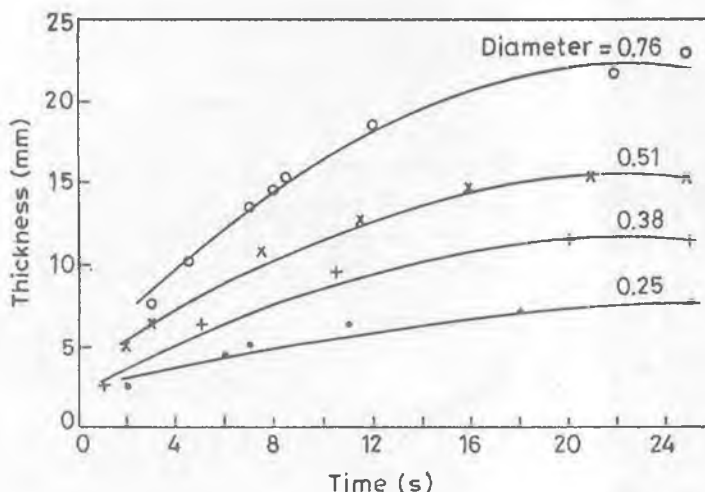


Fig. 8.8 Relationship between thickness of material and drilling time for various diameter hole sizes (mm) [James and Mike, 1989].

Drilling

This process is extensively used for making **small holes** (microhole dia. < 1 mm; small hole dia. 1.0-3.2 mm [Yeo *et al.*, 1994]) and also known as laser percussion hole drilling. The workpiece is placed at or near the focal point of the laser beam. The localized high intensity heat results in melting of a part of the material and a small part may vaporize also. Escaping of vaporized material results in most of the volume of molten material to be removed as a spray of the droplets.

Superalloys due to their properties like toughness, creep strength, and hot corrosion resistance at high temperatures, are commonly used materials for the turbine components like blades, guide vanes, afterburners and casings where temperatures as high as 2000°C can reach. A large number of **cooling holes** are required to be drilled in some of these components. Laser beam drilling (LBD) among small hole drilling processes (say, ECD) is more commonly used [Yeo *et al.*, 1994].

The process has been used to drill small holes (diameter, 0.125 to 1.25 mm) with depth to diameter ratio as high as 100:1. It has been used for drilling miniature holes in diamond dies for wire drawing, in sapphire and ruby bearings for watches, holes in turbine blades for cooling, etc. The drilled holes are found to have a taper, rough shape with low degree of roundness, recast layer and heat affected zone (\approx 0.0025 to 0.1 mm). The actual values of these characteristics (taper, roundness, etc) depend upon the workpiece material, thickness of the workpiece and the machining parameters. Diametral repeatability of this process is about ± 0.025 mm or $\pm 10\%$ of the diameter (whichever is greater). It is also reported [Sona, 1987] that a better quality hole and improved performance of the process can be achieved if high frequency pulses of low energy are used in place of high energy single pulse.

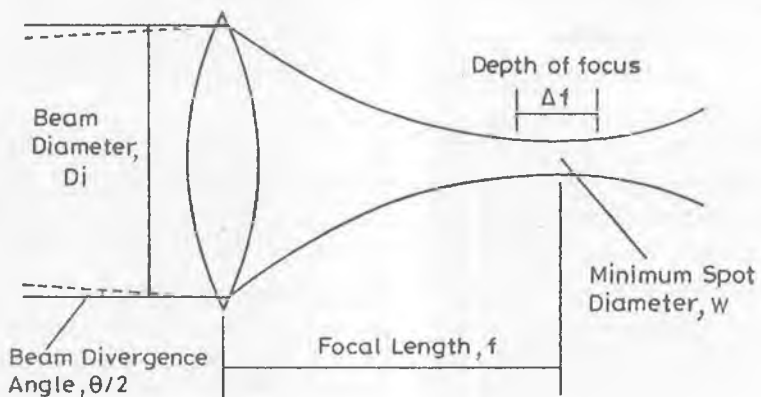


Fig. 8.9 Focal pattern of a converging lens [James and Mike, 1989].

The **beam divergence** (beam spread, or an increase in beam diameter for unit distance of beam travel) depends on the average output power of the laser [Bolin, 1982]. Laser beam with low divergence should be recommended for deep hole drilling. Apart from low divergence, laser beam should also have long focal length. To have straight sided hole, focal point of the laser beam should be located just below the surface of the material being machined. The beam is always focussed to a "waist" rather than infinitely small spot due to divergence and diffraction. The depth of focus (Fig. 8.9) is the length of the beam over which the waist diameter does not change appreciably. A lens of larger focal length gives a larger depth of focus. The depth of focus (Δf) can be calculated using Eq. (8.1).

where, f is focal length of the lens (mm), W (in mm) is the focussed diameter ($= f \cdot \theta$), θ is the total beam divergence angle (radians), and D_i^* is the beam diameter (mm).

Cutting

Larger sized holes (> 1.2 mm diameter) can't be drilled by this process because of low power density of the focussed beam. Hence, larger sized holes are trepanned (or cut) rather than drilled. Laser cutting does not involve any mechanical type of forces. Cutting is done at high speed and it is capable to pierce the workpiece at any location and can cut omnidirectionally. The laser beam goes towards the optical assembly having a focusing lens and a coaxial gas jet system. The laser beam and a gas jet are directed to the workpiece. The gas jet assists in clearing the material from the cut, and also to keep debris away from contaminating the focusing lens.

Nd:YAG laser gives low mean power beam but its intensity is quite high ($> 10^8$ W/cm²) mainly due to better focussing behaviour (beam divergence, 0.001 radian and focussed beam diameter, 0.08 mm). Due to low thermal load, Nd:YAG laser has been employed for cutting of brittle materials like SiC ceramics without crack damage [Tonshoff *et al*, 1989] with smaller kerf width and HAZ, as compared to CO₂ laser. Commercially available laser unit of about 800 W capacity can cut most metal plates up to 3 mm thick or so with cutting accuracy of about 0.8 mm.

Use of oxygen as a **jet gas** is often recommended for oxidizable material (viz, carbon steels). It gives higher cutting speed compared to other gases like air or nitrogen but oxidized edges of the machined components give larger HAZ. Argon gives very good cut edges, hence used for cutting workpieces which are to be welded or brazed at a later stage.

Cut shapes can be produced either by **trepanning** or **CNC cutting**. Trepanning is achieved by optomechanically sweeping the beam in the desired path on the workpiece. Large sized holes using laser beams are made by trepanning operation in which either laser beam or workpiece is moved according to the profile of the hole. The size of the trepanned hole does not depend on the size of the laser beam spot. This technique has been employed to drill holes in ceramics also.

Cycle time ranges from a fraction of a second to few seconds depending upon thickness of the workpiece material. Noncircular holes can be better machined by *CNC contour cutting*. Any programmable shape can be machined by this technique.

Marking

The marking system is used to imprint letters, numerals and symbols on metal and nonmetal workpieces. The system is made up of **pulsating laser system** and a computer-controlled beam scanning system. As the beam scans the workpiece, the localized area in the form of overlapping blind holes is vaporized to produce blind grooves of maximum width and maximum depth of 0.25 mm. The depth can be as low as 0.005 mm but it also depends on the selected machining parameters. To obtain high quality marking (blind features in workpieces) with minimum surface damage, a high power density pulsing laser beam lasting only for nanoseconds is used. To control the position of laser beam and timings of the laser pulses, a microcomputer is used. The necessary information to generate different characters is stored in the computer. As the system is put on, the beam scans the workpiece in the form of desired patterns at the rate as high as 30 characters/second. The quality of the characters obtained is quite high.

Miscellaneous Applications

LBM is being employed for both micro machining as well as macro machining. A **three-dimensional laser beam machining** process, utilizing two laser beams, for operations like threading, turning, grooving (Fig. 8.10a), etc has been employed [*Chryssolouris et al., 1989*]. During 3-D cutting, two independent lasers are simultaneously used to cut two grooves which are moving closer to each other. When these two grooves converge, a volume is cut off without being melted/vaporized (Fig. 8.10b).

Laser energy has also been employed to fracture in a controlled fashion delicate items. Absorption of laser energy by workpiece results in thermal gradients leading to the mechanical stresses. Finally, it results in a controlled fracture.

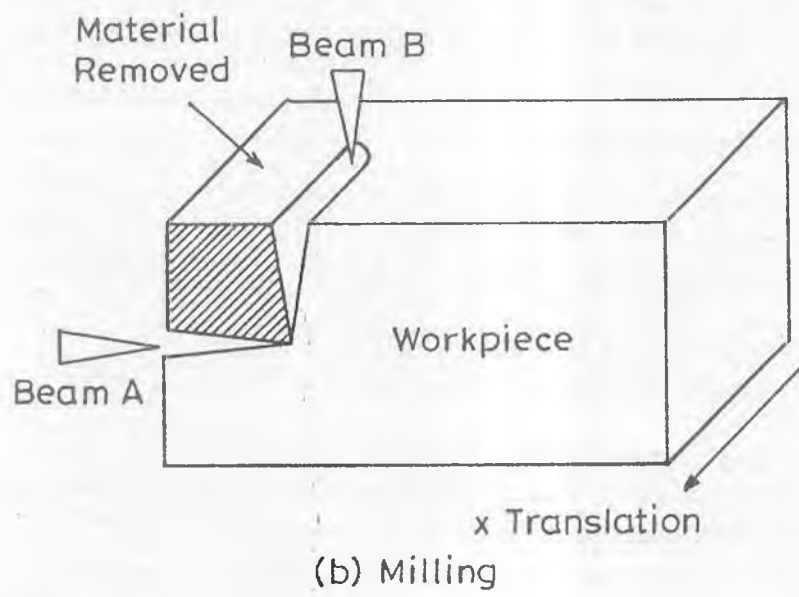
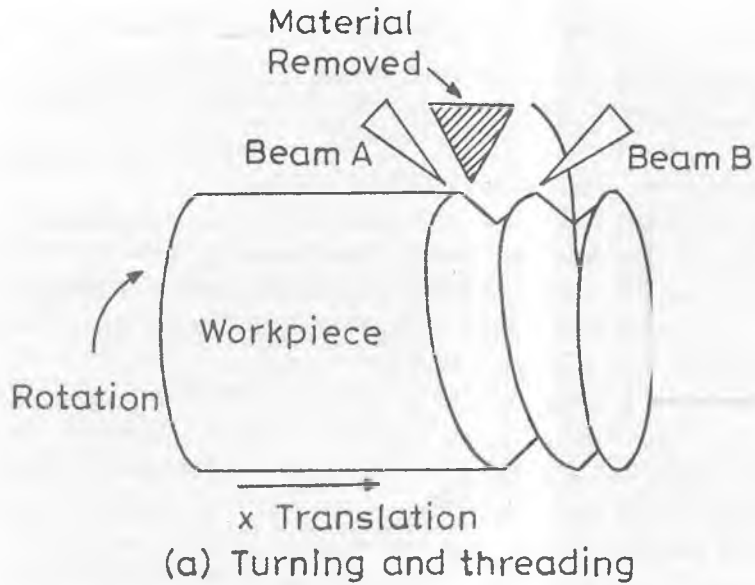


Fig. 8.10 Schematic diagram of (a) turning/threading, (b) milling, using two laser beams [Chryssolouris *et al*, 1989].

BIBLIOGRAPHY

1. Benedict G.F. (1987), *Non-traditional Manufacturing Processes*, Marcel Decker Inc., New York.
2. Bhattacharya A. and Brain K. (1989), Drilling: Working through the Benefits, *Machining Prod. Engg.*, Vol. 147(3765), pp. 73-83.
3. Bolin S.R. (1983), Nd:YAG Laser Application Survey, *Laser Material Processing* (Ed: M.Boss), North Holland Co., Amsterdam, pp. 407-438.
4. Bolin S.R. (1982), The Effect of F # and Beam Divergence on Quality of Holes Drilled with Pulsed Nd:YAG Laser, *Proc. Mat. Process. Symp.*, Laser Institute of America, Vol. 31, pp. 135-140.
5. Chryssolouris G., Schonbeck J., Choi W. and Sheng. P. (1989), Advances in three Dimensional Machining, paper presented to *WAM of ASME (PED-VOL)*, held at San Francisco, p. 17.
6. Chryssolouris G., Bredt J., Kordas S. and Wilson E. (1988), Theoretical Aspects of a Laser Machine Tool, *Trans. ASME, J. Engg. for Ind.*, Vol. 110, pp. 65-70.
7. Chryssolouris G., Choi W.C., Kyi S.B. and Sheng P. (1988), Investigation of the Effect of a Gas Jet in Laser Grooving, *Proc. 16th NAMRC*, pp. 217-223.
8. Chryssolouris G. and Yablon A. (1993), Depth Prediction in Laser Machining with the Aid of Surface Temperature Measurement, *Annls CIRP*, Vol. 42(1), pp. 250-257.
9. Gracia de Vicuna G.E., Beitialarrangoitia J.C. and Ghosh S.K. (1989), Defects Arising from Laser Machining of Materials, in *High Power Lasers*, (Eds.) A. Niku-Lari and B.L. Mordike, pp. 227-249.
10. Huber J. and Marx W. (1979), Production Laser Cutting, *ASM Conf. Applcat. Lasers Mater. Processing*, Washington DC, pp. 273-290.
11. James J. and Mike P. (1989), Deep Hole Drilling with Lasers, *Mod. Mach. Shop*, pp. 53-63.
12. Jiang C.Y., Lau W.S., Yue J.M. and Chiang L. (1993), On the Maximum Depth and Profile of Cut in Pulsed ND:YAG Laser Machining, *Annls CIRP*, Vol. 42(1), pp. 223-226.
13. Kobayashi A. (1984), Recent Progress in Laser Processing in Japan, Proc. 5th *Int. Conf. Prod. Engg.*, held at Tokyo, pp. 459-465.

14. McGeough J.A. (1988), *Advanced Methods of Machining*, Chapman and Hall, London.
15. Scott B.F. (1976), Laser Machining and fabrication – A Review, Proc. 17th *Int. Mach. Tool Des. Res. Conf.*, Birmingham, Macmillan Press, pp. 335-339.
16. Sona A. (1987), Metallic Materials Processing: Cutting and Drilling, in: ODD Soares and M. Perez Amor (Eds) *Applied Laser Tooling*, Nijhoff Boston, pp. 105-113.
17. Tonshoff H.K. and Emmelmann C. (1989), Laser Cutting of Advanced Ceramics, *Annls CIRP*, Vol. 38, pp. 219-222.
18. Ye. O C.Y., Tam S.C., Jana S., Michael W.S. Lau (1994), A Technical Review of the Laser Drilling of Aeroplane Materials, *J. Materials Process Tech.*, Vol. 42, pp. 15-49.

SELF-TEST QUESTIONS

- Q1. Make the correct choice(s).
- (a) LBM system cannot effectively machine
 - (i) refractory materials, (ii) tungsten carbide, (iii) copper, (iv) M.S.
 - (b) The efficiency of LBM system is about
 - (i) 3 to 5%, (ii) 13 to 15%, (iii) 0.3 to 0.5%, (iv) 30 to 50%.
 - (c) While drilling deep hole by LBM process, it is (with reference to top surface)
 - (i) straight sided, (ii) converging, (iii) diverging, (iv) none of these.
 - (d) You can use LBM for machining soda lime glass
 - (i) yes (ii) no.
 - (e) The suitable process(es) for 5 mm deep blind and complex contoured slot in M.S. sheet of 20 mm thickness is (are)
 - (a) LBM, (b) EDM, (c) ECM, (d) AFM.
 - (f) Commonly used process for making cooling holes in a turbine blade is
 - (a) USM, (b) AWJM, (c) LBM, (d) EBM, (d) EDM.

REVIEW QUESTIONS

- Q2. Answer in brief.
- (a) Write the full form of the following acronyms: LASER, MASER, and HAZ.
 - (b) Explain the effect of ‘focussing’ on the performance of LBM.

(c) LBM and EDM both are thermal processes. However, it is found that the first one results in more thermal damage to the machined component than the second one. Is it true? Justify your answer.

Q3. Explain the production of laser beam and working principle of LBM.

NOMENCLATURE

Di* Beam Diameter

E,p,q Energy levels

f Focal length

Δf Depth of focus

W Minimum spot diameter

θ Beam divergence angle

ACRONYMS

CNC Computer numerical control

HAZ Heat affected zone

HR Highly reflecting

LASER Light Amplification by Stimulated Emission of Radiation

MASER Microwave Amplification by Stimulated Emission of Radiation

CHAPTER 8
AT-A-GLANCE
LASER BEAM MACHINING
(LBM)

PRODUCTION OF LASER

- HYPOTHESIS OF EINSTEIN → POSSIBLE TO USE LIGHT ENERGY TO STIMULATE ELECTRONS → EMIT LIGHT OF SAME CHARACTERISTICS
- AN ATOM BROUGHT TO HIGH ENERGY LEVEL 'E2' BY OUTSIDE ENERGY SOURCE (LIGHT, HEAT, etc)
- THIS ATOM ALLOWED TO DECAY BACK TO GROUND STATE ENERGY LEVEL (E1) → A PHOTON IS RELEASED
- THIS PHOTON CONTACTS OTHER ATOM <- WILL ALSO DECAY BACK → CHAIN REACTION → STIMULATED EMISSION
- ENERGY SOURCE → SO POWERFUL → MOST OF THE ATOMS OF LASING MATERIAL ARE AT HIGHER ENERGY LEVEL

FEEDBACK MECHANISM

- CAPTURES AND REDIRECTS A FEW COHERENT PHOTONS BACK INTO THE ACTIVE MEDIUM
 - STIMULATES THE EMISSION OF SOME MORE PHOTONS
 - ALSO PERMITS A SMALL PERCENTAGE OF COHERENT PHOTONS TO EXIT AS LASER LIGHT

LIGHT AMPLIFICATION BY STIMULATED EMISSION OF RADIATION

WORKING PRINCIPLE

- ELECTRODES AT BOTH ENDS OF THE TUBE
- ELECTRIC CURRENT → STIMULATES GAS ATOMS / MOLECULES IN THE TUBE
- FEEDBACK MECHANISM → PARALLEL MIRRORS AT THE ENDS OF THE TUBE
 - + ONE MIRROR → FULLY REFLECTIVE
 - + OTHER ONE → PARTIALLY TRANSPARENT → LASER OUTPUT
- LASER LIGHT → MONOCHROMATIC
- WAVELENGTH → VERY NARROW PORTION OF THE SPECTRUM
 - + A SIMPLE LENS FOCUSES & CONCENTRATES → VERY SMALL DIAMETER & HIGH INTENSITY BEAM
 - + LASER LIGHT COHERENT (TRAVELS IN PHASE) IN NATURE & LOW DIVERGENCE RATE

- USE OF LASER IN MATERIALS PROCESSING → HIGH POWER DENSITY
- MACHINING OPERATION → 1.5×10^6 - 1.5×10^8 W/cm²
- W/P KEPT VERY NEAR TO FOCUS

TYPES OF LASERS

→ SOLID STATE LASERS → RUBY, Nd : YAG



- GAS LASERS → CO₂, H₂, N₂, ETC
- GASES RECIRCULATED & REPLENISHED
 - + FOLDED RESONATOR AXIAL FLOW CO₂ LASER → 1500 W
 - + FOR VERY HIGH POWER → TRANSVERSE FLOW / GAS TRANSPORT LASER
- LARGE AMOUNT OF GAS VOLUME
- BEAM REFLECTED SEVERAL TIMES BEFORE ESCAPE
- COMPUTER CONTROL TO TAKE ADVANTAGE OF HIGH SPEED PROCESSING
- MOTION → W/P OR BEAM OR BOTH

PROCESS CHARACTERISTICS

- LOW FATIGUE STRENGTH
- THICKNESS OF HAZ → FEED RATE, GAS PRESSURE, NTD, AND GAS NOZZLE DIAMETER
- NO MECHANICAL FORCES
- CAN NOT BE APPLIED TO → HIGH HEAT CONDUCTIVITY & HIGH REFLECTIVITY MATERIALS → Al, Cu



MACHINING TABLE → ALUMINIUM

- QUITE INEFFICIENT SYSTEM (< 1%)

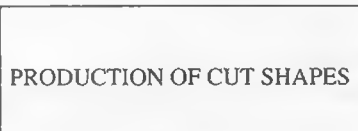
APPLICATIONS

DRILLING HOLES

- W/P PLACED AT/NEAR FOCAL POINT
- MELTING AS WELL AS VAPORIZATION
- HOLE DIAM → 0.125 - 1.25 mm, ASPECT RATIO → 100 : 1 TAPERED, LOW DEGREE OF ROUNDNESS, RECAST LAYERED WALLS. HAZ (2.5×10^{-3} - 10×10^{-3} mm)
- DIAMETER REPEATABILITY ± 0.025 mm, OR ± 10% OF THE DIAMETER (WHICHEVER IS GREATER)

CUTTING

- LARGE SIZED HOLES → CUT (TREPANNED) RATHER THAN DRILLED
- NO MECHANICAL FORCES → HIGH SPEED CUTTING
- GAS JET ASSISTS → CLEARING THE CUT MATERIAL.
 OXYGEN FOR OXIDIZABLE MATERIALS → HIGHER CUTTING SPEED
 BUT OXIDIZED EDGES → LARGER HAZ
- ARGON → GOOD CUT EDGES



→ CNC CONTOUR CUTTING



ANY PROGRAMMABLE SHAPE

↓
TREPANNING
↓

OPTOMECHANICALLY SWEEPING BEAM → DESIRED PATH
↓

CYCLE TIME → FEW SECONDS

MARKING

- TO MAKE LETTERS, NUMERALS, AND SYMBOLS → METALS & NON-METALS BOTH
- PULSATING LASER SYSTEM AND COMPUTER CONTROLLED BEAM SCANNING SYSTEM
- BLIND GROOVES OF VERY SMALL DEPTH (0.005 - 0.25 mm)



SELECTED MACHINING PARAMETERS

- FOR HIGH QUALITY MARKING → LASER BEAM LASTS FOR NANO-SECONDS
- MICROCOMPUTER TO CONTROL → POSITION AND TIMINGS
- 30 CHARACTERS/SECOND

PLASMA ARC MACHINING (PAM)

WORKING PRINCIPLE

A gas molecule at room temperature consists of two or more atoms. When such a gas is heated to a high temperature of the order of 2000°C or so, the *molecules separate out as atoms*. If the temperature is raised to 3000°C, the electrons from some of the atoms dissociate and the gas becomes ionized consisting of ions and electrons. This state of gas is known as plasma.

Thus, **plasma** is the glowing, ionized gas that results from heating of a material to extremely high temperature. It is composed of free electrons dissociated from the main gas atoms. A gas in plasma state becomes electrically conductive as well as responsive to magnetism. Because of such behaviour, plasma is also known as a *fourth state of matter*. The plasma is encountered in electrical discharges. The source of heat generation in plasma is the recombination of electrons and ions into

atoms, or recombination of atoms into molecules. This liberated bonding energy is responsible for increased kinetic energy of the atoms or molecules formed by recombination.

The temperature of plasma can be of the order of 33,000°C. When such a high temperature source reacts with work material, the work material melts out and may even vaporize, and finally is cut into pieces. Many materials (say, aluminum, stainless steel, etc) have high thermal conductivity, large heat capacity, and/or good oxidation resistance. As a result, such materials cannot be cut by conventional techniques like oxyfuel cutting. But these materials can be easily cut by plasma arc cutting (PAC).

PLASMA ARC CUTTING SYSTEM

PAC system uses DC power source. PAC systems operate either on non-transferred arc mode or transferred arc mode (Fig. 9.1). In the earlier case, the thermal efficiency is low (65–75%) and power is transferred between the electrode and the nozzle. This **non-transferred arc** ionizes a high velocity gas that is streaming towards the workpiece. The workpiece may be electrically conductive or non-conductive.

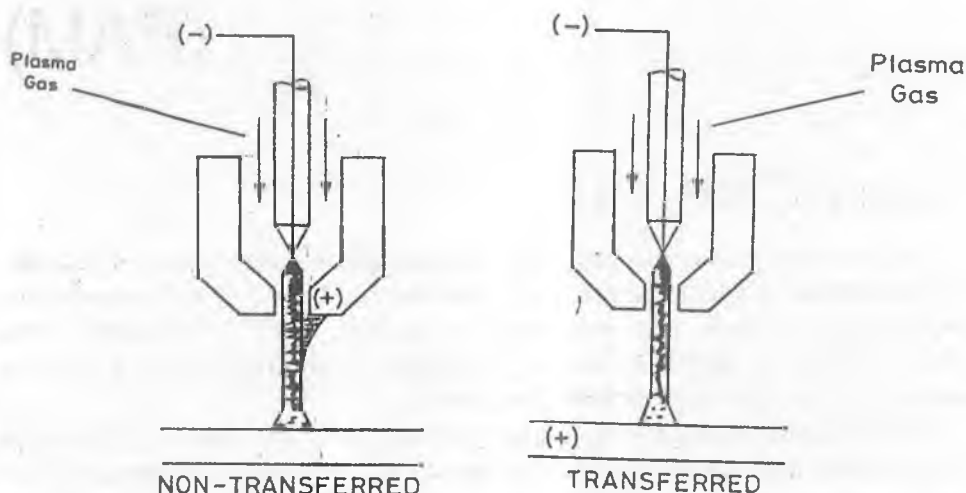


Fig. 9.1 Schematic diagram for non-transferred and transferred arcs.

In case of a **transferred arc mode**, the arc is maintained between the electrode (negative polarity) and the electrically conductive workpiece (positive polarity). Note that only *electrically conductive workpiece* can be machined or cut by transferred arc system. The arc heats a coaxial-flowing gas and maintains it in a plasma state. The electrothermal efficiency is up to 85–90%. PAC system can deliver up to 1000 A at about 200 V (DC). The flowing gas pressure may be up to 1.4 MPa resulting in a plasma velocity of several hundred metres/second. Higher the gas flow rate, more will be momentum of the plasma jet. It will ease out removal of the molten material from the machining zone. The plasma jet is constricted by the flowing gas which acts as a cooling agent sandwiched between the nozzle wall and the plasma jet.

In case of PAC, the material may be removed either by melting, or by melting and vaporization both. In either case, the material (in molten state or vaporized state) is blown off from the machining zone by high velocity plasma jet.

ELEMENTS OF PLASMA ARC CUTTING SYSTEM

The important **elements** of a PAC system are *power supply, gas supply, cooling water system, control console and plasma torch*. There are many torch designs which are practically used, for example air plasma, dual gas, oxygen injected, and water injected plasma torch.

Air plasma torch (Fig. 9.2) uses compressed air as the gas that ionizes and does cutting. The air to be used should be uncontaminated. The nozzle of this torch may result in premature failure because of *double arcing* (not shown in the figure), i.e. arcing between the electrode and the nozzle, and between the nozzle and the workpiece. Air plasma cutting results in a high degree of *tapered machined surface*. Zirconium or hafnium (electrode life ≈ 2 hr of cutting time) are used as electrode material because of their higher resistance to oxidation. Because of poor oxidation resistance, tungsten electrode does not last for more than a few seconds.

To avoid oxidation of electrode (or to enhance the life of the electrode), **oxygen injected torch** (Fig. 9.3) uses nitrogen as the plasma gas. Oxygen is injected downstream of the electrode. However, it lowers down the nozzle life. This torch gives high MRR and poor squareness of the cut edges. It is commonly used for mild steel plate cutting. The presence of oxygen in the air helps in increasing MRR in case of oxidizable materials like steel. In case of certain ferrous metals, cutting speed is increased by about 25%. It is possible because oxygen backs up

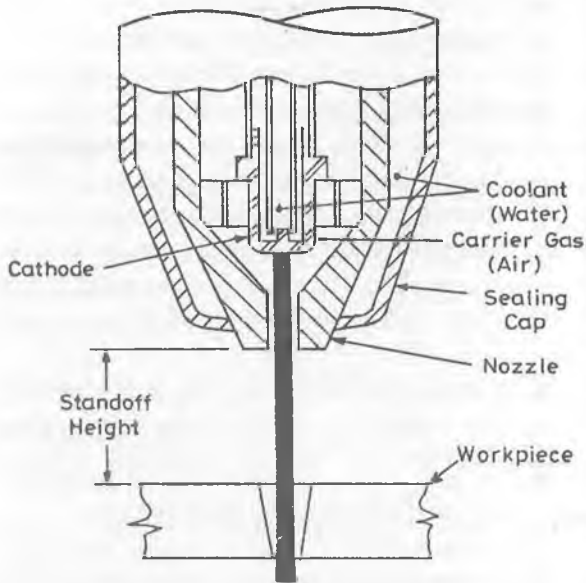


Fig. 9.2 Details of air plasma torch construction [Benedict, 1987;
Courtesy: W.A. Whitney Corp. Rockford, III.]

the exothermic burning of oxidizable metals.

Dual gas system (Fig. 9.4) uses one gas (nitrogen) as the plasma gas while another gas as the shielding gas (O_2 , CO_2 , argon-hydrogen, etc). Secondary or shielding gas is chosen according to the material to be cut. Secondary gas system helps in maintaining sharp corners on the top side of the cut edges.

In water injected torch (Fig. 9.5), water (pressure ≈ 1.2 MPa) is injected (radially or swirling vertically) to constrict the plasma. A small quantity (about 10%) of water vaporizes. This thin layer of steam constricts the plasma [McGeough, 1988] and also insulates the nozzle. Nitrogen at about 1 MPa is used as the plasma gas. To avoid double arcing, the lower part of the nozzle is made of ceramic. Water constriction helps in reducing smoke, enhancing nozzle life, reducing HAZ, and limiting formation of oxides on the cut edges of the workpiece. In some systems, shielding gas or water is given swirling motion. As a consequence of this, plasma is also forced to swirl. This results in one edge of the cut being almost perfectly straight.

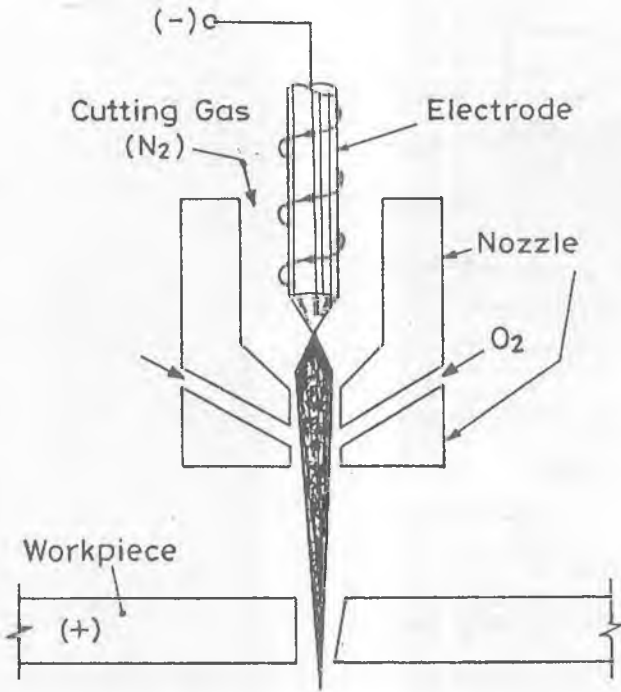


Fig. 9.3 Schematic diagram of oxygen-injected torch construction
[Benedict, 1978; Hypertherm Inc., Hanover, N.H.]

Water muffler (a device that produces a covering of water around the plasma torch and extends down to the work surface) helps in reducing smoke and noise. Water mixed with a dye also absorbs part of the ultraviolet rays produced in PAC. In some cases, a water table is also used to reduce the level of noise and extent of sparks. Water below the workpiece quenches sparks and damps sound level. **Underwater PAC systems** are also available which effectively reduce the noise and smoke levels.

PROCESS PERFORMANCE

As the surface speed during PAC is increased, volumetric material removal rate is found to attain a maximum value and then starts decreasing. PAC has been employed to cut materials as thick as 150 mm. Cutting speed is affected by

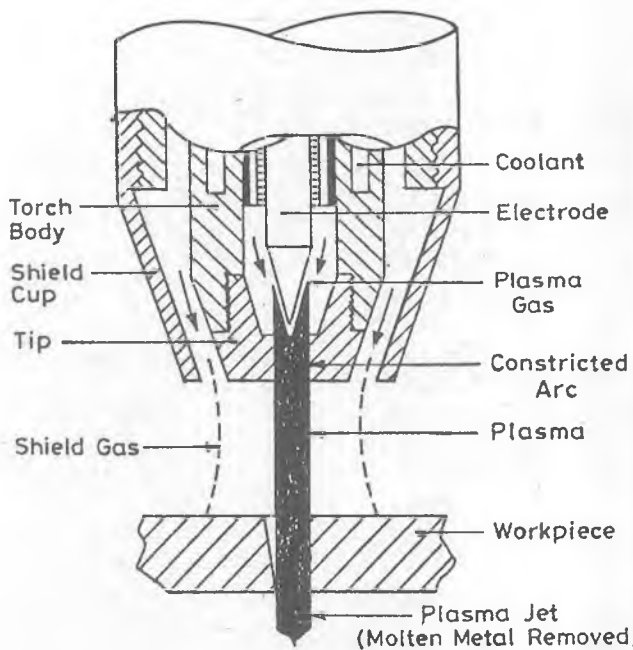


Fig. 9.4 Constructional details of dual gas plasma torch [Benedict, 1978:
Courtesy: W.A. Whitney Corp., Rockford 111.]

the thickness (t) of the material being cut, type of the material being cut, and the current (I) being used during cutting. Cutting speed (' S ' in m/min) is found to decrease with an increase in thickness (' t ' in mm) of the material being cut.

$$S = 25.4/t \quad (\text{for } I = 500 \text{ A}). \quad \dots(9.1)$$

The tolerances obtained are poor and depend on the thickness of the material being cut. For example, the tolerance value of ± 0.8 mm may be achieved if $t < 25.0$ mm, and ± 3.0 mm if $t > 25.00$ mm. Width of cut is also quite high (2.5–9.5 mm) and taper depends on whether swirling is used or not (without swirling 5–7°). Surface finish of the cut edges ranges from 5–75 μm . Thickness of HAZ is governed by the material thickness, PAC system, type of material being cut and cutting conditions. It ranges from 0.75–5.0 mm.

It should be noted that for an appropriate performance of PAC system, an increase in power requires a corresponding rise in the gas flow rate.

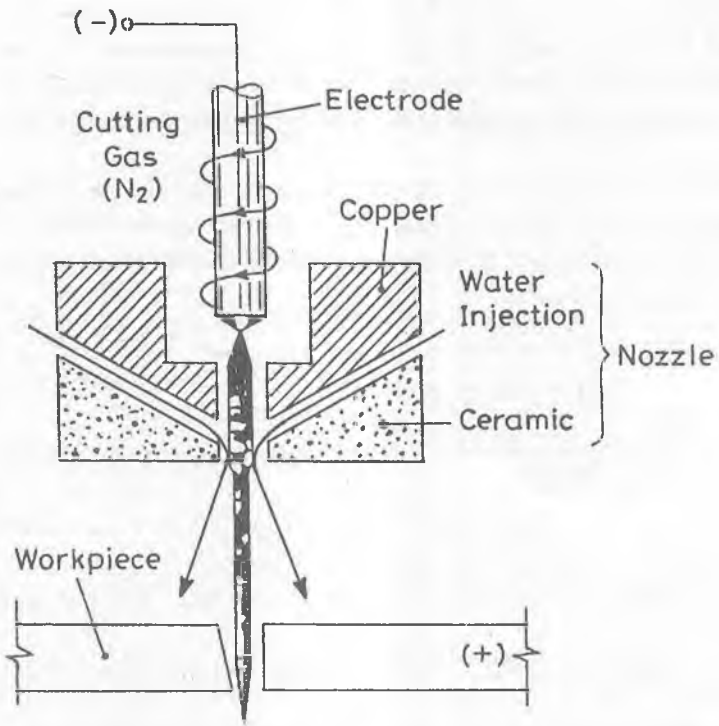


Fig. 9.5 Constructional details of water-injected plasma torch [Benedict, 1978, Courtesy: Hypertherm Inc., Hanover, N.H.]

APPLICATIONS

Multiple torch system is used for simultaneously cutting varieties of shapes from one plate. It is commonly used for preparing ends of a pipe section before welding. To achieve a bevel cut on the end of a pipe, mount the torch at a fixed angle and rotate the pipe underneath the torch.

Computer numerical control (CNC) PAC systems are also available in the market. They are useful for punching type of operations as well as for shape cutting on light duty plates made of stainless steel, aluminium and copper which are difficult to machine by oxy-fuel system.

Oxy-fuel system can cut the plates up to a definite thickness beyond which

only PAC system can do the job. In case of thick plates, PAC is much more economical than oxy-fuel system. In case of cutting of a groove, its shape and size are governed by arc power, traverse speed, angle and height of the plasma torch. In case of electrically non-conducting materials (using non-transferred arc), MRR is low.

PAM has also been employed for turning of difficult-to-machine materials. Plasma torch is mounted tangentially (at about 30°) to the workpiece. Attempts are being made to develop successful **underwater plasma machining** systems although associated with lower speeds.

BIBLIOGRAPHY

1. Benedict G.F. (1987), *Non-traditional Manufacturing Processes*, Marcel Dekker Inc., New York.
2. Lucey J.A. and Wyllie F.S. (Oct. 1967), Plasma Machining, *Proc. Conf. Machinability*, The Iron and Steel Institute, London, pp. 235-238.
3. McGeough J.A. (1988), *Advanced Methods of Machining*, Chapman and Hall, London.
4. Pandey P.C. and Shan H.S. (1980), *Modern Machining Processes*, Tata-McGraw Hill, New Delhi.
5. Trojan J. (April 1982), How to Apply Water Injected Plasma Cutting to a CNC Punching and Nibbling Machine, *Fabricator*, Apr., pp. 22-24.

REVIEW QUESTIONS

1. What do you understand by ‘fourth state of matter’? Explain in brief.
2. Can you machine electrically non-conductive materials by PAM?
3. How the molten material ejects out of the machining zone in PAC?
4. Why tungsten is not used as electrode material?
5. Write the specific applications of PAC.

CHAPTER 9
AT-A-GLANCE
PLASMA ARC MACHINING
(PAM)

PLASMA

- GAS HEATED TO 2000°C → MOLECULES SEPARATE OUT AS ATOMS (IF HAVING 2 OR MORE)
- AT 3000°C OR MORE, ELECTRONS DISSOCIATE FROM ATOMS AND GAS IONIZES
- THE GAS CONSISTING IONS & ELECTRONS RECOMBINES → AS ATOMS AND / OR ATOMS INTO MOLECULES
 - + CHARACTERISTICS OF PLASMA → GLOWING GAS, ELECTRICALLY CONDUCTIVE & RESPONSIVE TO MAGNETISM (FOURTH STATE OF MATTER)
 - + HEAT GENERATION → RECOMBINATION OF IONS & ELECTRONS AS ATOMS AND / OR RECOMBINATION OF ATOMS INTO MOLECULES



RELEASE OF BONDING ENERGY



TEMPERATURE AS HIGH AS 33000° C



CAN CUT ANY MATERIAL INCLUDING THOSE HAVING HIGH THERMAL CONDUCTIVITY, HIGH HEAT CAPACITY, AND/OR HIGH OXIDATION RESISTANCE



MATERIALS THAT CAN'T BE CUT BY CONVENTIONAL METHODS
→ PLASMA ARC CUTTING (PAC) CAN CUT THEM

- PAC USES DC POWER
- MATERIAL REMOVAL MECHANISM → MELTING AND / OR VAPORIZATION
 - MOLTEN MATERIAL IS BLOWN OFF BY HIGH VELOCITY GAS

PAC SYSTEM



ARC MODES



NON-TRANSFERRED ARC



TRANSFERRED ARC



- EFFICIENCY 65% - 75%
- ARC BETWEEN ELECTRODE & NOZZLE
- IONIZES HIGH VELOCITY GAS STREAMING TOWARDS W / P

- EFFICIENCY 85% – 90%
- ARC BETWEEN ELECTRODE & W/P
- W/P ELECTRICALLY CONDUCTIVE
- GAS PRESSURE (~1.4 MPa)
- VELOCITY SEVERAL HUNDRED m/s



- ▽ REMOVES OUT MOLTEN MATERIAL FROM MACHINING ZONE.
- ▽ FLOWING GAS CONSTRICTS PLASMA JET & ACTS AS A COOLING AGENT

ELEMENTS OF PAC SYSTEM

1. POWER SUPPLY
 2. GAS SUPPLY
 3. COOLING WATER SYSTEM
 4. CONTROL CONSOLE
 5. PLASMA TORCH
- ▽ AIR AS PLASMA GAS → IONIZED & DOES CUTTING
- ▽ TORCH MAY FAIL PREMATURELY → DOUBLE ARCING BETWEEN → ELECTRODE & NOZZLE, AND NOZZLE & W/P
- ▽ HIGH DEGREE OF TAPERED MACHINED SURFACE
- ▽ ELECTRODE MATERIALS
- ZIRCONIUM OR HAFNIUM (LIFE ~ 2 HR) → HIGH RESISTANCE TO OXIDATION
 - TUNGSTEN ELECTRODE → LIFE ONLY A FEW SECONDS → POOR OXIDATION RESISTANCE

OXYGEN INJECTED TORCH

- HOW TO ENHANCE ELECTRODE LIFE?
 - + TO AVOID OXIDATION OF ELECTRODE
 - ↓
 - + USE OXYGEN INJECTED TORCH
 - ↓
 - + USE NITROGEN AS PLASMA GAS
- THIS TORCH → HIGH MRR & POOR SQUARENESS
 - ↓
 - USED FOR M.S. (OXIDIZABLE) CUTTING
- PRESENCE OF OXYGEN IN AIR
 - ↓
 - + HIGHER MRR FOR OXIDIZABLE METAL (STEELS)
 - + CUTTING SPEED MAY GO UP → 25%
 - + OXYGEN BACKS UP EXOTHERMIC BURNING OF OXIDIZABLE METALS

DUAL GAS SYSTEM

PLASMA GAS (NITROGEN) & SHIELDING GAS (O₂, CO₂, ETC)

- ACCORDING TO THE MATERIAL TO BE CUT
- HELPS IN MAINTAINING SHARP CORNERS

WATER INJECTED TORCH

- WATER INJECTED (SWIRLING) → CONSTRICTS PLASMA
10% VAPOURIZES
- VAPOUR LAYER CONSTRICTS PLASMA & INSULATES NOZZLE
- NITROGEN (1 MPa) → USED AS PLASMA GAS
- TO AVOID DOUBLE ARCING → LOWER PART OF NOZZLE → CERAMIC
- WATER CONSTRICTION → REDUCES SMOKE, HIGHER NOZZLE LIFE,
SMALLER HAZ, LIMITED OXIDATION
- SWIRLING MOTION → SHIELDING GAS / WATER
 - ↓
SWIRLING OF PLASMA
 - ↓
ONE CUT EDGE → PERFECTLY STRAIGHT

WATER MUFFLER

- A COVERING OF WATER AROUND PLASMA TORCH & EXTENDS DOWN TO THE W/P SURFACE
- REDUCES SMOKE & NOISE
- DYE MIXED WITH WATER → ABSORBS ULTRAVIOLET RAYS FROM PLASMA ARC
- WATER TABLE → REDUCES LEVEL OF NOISE & DAMPS SOUND LEVEL
- UNDERWATER PAC SYSTEMS → REDUCE NOISE & SMOKE LEVELS

PERFORMANCE

- SURFACE SPEED & MRR → OPTIMUM
- MAX. CUT THICKNESS → 150 mm
- CUTTING SPEED = ϕ (MATL. THICKNESS (T) AND TYPE) → DECREASES WITH INCREASE IN "THICKNESS"
 $S(m/min) = 25.4/T(mm)$ FOR I = 500 A
- POOR TOLERANCES → ± 0.8 mm ($T < 25.0$ mm); ± 3.0 mm ($T > 25.0$ mm)
- WIDTH OF CUT → 2.5 - 9.0 mm
- TAPER → 5 - 7°
- SURFACE FINISH → 5 - 75 μm
- HAZ (0.75 - 5.0 mm) = ϕ (T, PAC SYSTEM, CUTTING CONDITIONS, & MATERIAL TYPE)

APPLICATIONS

- MULTIPLE TORCH SYSTEM → VARITIES OF SHAPES ON A PLATE
- BEVEL CUT ON THE END OF A PIPE
- CNC PAC SYSTEM → PUNCHING TYPE OPERATION ON LIGHT DUTY PLATES
→ SS, Al, Cu, ETC ← CANNOT BE CUT BY OXY-FUEL SYSTEM
- OXY-FUEL CANNOT CUT BEYOND A THICKNESS → PAC DOES
- SHAPE & SIZE OF A GROOVE = ϕ (ARC POWER, TRAVERSE SPEED · OF PLASMA, TORCH HEIGHT)
- NON-TRANSFERRED ARC → LOW MRR
- UNDERWATER PAC SYSTEM ← UNDER DEVELOPMENT

ELECTRON BEAM MACHINING (EBM)

WORKING PRINCIPLE

Electron beam machining (EBM) process is classified into two categories, viz '*Thermal type*' and '*Non-thermal type*'. In the thermal type EBM process, the surface of thermoelectronic cathode is heated to such a high temperature that the electrons acquire sufficient speed to escape out to the space around the cathode. The stream of these large number of electrons moves as a small diameter beam of electrons towards the anode. As a result, the workpiece is heated by the bombardment of these electrons in a localized area, to such a high temperature that it is melted and vaporized at the point of bombardment. In the second type

(*non-thermal* EBM) process, the electron beam is used to cause a chemical reaction. Here, only the first type of EBM process (*thermal type*) is discussed.

The high velocity beam of electrons strikes the workpiece. The kinetic energy of electrons converts into heat which is responsible for melting and vaporization of workpiece material. This process can produce any shape of hole; however, round holes are usually drilled in metals, ceramics, plastics, etc. It can machine electrically conducting as well as non-conducting materials. Before machining starts, vacuum is created in the machining chamber.

The diameter of the electron beam focussed onto the work should be slightly smaller than the desired hole diameter. As the electron beam strikes the workpiece, the material gets heated, melted and partly vaporized. On the exit side of the hole, the *synthetic or organic backing material* is used. The electron beam after complete penetration into the workpiece, also partly penetrates in the auxiliary backing material. The backing material vaporizes and comes out of hole at a high pressure. The molten material is also expelled along with the vaporized backing material. In case of a *non-circular hole* to be produced, the electron beam is deflected with the help of the *computer control*, along the perimeter of the hole to be produced. As an alternative method, the beam can be kept stationary but the work-table can be moved in the desired path with the help of CNC.

ELECTRON BEAM MACHINING SYSTEM

There are three important elements of EBM system, viz vacuum system, electron beam gun and power supply.

(i) Electron Beam Gun

It is used to produce electron beam (Fig. 10.1) of the desired shape and to focus at the predetermined location. EBM gun is operated in the pulsed mode. A super-heated cathode (tungsten filament type) generates the electrons cloud. Sometimes cathode may be used as a solid block indirectly heated by radiation emitted from a filament. Due to force of repulsion from the cathode, electrons move at a very high acceleration towards the anode which attracts them. The velocity with which electrons pass through the anode is approximately 66% that of light. On the path of electrons, there is a kind of **switch** (bias electrode) which generates the pulses.

A **magnetic lens** is used to shape the electron beam into a converging beam. This beam is passed through a variable aperture to reduce the diameter of the

focussed beam by removing the stray electrons. Magnetic lenses are used to pin point the location of the beam, deflect it, and make it a round beam falling on the workpiece.

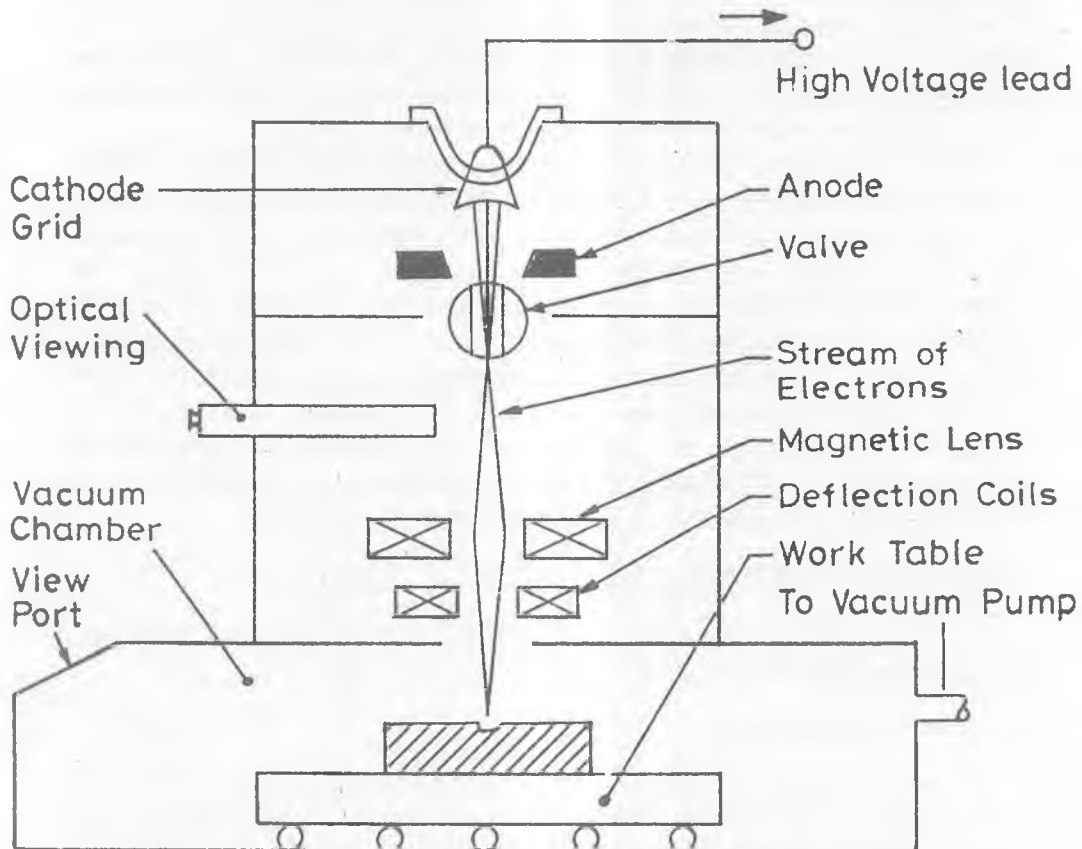


Fig. 10.1 Schematic diagram of electron beam machining system.

(ii) Power Supply

The power supply generates a voltage as high as 150 kV to accelerate electrons. The EBM gun of a powerful system is usually operated at about 12 kW and

an individual pulse energy as 120 J/pulse. The *power density* at the work surface is too high that is why it is capable to melt and vaporize the workpiece material. Thus, material removal in EBM is basically due to vaporization.

(iii) Vacuum System and Machining Chamber

The electron beam generation, its travel in the space, and resulting machining take place in a vacuum chamber. The vacuum does not allow rapid oxidation of incandescent filament and there is no loss of energy of electrons as a result of collision with air molecules. The vacuum in the chamber is of the order of 10^{-4} – 10^{-5} torr.

PROCESS PARAMETERS

The *important parameters* in EBM process are *beam current, duration of pulse, lens current* and signals for the deflection of beam. The values of these parameters during EBM are controlled with the help of a computer.

Beam current varies from 100 μ A to 1A and it governs the energy/pulse being supplied to the workpiece. Higher the energy/pulse more rapidly the hole can be drilled. Pulse duration during EBM varies in the range of 50 μ s to 10 ms depending upon the depth and diameter of the hole to be drilled. Drilling using longer pulse duration results in a wider and deeper drilled hole. It also affects HAZ as well as the thickness of the recast layer which is normally 0.025 mm or less. The extent of both these effects should be minimum possible.

The working distance (i.e. the distance between the electron beam gun and the focal point) and the focussed beam size (diameter) are determined by the magnitude of lens current. The *shape of the hole* along its axis (straight, tapered, etc.) is determined by the position of the focal point below the top surface of the workpiece. To obtain the *hole shape other than circular*, the movement of the beam can be programmed.

The **material removal rate** (MRR) at which the workpiece material is vaporized can be calculated from Eq. (10.1).

$$MRR = \eta \frac{P}{W} \quad \dots(10.1)$$

where, η is the cutting efficiency, P is the power (J/s) and W is the specific energy (J/cm^3) (Eq. (10.2)) required to vaporize the work-material. Specific energy (W) can be calculated as follows:

$$W = C_{ps}(T_m - T_i) + C_{pl}(t_b - t_m) + H_f + H_v \quad \dots(10.2)$$

where, C_p is specific heat, T_m is melting temperature, T_i is initial temperature of workpiece, T_b is boiling temperature, H_f is latent heat of fusion, and H_v is the latent heat of vaporization. The cutting efficiency is usually below 20%. Here, C_p is assumed constant although it varies with temperature. Suffix s and l indicate solid and liquid states, respectively.

CHARACTERISTICS OF THE PROCESS

This process can be used to machine both electrically conductive as well as non-conductive materials, viz Ni, Cu, Al, ceramics, leather, plastics, etc. It has been observed that at the entry side of the electron beam, a small sized burr (a solidified layer) may be left out. In general, performance (viz MRR) of the EBM process is not significantly influenced by the properties (physical, mechanical and metallurgical) of workpiece material.

This process can machine small diameter holes (0.1 to 1.4 mm) to a large depth (say, 10 mm) or in other words, a hole with high *aspect ratio* (up to 15:1). The geometry of the hole and depth of the hole to be drilled, determine the average machining rate (or penetration rate). Further, no mechanical force is applied on the job; hence fragile (or brittle), thin, and/or low strength workpieces can be easily machined. *Off-the-axis holes* (or inclined holes) can also be machined by this process.

There is no distortion due to mechanical forces; however, very high temperature gradient would result in **residual thermal stresses**. Another limitation of the process is very high cost of the equipment. The operator also should be skilled one. The quality of the edges produced is determined by the thermal properties of the workpiece material and the pulse energy [Kaczmarek, 1976]. The heat affected zone (HAZ) depends upon pulse duration and the diameter of the hole being drilled.

APPLICATIONS

EBM is more popular in **industries** like *aerospace, insulation, food processing, chemical, clothing, etc.* It is very useful in those cases where number of holes (simple as well as complex shaped) required in a workpiece may range from *hundreds to thousands* (perforation of sheets, etc). This Process is also used for drilling thousands of holes (diameter < 1.00 mm) in very thin plates used for tur-

bine engine combustor domes. Many thousand holes (diameter < 1.0 mm) in a cobalt alloy fibre spinning head of thickness around 5 mm are drilled by EBM. This drilling is claimed to be 100 times faster than EDM. Holes in the filters and screens used in food processing industries are also made by this process.

The *applications of EBM* also encompass the areas like making of fine gas orifices in space nuclear reactors, holes in wire drawing dies, cooling holes in turbine blades, metering holes in injector nozzles of diesel engines, etc. EBM is also being employed for *pattern generation* for integrated circuit fabrication.

In EBM, the beam power, focus, pulse duration and mechanical motion have been *controlled numerically*. This would permit more accurate and complex shaped machining using numerically controlled EBM system (NC-EBM).

BIBLIOGRAPHY

1. Bellows G. and Kohls J.B. (March 1982), Drilling without Drills, Special Report 743, *Am. Machinist*, pp. 173-188.
2. Bhattacharyya A. (1973), *New Technology*, The Institution of Engineers (I), Calcutta, India.
3. Kaczmarek J. (1976), *Principles of Machining by Cutting, Abrasion and Erosion*, Peter Pergrinus Ltd., Stevenage, pp. 514-528.
4. McGeough J.A. (1988), *Advanced Methods of Machining*, Chapman and Hall, London, pp. 11-33.
5. Pandey P.C. and Shan H.S. (1980), *Modern Machining Processes*, Tata-McGraw Hill, Publishing Co. Ltd., New Delhi.

PROBLEMS

- (1) Explain the working principle of EBM process. Make the necessary sketch.
- (2) Can you machine electrically non-conducting materials using EBM process?
- (3) How the work-table is protected from getting damaged by the electron beam which has completely penetrated the workpiece?
- (4) How a complex shape can be cut using EBM process?
- (5) Write an equation to compute specific energy of vaporization.
- (6) Write four specific applications where you feel that EBM should be the preferable choice.

NOMENCLATURE

C_{ps}	Specific heat of solid
C_{pl}	Specific heat of liquid
H_f	Latent heat of fusion
H_v	Latent heat of vaporization
P	Power
T_b	Boiling temperature
T_i	Initial temperature of the workpiece
T_m	Melting temperature
W	Specific energy
η	Cutting efficiency

CHAPTER 10
AT-A-GLANCE
ELECTRON BEAM MACHINING
(EBM)

ELECTRON BEAM MACHINING



↓
THERMAL TYPE
↓

CATHODE HEATED

↓
NON THERMAL TYPE
↓

ELECTRON BEAM
CAUSES CHEMICAL
REACTION

↓
STREAM OF A LARGE NO. OF ELECTRONS
AS A SMALL DIAMETER BEAM

↓
MOVES TOWARDS WORKPIECE

↓
BOMBARDMENT OF ELECTRONS IN A LOCALIZED AREA

↓
VERY HIGH TEMPERATURE

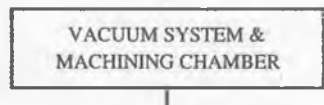
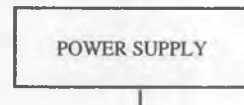
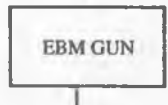
↓
MELTING AND VAPORIZATION OF W/P MATL.

KINETIC ENERGY OF BEAM CONVERTS INTO HEAT

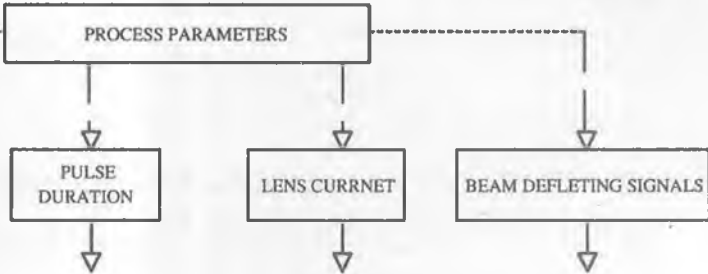


- ▽ CAN PRODUCE HOLES OF DIFFERENT SHAPES
- ▽ CONDUCTING AS WELL AS NON-CONDUCTING MATERIALS
- ▽ VACUUM REQUIRED IN MACHINING CHAMBER
- ▽ BEAM SIZE < DESIRED HOLE SIZE
- ▽ EJECTION OF MOLTEN WORKPIECE MATERIAL
 - VAPORIZED BACKING MATERIAL COMES OUT AT HIGH PRESSURE
 - EXPELS MOLTEN WORKPIECE MATERIAL
- ▽ NON-CIRCULAR HOLES → MOVE ELECTRON BEAM BY COMPUTER CONTROL ALONG HOLE PERIMETER

ELEMENTS OF EBM SYSTEM



- OPERATION IN PLUSED MODE
 - PRODUCES & FOCUSES ELECTRON BEAM AT PREDETERMINED LOCATION
 - SUPERHEATED CATHODE
 - ELECTRONS CLOUD REPELLED FROM CATHODE & ATTRACTED BY ANODE
 - MAGNETIC LENS → CONVERGES BEAM
 - STRAY ELECTRONS REMOVED → REDUCED DIAMETER OF BEAM
 - GENERATES VOLTAGE → 150 kV
POWER → 12 kW
 - PLUSE ENERGY → 120 J/PULSE
 - COMPUTER CONTROL OF PROCESS VARIABLES
 - HIGH POWER DENSITY
- ▽
- MELTING &
VAPORIZATION
- MATERIAL REMOVAL BY VAPORIZATION
 - BEAM GENERATION & TRAVEL → VACUUM
 - NO OXIDATION OF FILAMENT
 - NO COLLISION OF ELECTRONS & AIR MOLECULES
 - VACUUM 10^4 TO 10^3 TO RR



- ▽ 100 µA TO 1 A
- ▽ GOVERNS ENERGY / PLUSE
- ▽ HIGHER VALUE → HIGHER MRR
- ▽ PULSE DURATION → 50 µs TO 10 ms
- ▽ LONG DURATION → WIDER & DEEPER HOLE
- ▽ AFFECTS HAZ & RECAST LAYER (≤ 0.025 mm)
- ▽ DETERMINES WORKING DISTANCE & BEAM SIZE
- ▽ SHAPE OTHER THAN CIRCULAR → BEAM MOVEMENTS ARE PROGRAMMED
- ▽ HOLE SHAPE → POSITION OF FOCAL POINT BELOW TOP SURFACE OF W/P

- $MRR = \eta P/W$
- $W = C_{Ps} (T_M - T_i) + C_{Pl} (T_B - T_M) + H_F + H_V$

CHARACTERISTICS

- ▽ FOR CONDUCTIVE AS WELL AS NON-CONDUCTIVE MATERIALS
- ▽ AT ENTRY SIDE OF BEAM → A SMALL SIZED BURR
- ▽ W/P MATERIAL PROPERTIES DO NOT AFFECT PERFORMANCE
- ▽ SMALL DIAMETER HOLES (0.1 TO 1.4 mm)
- ▽ ASPECT RATIO = 15 : 1
- ▽ NO MECHANICAL FORCE → FRAGILE, THIN, LOW STRENGTH COMPONENTS → EASILY MACHINED
- ▽ OFF-AXIS HOLES EASILY MADE
- ▽ RESIDUAL THERMAL STRESSES ← HIGH TEMPERATURE GRADIENT
- ▽ VERY HIGH INVESTMENT COST
- ▽ SKILLED OPERATOR
- ▽ MACHINED EDGE QUALITY → THERMAL PROPERTIES OF W/P MATERIAL & PULSE ENERGY
- ▽ HAZ → ϕ (PULSE DURATION & HOLE DIAMETER)

APPLICATIONS

- ▽ MORE POPULAR → AEROSPACE, INSULATION, FOOD PROCESSING, CHEMICAL, CLOTHING, ETC
- ▽ HUNDREDS TO THOUSANDS OF HOLES IN A W/P ← COMPLEX-SHAPED, DIFFICULT-TO-MACHINE MATERIAL, PERFORATION, ETC
 - EXAMPLE : TURBINE ENGINE COMBUSTOR DOME
 - FIBER SPINNING HEAD (THICKNESS < 5 mm), MUCH FASTER THAN EDM
 - HOLES IN FILTERS & SCREENS ← FOOD INDUSTRY
 - COOLING HOLES IN TURBINE BLADES
 - METERING HOLES IN INJECTOR NOZZLES

ELECTROCHEMICAL AND CHEMICAL ADVANCED MACHINING PROCESSES

ELECTROCHEMICAL AND CHEMICAL ADVANCED MACHINING PROCESSES

- ELECTROCHEMICAL MACHINING
- ELECTROCHEMICAL GRINDING
- ELECTROCHEMICAL DRILLING
- ELECTROCHEMICAL DEBURRING
- SHAPED TUBE ELECTROLYTIC MACHINING
- CHEMICAL MACHINING
- ANODE SHAPE PREDICTION AND TOOL DESIGN IN ECM

ELECTROCHEMICAL MACHINING (ECM)

INTRODUCTION

Electrolysis

Electrical energy is transported through metals by conduction of electric charges from one place to another. As opposed to the metallic conduction, where only electrons are the charge carriers, salt solutions conduct electrical energy by the migration of ions in the medium.

Fig. 11.1 shows an **electrolytic cell** in which DC battery sends electric current

through the molten sodium chloride salt. Electrons from the battery enter the melt at the cathode, and when the circuit is complete, they leave the melt at the anode returning to the battery. Sodium ions (Na^+) from the medium combine with the electrons available at the cathode, and produce sodium metal which accumulates at the cathode region as

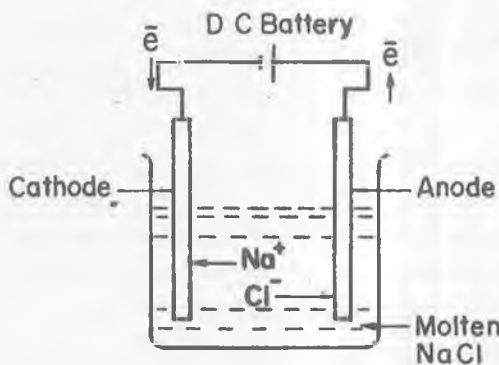
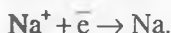
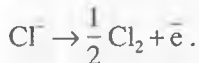


Fig. 11.1 The electrolysis of molten sodium chloride salt.

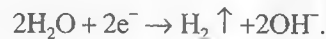
Thus, sodium ions are reduced (*reduction process* involves the addition of electrons) at the cathode. At the same time, chloride ions migrate towards the anode and are oxidized (in *oxidation process* electrons are released) to chlorine as:



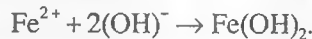
In order to get a sustained flow of current, and to avoid accumulation of ions at the electrode, reactions must keep occurring at the electrode, to maintain electrical neutrality. Thus, the external circuit feeds electrons into the medium at the cathode. These electrons are consumed at the cathode by the positive ions (or *cations* → since they migrate to the cathode), and are released by the negative ions (or *anions*) of the medium at the anode.

Electrochemical Machining (ECM)

Electrolysis has been successfully put to work in the areas like electroplating, electroforming and electropolishing. The process of metal removal by electrochemical dissolution was known as long back as 1780 AD but it is only over the last couple of decades that this method has been used to advantage. It is also known as *contactless electrochemical forming* process. The noteworthy feature of electrolysis is that the electrical energy is used to produce a chemical reaction, therefore, the machining process based on this principle is known as *electrochemical machining (ECM)*. This process works on the principle of Faraday's laws of electrolysis. In ECM, small electric DC* potential (5–25 V) is applied across the two electrodes, i.e. cathode and anode (anode is work and cathode is tool) immersed in electrolyte (Fig. 11.2). The transfer of electrons between the ions and the electrodes completes the electrical circuit. The metal is detached, atom by atom, from the anode surface and appears in the electrolyte as positive ions. In electrochemical machining, detached metal appears as precipitated solid of metal hydroxides. During the electrolysis of water, its molecules gain electrons from cathode so that they separate into free hydrogen gas and hydroxyl ions.



As the anode dissolves, negatively charged hydroxyl ions are electrically balanced by positively charged metal ions entering into the electrolyte.



Metal ions do not remain as ions in the solution when neutral electrolytes are used, but combine with the hydroxyl ions to form **metal hydroxides**. These hydroxides are insoluble in water hence they appear as solid precipitates and no longer affect the electrochemical reaction.

*The application of direct current through a solution of electrolyte results in redox (reduction and oxidation) reactions, while the application of an alternating current (AC) leads to conduction only. The reason being that the electrodes change their polarities very fast hence the electrode reaction occurring in the first half of the cycle is reversed in the later half of the cycle. Hence, only DC is used in this application.

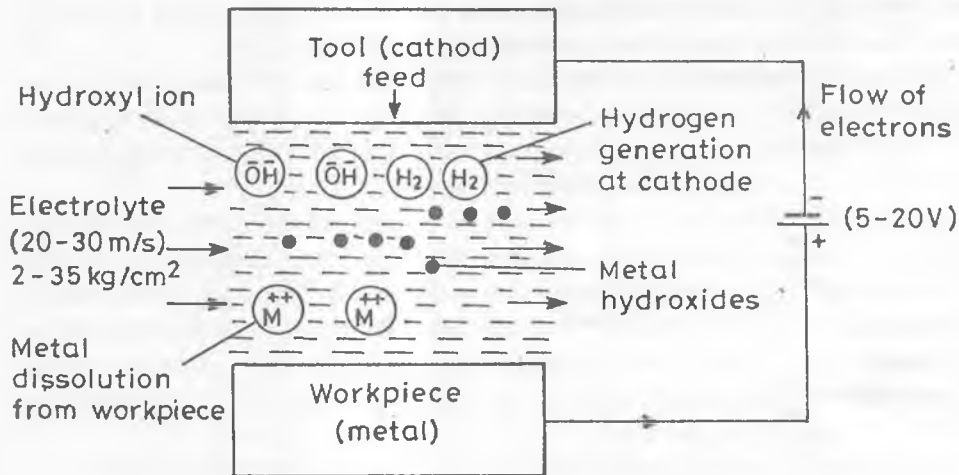


Fig. 11.2 The schematic diagram of electro-chemical machining.



Ferrous hydroxides may further react with water and oxygen to form ferric hydroxide:



Smaller the **interelectrode gap (IEG)** (the gap, y , between the two electrodes), greater will be the current flow because resistance (py/A) decreases and higher will be the rate of metal removal from the anode. High current density, in the small spacing (usually about 0.5 mm or less), promotes rapid generation of **reaction products**, viz. hydroxide solids and gas bubbles. These reaction products act as a barrier to the flow of electrolyzing current and their effect is minimized by supplying the electrolyte at a pressure of 2 to 35 kg cm^{-2} , leading to the electrolyte flow velocity as high as 20–30 m/s.

Electrolytes used in ECM consist of either acids or, more generally, basic salts

dissolved in water. Electrolyte flowing at high velocity in the IEG serves multifarious functions, viz dilutes the electrochemical reaction products and removes them out from the gap, dissipates heat at a faster rate, and limits the concentration of ions at the electrode surface to give higher machining rates. Electrolyte flow rate (volumetric) is determined based upon the desired flow velocity of electrolyte, *IEG*, and the size of the component being machined.

Electrolyte properties (composition, concentration, pH value, temperature and concentration of foreign elements) together with tool shape should be closely controlled because these are the important variables which determine the geometry of the machined component (anode profile).

Amount of hydroxides in the electrolyte is confined by continuous removal using large settling tanks, filters, and centrifuging pumps. Composition, concentration and pH value of electrolyte solution are controlled by adding water and salt solution. Their quantity to be added depends upon the periodic analysis of the check samples. Temperature is another important factor which governs the **electrical properties** of the electrolyte. It is controlled (within $\pm 1^\circ \text{C}$) by heating or cooling the electrolyte while in the tank.

The cathode is moved towards the anode at the same rate at which the work is being dissolved so that the gap (spacing) between the two electrodes remains constant. It really does not matter even if work is fed towards the tool. This will help in maintaining a constant **material removal rate (MRR)**. Smaller gap at various points (Fig. 11.3a) between confronting surfaces of the electrodes-tool and work-will result in higher current density (J) and hence higher MRR. With the progressive movement of cathode towards the anode, ultimately the two surfaces will closely match (Fig. 11.3b).

Selection of electrolyte is quite important. However, inexpensive, easily available and commonly used electrolyte is sodium chloride (common salt). It is also necessary to pump the electrolyte at very high pressure through the IEG, so that the desired MRR can be maintained.

Thus, the anode profile to be produced depends upon so many factors but they can be narrowed down to only two, current density and cathode shape.

The principle of electrochemical machining (ECM) discussed above has been applied for performing a variety of **operations** as listed in Fig. 11.4. Some more operations can still be included in this list; however, the principle of working of all these operations remains the same, ie electrochemical dissolution of anode.

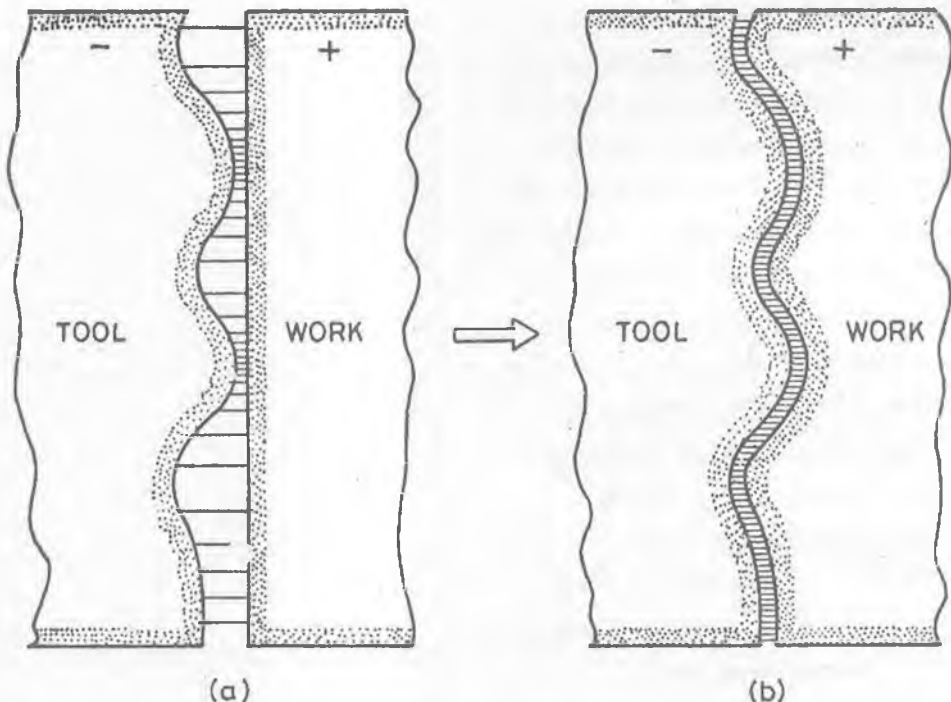


Fig. 11.3 Electrochemical machining: (a) Initial condition, (b) final condition.

ECM MACHINE TOOL

ECM machine tool (m/t) consists of mainly four sub-systems [Jain, 1980]:

- (i) power source,
- (ii) electrolyte supply and cleaning system,
- (iii) tool and tool-feed system, and
- (iv) workpiece and work-holding system.

A schematic diagram of the horizontal type ECM m/t is shown in Fig. 11.5.

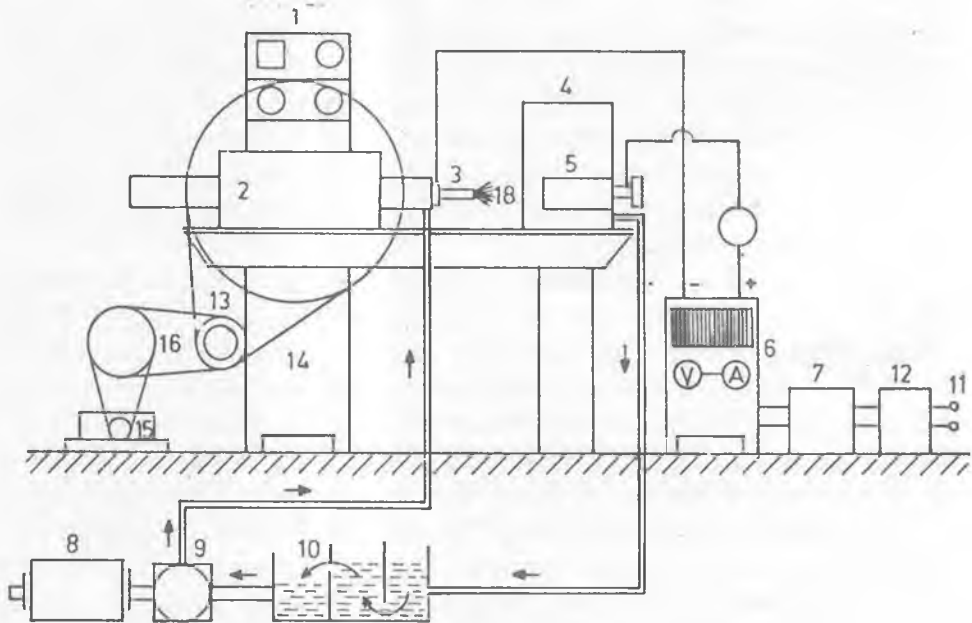
(i) Power Source

During ECM process, a high value of direct current (may be as high as 40,000 A) and a low value of electric potential (in the range of 5–25 V) across the IEG is desirable. The highest current density achieved so far is around $20,000 \text{ A/cm}^2$.

- ECB (Electrochemical Boring) [15]
- ECB_r (Electrochemical Braoching) [18]
- ECB_s (Electrochemical Ballizing) [13]
- ECD (Electrochemical Drilling) [14]
- ECD_e (Electrochemical Deburring) [9]
- ECDS (Electrochemical Die Sinking) [7]
- ECG (Electrochemical Grinding) [6]
- ECH (Electrochemical Honing) [19]
- ECM (Electrochemical Machining) [16]
- ECM_i (Electrochemical Milling) [11]
- ECMM (Electrochemical Micromachining)
- ECS (Electrochemical Sawing)
- ECT (Electrochemical Turning)
- ECT_r (Electrochemical Trepanning)
- ECWC (Electrochemical Wire Cutting)
- ESD (Electrostream Drilling)
- STEM (Shaped Tube Electromachining)

Fig. 11.4 Various machining operations based on electrochemical dissolution of anode (*Jain and Pandey, 1991*).

Hence, with the help of a rectifier and a transformer, three phase AC is converted to low voltage, high current DC. Silicon controlled rectifiers (SCRs) are used both for rectification as well as for voltage regulation because of their rapid response to the changes in the process load and their compactness. Voltage regulation of $\pm 1\%$ is adequate for most of the precision ECM works. However, lack of process control, equipment failure, operator's error, and similar other reasons may result in sparking between tool and work. The electrical circuitry detects these events and power is cut off (using devices like SCRs) within 10 μ s to prevent severe damage to the work and tool. In case of precision works, even a small damage to an electrode is not acceptable. It may be minimized by using a bank of SCRs placed across the DC input to ECM m/c.



Schematic layout of ECM setup

- (1) Switch board (2) Linear drive head (3) Tool (4) Perspex box
- (5) Work piece (6) Rectifier (7) Voltage Regulator (8) Motor (9) Pump
- (10) Tank (11) Mains (12) Transformer (13) Flat Pulley (14) Flat belt
- (15) V-pulley (16) Split V-pulley (17) Motor (18) Electrolyte.

Fig. 11.5 A schematic diagram of horizontal type ECM m/t [Jain, 1980].

(ii) Electrolyte Supply and Cleaning System

The electrolyte supply and cleaning system consists of a pump, filters, pipings, control valves, heating or cooling coils, pressure gauges and a storage tank (or reservoir). Electrolyte supply ports may be made in the tool, work, or fixture, depending upon the requirements of the mode of electrolyte flow. Small inter-electrode gap, usually smaller than 1 mm, should be maintained for achieving high MRR and high accuracy. For this purpose, smooth flow of electrolyte should be maintained, and any blockade of such a small gap by particles carried by the electrolyte, should be avoided. Hence, electrolyte cleanliness is imperative. It is normally done with the help of filters made of stainless steel, monel, or any other anti-corrosive material. Filters should be periodically cleaned for their proper functioning. To achieve good results, filters can be placed in the supply pipe just prior to the work enclosure.

It should be ensured that the piping system does not introduce any foreign materials like corroded particles, scale, or pieces of broken seal material. Piping system is therefore made of stainless steel, glass fibre-reinforced plastics (GFRP), plastic lined mild steel, or similar other anti-corrosive materials. If the metallic piping is used, all the metallic parts should be earthed to prevent their anodic corrosion. Tables and fixtures should also be insulated from the anode. In case of heavy structures; if it is not possible to insulate from anode, they must carry a cathodic potential to prevent corrosion. The required minimum capacity of electrolyte tank is about 500 gallons for each 10,000 A of current. Fig. 11.5 shows a **single tank system** having three compartments. Reaction products from the electrolyte are separated by natural sedimentation in the first compartment. Electrolyte is then made to go to compartment 2 via a filter, and finally to the last compartment via a passage between the compartments 2 and 3. Electrolyte is further cleaned by a filter attached at the exit port of the tank.

ECM system is supposed to machine different metals and alloys at optimum machining conditions, and with varying requirements of accuracy, surface texture, etc. Under such situations, a single tank system is not recommended because of loss of time and wastage of electrolyte during draining, cleaning, mixing, or filling of new electrolyte in the tank. It results in higher cost and poor accuracy of electrochemically machined components and also poor control of operating conditions. *More than one tank* therefore, can be used and their number would depend upon the range of electrolytes needed to meet the work load. Use of more

than one tank is justified when several ECM machines are in use. Further, concrete tank or swimming pool type of tank are pleaded because of their low cost, easy maintenance, and reliability.

(iii) Tool and Tool Feed System

Use of anti-corrosive material for tools and fixtures is important because they are required for a long period of time to operate in the corrosive environment of electrolyte. High thermal conductivity and high electrical conductivity of tool material are the main requirements. Easy machining of tool material is equally important because dimensional accuracy and surface finish of the tool directly affect the workpiece accuracy and surface finish. Aluminium, brass, bronze, copper, carbon, stainless steel and monel are a few of the materials used for this purpose. Further, those areas on the tool where ECM action is not required, should be insulated. For example, lack of insulation on the sides of a die sinking tool causes unwanted machining of work, and results in a loss of accuracy of the machined workpiece. However, under such situations use of **bit type of tools** can be recommended [Jain and Pandey, 1982]. Fig. 11.6 shows three categories of tools, viz bare tool, coated tool, and bit type of tool with the expected drilled hole profiles.

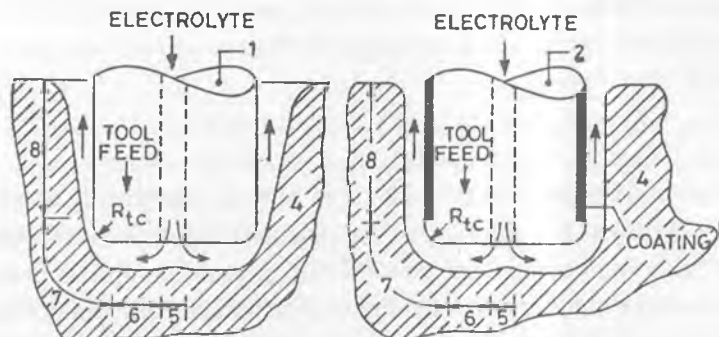
Use of non-corrosive and electrically non-conducting materials for making fixtures is recommended. Also, the fixtures and tools should be rigid enough to avoid vibration or deflection under the high hydraulic forces to which they are subjected.

(iv) Workpiece and Work Holding System

Only electrically conductive *work materials* can be machined by this process. The chemical properties of anode (work) material largely govern the material removal rate (MRR). *Work holding devices* are made of electrically non-conductive materials having good thermal stability, and low moisture absorption properties. For example, graphite fibres-reinforced plastics, plastics, perspex, etc are the materials used for fabricating the work holding devices.

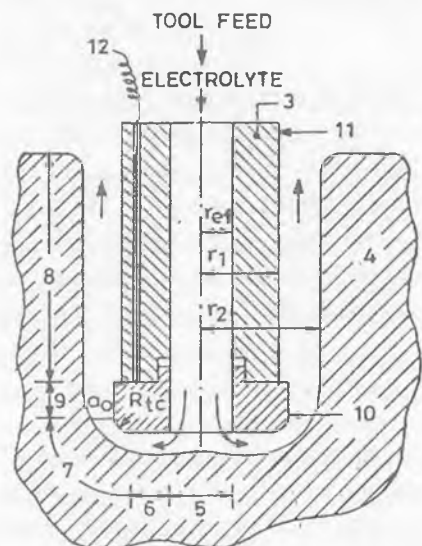
ADVANTAGES AND LIMITATIONS

ECM offers impressive and long lasting **advantages**. It can machine highly complicated and curved shapes in a single pass. A single tool has been used to machine a large number of pieces without any loss in its shape and size. Theoretically, tool life in ECM is very high. The process offers several advantages, viz



(a)

(b)



(c)

Fig. 11.6 Various types of tools: (a) bare tool, (b) coated tool, (c) bit type of tool¹ [Jain and Pandey, 1987].

1. bare tool, 2. coated tool, 3. bit type of tool, 4. workpiece, 5. Stagnation zone, 6. Front zone, 7. transition zone, 8. side zinc, 9. tapered side, 10. tool bit, 11. perspex tool bit holder, 12. connecting wire

the machinability of the work material is independent of its physical and mechanical properties. Machined surfaces are stress and burr free having good surface finish (best surface finish obtained is in the range of 0.1 to 1.0 μm), better corrosion resistance, and better accuracy. It yields low scrap, almost automatic operation, low overall machining time, and reduced inventory expenses.

ECM has its own **limitations**, and it can be used only for electrically conductive work-materials. Further, the accuracy of the machined components depends upon the factors like tool design, degree of the process control imposed, complexity in the shapes produced, etc. Machining of materials consisting of hard spots, inclusions, sand and scale present some practical difficulties. ECM, under certain circumstances, is found to be incapable of economically producing the dimensional tolerances desired on the workpiece. It cannot produce sharp corners and edges. To overcome this, researchers are constantly and continuously engaged in improving upon the ECM system technology and equipment.

APPLICATIONS

Over the years, ECM principle has been employed for performing a number of **machining operations** (Fig. 11.4), viz turning, trepanning, broaching, grinding, fine hole drilling, die sinking, piercing, deburring, plunge cutting, etc; it is being widely used in **industries** related to aeronautics, nuclear technology, space vehicles, automobiles, turbines, etc. Some of the *typical examples* of ECM applications are: machining of turbine blades made of high strength temperature resistant (HSTR) alloys, copying of internal and external surfaces, cutting of curvilinear slots, machining of intricate patterns, production of long curved profiles, machining of gears, production of integrally bladed nozzle for use in diesel locomotives, production of stellite rings and connecting rods, machining of thin large diameter diaphragms, etc.

This process has attracted the maximum attention of those involved in machining of hard and tough materials, specially with complex contours. However, the capabilities of this process have not been exploited to its fullest extent mainly because of the inherent problems associated with tool design [Jain and Pandey, 1980], and environment friendliness.

MECHANICAL PROPERTIES OF ECM'd PARTS

It is important to know the effects of ECM on the mechanical properties of electrochemically machined (ECM'd) components. This will greatly affect the acceptability of the process in different industries. Hardly any evidence is available about the hydrogen embrittlement of the ECM'd components. The basic reason being that hydrogen is evolved at the cathode while metal removal is taking place due to anodic dissolution at the anode. It has been reported that there is no effect of ECM on ductility, yield strength, ultimate strength, and microhardness of the machined component.

Surface layers damaged during conventional machining or by some other processes, may be removed by ECM and this may result in improvement in the properties of the work material. However, such removal of layers from the work surface reduces *fatigue strength* of a conventionally machined component. The conventionally machined surfaces have compressive residual stresses responsible for higher **fatigue strength**. This fact has been verified experimentally [Evans et al, 1971]. However, the required fatigue strength can be restored by further appropriate post mechanical finishing treatment. These subsequent mechanical treatments impart compressive stresses to the surface, so that the resulting work-piece can exhibit fatigue properties comparable to or better than those of mechanically finished parts.

The **surface finish** produced by ECM may also be the source of reduction in fatigue properties. The surfaces produced by ECM generally have better wear, friction, and corrosion resistance properties than those produced by mechanical means [Gurkis, 1965]. Table 11.1 gives and idea of the effect of type of finish on fatigue strength [Evans et al, 1971].

Table 11.1 Fatigue lives obtained [Evans et al, 1971] after ECM at a stress of $\pm 386 \text{ MN/m}^2$

Surface Finish	Fatigue Life, $10^5 \times \text{cycles}$
Electrochemically polished	4.9
Etched	4.4
Intergranular attack	4.25
Hemispherical pits	3.3

Micro examination of the specimen has revealed that fatigue cracks usually originate from pits. Due to flowing electrolyte, these defects are more severe than those found in electropolishing. However, reduction in fatigue life is low and depth of intergranular attack measured is about hundredth of a millimeter or even less. Removal of compressive stress layer seems to be the main reason, and intergranular attack and other defects induced during ECM appear to be the secondary reasons for reduction in the fatigue strength. Improper combination of work and electrolyte, or inappropriate selection of operating conditions may result in non-uniform dissolution of metals and alloys. It would lead to selective etching, intergranular attack, or pitting. But, such defects can be minimized by employing proper heat treatment procedure, and also by developing an appropriate electrolyte and selecting proper operating conditions.

THEORY OF ECM

There are many *industrial processes* which work based on the principle of Faraday's laws of electrolysis. ECM is one of them. It is considered as the reverse of electroplating process. But, there are two major differences between ECM process and other electrolytic processes (viz, electropolishing, electrolytic pickling, etc). In ECM, it is not merely to remove metal from the workpiece but also change the shape and size of the workpiece in a controlled manner. Secondly, the magnitude of minimum current density employed in ECM is very high (8 A mm^{-2}) as compared to that used in electroplating or electrolytic pickling.

Faraday's Laws of Electrolysis

During ECM, metal from the anode (or workpiece) is removed atom by atom by removing negative electrical charges that bind the surface atoms to their neighbours. The ionized atoms are then positively charged and can be attracted away from the workpiece by an electric field. In an *electrolytic cell* (or ECM cell), material removal is governed by *Faraday's laws* of electrolysis given below.

- (i) The amount of chemical change produced by an electric current (or the amount of substance deposited or dissolved) is proportional to the quantity of electricity passed.
- (ii) The amounts of different substances deposited or dissolved by the same quantity of electricity are proportional to their chemical equivalent weights.

These laws can be expressed in mathematical form as follows:

$$m \propto I t E$$

$$m = I t E / F$$

...(11.1)

or,

where, I is the current strength (amperes), t is the time (seconds), E is the gram equivalent weight of material (or A/Z, where A is atomic weight and Z is valency of dissolution), F is Faraday's constant (96500 As), and m is mass in grams. Eq. (11.1) is used to calculate MRR_g (= IE/F). Table 11.2 gives the values of 'A' and 'Z' for some metals, their density, and theoretical material removal rate.

This equation is based on the number of simplified assumptions and does not account for the effects of some of significant process variables, viz change in valency of electrochemical (EC) dissolution during the operation, gas evolution and bubble formation, electrolyte's electrical conductivity (k) and temperature variation along the electrolyte flow path, overpotential, presence of passivation film, etc. Passivity arises as a result of chemical and electrochemical behaviour of metals which results in the formation of protective film on their surfaces. Further, dissolution of iron in NaCl solution, depending upon the machining conditions, may be either in the form of ferrous hydroxide (Fe²⁺) or ferric hydroxide (Fe³⁺). Mode of dissolution during machining of alloys, is still more difficult to know. The preferential valency mode of dissolution has been found to depend upon the electrolyte flow rate, IEG and length of electrolyte flow path.

Electrochemical Equivalent of Alloys

Eq. (11.1) has been used for evaluating the amount of metal (m) removed from an anode made of single element. The evaluation of 'm' becomes difficult when the anode is made up of an alloy because the value of electrochemical equivalent of the alloy (A/Z)_a is not known. However, two methods have been suggested to solve this problem, viz, '*percentage by weight method*' and '*superposition of charge*' method.

In the **first method**, the value of electrochemical equivalent of an alloy is calculated by multiplying the chemical equivalent of individual elements (A_i/Z_i) by their respective proportions by weight X_i, and then summing them up as given in Eq. (11.1a)

$$\left(\frac{A}{Z}\right)_a = \frac{1}{100} \sum_{i=1}^n \left(\frac{A_i}{Z_i}\right) X_i \quad ... (11.1a)$$

where, n is the number of the constituent elements.

Table 11.2 Theoretical material removal rates for a current of 1000 A [McGeough, 1974].

Metal	Atomic Weight (g)	Valency	Density (g/cm ³)	Removal rate (g/s)	(10 ⁻⁶ m ³ /s)
Aluminium	26.97	3	2.67	0.093	0.035
Beryllium	9.0	2	1.85	0.047	0.025
Chromium	51.99	2	7.19	0.269	0.038
		3		0.180	0.025
		6		0.090	0.013
Cobalt	58.93	2	8.85	0.306	0.035
		3		0.204	0.023
Niobium	92.91	3	9.57	0.321	0.034
(Columbium)		4		0.241	0.025
		5		0.193	0.020
Copper	63.57	1	8.96	0.660	0.074
		2		0.329	0.037
Iron	55.85	2	7.86	0.289	0.037
		3		0.139	0.025
Magnesium	24.31	2	1.74	0.126	0.072
Manganese	54.94	2	7.43	0.285	0.038
		4		0.142	0.019
		6		0.095	0.013
		7		0.081	0.011
Molybdenum	95.94	3	10.22	0.331	0.032
		4		0.248	0.024
		6		0.166	0.016
Nickel	58.71	2	8.90	0.304	0.034
		3		0.203	0.023

Table 11.2 (Contd.)

Silicon	28.09	4	2.33	0.073	0.031
Tin	118.69	2	7.30	0.615	0.084
		4		0.307	0.042
Titanium	47.9	3	4.51	0.165	0.037
		4		0.124	0.016
Tungsten	183.85	6	19.3	0.317	0.016
		8		0.238	0.012
Uranium	238.03	4	19.1	0.618	0.032
		6		0.412	0.022
Zinc	65.37	2	7.13	0.339	0.048

In the **second method** (superposition of charge method), the amount of electrical charge required to dissolve the mass contribution of individual constituent element of the alloy is calculated. The total electric charge required to dissolve 1g of the alloy is given by $(Z/A)_a F$ coulombs (from Eq. (11.1)).

Now, equate the electrical charge required by each element to dissolve their individual mass contribution to the total charge required for dissolving 1 gram of alloy,

$$\left(\frac{Z}{A}\right)_a F = F \sum_{i=1}^n \frac{X_i}{100} \left(\frac{Z_i}{A_i}\right),$$

or,

$$\left(\frac{A}{Z}\right)_a = \frac{100}{\sum_{i=1}^n X_i \left(\frac{Z_i}{A_i}\right)}. \quad \dots(11.1b)$$

The values of electrochemical equivalent of alloys calculated by these two methods are not exactly same. Hence, one should be careful while choosing a particular method for calculating $(A/Z)_a$.

All of the current (I) is not utilized only in dissolving metal from the work-piece. Hence, actual MRR depends on the **current efficiency**, η . It ranges from 75% to 100%. Theoretical MRR depends upon the current passing through the

workpiece and its chemical composition. As soon as machining starts, the tool is fed towards the workpiece so that the gap can be maintained at a constant value. The feed rate is approximately equal to the linear material removal rate (MRR_i, i.e. penetration rate).

Example 11.1

An alloy consists (% by weight) nickel (72%), chromium (20%), iron (5%), titanium (0.5%), copper (0.5%), silicon and manganese (1.0% each). Determine chemical equivalent (using both methods) and density of the alloy. Use the lowest valency of dissolution (Table 11.2). Compare MRR_g in the two cases for a current value of 500 A at 100% current efficiency.

Solution

The density of an alloy can be determined as follows:

Consider one gram of alloy having density as ρ_a and volume as V_a . Then,

$$\rho_a V_a = 1$$

or,

$$\rho_a = \frac{1}{V_a} = \frac{1}{V_1 + V_2 + V_3 + \dots + V_n}$$

For constituent 1, $V_1 \rho_1 = 0.72$ g

Therefore,

$$V_1 = \frac{0.72}{\rho_1} = \frac{72}{100\rho_1}$$

Similarly,

$$V_2 = \frac{20}{100\rho_2}$$

$$V_n = \frac{X_n}{100\rho_n}$$

Therefore,

$$\rho_a = \frac{1}{\frac{x_1}{100\rho_1} + \frac{x_2}{100\rho_2} + \dots + \frac{x_n}{100\rho_n}}$$

$$\rho_a = \frac{100}{\sum X_i/\rho_i}$$

Substitute the values in the above equation.

$$\begin{aligned}\rho_a &= \frac{100}{\frac{72}{8.90} + \frac{20}{7.19} + \frac{5}{7.86} + \frac{0.5}{4.51} + \frac{0.5}{8.69} + \frac{1}{2.33} + \frac{1}{7.43}} \\ &= \frac{100}{8.09 + 2.78 + 0.64 + 0.11 + 0.058 + 0.43 + 0.13} \\ &= 8.17 \text{ g/cm}^3.\end{aligned}$$

Now, chemical equivalent of the alloy using percentage by weight method is calculated as given below:

First Method (Eq. 11.1a)

$$\begin{aligned}\left(\frac{A}{Z}\right)_a &= \frac{1}{100} \sum_{i=1}^n \left(\frac{A_i}{Z_i}\right) X_i \\ &= 0.72 \times \frac{58.71}{2} + 0.20 \times \frac{51.99}{2} + 0.05 \times \frac{55.85}{2} + 0.005 \times \frac{47.9}{3} \\ &\quad + 0.005 \times \frac{63.57}{1} + 0.01 \times \frac{28.09}{4} + 0.01 \times \frac{54.94}{2} \\ &= 21.135 + 5.199 + 1.396 + 0.080 + 0.318 + 0.070 + 0.275 \\ &\approx 28.473 \text{ g}\end{aligned}$$

Second Method

$$\left(\frac{A}{Z}\right)_a = \frac{100}{\sum_{i=1}^n \left(\frac{Z_i}{A_i}\right) X_i}$$

$$= \frac{100}{72 \times \frac{2}{58.71} + 20 \times \frac{2}{51.99} + 0.5 \times \frac{2}{55.85} + 0.5 \times \frac{3}{47.9} + 0.5 \times \frac{1}{63.57} + 1 \times \frac{4}{28.09} + 1 \times \frac{2}{54.94}}$$

$$\approx \frac{100}{2.453 + 0.769 + 0.018 + 0.031 + 0.008 + 0.142 + 0.036}$$

$$\approx 28.927 \text{ g.}$$

Material removal rates (in grams – MRR_g) using (A/Z)_a obtained from the two different methods are calculated as given below:

$$\text{MMR}_{g_1} = \frac{IE}{F} = 500 \times \frac{28.473}{96500}$$

$$\approx 0.1475 \text{ g/s.}$$

$$\text{MRR}_{g_2} = \frac{IE}{F} = \frac{500 \times 28.927}{96500}$$

$$\approx 0.1499 \text{ g/s.}$$

Material Removal Rate in ECM

It is always desirable to have minimum possible gap (usually ≤ 0.5 mm) between the two electrodes (tool and work) mainly to get accurate reproduction of tool shape on the workpiece. To simplify the analysis given in this section, the following assumptions are made:

- (i) Electrical conductivity (k) of electrolyte in the IEG remains constant.
- (ii) Electrical conductivities of tool and work materials are very large ($1,00,000 \Omega^{-1} \text{ cm}^{-1}$) as compared to that of electrolyte (less than $1.0 \Omega^{-1} \text{ cm}^{-1}$). Hence, surfaces of the electrodes can be considered as equipotentials.
- (iii) Effective voltage working across the electrodes is ($V - \Delta V$), where ΔV is a small fraction of V and includes electrode voltage, overvoltage, etc. It is assumed to remain constant.
- (iv) The anode dissolves at one fixed valency of dissolution.

For the simplicity of mathematical modelling, a case of plane parallel electrodes normal to feed direction [Tipton, 1964] is considered (Fig. 11.7). The equations derived in the following will be applicable mainly for such cases.

Electrolyte is assumed to flow in the direction of increasing X across the gap between two electrodes. It is also assumed that the properties of electrolyte remain unchanged in the Z direction, i.e. the problem is two-dimensional in nature.

The Eq. (11.1) can be used to calculate material removal rate (in grams MRR_g, or in terms of volume as MRR_v):

$$m(MRR_g) = \eta I E / F, \quad \dots(11.1c)$$

$$MRR_v = \eta I E / F \rho_a. \quad \dots(11.1d)$$

where, η is current efficiency.

Leaving aside a few specific applications of ECM (for example, deburring), tool (cathode) is usually fed towards the workpiece (anode) at a constant rate. During equilibrium, feed rate (f) of the cathode is equal to the rate at which the thickness of the anode is being reduced, i.e. MRR₁. It is given by the following equation (divide both sides of the last equation by the common area 'A' through which current is flowing):

$$MRR_1 = \frac{J E \eta}{\rho_a F}, \quad \dots(11.1f)$$

where, $J = I/A$ (A/mm^2), and ρ_a is density (g/mm^3) of the anode material. In ECM, a properly shaped tool concentrates electric current on those areas of the workpiece from which preferential removal of the metal is desired. Metal removal rate (MRR) from an area on the workpiece is controlled by current density on that area. Current density during ECM is a function of shapes of the electrodes (work and tool, Fig. 11.3), their distance apart, voltage applied across them, and electrical conductivity of electrolyte flowing through the gap. Current density can also be written (Eq. 11.2a) as a multiplication of potential gradient ($(V - \Delta V)/y$) in the IEG, and electrolyte conductivity (k).

$$J = \frac{(V - \Delta V)k}{y}. \quad \dots(11.2a)$$

Here, $(V - \Delta V)$ is the voltage available for driving current through the electrolyte. In Eq. (11.1f), MRR₁ is nothing but penetration rate, or rate of change of IEG, i.e. dy/dt .

$$\frac{dy}{dt} = \frac{JE\eta}{\rho_a F}. \quad \dots(11.2b)$$

During actual ECM, tool is usually moved towards the workpiece at a rate of ' f ' units/s. Hence, effective rate of change of IEG is given by

$$\frac{dy}{dt} = \frac{JE\eta}{\rho_a F} - f. \quad \dots(11.2c)$$

Under equilibrium conditions, $\frac{dy}{dt} = 0$. $\dots(11.3a)$

Therefore, under equilibrium condition, feed rate is given by

$$\frac{JE\eta}{\rho_a F} = f. \quad \dots(11.3b)$$

Substitute the value of 'J' from Eq. (11.2a),

$$\frac{(V - \Delta V)k}{y_e} \frac{E\eta}{\rho_a F} = f \quad \dots(11.3c)$$

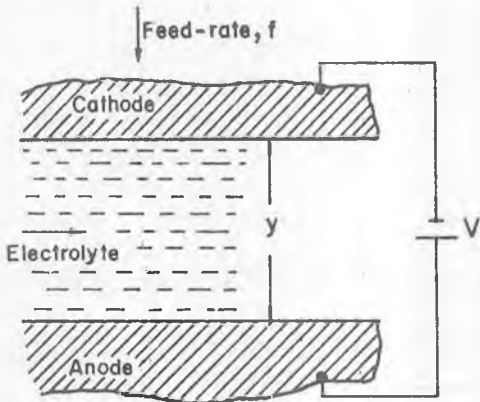


Fig. 11.7 Electrochemical machining with plane parallel electrodes at a constant voltage.

Inter-electrode Gap in ECM

Eq. (11.3c) can be used to evaluate equilibrium interelectrode gap (y_e)

$$y_e = \frac{(V - \Delta V)\eta k E}{\rho_a f F} \quad \dots(11.4)$$

y_e can be achieved only if the feed rate (f) and applied voltage (V) are constant throughout machining. It is not important whether the work is stationary and the tool is fed towards it or vice versa. Since the tool surface during ECM remains unchanged, it is preferable to use it as a reference surface.

Example 11.2

During machining of iron (atomic weight = 55.85, valency = 2, density = 7.85 g/cm³), the equilibrium gap is approximately 0.125 mm and the measured value of specific conductance of electrolyte = 0.2 Ω⁻¹ cm⁻¹. Faraday's constant is 26.8 Ah, applied voltage is 10 V, and overvoltage is 1.5 V. Calculate the value of feed rate, f.

Solution

Substitute the values in Eq. (11.4)

$$f = \frac{(V - \Delta V)k E}{y_e \rho_a F} = \frac{(10 - 1.5)0.2(55.85/2)}{0.0125 \times 7.85 \times (26.8 \times 60)}$$

or

$$f = 0.3 \text{ cm/min.}$$

$$f = 0.05 \text{ mm/s.} \quad \boxed{\text{Ans.}}$$

The rate of change of IEG (y) can be calculated from Eq. (11.5) [Tipton, 1964].

$$\frac{dy}{dt} = \frac{E(V - \Delta V)k}{F \rho_a y} - f \quad \dots(11.5)$$

However, in case of equilibrium condition, dy/dt will attain the value as zero. In a more convenient form, above Eq. (11.5) can be written in terms of f, y and machining constant, C (mm² s⁻¹) ($C = E(V - \Delta V)k/F\rho_a$ is a constant for a particular work and electrolyte combination only if, $(V - \Delta V)$ and k remain constant during the process):

$$\frac{dy}{dt} = \frac{C}{y} - f. \quad \dots(11.6)$$

It is a basic differential equation of the system.

In actual practice, two cases arise for which Eq. (11.6) can be solved, zero feed rate ($f = 0$) and finite feed rate ($f \neq 0$).

Zero Feed Rate

For $f = 0$, Eq. (11.6) can be written as:

$$\frac{dy}{dt} = \frac{C}{y},$$

or,

$$y \cdot dy = C dt. \quad \dots(11.7)$$

Integrate both sides to get

$$y^2 = 2Ct + K$$

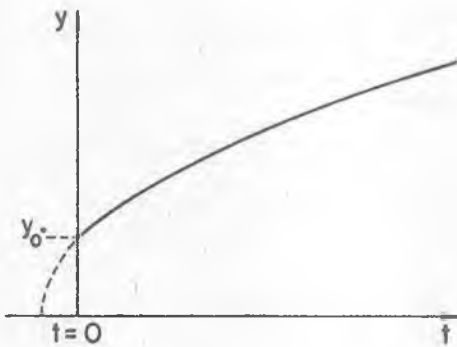


Fig. 11.8 The variation of the gap thickness (y) with time at zero feed-rate.

For the initial condition as $y = y_0$ at $t = 0$, above equation gives, $K = y_0^2$. Eq. (11.8) is obtained by substituting the value in the above equation.

$$y = (2Ct + y_0^2)^{1/2} \quad \dots(11.8)$$

It means that the gap increases in proportion to the square root of the time (Fig. 11.8).

Finite Feed Rate

For $f \neq 0$, the IEG during equilibrium condition will remain constant ($dy/dt = 0$) and from Eq. (11.6) we get

$$y = y_e = \frac{C}{f}, \quad \dots(11.9)$$

where, y_e is *equilibrium gap*. The IEG always tends to attain the equilibrium value during ECM. To make the analysis more generalized, some of the parameters (time and IEG) are made dimensionless, i.e.

$$\left. \begin{aligned} y' &= \frac{y}{y_e} = \frac{y f}{C} \\ t' &= \frac{t}{(y_e/f)} = t \frac{f^2}{C} \end{aligned} \right\} \quad \dots(11.10)$$

Here, y' indicates the ratio of the gap to the equilibrium gap, and t' indicates the number of times required to machine one ' y_e ' distance.

Now, from Eq. (11.6) and Eq. (11.10), we get

$$\frac{dy'}{dt'} = \frac{1}{y'} - 1.$$

This equation can also be written as

$$\frac{dt'}{dy'} = \frac{y'}{1-y'}, \quad \dots(11.11a)$$

or,

$$\begin{aligned} dt' &= \left(\frac{y'}{1-y'} \right) dy' \\ &= \left(\frac{-1+y'+1}{1-y'} \right) dy' \end{aligned}$$

$$t' = -y' - \ln(y' - 1) + K \quad \dots(11.11b)$$

Solve the above Eq. (11.11a) to give Eq. (11.11b). Substitute the initial condition as $y' = y'_0$ at $t' = 0$ in Eq. (11.11b), to give the following:

$$0 = -y'_0 - \ln(y'_0 - 1) + K$$

$$\therefore K = y'_0 + \ln(y'_0 - 1).$$

Substitute the value of K in Eq. (11.11b).

$$t' = -y' - \ln(y' - 1) + y'_0 + \ln(y'_0 - 1)$$

$$t' = y'_0 - y' + \ln \frac{(y'_0 - 1)}{(y' - 1)}. \quad \dots(11.12)$$

In the above Eq. (11.12), only positive values of y' are possible, and $y' = 0$ implies a short circuit between the tool and workpiece.

For the case of $f \neq 0$, solution of Eq. (11.5) can also be obtained [McGeough, 1974] when parameters are not non-dimensionalised, as given below:

$$t = \frac{1}{f} \left[y_0 - y_t + y_e \ln \left(\frac{y_0 - y_e}{y_t - y_e} \right) \right] \quad \dots(11.13)$$

where, y_t is IEG at any time 't'.

Self-Regulating Feature

To illustrate *self-regulating feature* of the ECM process, Eq. (11.12) has been plotted in Fig. 11.9 where y' is asymptotic to $y' = 1$ (ie MRR_1 is equal to feed rate, or $y = y_e$).

Three relationships are possible between 'f' and 'MRR₁': $f = MRR_1$, $f > MRR_1$, and $f < MRR_1$.

- (i) If $f = MRR_1$, stable machining will take place and IEG will be equal to the equilibrium gap ($y = y_e$).
- (ii) If $f < MRR_1$, then initially the IEG will increase and it will attain a value greater than the equilibrium gap value ($y > y_e$). Because of this, current density will decrease as compared to the current density at the time when the gap is equal to the equilibrium gap. As a result, MRR_1 will also decrease. Or the difference between f and MRR_1 will decrease. Finally, the

IEG will start decreasing and it will attempt to attain the equilibrium gap ($MRR_l = f$).

- (iii) If $f > MRR_l$, then initially the gap will be smaller than the equilibrium gap ($y < y_e$). As a result, current density will increase as compared to the situation when $y = y_e$, hence MRR_l will also increase. In other words, the difference between f and MRR_l will decrease. Finally, the gap will tend to attain the equilibrium gap (or $MRR_l = f$) value.

This characteristic has been utilized to illustrate the levelling up or shaping process.

Generalized Equation for Inter-electrode Gap

A quadratic Eq. (11.8) predicts an infinite value of the gap as 't' approaches infinity. However, in practice, as the gap increases, the current density decreases so that MRR gradually diminishes, and for a very large value of the gap the process would come to a *stand still*. This aspect is not well reflected in Eq. (11.8). Eqs. (11.12) and (11.13) are *implicit equations*, and can be solved *iteratively* for y (or y'). But, it consumes a lot of computer time. In order to evaluate the IEG at any instant of time t , solution of Eq. (11.13) is a bit tedious. Further, these equations are not convenient to handle specially in those cases where numerical methods like finite element method (FEM), finite difference method (FDM), or boundary element method (BEM) are applied to analyze the ECM process. Keeping this in view, a single equation has been derived [Jain and Pandey, 1981] which can be conveniently used in case of FEM, FDM, or BEM, and it is applicable simultaneously for both the cases, i.e zero feed rate ($f = 0$) as well as finite feed rate ($f \neq 0$). Eq. (11.5) can be written as

$$\frac{dy}{dt} = \frac{EJ\eta}{F\rho_a} - f,$$

where, η is current efficiency.

$$dy = \left(\frac{EJ\eta}{F\rho_a} - f \right) dt. \quad \dots(11.14a)$$

In the parentheses on the right hand side of the Eq. (11.14a), all the factors are constant except J . In FEM, BEM, and FDM, element size is quite small. Hence,

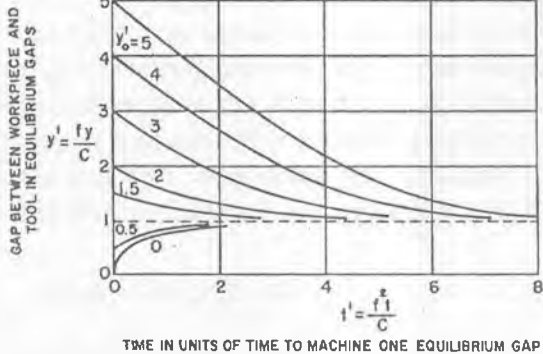


Fig. 11.9 y' approaches to the equilibrium gap ($y' = 1$) for a constant feed rate and for various initial gaps y'_o .

within an element, J can be assumed to remain constant over a small interval of time dt . Above equation therefore, can be written as

$$dy = (c - f)dt. \quad \dots(11.14b)$$

After integration, Eq. (11.14b) can be written as

$$y = (c - f)t + C'.$$

At time $t = 0$, $y = y_o$, then the above equation can be written as

$$C' = y_o.$$

Therefore,

$$y = y_o + (c - f) t. \quad \dots(11.15)$$

Eq. (11.15) is valid for a small interval of time Δt , hence, more conveniently, it can be written as

$$y = y_o + (c - f) \Delta t.$$

 $\dots(11.16)$

Table 11.3 [Jain and Pandey, 1980] shows that the values of different parameters for three different problems obtained from the above discussed two different methods are very close to each other. It establishes the *validity* of a single and simple Eq. (11.16) applicable to both the cases of feed rate ($f = 0$ and $f \neq 0$).

However, computer time required to solve ECM problems by employing the two Eqs. (11.13) and (11.16) and using numerical methods, would be very different.

One may come across a case when a plane parallel *gap is inclined* at an angle θ to the feed direction, Fig. 11.10. In such cases, feed rate 'f' should be replaced by its component (' $f \cos \theta$ ') in the above analysis. When $\theta = 90^\circ$, the feed rate normal to the work is zero and hence the condition $f = 0$ would apply. Note that here, angle θ is measured between a normal to the work surface and the feed direction.

Table 11.3 Comparison of Eqs. (11.13) and (11.16) with the data for anode shape ($t = 300$ s) after [Jain and Pandey, 1980].

x, mm	y (mm), 10^{-1}		Temperature rise (°C)		
	Eq. (11.13)	Eq. (11.16)	Eq. (11.13), $y_0 = 0.8$	Eq. (11.16), $y_0 = 0.8$	Experimental
7.0	7.8500	7.8477	5.2595	5.2623	5.0
17.0	9.0419	9.0452	13.7024	13.6954	11.625
22.0	9.7153	9.7192	18.4565	18.4422	15.0*
7.0	3.4808	3.3670	5.7189	5.3100	—
17.0	4.0584	4.0890	14.9660	15.0073	15.8687
22.0	4.3841	4.3980	20.1821	20.4389	22.45*
7.0	5.0018	5.0027	6.3056	6.3056	10.0875
17.0	5.9177	5.9176	16.6205	16.6170	—
22.0	6.4434	6.4426	22.5309	22.5336	23.6*

* $x = 21.5$ mm

MAXIMUM PERMISSIBLE FEED RATE IN ECM

Equation for volumetric material removal rate (MRR_v) can be written as

$$MRR_v = \frac{EI\eta}{96500 \rho_a} . \quad \dots(11.17)$$

The current efficiency (η) is close to 100% while using aqueous solution of NaCl as electrolyte. It is somewhat lower than 100% in case of nitrate and sulphate

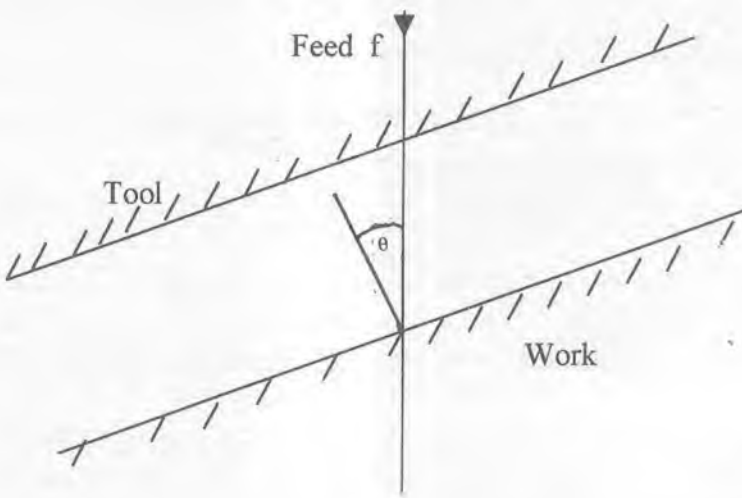


Fig. 11.10 Feed direction inclined at an angle θ measured between the normal to the work surface and feed direction.

electrolytes. In some cases, efficiency has been reported [De Barr and Oliver, 1975] to be more than 100% also specially when electrically non-conducting inclusions (Fig. 11.11) are there in the anode.

From Eq. (11.17), specific metal removal rate ($\text{m}^3 \text{A}^{-1} \text{s}^{-1}$) can be written as

$$\text{MRR}_s = \frac{\eta}{96500} \frac{E}{\rho_a} (\text{m}^3 \text{A}^{-1} \text{s}^{-1}). \quad \dots(11.18)$$

Therefore, electrode feed rate (m/s) is given by

$$f = J \cdot \text{MMR}_s$$

$$= \frac{(V - \Delta V)}{y} k \cdot \frac{E \eta}{96500 \rho_a} \text{ ms}^{-1} \text{ (y in metre)} \quad \dots(11.19)$$

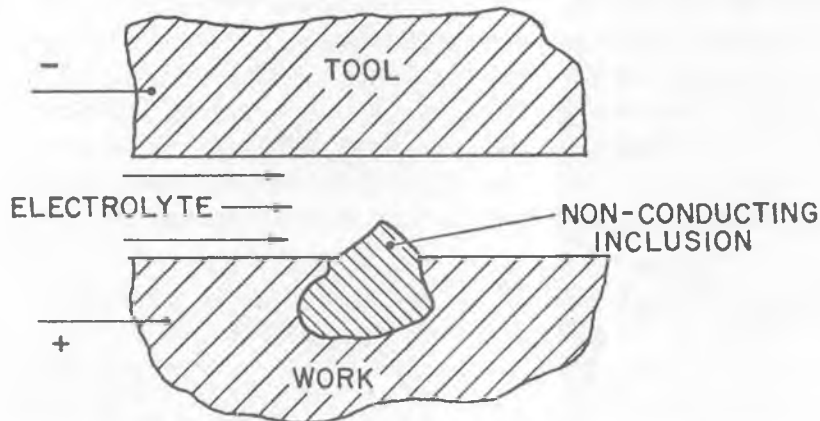


Fig. 11.11 Dissolution of anode with electrically non-conducting inclusion.

One of the important functions of the electrolyte is to carry away the heat out of the IEG. There is always an upper limit to the electrolyte flow rate that can be achieved from a given electrolyte flow system. This constraint in turn also poses a limit to the maximum feed rate that can be used during ECM without permitting the electrolyte to boil. In the worst case, it can be assumed that the electrolyte is *allowed to heat up to the boiling temperature*. Assuming that only Ohmic heating is significant, an approximate expression for maximum permissible feed rate can be derived [Pandey and Shan, 1980].

Using the law of **conservation of heat**, heat (H_o) required to raise the electrolyte temperature from T_i (temperature at inlet) to T_b (electrolyte boiling temperature) can be evaluated as:

$$H_o = m_e C_e (T_b - T_i),$$

where, m_e is the mass of electrolyte and C_e is the specific heat of electrolyte. It can also be written as

$$H_o = \bar{V}_e \rho_e C_e (T_b - T_i),$$

$$\frac{H_o}{t} = \frac{\bar{V}_e}{t} \rho_e C_e (T_b - T_i),$$

or,

where, \bar{V}_e and ρ_e are the volume of electrolyte flowing in time 't' and density of electrolyte (assumed invariable with temperature), respectively.

Let \dot{q} be the *volumetric flow rate* of electrolyte; then power (P) required for its heating is given by (1 Cal = 4.186 Joules):

$$P = 4.186 \dot{q} \rho_e C_e (T_b - T_i),$$

or,

$$I_m^2 R = 4.186 \dot{q} \rho_e C_e (T_b - T_i),$$

or,

$$I_m = \sqrt{\frac{4.186 \dot{q} \rho_e C_e (T_b - T_i) A}{y}}, \quad \dots(11.20)$$

where, I_m is the permissible maximum current (A) and R ($=y/kA$) is the gap resistance. An increase in current (or current density) would require increased feed rate for machining under equilibrium conditions.

Using above equations (11.18-11.20), *maximum permissible feed rate* (f_m) can be calculated as:

$$\begin{aligned} f_m &= J MRR_s = \frac{I_m}{A} MRR_s \\ &= \sqrt{\frac{4.186 \dot{q} \rho_e C_e (T_b - T_i) A}{y}} \cdot \frac{1}{A^2} \cdot \frac{\eta E}{\rho_a 96500} \\ &= \frac{\eta E}{\rho_a 96500} \sqrt{\frac{4.186 \dot{q} \rho_e C_e (T_b - T_i) k}{y A}} \quad \dots(11.21) \end{aligned}$$

Eq. (11.21), after simplification (as given in the following), can also be used to calculate change in temperature ($\Delta T = T_b - T_i$) for the specified feed rate (f).

$$\Delta T = 2.23 \times 10^9 \left[\frac{y A}{k \dot{q} C_e \rho_e} \right] \left[\frac{f \rho_a}{E \eta} \right]^2$$

ELECTROLYTE CONDUCTIVITY (k)

In the above analysis, electrolyte's electrical conductivity has been assumed to remain constant throughout the gap. However, in actual practice, it is not so. Its conductivity is a function of local temperature, presence of bubbles, and contamination of the electrolyte by sludge. Size and distribution of hydrogen gas bubbles

(ignoring oxygen, water vapour, and other gas bubbles) will affect the magnitude by which the electrolyte conductivity changes. Temperature increases the value of k while hydrogen gas bubbles decrease its value. As a result, the gap gets tapered, ie IEG varies along the electrolyte flow direction (Fig. 11.12). Fig. 11.13 shows the effect of variation in temperature and concentration on the conductivity of NaCl and HCl. The effects of temperature and gas bubbles on the electrolyte conductivity will be discussed now.

Effect of Temperature (T)

In the following analysis, it is assumed that heat generated due to viscous flow of electrolyte, heating due to overvoltage and chemical reactions, and heat transferred through the electrodes are all negligible.

Using the law of conservation of heat, temperature gradient along the path of electrolyte flow can be derived as follows:

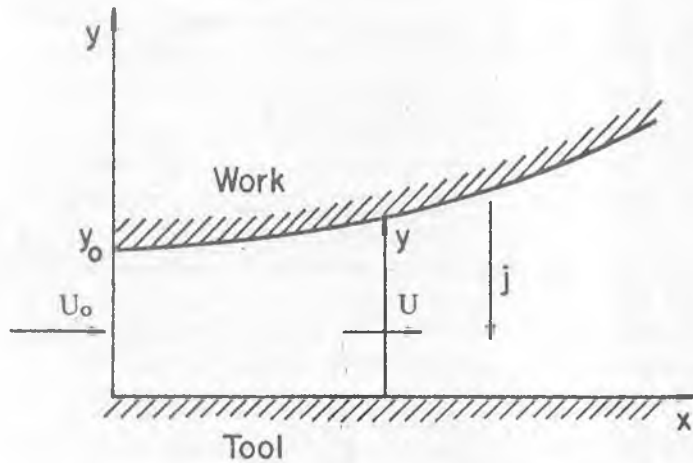


Fig. 11.12 The equilibrium gap with variable conductivity [Tipton, 1964].

$$I^2 R = U \rho_e C_e (\Delta T) y$$

(where, U is electrolyte flow velocity)

or,

$$\frac{(V - \Delta V)^2}{y} k . dx = U \rho_e C_e (\Delta T) y$$

(Assuming unit width in z direction)

or,

$$\frac{dT}{dx} = \frac{(V - \Delta V)^2}{U \rho_e C_e y^2} \cdot k$$

where, ρ_e and C_e are assumed to remain constant in the IEG.

It is also safe to assume IEG and electrolyte flow velocity at inlet (y_o and U_o) to be constant. Then, initial temperature distribution in a plane parallel gap of thickness y_o is given by

$$\frac{dT}{dx} = \frac{(V - \Delta V)^2}{U_o \rho_e C_e y_o^2} = A \cdot k. \quad \dots(11.22)$$

Conductivity of the electrolyte varies linearly with temperature

$$k = k_o (1 + \alpha(T - T_o)), \quad \dots(11.23)$$

where, α is the temperature coefficient of specific conductance ($= dk/(k_o dT)$) with the units as per °C. From Eqs. (11.22) and (11.23),

$$\frac{dT}{1 + \alpha(T - T_o)} = Ak_o dx.$$

Integration of the above equation gives,

$$\ln[1 + \alpha(T - T_o)] = \alpha Ak_o x$$

or,

$$(T - T_o) = \frac{1}{\alpha} [\exp(\alpha Ak_o x) - 1].$$

The current density, J also varies along the gap and can be calculated as follows:

$$J = \frac{(V - \Delta V)k}{y}$$

$$= \frac{(V - \Delta V)}{y} k_o [1 + \alpha(T - T_o)]$$

$$= \frac{(V - \Delta V)}{y} k_o [\exp(\alpha Ak_o x)]$$

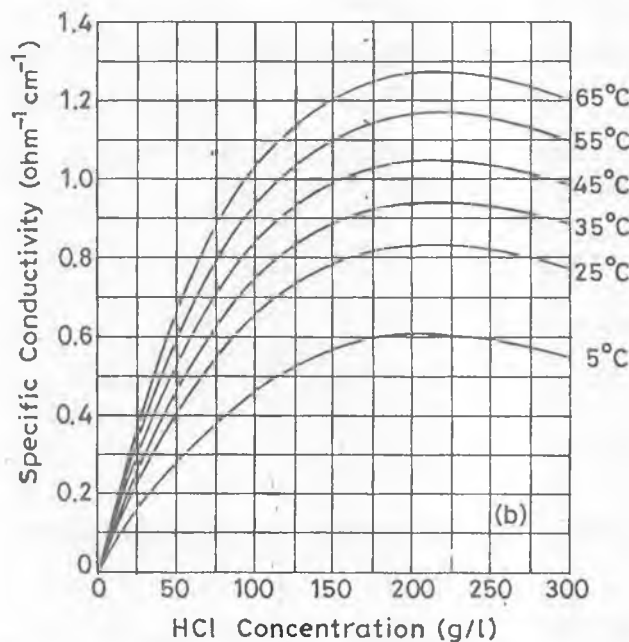
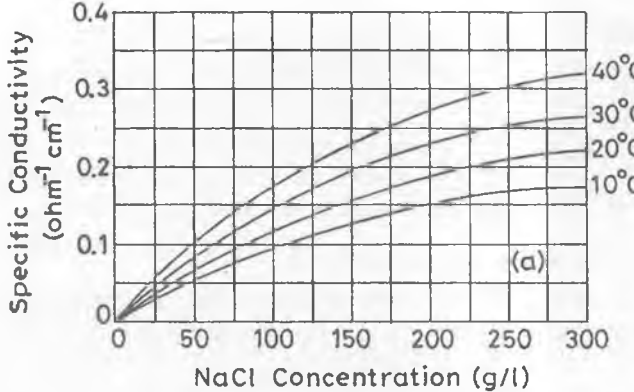


Fig. 11.13 Specific conductivity variation with electrolyte concentration of (a) NaCl, (b) HCl, at various temperatures.

To accurately predict variation in the gap along the electrolyte flow path, it is also desirable to consider the effect of hydrogen gas bubbles and the presence of sludge on k . The quantitative analysis of the effect of sludge on the value of k is not available in the literature; hence the effect of only hydrogen gas bubbles on k has been discussed in what follows.

Effect of Hydrogen Bubbles

Rate of evolution of hydrogen gas bubbles at the cathode surface is governed by current density on its surface. Since the hydrogen bubbles are swept away by flowing electrolyte, their mass concentration will increase in the downstream direction. The net effect of the presence of hydrogen gas bubbles is to decrease the electrolyte's electrical conductivity. Thus, it would decrease the local anodic dissolution rate.

The effect of hydrogen gas bubbles on electrolyte conductivity is governed by the size and distribution of the bubbles in the gap. It is easy to calculate the volume of hydrogen gas evolved and the effect of temperature and pressure on it. But, it is very difficult to estimate anything about the hydrogen bubbles sizes and their distribution under the complex hydrodynamic conditions present in the IEG.

However, some qualitative studies about the effect of different parameters on the size of bubbles have been reported [Landolt *et al*, 1970; Hopenfeld and Cole, 1966, 1969]. The important conclusions of the study are as follows:

The thickness of the bubbles-layer increases in the downstream direction along the gap. However, its thickness decreases if the electrolyte flow rate is increased. The size of individual bubbles decreases as the electrolyte velocity or pressure, or both are increased. But, bubbles size is seen to increase with the increase in current density, keeping other variables as constant. It is also observed that the gas bubbles are concentrated near the cathode, and they are not dispersed uniformly throughout the IEG. It is also to be noted that the gas bubbles may be formed due to evolution of oxygen at the anode and also the cavitation phenomenon. However, only evolution of hydrogen at the cathode is considered for calculation purposes.

To incorporate the effect of temperature as well as hydrogen gas bubbles on electrolyte conductivity, the following equation has been suggested [Hopenfeld and Cole, 1969; Thorpe and Zerkle, 1969]:

$$k = k_o(1 + \alpha\Delta T)(1 - \alpha_v)^n \quad \dots(11.24)$$

where, α , is void fraction and n is an exponent. The value of exponent 'n' in Eq. (11.24) depends on the distribution of voids in the IEG. For uniform void distribution, *Hopenfeld and Cole [1969]* suggested a value of $n = 1.5$, and for non-uniform distribution when bubbles are concentrated near the cathode, *Thorpe and Zerkle [1969]* suggested a value of $n = 2.0$. But, during electrochemical drilling (ECD) and electrochemical bit drilling (ECBD), it is extremely difficult to know the distribution of voids in the IEG. Hence, an average value of $n = 1.75$ has also been used [*Jain et al, 1987*].

BIBLIOGRAPHY

1. Abdel Mahboud A.M. (1986), Improving accuracy and economics of ECM: Modelling, simulation and control., *ASME Press*, Vol. 7(1), pp. 23-23.
2. Benedict G.. (1987, *Nontraditional Manufacturing Processes*, Marcel Dekker, New York.
3. Datta M., Romankiw L.T., Vigliotti D.R. and Von Gutfeld R.J. (1989), Jet and laser jet electrochemical micromachining of nickel and steel, *J. Electrochem. Soc.*, Vol. 136, No. 8, pp. 2251-2256.
4. DeBarr A.E. and Oliver D.A. (Ed) (1975), *Electrochemical Machining*, Macdonald & Co. Ltd., London.
5. Evans J.M., Boden P.J. and Baker A.A. (1971), Effects of surface finish produced during ECM upon the fatigue life of Nimonic- 80A, *Proc. 12th Int. Mach. Tool Des. & Res. Conf.*, p. 271.
6. Gurklis J.A. (1965), Metal removal by electrochemical methods and its effects on mechanical properties of metals, *Defense Metals Information Centre Report 213, Bettle Memorial Institute*.
7. Hewidy M.S., Rajurkar K.P., Royo G.F. and Fattouh M. (1989), Theoretical and experimental investigations of electrochemical ballizing, *Int. J. Prod. Res.*, Vol. 27, No. (8), pp. 1335-1347.
8. Hofstede A. and Berkel Van den (1970), Some remarks on electrochemical turning, *Annls CIRP*, Vol. 18, pp. 93-106.
9. Jain V.K. (1980), *An Analysis of ECM process for anode shape prediction*, Ph.D. Thesis, Roorkee University, India.
10. Jain V.K. and Pandey P.C. (1980), Tooling design for ECM, *Precision Engg.*, Vol. 2, pp. 195-206.

11. Jain V.K. and Pandey P.C. (1980), CAD of Tools in ECM, *Computer Aided Design*, Vol. 12, No. 6, pp. 309-315.
12. Jain V.K. and Pandey P.C. (1981), Tooling design for ECM: A finite element approach, *Trans. ASME, J. Engg. for Ind.*, Vol. 103, pp. 183-191.
13. Jain V.K. and Pandey P.C. (1982), Some investigations into the anode profile in the transition zone in an electrochemical hole sinking operation, *J. Appl. Electrochem.*, Vol. 12, pp. 497-500.
14. Jain V.K. and Pandey P.C. (1982), Investigations into the use of bits as a cathode in ECM, *Int. J. Mach. Tool Des. & Res.*, Vol. 22, No. 4, pp. 341-352.
15. Jain V.K. Tandon S. and Kumar Prashant (1990), Experimental investigations into electrochemical spark machining of composites, *Trans ASME, J. Engg. for Ind.*, Vol. 112, No. 2, pp. 194-197.
16. Jain V.K., Jain Vinod K. and Pandey P.C. (1984), Corner reproduction accuracy in electrochemical drilling of blind holes, *Trans. ASME, J. Engg. for Ind.*, Vol. 106, pp. 55-61.
17. Jain V.K., Yogindra P.G. and Murugan S. (1987), Prediction of anode profile in ECB and ECD operations, *Int. J. Mach. Tools Manuf.*, Vol. 27, No. 1, pp. 113-134.
18. Janseen J.W. (1989), New horizons for STEM drilling, *Proc. Nontraditional Machining Conf.*, Orlando, pp. MS89-81-8-1 to MS89-81-8-7.
19. Kawafune K., Mikoshiba T., Noto K. and Hirta K. (1967), Accuracy in cavity sinking by ECM, *Annls CIRP*, Vol. 15, pp. 443-455.
20. Krabacher E.J., W.A. Haggerty, Allison C.R. and Devis M.F. (1962), Electrical methods of machining, *Int. Conf. Production Research organised by ASME*, pp. 232-241.
21. Landolt D., Acosta R., Mullor R.H. and Tobias C.W. (1970), An optical study of cathodic hydrogen evolution in high rate electrolysis, *J. Electrochem. Soc.*, Vol. 117, No. 6, pp. 839-845.
22. McGeough J.A. (1974), *Principles of ECM*, Chapman and Hall, London.
23. Merchant M.E. (1962), Newer methods for the precision working of metals: Research and present status, *Proc. Int. Conf. Prod. Res.*, ASME, pp. 93-107.
24. Molley J. (1966), Electrochemical machining, *Machinery & Prod. Engg.*, pp. 13-17.
25. Pandey P.C. and Shan H.S. (1980), *Modern Machining Processes*, Tata-McGraw Hill, New Delhi, India.

26. Pourassamy A., Santosh Kumar K.J., Krishnan A. and Rajgopalan S.R. (1987), Investigations on the insulation of electrochemical trepanning tool, *Indian J. Technol.*, Vol. 25, pp. 617-620.
27. Ranganathan V. (1976), Electrochemical grinding of titanium, *Proc. 7th AIMTDR Conf.*, pp. 164-168.
28. Rolsten R.F. and Manning E.J. (1969), Electrochemical deburring, *Tool Manuf. Engr.*, pp. 4-16.
29. Thorpe J.F. and Zerkle R.D. (1969), Analytical determination of the equilibrium gap in electrochemical machining, *Int. J. Mach. Tool Des. Res.*, Vol. 9, pp. 131-144.
30. Tipton H. (1964), The dynamics of electrochemical machining, *In Advances in Machine Tool Design and Research*, Pergamon Press, Birmingham.
31. Wilson J.F. (1971), *Practice and Theory of Electrochemical Machining*, Wiley Interscience, New York.

SELF-TEST QUESTIONS

Q1. Write the correct answer(s). More than one may be correct.

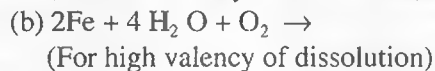
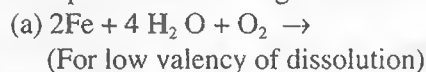
- (i) Which of the following workpiece properties affect MRR during ECM?
(a) Physical, (b) Mechanical, (c) Chemical, (d) None.
- (ii) Desirable properties of electrolytes used in ECM are:
(a) high electrical conductivity, (b) high thermal conductivity,
(c) low specific heat, (d) high specific heat.
- (iii) Theoretically the ratio of MRR to tool wear rate during electrochemical drilling is:
(a) Zero, (b) usually ≈ 1 , (c) depends on the type of work material and electrolyte combination, (d) none of these.
- (iv) Value of void fraction along the path of flow of electrolyte is increasing but temperature of the electrolyte remains approximately constant.
Slope of the machined surface will be
(a) zero, (b) varying linearly, (c) varying nonlinearly, (d) unpredictable.
- (v) Electrochemically machined surfaces have
(a) high residual stresses and improved fatigue strength,

- (b) high residual stresses and reduced fatigue strength,
- (c) insignificant residual stresses and reduced fatigue strength,
- (d) insignificant residual stresses and improved fatigue strength.

Q2. Write whether the following statements are true or false:

- (i) Electrolyte is not consumed in ECM. Type of electrolyte used during ECM, therefore, has no effect on MRR.
- (ii) Electrochemically ground surface requires deburring.
- (iii) Theoretically tool wear rate during ECM is zero.
- (iv) IEG during ECM is usually in the range of 1-3 mm.
- (v) Feed rate during ECD_e is usually low.

Q3. (i) Complete the following chemical reactions (ECM)



- (ii) During ECM of iron using aqueous solution of NaCl as electrolyte, what are the possible reactions at anode and cathode?
- (iii) Complete the following equations:

(a) $J = (V - \Delta V)$

(b) $\dot{m} = A$

(c) $f = J$

Q4. Write the correct answer from the given choices. Show all the calculations necessary to arrive at your answer.

- (i) During ECM of an iron plate, ferrous hydroxide is formed and MRR_v obtained is 300 mm³/s. What would be MRR_v (mm³/s) if iron dissolves as ferric hydroxide in place of ferrous hydroxide.
(a) 200, (b) 450, (c) 300, (d) none of these.
- (ii) During ECM, electrode feed rate is calculated as 2 mm/min. The electrolyte conductivity is $0.2 \Omega^{-1} \text{cm}^{-1}$. It is now decided to change the feed rate to 3 mm/min without changing any other parameter except conductivity. What is the new value of conductivity ($/\Omega\text{-cm}$) for the same performance of the process?
(a) 0.4, (b) 0.3, (c) 0.133, (d) none.

- (iii) In ECM, the maximum permissible feed rate is f_1 while using electrolyte 'A' having sp. heat as C_1 and electrolyte density as ρ_{el} . In the second case, while using electrolyte 'B', the maximum permissible feed rate becomes f_2 . In this case, specific heat of electrolyte 'B' is $1.125 C_1$ and density as $2\rho_{el}$. If the highest allowable temperature of the electrolyte and the values of other parameters remain the same, what is the ratio of f_1/f_2 ?
 (a) 1.0, (b) 0.667, (c) 2.25, (d) 1.5.

PROBLEMS

- Q1. (i) The composition (% by weight) of Nimonic 75 alloy is given in the accompanying table:

Element:	Ni	Cr	Fe	Ti	Si	Mn	Cu
% by weight:	72.0	20.00	5.00	0.50	1.00	1.00	0.50
Atomic weight:	58.71	51.99	55.85	47.90	28.09	54.94	63.50
Valency:	2, 3	2, 3, 4	2, 3	3, 4	4	2, 4, 6, 7	1, 2
Density:	8.90	7.19	7.89	4.51	2.33	7.43	8.96

- (a) Calculate MRR (specific MRR and volumetric MRR) when a current of 2000 A is used. Use the lowest valency of dissolution in each case.
 (b) Determine the equilibrium gap if applied voltage = 15 V, over potential = 1.5 V, $k = 0.21/\Omega\text{-cm}$, and $f = 1 \text{ mm/min}$.
 (c) Calculate rise in temperature for the following machining conditions: feed rate = 0.05 mm/s, room temperature = 38°C , electrolyte density = 1.05 g/cm^3 , $\eta = 100\%$, electrolyte flow rate = 120 litres/min, flow velocity = 2000 cm/s and specific heat, $C_e = 1.06 \text{ cal/g}\cdot^\circ\text{C}$.
- (ii) Geometry of the workpiece surface with single curvature is given by the equation

$$y = 10 + 0.20x - 0.05x^2$$

where, x and y are in centimetres. The other details are as follows:

Applied voltage = 15 V, Over potential = 0.67 V, $f = 0.75 \text{ mm/min}$, work material = copper ($A = 63.57$, $Z = 1$), $\rho = 8.96 \text{ g/cm}^3$, $k =$

$0.2/\Omega\text{-cm}$.

Determine the equation of the required tool surface geometry and write the assumptions, if any.

- (iii) Derive an equation for the maximum permissible feed rate during ECM. Also deduce the relationship for electrolyte temperature change for a given feed rate of tool.
- (iv) Calculate the maximum permissible feed rate if boiling temperature of electrolyte = 98°C , room temperature = 38°C , $\rho_e = 1.05 \text{ g/cm}^3$, $\eta = 100\%$, electrolyte flow rate = 22 litres/s, electrolyte flow velocity = 20 m/s and specific heat = $1.07 \text{ cal/g-}^\circ\text{C}$.

Derive the following equation:

$$(T_o - T_i) = \frac{1}{\alpha} [\exp(Ak_i \alpha x) (1 - \alpha_v)^n - 1]$$

where, T_o and T_i are outlet and inlet temperatures respectively, k_i is inlet electrolyte conductivity, and A is given by

$$A = \frac{(V - \Delta V)^2}{U \rho_e C_e y^2}$$

where, x = distance along electrolyte flow direction, α = coefficient of change in electrolyte conductivity with temperature, α_v = void fraction, n = exponent, C_e = specific heat of electrolyte, V = applied voltage and y = IEG.

- (v) Derive one single equation for computing IEG during both zero feed rate as well as finite feed rate. Write the assumptions clearly.
- (vi) While using numerical method like FEM, FDM, or BEM for anode shape prediction, which of the two equations-implicit equation or equation derived in (v) above-will you recommend? Give the reasons.

- Q2. (i) During ECM, 10 V DC supply is used. Initial conductivity of the electrolyte used is $0.2 \Omega^{-1} \text{ cm}^{-1}$. Feed rate used is 1.0 mm/min. Calculate the IEG at 10, 20 and 30 mm distance from the inlet after 10s. Use the following given conditions (assume linear variation of α_v along x direction):

$T = 30^\circ\text{C}$, $\alpha_v = 0.0$ at $x = 0.00 \text{ mm}$,

$T = 60^\circ\text{C}$, $\alpha_v = 0.3$ at $x = 40.0 \text{ mm}$

Take n (exponent) = 1.75, atomic weight of anode = 55.9 g, density of anode = 7.86 g/cm³, initial IEG = 0.4 mm, valency of dissolution = 2, overpotential = 1.5 V, and α = 0.002. Also calculate the mean equilibrium gap.

- (ii) Using Faraday's laws of electrolysis, derive an equation to compute maximum permissible feed rate. Modify this equation to take into consideration the effect of temperature and void fraction on the electrolyte conductivity.
- (iii) The composition of nimonic alloy turbine blade is 18% cobalt, 62% Ni, and 20% chromium. Take I = 1500 A, and p_a = 8.3 g cm⁻³. Use valency of dissolution for chromium, nickel and cobalt as 6, 2 and 2, respectively. Gram atomic weights are as follows: Ni = 58.7, Cr = 52.0 and Co = 59.9. Calculate the volumetric MRR, and state assumptions, if any.
- (iv) Explain the 'self regulating (or adjusting) feature' of ECM.

NOMENCLATURE

A	Atomic mass, area of cross-section
C	Specific heat
E	Gram equivalent mass of material
f	Feed rate
F	Faraday's constant
H	Heat required
I	Current
J	Current density
k	Electrolyte conductivity
m	Mass of the material removed
n	Number of the constituent elements
q	Volumetric flow rate of electrolyte
R	Resistance
t	Time
T	Temperature
ΔT	Change in temperature
U	Electrolyte flow velocity
V	Applied voltage
V_e	Volume of electrolyte flowing
ΔV	Over voltage

X_i	Proportion by weight of i th element
x	Coordinate direction
y	Interelectrode gap, coordinate direction
Z	Valency of dissolution
z	Coordinate direction
α	Temperature coefficient of specific conductance
ρ	Density
η	Machining efficiency

Subscripts

a	Alloy, anode (workpiece)
b	Boiling
e	Equilibrium, electrolyte
g	Grams
i	Inlet
l	Linear
m	Maximum
o	Condition at time $t = 0$, or initial condition, outlet
s	Specific, second
t	At any time 't'
v	Volumetric

Acronyms

AC	Alternating current
DC	Direct current
ECM	Electrochemical machining
GFRP	Glass fiber reinforced plastics
IEG	Interelectrode gap
m/c	Machine
m/t	Machine tool
MRR	Material removal rate
SCRs	Silicon controlled rectifiers
TWR	Tool wear rate

CHAPTER 11
AT-A-GLANCE
ELECTROCHEMICAL MACHINING
(ECM)

- ECM PROCESS IS ALSO KNOWN AS : CONTACTLESS ELECTROCHEMICAL FORMING PROCESS

ECM PRINCIPLE

- FARADAY'S LAWS OF ELECTROLYSIS
- ELECTROCHEMICAL ENERGY DETACHES METAL FROM ANODE
→ ATOM BY ATOM
- POSITIVE IONS CONVERT AS HYDROXIDES
 - ACIDIC
- ELECTROLYTES →
 - ALKALINE
 - NEUTRAL
- $2H_2O + 2e \rightarrow H_2 \uparrow + 2 OH^-$
- $2Fe - 2e \rightarrow 2Fe^{++}$
- $Fe^{++} + 2OH^- \rightarrow Fe(OH)_2 \downarrow$
- $Fe(OH)_2 \rightarrow$ "INSOLUBLE IN WATER"
- SMALLER IEG → HIGHER MRR
- REACTION PRODUCTS → BARRIER TO THE FLOW OF ELECTROLYZING CURRENT <- TO MINIMIZE THIS EFFECT → ELECTROLYTE FLOW VELOCITY 20-30 m/s (2 - 35 kgf/cm²)
 - LIMITS ION CONCENTRATION AT THE ELECTRODE SURFACE → HIGHER MRR
 - DILUTES REACTION PRODUCTS
 - DISSIPATES HEAT AT A FASTER RATE
- FLOWING ELECTROLYTE →
 - LIMITS ION CONCENTRATION AT THE ELECTRODE SURFACE → HIGHER MRR
 - DILUTES REACTION PRODUCTS
 - DISSIPATES HEAT AT A FASTER RATE
- FEED RATE = MRR → CONSTANT IEG → CONSTANT MRR
- FACTORS GOVERNING ANODE PROFILE
 - ELECTROLYTE PROPERTIES, COMPOSITION, CONCENTRATION, TEMPERATURE, ETC. → CHANGE IN CURRENT DENSITY → MRR
 - FEED RATE
 - VOLTAGE
 - TOOL SHAPE
- ELECTROCHEMICAL DISSOLUTION BASED MACHINING OPERATIONS (FIG. 11.2)

- POWER SOURCE
- ELECTROLYTE CLEANING AND SUPPLY SYSTEM
- TOOL & TOOL FEED SYSTEM
- WORK & WORK HOLDING SYSTEM

POWER SOURCE

- RECTIFIER CONVERTS & TRANSFORMS 220V/440V AC → LOW VOLTAGE → (5 - 20 V) HIGH CURRENT → (AS HIGH AS 40 kA) DC
- VOLTAGE REGULATION → ± 1 %
- SPARKING DETECTED (WITHIN 10 μ s) → DEVICES LIKE SCR → PEEVENT DAMAGE TO TOOL & W/P
- TO MINIMIZE DAMAGE DUE TO A SPARK → USE OF SCR BANKS ACROSS DC INPUT

ELECTROLYTE SUPPLY AND CLEANING SYSTEM

- PUMP, FILTERS, PIPINGS, CONTROL VALVES, HEATING / COOLING COILS, PRESSURE GAUGE & RESERVOIR
- SUPPLY PORTS IN TOOL / WORK / FIXTURE ← MODE OF ELECTROLYTE FLOW
- TO MAINTAIN SMALL IEG (≤ 1 mm) → SMOOTH FLOW OF ELECTROLYTE AND NO BLOCKAGE OF GAP
- PROPER CLEANLINESS OF ELECTROLYTE USING FILTERS MADE OF ANTI-CORROSIVE MATERIALS
- PIPING SYSTEM : STAINLESS STEEL, GFRP, PLASTIC LINED M.S, OTHER ANTI-CORROSIVE MATERIALS
- : METALLIC PIPING ← EARTHED TO PREVENT ANODIC CORROSION
- TABLES, FIXTURES : EARTHED/CARRY CATHODIC POTENTIAL TO PREVENT CORROSION
- ELECTROLYTE TANK CAPACITY : 500 gal/1000 A
- ELECTROLYTE TEMPERATURE: ± 1°C → HEATIN/COOLING
 - | → PERIODICALLY CLEANED FOR PROPER FUNCTIONING
- FILTERS →
 - | → PLACED IN SUPPLY PIPE JUST PRIOR TO THE WORK ENCLOSURE
- SINGLE TANK SYSTEM (FIG 11.3)
- ECM : DIFFERENT METALS & ALLOYS, OPTIMUM MACHINING CONDITIONS, REQUIREMENTS OF ACCURACY & SURFACE FINISH
- USE OF SINGLE TANK → LOSS OF TIME & WASTAGE OF ELECTROLYTES RECOMMENDATION OF MORE THAN ONE TANK.

TOOL AND TOOL FEED SYSTEM

- TOOL MATERIAL —>
 - | HIGH THERMAL & ELECTRICAL CONDUCTIVITY
 - | ANTI-CORROSIVE IN NATURE
 - | HIGH MACHINABILITY
- TYPES : ALUMINIUM, BRASS, COPPER, MONEL, BRONZE, ETC
- INSULATION OF TOOL / BIT TYPE OF TOOL
- ACCURACY & SURFACE FINISH OF TOOLS → AFFECT W/P ACCURACY
 - |→ NON-CORROSIVE & ELECTRICALLY NON-CONDUCTING MATERIALS
- FIXTURES —>
 - |→ MINIMUM VIBRATION & DEFLECTION UNDER HYDRAULIC FORCES

WORKPIECE AND WORK HOLDING SYSTEM

- W/P MATERIAL : ELECTRICALLY CONDUCTIVE
- W/P HOLDING DEVICE :
 - * ELECTRICALLY NON-CONDUCTING
 - * GOOD THERMAL STABILITY
 - * LOW MOISTURE ABSORPTION
 - * GFRP, PLASTICS, PERSPEX

METAL REMOVAL IN ECM

- FARADAY'S LAWS OF ELECTROLYSIS
- IN ECM → W/P SHAPE & SIZE ARE CHANGED
- HIGH CURRENT DENSITY (MIN 8 A/mm²)
- PREFERENTIAL REMOVAL OF METAL IS DESIRABLE
- $m = (E I t)/F$ (BASED ON SIMPLIFIED ASSUMPTIONS & DOES NOT ACCOUNT FOR CHANGE IN VALENCY, PROTECTIVE FILM, GAS EVOLUTION EFFECTS, OVER-POTENTIAL, ETC)
- PART OF CURRENT GOES AS A WASTE, $\eta \rightarrow 75\% - 100\%$
- IEG ≤ 1.0 mm
- $f = MRR_i$ (MAINTAIN CONSTANT TOOL FEEDING)
- TOOL LIFE: THEORETICALLY INFINITE UNDER IDEAL CONDITIONS

ELECTROLYTE

- MEDIUM FOR CURRENT TO FLOW, TAKES AWAY HEAT GENERATED, REMOVES REACTION PRODUCTS, ETC
- NaCl COMMONLY USED
- RECIRCULATION
- VERY HIGH FLOW VELOCITY

MECHANICAL PROPERTIES OF ECM'D JOBS

- NO EVIDENCE ABOUT HYDROGEN EMBRITTLEMENT → HYDROGEN EVOLUTION AT THE CATHODE
- NO EFFECT ON DUCTILITY, YIELD STRENGTH, ULTIMATE STRENGTH, & MICRO-HARDNESS OF MACHINED COMPONENTS
- REDUCED FATIGUE STRENGTH AFTER ECM ← IMPROVE BY POST PROCESSING
- SURFACE FINISH AFFECTS FATIGUE STRENGTH
- FATIGUE CRACKS ORIGINATE FROM PITS
- DEPTH OF INTERGRANULAR ATTACK ← 0.01 mm

ADVANTAGES

- MACHINES COMPLICATED SHAPES IN SINGLE PASS
- MACHINABILITY ← INDEPENDENT OF PHYSICAL & MECHANICAL PROPERTIES OF W/P
- STRESS & BURR-FREE
- GOOD FINISH (0.1-1.0 μm)
- GOOD ACCURACY
- LOW MACHINING TIME
- LOW SCRAP
- AUTOMATIC OPERATION

LIMITATIONS

- ONLY ELECTRICALLY CONDUCTIVE W/P
- ACCURACY → (TOOL DESIGN, DEGREE OF PROCESS CONTROL, SHAPE'S COMPLEXITY, ETC)
- DIFFICULTIES → HARD SPOTS, INCLUSIONS, SAND, ETC
→ SHARP CORNERS & EDGES

APPLICATIONS

- OPERATIONS : TURNING, TREPANNING, ETC
- INDUSTRIES : AERONAUTICS, NUCLEAR TECHNOLOGY, SPACE VEHICLES, AUTOMOBILES, ETC
- PRODUCTS : TURBINE BLADES, CURVILINEAR SLOTS, GEARS, INTEGRALLY BLADED NOZZLE RING, ETC
- MATERIALS : SPECIALLY DIFFICULT-TO-MACHINE METALS AND ALLOYS
- FULL CAPABILITIES OF THE PROCESS HAVE NOT BEEN EXPLOITED

▽

PROBLEMS IN TOOL DESIGN

ELECTROCHEMICAL GRINDING (ECG)

INTRODUCTION

Conventional grinding produces components with good surface finish and dimensional tolerances but such components are also associated with burrs, comparatively large heat affected zone (HAZ), and thermal residual stresses. These defects are not found in electrochemically ground workpieces (anodes). During electrochemical grinding (ECG), material is removed by mechanical abrasive action (about 10%) and by electrochemical dissolution (about 90%) of anodic workpiece. As in any other electrochemical dissolution based process, workpiece should be electrically conductive. Electrolyte is recirculated in ECG, hence, an

effective and efficient electrolyte supply and filtration system is needed. The commonly used electrolytes are sodium chloride (NaCl) and sodium nitrate (Na-NO₃).

In ECG, there is a **grinding wheel** (cathode) similar to a conventional grinding wheel except that the bonding material is electrically conductive. Electrolyte is supplied through inter electrode gap (IEG) between the wheel and the workpiece. The height of abrasive particles protruding outside bonding material of the wheel helps in maintaining a constant IEG because the abrasive particles act as spacers. *Life of the ECG wheel* is about ten times more than that of the conventional grinding wheel. Two factors are responsible for such a high wheel-life: only 10% contribution by abrasive action towards the total material removal, and very small length of arc of contact.

In ECG, the area in which machining is taking place can be divided into 3 zones (*named as, zone I, zone II, and zone III*) as discussed in the following. Fig. 12.1 shows a schematic diagram for ECG set-up.

In **zone I** (Fig. 12.2), material removal is purely due to *electrochemical dissolution* and it occurs at leading edge of the ECG wheel. Rotation of the ECG wheel helps in drawing electrolyte into the IEG. As a result of electrochemical reaction in zone I, reaction products (including gases) contaminate electrolyte resulting in lower conductivity. In fact, presence of sludge, to some extent, increases conductivity of the electrolyte [Jain *et al*, 1990], while that of gases decreases it. Net result is a decrease in the value of conductivity of the electrolyte. It yields a lower value of IEG. As a result, abrasive particles touch the workpiece surface and start removing material by abrasive action. Thus, a small part of material is removed in the form of chips. Further, electrolyte is trapped between the abrasive particles and workpiece surface, and it forms a tiny electrolytic cell as shown in Fig. 12.2. In each electrolytic cell, small amount of material from the workpiece is electrochemically dissolved.

The electrolyte is being forced into the IEG in **zone II** by rotational motion of the wheel. As a result, local electrolyte pressure increases in this part of the IEG (zone II). It suppresses formation of gas bubbles in the gap yielding higher MRR. Chemical or electrochemical reaction may result in the formation of passive layer on the workpiece-surface. In this zone II, abrasive grains remove material from the work surface in the form of chips and also remove *non-reactive* oxide layer. Most of the metal oxides formed are insoluble in water, and electrically non-conductive.

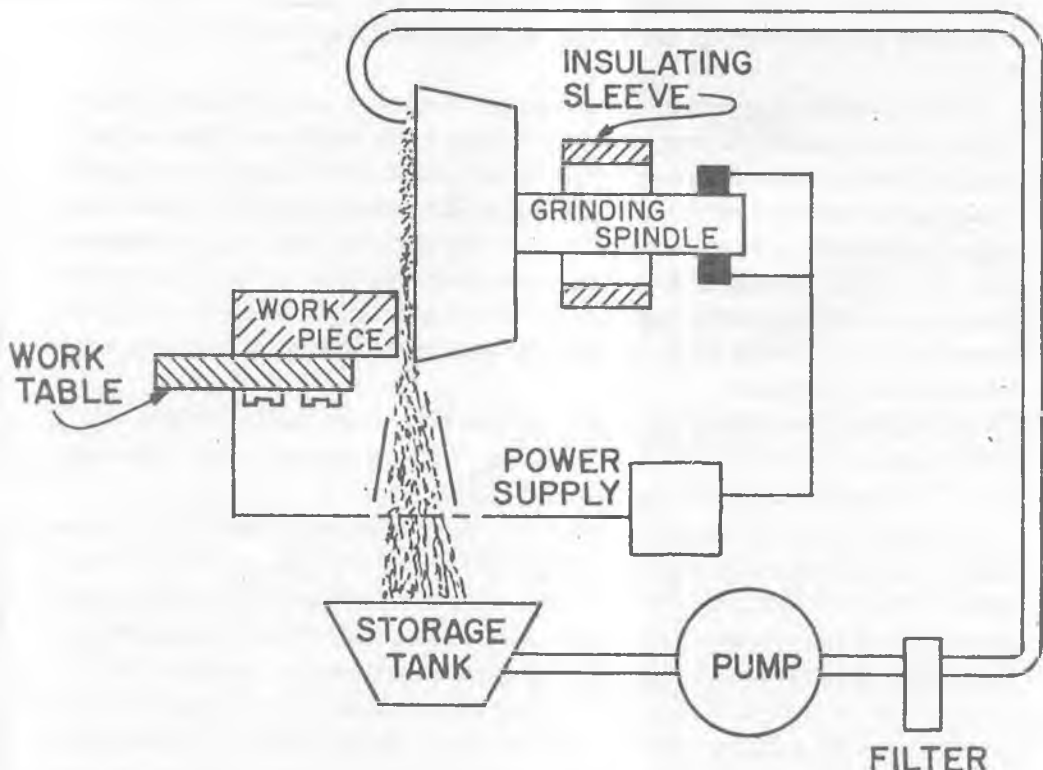


Fig. 12.1 Schematic diagram of electrochemical grinding set-up.

Removal of non-reactive oxide layer promotes electrolytic dissolution. It exposes fresh metal for further electrolytic action. Hence, it is also called [Bhattacharyya, 1973] as “mechanical assisted electrochemical grinding” process.

In **zone III**, material removal is totally by electrochemical dissolution. Zone III starts at the point where wheel lifts off the work-surface. In this zone, pressure is released slowly. This zone contributes to the removal of scratches or burrs that might have formed on the workpiece in zone II.

ECG MACHINE TOOL

The ECG systems are very similar to conventional grinders (Fig. 12.3). In ECG

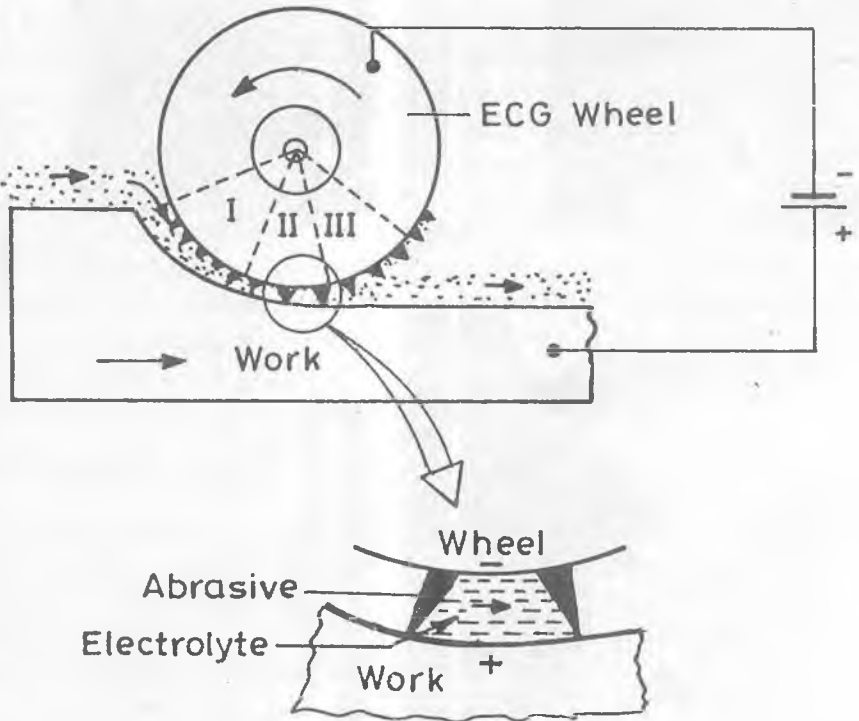
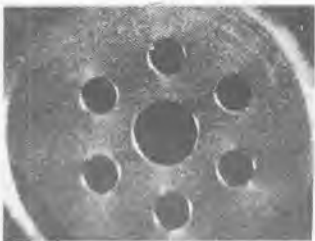


Fig. 12.2 Three machining zones and tiny electrochemical cell formation in ECG.

system, machining area is made up of non-corrosive materials. Power is supplied through spindle either with the help of brushes or mercury coupling. The latter can carry more current than the previous one. The probability of **short circuiting** during ECG is very low because of the presence of protruding abrasives which create a positive IEG. Hence, in this system, there is less need of having short circuit cut-off devices.

Five different kinds of ECG operations can be performed, viz electrochemical (EC) cylindrical grinding, electrochemical form grinding, EC surface grinding, EC face grinding and EC internal grinding. EC cylindrical grinding is the slowest process because of the limited area of contact between the



Hammond Machinery
Inc.
1600 DOUGLAS KALAMAZOO • MI 49007
616 345-7151

Fig. 12.3 Electrochemical grinder [Hammond Machinery, USA].

wheel and the workpiece. However, EC face grinding is the fastest process because of maximum area of contact between the anode and the cathode. Uneven wheel wear can be controlled by providing oscillating motion to the workpiece. In EC surface grinding, the workpiece reciprocates. EC internal grinding and EC form grinding are the same as conventional internal and form grinding operations.

except that the ECG wheel is electrically conducting and the electrolyte is present in the IEG.

Metal bonded grinding wheels have many advantages over resinoid bonded wheels. In ECG wheel, the commonly used bonding materials are copper, brass, nickel, or copper impregnated resin. Such metal bonded wheels are effectively dressed using electrochemical process. To prepare (or dress) them, reverse the current (or make the wheel as anode) and do the grinding on the scrap piece of metal. It will deplate the metal bond. The commonly used abrasive is alumina (grit mesh size 60-80). ECG does not require frequent wheel dressing. Dissolution of bond metal usually makes mechanical shear unnecessary. Trueing of the metal bonded grinding wheel is done, in-process, during electrochemical dressing. Further, the electrolyte used in ECG should be chemically inert to the conductive wheel bond material and workpiece. Current rating of these machines is usually 50-3000 A.

PROCESS CHARACTERISTICS

Performance of ECG process depends on various process parameters such as wheel speed, workpiece feed, electrolyte type, concentration and delivery method, current density, wheel pressure, etc. By selecting appropriate values of these parameters, MRR and surface finish obtainable during the process can be varied over a wide range [Kuppuswamy, 1976].

Current density is one of the most important parameters that influences the process performance. Material removal rate (MRR) in ECG is also governed by *current density*. With higher current density, both MRR and surface finish improve. If the applied voltage is very high (usual range is 4-15 V), it may deteriorate surface finish of the machined workpiece as well as damage the tool (grinding wheel). Presence of such condition is perceived by spark formation at the front of the wheel.

Selection of an appropriate **feed rate** to the tool is important. If it is higher than the required one, the abrasive particles will prematurely detach from the wheel, leading to excessive wheel wear. If it is lower than the required one, a large over-cut (or poor tolerances) and poor surface finish will result. The IEG is usually a quarter of a millimetre while using a freshly dressed wheel. Surface speed of the wheel is in the range of 1200-1800 m/min. The depth of cut is usually below 2.5 mm and it is limited by the wheel contact arc length, which should never exceed

19 mm; otherwise electrolyte becomes ineffective because of higher concentration of H₂ gas bubbles and sludge [Benedict, 1987].

MRR achieved during ECG may be high as 10 times compared to conventional grinding on hard materials (hardness \geq 65 HRC). But tolerances obtained in ECG are poorer (± 0.0025 mm). Minimum inside corner radius of 0.25 mm and outside corner radius of 0.025 mm can be produced by this process. Abrasive particles maintain electrical insulation between cathode and anode, and determine the effective gap between them (may be as low as 0.025 mm). Surface finish obtained by ECG ranges from 0.12 and 0.8 μm . The **surface produced** by ECG is free of grinding scratches and burrs. Surface finish produced on non-homogeneous materials during ECG is better than that produced during conventional grinding. In spite of more initial investment, the cost of EC grinding is lower than that of conventional grinding due to much higher MRR during ECG. Risk of thermal damage is also reduced.

Electrochemical grinding of WC-Co has been reported [Levinger and Malkin, 1979]. The initial specific etching rate of cobalt phase is higher than that of WC phase. In addition to the direct dissolution of material, the electrolysis process in ECG weakens the cermet material by selective removal of cobalt. When the in-feed rate during ECG is less than the initial specific etching rate of cobalt phase, selective etching of cobalt occurs that reduces mechanical power requirement for machining. At higher in-feed velocities, the reduction in mechanical power requirement is marginal. Study of surface roughness produced during ECG [Geva *et al.*, 1976] clearly indicates that there is selective electrochemical etching of the metal phase (Cobalt). It weakens the composite material and, thereby, reduces the forces required for mechanical grinding.

Kuppuswamy and Venkatesh [1979] conducted experimental study to investigate the **effect of magnetic field** on electrolytic grinding using diamond, SiC, and Al₂O₃ wheels. It has been found that the magnetic field in case of a diamond wheel, improves the process performance but the same is not true for Al₂O₃ wheel. In case of SiC wheel, the improvement obtained is marginal. The magnetic field interacts with the moving charged particles and may affect the rates of both mass transport and charge transfer processes [Dash and King, 1972]. The magneto-hydrodynamic force leads to stirring of electrolyte particularly in the neighbourhood of electrodes. It leads to enhanced mobility and hence an increased rate of electro-chemical reactions. *Gedam and Noble* [1971] concluded that fine grits and low concentration wheels show a tendency to draw more cur-

rent and thereby achieve greater MRR than coarse grits and high concentration wheels.

ECG is a **cold process** (bulk temperature < 100°C), thus prevents structural damage and grinding cracks. However, electrochemically ground specimens show relatively poor fatigue strength, possibly due to stray current attack of the surface, which leaves a series of 'pits' that would act as sites for fatigue crack initiation [DeBarr and Oliver, 1968].

Declogging of the grinding wheel can be done by reversing its polarity (making the tool as anode) for a short period. It may, however, result in longer machining time and degeneration of the wheel-shape.

APPLICATIONS

Electrochemical grinding is economical for grinding carbide cutting tool inserts. Microscopic study of electrochemically ground surfaces of the cemented carbide do not reveal any damage to the microstructure, microcracks, or any other defects. This process is also used to reprofile worn locomotive traction motor gears. Usually wear marks from the gear tooth surfaces are removed by removing as much as 0.38 mm thick layer of material. ECG does not have any effect on gear hardness. ECG is also used for burr-free sharpening of hypodermic needles, grinding of superalloy turbine blades, and form grinding of fragile aerospace honeycomb metals.

BIBLIOGRAPHY

1. Benedict G.F. (1987), *Non-traditional Manufacturing Processes*, Marcel Dekker Inc., London.
2. Bhattacharyya A. (1973), *New Technology*, The Institution of Engineers (I), Calcutta.
3. Buttner A. and Lindenback D.A. (1969), Electrolytic dressing of diamond wheels for use in steel grinding, *Ind. Diamond Rev.*, pp. 450-454.
4. Dash J. and King W.W. (1972), Electrothinning and electrodeposition of metals in magnetic fields, *J. Electrochem Soc.*, Vol. 119, pp. 51-56.
5. DeBarr A.E. and Oliver D.A. (1968), *Electrochemical Machining*, MacDonald, London.
6. Gedam A. and Noble C.F. (1971), An assessment of the influence of some wheel variables in peripheral electrochemical grinding, *Int. J. Mach. Tool*

7. Kuppuswamy G. (1976), Electrochemical grinding: an investigation of the metal removal rate, *Proc. 7th AIMTDR Conf.* held at Coimbatore (India) pp. 337-340.
8. Kuppuswamy G. and Venkatesh V.C. (1979), Wheel parameters and effect of magnetic field on electrolytic grinding, *J. Inst. Engrs. (I), Part ME(I)*, Vol. 60, pp. 17-20.
9. Levinger R. and Malkin S. (1979), Electrochemical grinding of WC-Co cemented carbides, *ASME Paper No. 78-WA/PROD-26, WAM*, San Francisco, pp. 1-10.
10. McGeough J.A. (1988), *Advanced Methods of Machining*, Chapman and Hall, London.
11. Pandey P.C. and Shan H.S. (1980), *Modern Machining Processes*, Tata-McGrawHill, New Delhi.
12. Jain V.K., Tandon S. and Kumar Prashant (1990), Experimental investigation into electrochemical spark machining of composites, *Trans. ASME, J. Engg. Ind.*, Vol. 12, pp. 194-197.
13. Verma M.M. (1981), A study of process parameters in electrochemical grinding, *M. Tech. Thesis*, IIT Kanpur (India).

REVIEW QUESTIONS

- (1) Why there is no need to have ‘short circuit’ protection device in ECG system?
- (2) Explain the mechanism of material removal during ECG and how it is different from ECM.
- (3) Why the life of the ECG wheel is much higher than conventional grinding wheel?
- (4) Why some researchers prefer to call this process as “mechanically assisted ECG”?
- (5) What are the factors responsible to improve ECG (with diamond wheel) process performance while using magnetic field?
- (6) What do you understand by in-process dressing during ECG? Write its merits and demerits.

CHAPTER 12
AT-A-GLANCE
ELECTROCHEMICAL GRINDING
(ECG)

CONVENTIONAL GRINDING

- GOOD SURFACE FINISH & TOLERANCES
- PRESENCE OF BURRS, HAZ, & THERMAL RESIDUAL STRESSES
- 100 % REMOVAL BY ABRASIVE ACTION

ECG

- W/P → ELECTRICALLY CONDUCTIVE
- ELECTROLYTE RECIRCULATED
- GRINDING WHEEL BONDING MATERIAL → ELECTRICALLY CONDUCTIVE
- MECHANICAL ABRASIVE ACTION → 10 %
- ELECTROCHEMICAL DISSOLUTION → 90 %
- LONG WHEEL LIFE
- COMMON ELECTROLYTES : NaCl & NaNO₃

3 ZONES OF IEG

ZONE 1

- PURE ELECTROCHEMICAL DISSOLUTION
- WHEEL ROTATION HELPS IN DRAWING THE ELECTROLYTE
- CONTAMINATION BY REACTION PRODUCTS & GASES
- CONDUCTIVITY CHANGES
- ELECTROLYTE TRAPPED ⇒ GRIT & W / P → ELECTROLYTIC CELL FORMATION
- SMALL AMOUNT OF MATERIAL REMOVED

ZONE 2

- HIGHER PRESSURE SUPPRESSES FORMATION OF GAS BUBBLES → HIGHER MRR
- ABRASIVE GRAINS → REMOVE W/P MATERIAL IN THE FORM OF CHIPS
- REMOVAL OF OXIDE LAYER HELPS IN EC DISSOLUTION

ZONE 3

- MATERIAL REMOVAL BY ELECTROCHEMICAL DISSOLUTION
- WHEEL STARTS LIFTING OFF THE WORK SURFACE
- REMOVES SCRATCHES & BURRS ← FORMED IN ZONE 2

- VERY HIGH VOLTAGE → SPARKING → DETERIORATES SURFACE FINISH & DAMAGES GW
- MATERIAL REMOVAL IS AS HIGH AS 10 TIMES OF CONVENTIONAL GRINDING ON HARD MATERIAL (> 65 HRC)

OPERATIONS

- CYLINDRICAL, FORM, SURFACE, FACE & INTERNAL ECG
 - CYLINDRICAL →
 - SLOWEST
 - LIMITED AREA OF CONTACT
 - FACE →
 - FASTEST
 - MAXIMUM AREA OF CONTACT

GRINDING WHEEL

- BONDING MATERIAL →
 - COPPER, BRASS, NICKEL
- DRESSING →
 - REVERSE THE CURRENT & DO ECG ON A SCRAP PIECE
 - DEPLATE THE METAL BOND EXPOSING ABRA-SIVE PARTICLES

APPLICATIONS

- ECONOMICAL IN GRINDING CARBIDE CUTTING TOOLS
- EC GROUND CEMENTED CARBIDE W/P → NO DAMAGE TO MICROSTRUCTURE & NO MICROCACKS
- FOR RE-PROFILING WORN LOCOMOTIVE TRACTION MOTOR GEARS
- NO EFFECT ON GEAR HARDNESS
- BURR-FREE SHARPENING OF HYPODERMIC NEEDLES
- SUPERALLOY, TURBINE BLADES & HONEYCOMB METALS

ELECTROSTREAM DRILLING (ESD)

INTRODUCTION

Standard electrochemical drilling (ECD) process uses a hollow metal tube as cathode through which electrolyte flows at high velocity. This tube moves in the hole as it is drilled hence, the hole diameter is always bigger than the outside diameter of the cathode tube. There are certain practical limitations because of which the cathode tube diameter cannot be reduced below a certain value. To drill a hole of diameter smaller than this value, a process named **electrostream drilling** was invented [Annon, 1976]. This process was employed for drilling thousands of small cooling holes in nickel and cobalt superalloys [Benedict, 1987].

In electrostream drilling (ESD), electrically negatively charged, high velocity, acid electrolyte stream is passed through electrically non-conducting nozzle (Fig. 13.1). This stream strikes positively charged workpiece and removes material in

the same way as in conventional ECM. This dissolved material (the sludge dissolved in the acid electrolyte) is flushed out from the machining zone in the form of metal ions in the solution. Since there is no sludge to restrict the flow of electrolyte, the limit on the minimum diameter of the hole that can be drilled is relaxed. This process can be used to drill very small holes at steep angles or curved holes (Fig. 13.2). By this method, it has been possible to drill holes of diameter as small as 0.127 mm to as large as 0.89 mm. But, the voltage used during ESD is very high (say, 150-850 V).

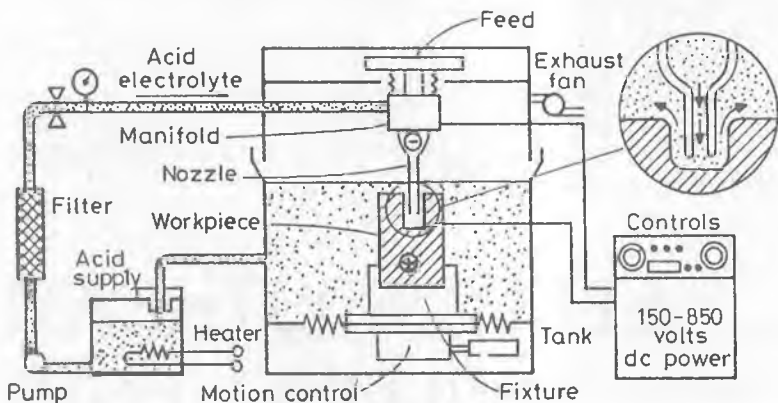


Fig. 13.1 Schematic diagram of electrostream drilling (ESD) set-up [Benedict, 1987].

In ESD, dilute solution of H_2SO_4 or HCl is used as **electrolyte**. Hydrochloric acid has proved to be better electrolyte for drilling materials like aluminium, titanium, etc. Sulfuric acid is the electrolyte preferred for drilling in carbon steel, cobalt alloys and stainless steel [Bellow and Kohls, 1982].

ESD can be performed in two ways, by giving no feed (or zero feed rate) and by providing finite feed to the nozzle. The first one is known as "**dwell drilling**" which is used when shallow, and less accurate holes are required. This technique is also employed under the circumstances when workpiece configuration or m/c capabilities do not permit movement of the nozzle. Nozzle tip is fixed at a pre-determined distance from the work surface, and drilling is done by the electrolyte stream, but it limits the depth of the drilled hole and obtainable accuracy (Fig. 13.3).

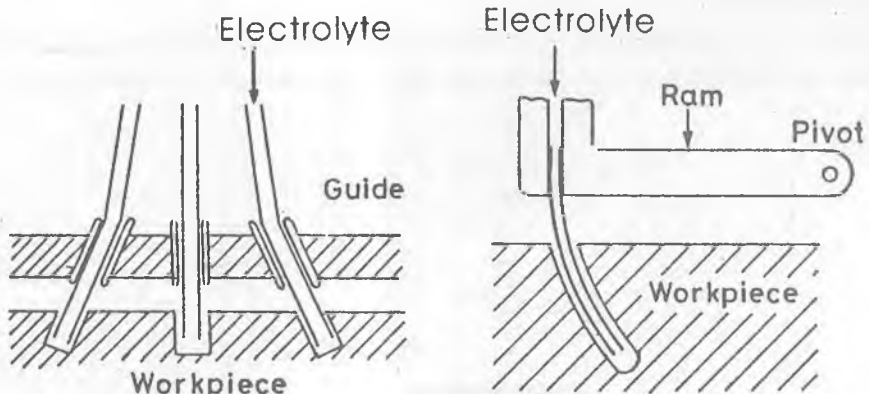


Fig. 13.2 Drilling of a curved hole using ESD.

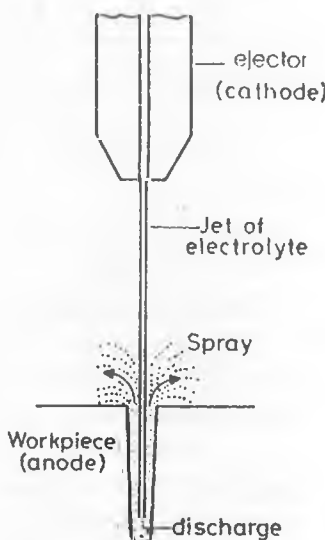


Fig. 13.3 Schematic of "Dwell drilling".

The second kind of ESD is known as "penetration drilling", and is used for deep and accurate hole drilling (Fig. 13.4). During ESD, the nozzle is fed towards the workpiece with a finite feed rate to maintain a constant inter electrode gap

(IEG). A gap sensing device is used to monitor the current being drawn, to slow down the feed, and trigger full power when the proper nozzle workpiece gap is detected.

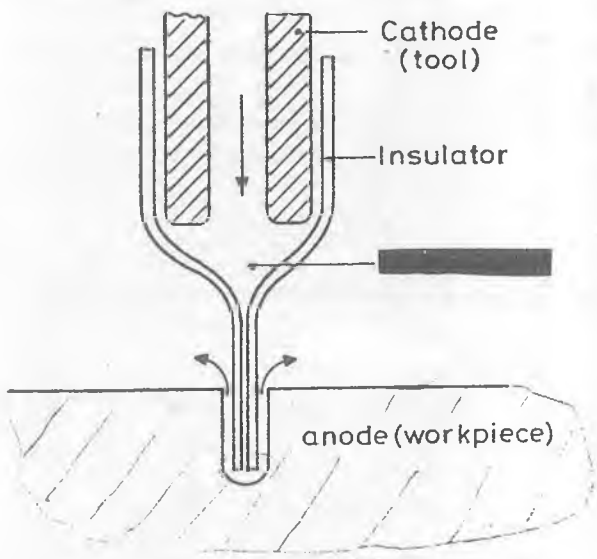


Fig. 13.4 Schematic of “Penetration drilling”.

Components of m/c and fixtures must be made of acid resistant materials. Nozzles designed for drilling round holes are made of glass tubing that is drawn to a small diameter, thus forming a capillary at one end. If a hole in the cavity is to be drilled at such an angle that the line of sight access is not available, a tool with a right angle bend at the tip is used (Fig. 13.5).

The outside diameter of the nozzle tip should be such that it fits within the hole being drilled as well as allows room for the repeatable escape of the used electrolyte [Bellow, 1967]. The length of the small diameter part of the tube should always be slightly greater than the depth of the hole to be drilled.

Charging of electrolyte can be done in two ways, either by the use of a metallic sleeve or by a small titanium wire (Fig. 13.6) which is placed inside the large diameter section of the ES nozzle. Metallic sleeve or titanium wire is kept as close to the throat as possible. Multiple nozzle applications require the use of a junction manifold with individual wires running from the electrolyte manifold to each nozzle.

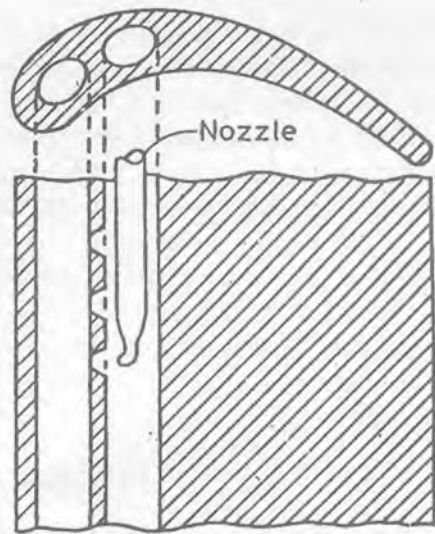
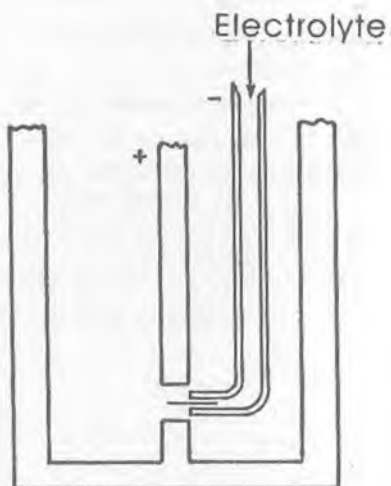


Fig. 13.5 Drilling of a right angled hole.

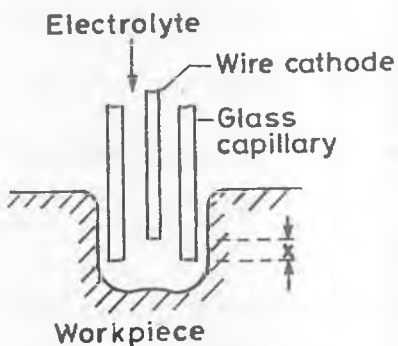


Fig. 13.6 Use of a small titanium wire to charge electrolyte.

PROCESS PERFORMANCE

The ESD process is being used for drilling holes having large depth and small diameter, ie high aspect ratio (in penetration drilling 40:1 and in dwell drilling 10:1), in any electrically conductive material without affecting its properties [Anon, 1976]. The maximum depth to which holes can be drilled in dwell drilling and penetration drilling are 5 mm and 19 mm, respectively. Machining rate that

that has been achieved in single nozzle or multiple nozzles (as many as 100 holes) is 1.5 mm min^{-1} . In a specific case, as many as 96 holes have been simultaneously drilled in a turbine blade in a period of just 1.5 min [Bellow et al., 1982]. By penetration drilling, shallow holes up to an angle of 75° from the normal to the work surface, tolerance up to $\pm 5\%$ of the diameter of the hole (but no less than 0.025 mm), and surface finish in the range of $0.25 \mu\text{m}$ to $1.67 \mu\text{m}$ have been achieved. Taper can be controlled to a value of 0.03 mm/cm . Machined component has burr free surfaces with no induced residual stresses. There is insignificant HAZ (heat affected zone) and no tool wear. Electrostream drilling has bell mouth hole entrance. To increase the production rate, simultaneous drilling of small holes is done.

BIBLIOGRAPHY

1. Annon (1967), Liquid stream drill holes in tough metals steel, *Steel*, April 24, pp. 49-62.
2. Benedict G.F., (1987), *Non-traditional Manufacturing Processes*, Marcel Dekker Inc., London.
3. Bellow G. (1967), New Non-conventional machining processes, *Am. Soc. Tool Manuf. Engg.*, Paper No. MR, pp. 67-141.
4. Bellow G. and Kohls J.B. (1982), Drilling without drills, *Am. Machinist*, pp. 173-188.

REVIEW QUESTIONS

1. Explain the working principle of ESD. In what respects it is different from conventional ECM?
2. Write a major difference between dwell drilling and penetration drilling.
3. In your opinion, what is the most interesting application of ESD?
4. What do you understand by charging of electrolyte.

CHAPTER 13
AT-A-GLANCE
ELECTROSTREAM DRILLING
(ESD)

- IN CONVENTIONAL ELECTROCHEMICAL DRILLING \Rightarrow HOLLOW METAL TUBE AS CATHODE
 - ELECTROLYTE FLOWS AT HIGH VELOCITY
 - CATHODE PENETRATES IN HOLE
 - HOLE DIAM \geq CATHODE OUTSIDE DIAM
 - TO DRILL A HOLE OF SMALL DIAM. \rightarrow ESD
 - SMALL COOLING HOLES IN SUPERALLOYS
 - HIGH VELOCITY NEGATIVELY CHARGED ACID - ELECTROLYTE STREAM
 - $0.127 \text{ mm} < \text{HOLE DIAM} < 0.890 \text{ mm}$
 - VOLTAGE $\rightarrow 150 - 850 \text{ V}$
 - ESD \Rightarrow ZERO FEED RATE \Rightarrow DWELL DRILLING \Rightarrow SHALLOW & LESS ACCURATE HOLES
- ↓
- LIMITED DEPTH OF HOLE
 - W/P CONFIGURATION, OR M/C CAPABILITIES DO NOT ALLOW NOZZLE MOVEMENT
 - MAXIMUM DEPTH $\rightarrow 5 \text{ mm}$
- ↓
- FINITE FEED RATE
(PENETRATION DRILLING)
↓
 - DEEP & ACCURATE DRILLING
 - CONSTANT GAP USING FINITE FEED RATE
 - A GAP SENSING DEVICE TO MAINTAIN CONSTANT GAP
 - MAXIMUM DEPTH $\Rightarrow 19 \text{ mm}$
 - MACHINING RATE $\rightarrow 1.5 \text{ mm/min}$
 - NO BURR
 - NO RESIDUAL STRESSES
 - INSIGNIFICANT HAZ
 - NO TOOL WEAR
 - BELL MOUTH HOLE ENTRANCE
 - MULTIPLE HOLE DRILLING

- M/C & FIXTURES MADE OF → ACID RESISTANT MATERIAL
- NOZZLE AND GLASS TUBING
- A TOOL WITH RIGHT ANGLE BEND ALSO
- LENGTH OF TUBE > DEPTH OF THE HOLE
- CHARGING OF ELECTROLYTE
 - ~ METALLIC SLEEVE
 - OR
 - ~ TITANIUM WIRE PLACED INSIDE TUBE.
- MULTIPLE NOZZLE APPLICATION



JUNCTION MANIFOLD



→ INDIVIDUAL WIRES RUNNING TO EACH NOZZLE

- $\text{H}_2\text{SO}_4 / \text{HCl} \rightarrow$ ELECTROLYTE



→ Al, Ti, ETC.

- * CARBON STEEL
- * COBALT ALLOYS
- * STAINLESS STEEL

ELECTROCHEMICAL DEBURRING (ECDe)

INTRODUCTION

A designer during the design phase of a component usually considers the aspects like material, form, dimensional accuracy, surface texture and heat treatment, but not the surface integrity and edge quality [K. Takazawa, 1988]. However, the last two factors are very important from the point of view of performance and the life of the product. Fig. 14.1 shows the concepts of surface technology. In this chapter, some discussion on how to achieve the desired edge quality (shape, dimension, tolerance and surface roughness) through electrochemical deburring is presented.

When a component is processed by a conventional machining method, usually, it is left with burrs specifically along the two intersecting surfaces. Such burrs are undesirable from the viewpoint of performance of a component as well as safety

of an operator, or for that matter whosoever works with this component. Such burrs can be removed by one of the deburring processes. Deburring is an important phase for manufacturing quality products, especially in large scale industries. The problems of burrs are still persisting and unsolved in many industries. Attempts are made to reduce burr level by various means, viz. by fixing speed, feed rates, and tool life, but this could not be achieved for certain reasons. Hence, the quality of the products is affected.

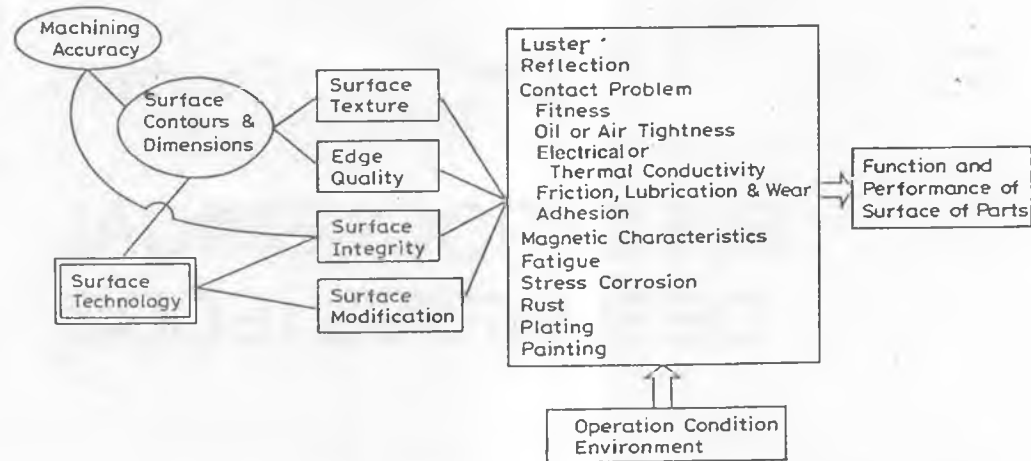


Fig. 14.1 Concepts of surface technology [K. Takazawa, 1988]

Definition of Burr: Burrs are three-dimensional in nature (Fig. 14.2) having length (l), height (h) and thickness (t) as described in the following:

- 1 (Burr length) : length of the edge along the burr axis.
- h (Burr height) : distance of the burr projected above the parental surface.
- t (Burr thickness) : thickness or width of the burr where it joins the parental surface.
- Burr Hardness : Hardness of the burr in the vicinity of the base of the burr.

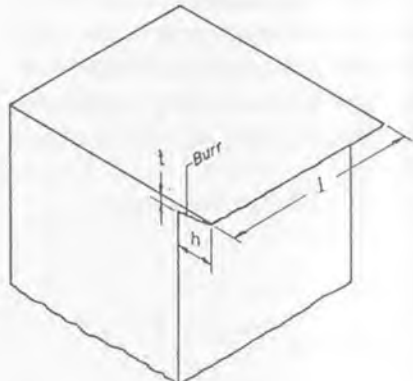
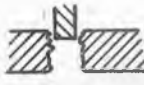


Fig. 14.2 Terminology of a burr [Naidu, M.G.J., 1991].

Types of Burrs Formed During Different Manufacturing Methods:

Types of Burrs	Figure of the Burr	Remarks
Compressive burr		The burr produced in blanking and piercing operations in which slug separates from the parent material under compressive stress.
Cutting off burr		A projection of material left when the workpiece falls from the stock.
Corner burr		Intersection of three or more surfaces.
Edge burr		Intersection of two surfaces.

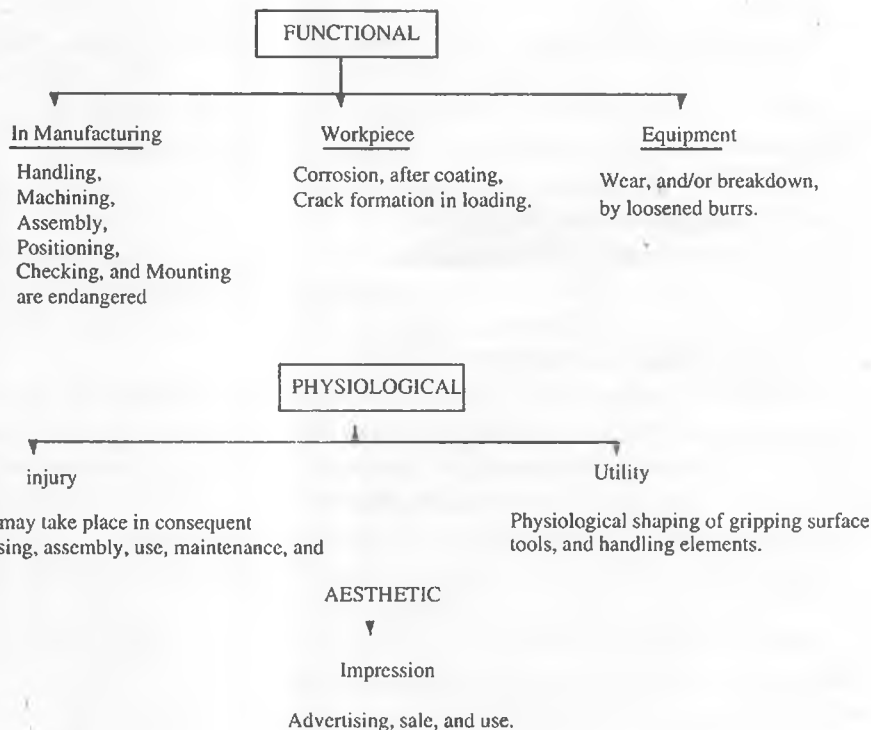
Types of Burrs	Figure of the Burr	Remarks
Entrance burr		Cutting tool enters in the workpiece.
Exit burr		Cutting tool exits the workpiece.
Feather burr		Fine or thin burr.
Flash burr		Portion of flash remaining on the part after trimming.
Hanging burr		Loose burr not firmly attached to the workpiece.
Roll over burr		Burr formed when it exits over a surface and allows the chips to be rolled away.
Tear burr		Formed from the sides of the tool as the tool tears the edge.

Basic Approach on Deburring

In the modern industrial technology, the deburring process has attained great importance because of rigid quality standards.

In analyzing the specific situations, one has to know 'why deburring is

required?" Burrs, to some extent, can be reduced by controlling cutting conditions, but cannot be eliminated completely. Hence, deburring becomes inevitable. However, deburring cost should not be very high. This requires careful considerations regarding effects of the presence of burrs on functional, physiological and aesthetic requirements [Naidu, 1991], as outlined in the following chart.



CLASSIFICATION OF DEBURRING PROCESSES

Deburring processes can be classified (Fig. 14.3) as:

1. Mechanical deburring,
2. Abrasive deburring,
3. Chemical and Electro-chemical deburring, and
4. Thermal deburring.

Mechanical deburring, using cutting tools, brushes, scrapers, belt sanders, etc, is generally unreliable as it is labour oriented and is only a burr-minimizing process. It does not meet the requirements of high edge quality because of the existence of fine burrs even after mechanical deburring operation.

In **abrasive deburring** like tumbling, barrel finishing, vibratory deburring, liquid abrasive flow, sand blasting,etc, the selection of abrasive medium, its shape and quantity play an important role. Deburring by this method generally affects other areas on the component where deburring is not required and has limitations on edge quality. The reliability, uniformity and MRR of these processes are low, and tend to charge the workpiece with grits.

In **thermal deburring** (TDe), components to be deburred are placed in the deburring chamber. The chamber is closed and filled with combustible gas mixture of oxygen and hydrogen. After ignition by an electric spark, the gas burns in few milliseconds and the temperature attained is over 3500°C. Due to this short heat wave, burrs and sharp edges on the component burn away.

Chemical deburring is the process where the burrs are dissolved in chemical media. It also may affect the areas where material removal is not required.

Principle of *anodic dissolution* (ECM) has also been applied [Benedict, 1987; Rumyantsev and Davydev, 1989] for the removal of burrs. However, in case of electrochemical deburring (ECDe) as compared to ECM, magnitude of current, electrolyte flow rate, and electrolyte pressure are all low. Secondly, tool is stationary. Fig. 14.4 shows an ECDe system.

Electrochemical deburring is generally employed for far away located as well as inaccessible places where other deburring processes are not effective. This process involves the use of flowing electrolyte for conducting electric current for the electrochemical reaction to take place. The current rating and duration of the current flow to suit a particular component are determined after extensive trials for each type of the component. The electrolyte commonly used is either sodium chloride or sodium nitrate. Because of the corrosive nature of the electrolyte

DEBURRING PROCESS

Much of this research and development has now made the transition from the laboratory into the production

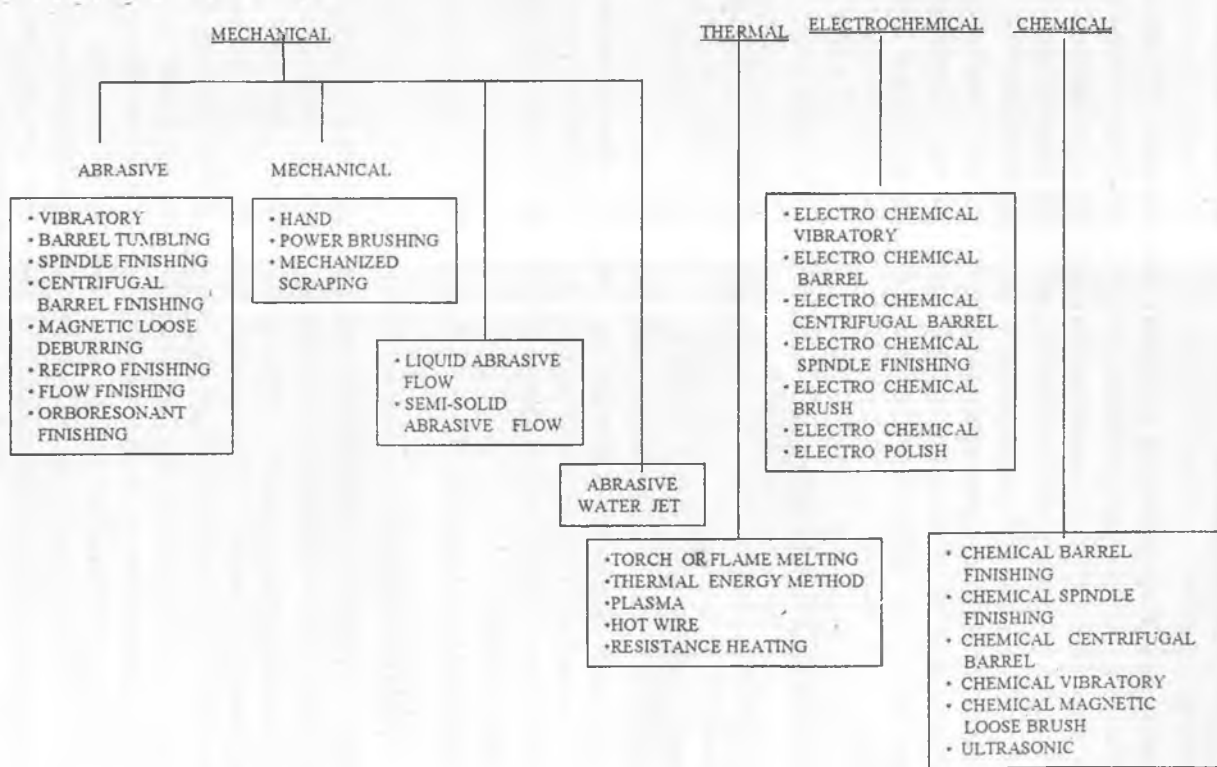


Fig. 14.3 Classification of deburring processes.

and ferrous hydroxide released by the process, machines are built with non-corrosive materials.

Electro polishing deburring (EPDe) is different from EC deburring. The metal removal and polishing simultaneously take place on all the surfaces in EPDe, whereas in ECDe, the metal removal is localised. In this process, a component which has roughness and some burrs, is subjected to selective electrochemical attack. As a result, microprofile is smoothened and levelled.

Selection of a process depends on the edge quality and other requirements of the component. Most of the modern industries are switching over to modern technologies like ECDe, EPDe and TDe due to obvious advantages including cost savings.

ELECTROCHEMICAL DEBURRING (ECDe)

This process has been tried out successfully on contours where the conventional deburring tools can not be used. The performance of the process is improved with higher current intensities. It requires specially engineered equipment for its use as manufacturing unit. It consists of:

1. Electrolyte system which provides high velocity to the electrolyte flow,
2. Electrical power system which supplies the electrolyzing current,
3. Mechanical structure which locates and provides movement/mounting to the electrodes, and
4. Separator which separates the sludge.

Principle of working

When a voltage is applied between two metal electrodes immersed in an electrolyte, current flows through the electrolyte from one electrode to the other. Unlike the conduction of electric current in the metals in which only the electrons move through the structure of the material, 'ions' (electrically charged groups of atoms) physically migrate through the electrolyte. The transfer of electrons between the ions and electrodes completes the electrical circuit and also brings about the phenomenon of metal dissolution at the positive electrode or anode (workpiece). Metal detached atom by atom from the anode surface appears in the main body of the electrolyte as positive ions, or as precipitated semi-solid of the metal hydroxide, which is more common in electrochemical deburring process.

The tool is usually insulated on all surfaces except a part which is adjacent to

the burr(s). Instead of insulated tool, a **bit type of tool** [Jain and Pandey, 1982] can also be used. The electrolyte is made to flow through inter electrode gap. However, setting of dimensions of the bare part of the tool, time of machining, and other machining conditions are all decided by '*trial and error*' method. The inter electrode gap (IEG) is usually kept in the range of 0.1-0.3 mm. The deburring tool-tip should normally overlap with the area to be worked by 1.5 to 2.0 mm.

ECDe machine tool (M/T) is usually designed with multiple work stations served from a single power supply. The electrolyte is properly filtered out before its re-circulation. Criteria for selection of tool material used is the same as for general ECM.

It is considered as a high-tech method when compared to the conventional methods of deburring. Before applying ECDe method for a particular type of job, one should know about thickness, shape, and repeatability of burrs on the job in hand. Almost identical shape and size of the burrs should be on the job otherwise efficient burr removal may not take place. Further, the part of the tool supposed to remove burrs should be shaped as a replica of the contour of the work. Fig. 14.5 shows a tracing from the micrograph of a sample deburred electrochemically.

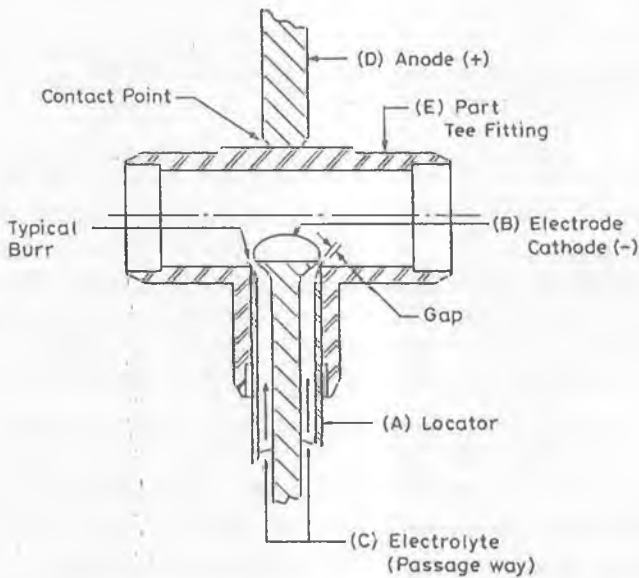


Fig. 14.4 Schematic diagram of electrochemical deburring.

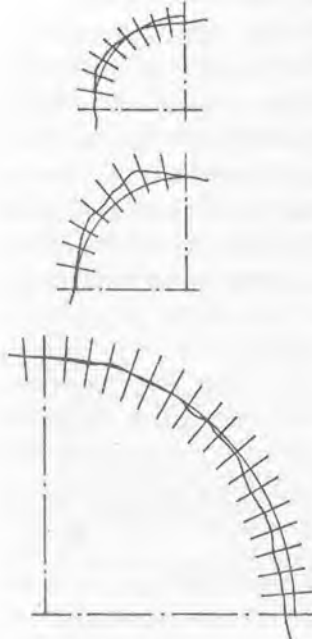


Fig. 14.5 Tracing from the micrograph of an electrochemically deburred samples [Rumyantsev and Davydev, 1989].

In some cases, deburring can also be done with the help of a **movable ECD_e** unit [Rumyanstev and Davydov, 1989] consisting of deburring gun, electrolyte supply tank, and power supply unit (≈ 50 A max. current). The deburring gun is supplied with electrodes of different diameter and length so that it can be used to deburr hard-to-get places. However, in some cases, tool of varying length may be needed. For this purpose, a *flexible tool* is used which consists of wire coiled into a closely wound spring. The details of the tool are shown in Fig. 14.6 (1-insulating spherical tip, 2-copper tip with a hole for electrolyte supply, 3-spring, 4-PVC sleeve, 5-copper shank press fitted to the spring. The flexible electrode is attached to the gun by means of shank 5). The deburring gun is also used to deburr edges of sheet metals. Deburring speed may be as 400-500 mm/min.

The data in the following table may be useful for practical deburring purposes:

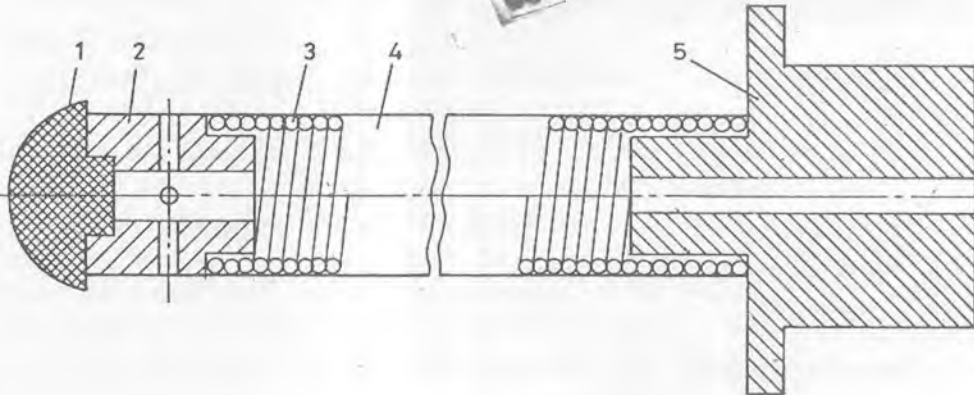


Fig. 14.6 A tool for a movable electrochemical deburring unit [Rumyantsev and Davydev, 1989].

Material	Electrolyte	Applied Voltage	Current Density	Deburring Time
Carbon and low carbon steel	5–15% NaNO ₃ + 2–5% NaNO ₂			
Copper alloys	5–15% NaNO ₃	12–24V	5–10 A/cm ²	5–100 s
Aluminium alloys	15–20% NaNO ₃			
Stainless steels	5% NaNO ₃ +NaCl			

ECDe is found suitable for removing burrs from tubes and pipes widely varying in configuration, length and cross-sectional area.

Functions of Electrolyte and its Importance

Depending upon the requirements of the process, sodium chloride (NaCl) and sodium nitrate (NaNO₃) are generally used as electrolytes. The other electrolytes like hydrochloric acid, potassium chlorate, etc. have certain disadvantages in the process application. Sodium nitrate and sodium chloride have certain variations in usage [Naidu, 1991] which are as follows:

Details	Sodium Nitrate	Sodium Chloride
1. Voltage requirements	High	Low
2. Reaction	Normal	Aggressive slow
3. Increase of pH value	Fast	Slow
4. Machining efficiency		
• Low carbon steel	60–80%	80–100%
• High carbon steel	Good	Poor
• Aluminium	Good	Poor
5. Machined surface		
• Roughness	About 5 μm	About 1 μm
• Colour	Dark grey	Bright grey
• Edges	Sharp & distinct	Blunt & dull
• Dimensional accuracy	Accurate	Not accurate
• Reach	Up to 1 mm	Up to 5 mm
• Effect on surrounding surface	Limiting stray machining and pitting of adjacent areas	Removes material from surrounding areas and pitting damages adjacent areas.
6. Cost	Costly	Not very expensive.

The deburred component shows a **localized deposit** (dark grey) which is a reaction product of the process. The composition of the reaction product while deburring ferrous component is Fe_3O_4 . It is a magnetic oxide of iron and its thickness is less than 1 μm . The adhesion of the deposit is very strong and it can be removed only mechanically. In specific cases, this deposit can be removed from unhardened components (unalloyed or low alloyed steels) as follows:

1. Anneal under air flow for more than 40-60 min at 430°C,
2. Pickle in hydrochloric acid for 1/2 min,
3. Anodically clean in alkaline bath for about 2 min.

In most of the cases, the deposit is electrolytically conductive and does not come in the way of galvanic deposits. This deposit disappears during heat treatment of the components.

APPLICATIONS

ECDe has applications in *industries* like consumer appliances, biomedical, aerospace, automobile, etc. ECDe is used for the components like gears, splines, drilled holes and milled components, fuel supply and hydraulic system components, etc. It is very successful even in the situations where two holes cross each other like crank shaft. Apart from economics of the process, it gives higher reliability, reduced operation time, and more uniformity. This process can be automated in an easier way than other processes. Fig. 14.7 shows a gear before and after deburring.

SPECIFIC FEATURES OF ECDe M/C

Specific features of an ECDe M/C are summarized as follows:

1. *Application:* Removal of thin and thick burrs at inaccessible and irregular areas within the restricted zone, and wherever edge rounding is required.
2. *Principle:* High velocity electrolyte (sodium chloride/sodium nitrate) is passed through the IEG between the tool-cathode and the component-anode connected to the electric potential. The undesired superfluous projections on the component are dissolved electrochemically within a preset cycle time of a few seconds. The dissolved burrs in the form of hydroxides settle down and the electrolyte is regenerated. The hydroxide is disposed through outlet drain.
3. *Equipment:* Consists of specially designed DC-power pack, working station, storage tank, and necessary controls. All the controls and safety requirements are interlocked in a logic system.
4. *Capacity:* It is decided *based on the area of deburring* and production quantity. Approximately 200 mm diameter gear with the tooth profile and spline slots are deburred within 45-60 s cycle time on a 500 A capacity machine.
5. *Consumables:* A 500 A capacity machine requires approximately 20 kg of electrolyte salt per week, working in two shifts. The cathode electrode wears out at the insulating areas where the component has heavy burrs, hence the life of the electrode is approximately 3000-25000 *components per electrode*.

The cost of such electrode varies from Rs. 1000 to 5000.

6. *Adoption:* It can be adopted to any material through the selection of an appropriate electrolyte. Generally sodium nitrate (NaNO_3) is used on steels, cast iron and aluminium for a precise deburring, and sodium chloride (NaCl) is used on steels for an aggressive deburring.

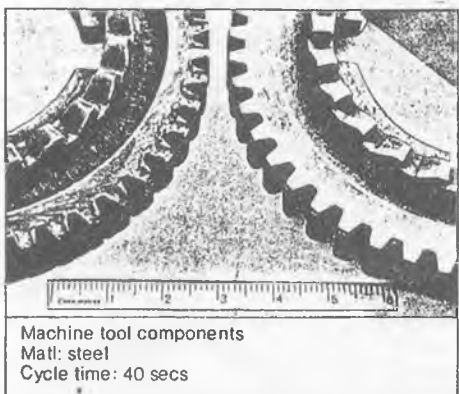


Fig. 14.7 A gear before and after deburring [Courtesy, EleChem Technik, Bangalore].

7. *Pollution:* Electrolyte is a domestic salt and solution is free from health hazard. The hydroxide removed from the drain valve is extensively being used as a raw material for the lapping paste.
8. *Quality:* The component having the burr root thickness less than 0.2 mm and the height less than or equal to 1 mm, can be precisely deburred by maintaining the edge rounding from 0.2–0.5 mm radius, and the cycle time for approximately 20–30s. If the burr size is larger than the above stated one, the edge quality after deburring would be of approximately 0.5–1.5 mm radius and cycle time required will be 60–90s depending upon the burr level. There will be discolouration at the adjacent area but no material removal; however, as the cycle time increases more than 30s, there will be slight material removal (approximately 0.05 mm) on a width of 1-2 mm adjacent to the deburred area. It can be controlled through tooling, if desired.
9. *Components Cleaning:* Before deburring, the components should be free from loose burrs which damage the electrodes, and from grease/oil which

contaminates the electrolyte. Hence, it is preferred to thoroughly wash the components just before deburring. After deburring, it should be dipped immediately in running water followed by dewatering fluid, thus protecting against corrosion.

Deburring is advised to be done usually before any surface treatment. There will be no hydrogen embrittlement.

BIBLIOGRAPHY

1. Benedict G.F. (1987), *Non-traditional Manufacturing Processes*, Marcel Dekker Inc., New York.
2. Naidu M.G.J. (1991), Electrochemical deburring for quality production, *Proc. Winter School on AMT* (Eds.: Jain V.K. and Choudhury S.K.), IIT Kanpur (India).
3. Pandey P.C. and Shan H.S. (1980), *Modern Machining Processes*, Tata-McGraw Hill, New Delhi.
4. Pramanik D.K., Dasgupta R.K. and Basu S.K. (1982), A study of electrochemical deburring using a moving electrode, *Wear*, Vol. 82, pp. 309-316.
5. Rumyantsev E. and Davydev A. (1989), *Electrochemical Machining of Metals*, Mir Publishers, Moscow.
6. Takazawa K. (1988), The challenge of burr technology and its worldwide trends, *Bull. JSPE*, Vol. 22, No. 3, pp. 165-170.
7. *Tool Design Manual for Electrochemical Deburring*, Chemtoal Inc., Minnesota, U.S.A.

REVIEW QUESTIONS

- Q1. (i) From which viewpoints it is important to have a deburred component?
(ii) Which type of burr is expected in the following type of machining operations: drilling, milling, turning and shaping?
(iii) How the presence of burrs at the intersecting holes will affect the functional requirements of a given component?
(iv) How can you protect the areas where dissolution of the work material during ECDe, is not desirable?
(Hint: See chemical machining).
- Q2. Write names of the two types of components from each of the five different industries, in which cases ECDe can be applied.

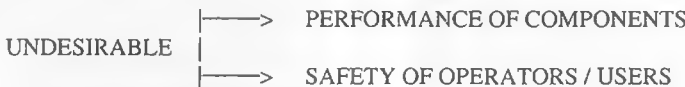
Q3. What is the usual feed rate in case of ECDe?

ACRONYMS

ECDe	Electrochemical deburring
ECM	Electrochemical machining.
EPD _e	Electropolish deburring
IEG	Interelectrode gap
M/C	Machine
M/T	Machine Tool
TDe	Thermal Deburring

CHAPTER 14
AT-A-GLANCE
ELECTROCHEMICAL DEBURRING
(ECDe)

- MACHINING OF MATERIALS BY CONVENTIONAL METHODS →
BURRS SPECIFICALLY AT INTERSECTING SURFACES



- REMOVAL OF BURRS
 - MECHANICAL → TUMBLING, BLASTING, ETC → NON-UNIFORMITY, LOW MRR, CHARGED WITH GRITS, ETC
 - THERMAL
 - ELECTROCHEMICAL → BASED ON ECM PRINCIPLE
- ECDe TOOL
 - INSULATED EXCEPT A PART ADJACENT TO BURRS
 - DIMENSIONS OF BARE PART OF TOOL, MACHINING TIME & MACHINING CONDITIONS
- ECDe M/C TOOL
 - MULTIPLE WORK STATIONS
 - SINGLE POWER SUPPLY
 - ELECTROLYTE IS RECIRCULATED AFTER FILTRATION
 - FOR PROPER DEBURRING → BURR CHARACTERISTICS SHOULD BE KNOWN

APPLICATIONS

- BIOMEDICAL, CONSUMER APPLIANCES, AEROSPACE, AUTOMOBILE, ETC
- COMPONENTS → GEARS, SPLINES, DRILLED HOLES, ETC
- HIGHER RELIABILITY, REDUCED OPERATION TIME & MORE UNIFORMITY

SHAPED-TUBE ELECTROLYTIC MACHINING (STEM)

INTRODUCTION

For drilling smaller diameter but deep holes in electrically conductive materials, shaped-tube electrolytic machining (STEM) process is used [Benedict, 1987]. Shaped-tube electrodrilling is quite commonly done in aerospace industries and difficult-to-machine superalloys. It was developed primarily for drilling high aspect ratio (up to 300:1) round and shaped holes in turbine engine airfoils. It uses

acid based electrolyte which ensures that the reaction products formed during electrolytic deplating are dissolved and carried away as metal ions. It eliminates clogging of the electrolyte flow path around the electrode. STEM uses an electrode as a hollow, shaped-tube covered with insulating coating on all exterior surfaces except at the tip [Bellow and Kohls, 1982].

Fig. 15.1 shows different **elements of a STEM system**. STEM is a low-voltage process (5-15 V DC). At higher voltages, drilling rates can be increased but boiling of electrolyte, plating of electrodes, and damage to the electrode coating may lead to serious problems. Feed rate depends on the machining parameters; however, it can be as high as 5 mm/min against a normal feed rate of 1.5 mm/min. For clarity, magnified view of overcut is shown in Fig. 15.1. Value of the overcut can be changed by varying the applied voltage and electrolyte flow velocity with the help of computer control. During STEM, taper obtained is 0.015 mm/cm and surface finish achieved is 0.8 to 3.1 μm . Surface finish depends upon work material and machining parameters.

Electrolyte normally used is 10% concentration of sulphuric acid or hydrochloric acid in water. Temperature of electrolyte is maintained between 37-40°C. To maintain a constant gap between tool and workpiece, a servo system is used. After drilling is over, the workpiece should be thoroughly washed by water to neutralize and remove residual acid. Tube material is pure titanium to resist acidic action of the electrolyte. Coating on the tube serves dual purpose, eg it saves from the attack of the electrolyte as well as eliminates stray cutting at the walls of the hole. Best results are obtained if the tip is dressed at an angle of 10°. Pinhole scratches and delaminations in the coating would result in stray cutting (i.e. non-uniform cutting). Multiple electrodes even with varying shapes and sizes, would be able to produce as many as 100 holes simultaneously. The components of the M/C which are likely to come in contact with electrolyte, should be made of corrosion resistant materials like titanium, stainless steel, plastics, and ceramics. Proper ventilation of machining chamber must be provided to extract corrosive electrolyte mist and hydrogen gas byproducts of the process.

Material removal is performed basically by the foot (or tip) of the tube, hence by changing its shape, the holes of different shapes can be obtained without changing the shape of the full tube. To increase productivity and to make the process more versatile, these tips may be made of different shapes and sizes even in multiple hole machining. An alternative method is to make these tips as independent, separate, **bit type of tube** of the desired shape and size, and then

fasten (by threading or otherwise) them to the bit holder (or electrode) [Jain and Pandey, 1982]. Electrolyte mist and hydrogen gas byproducts of the process should be properly removed from the machining chamber.

BIBLIOGRAPHY

1. Benedict G.F. (1987), *Non-traditional Manufacturing Processes*, Marcel Dekker Inc., New York.
2. Bellow G and Kohls J.B. (1982), Drilling without drills, *Am. Machinist*, pp. 173-188.
3. Jain V.K. and Pandey P.C. (1982), Investigations into the use of bit as a cathode in ECM, *Int. J. Mach. Tools Des. & Res.*, Vol. 22(4), pp. 341-352.

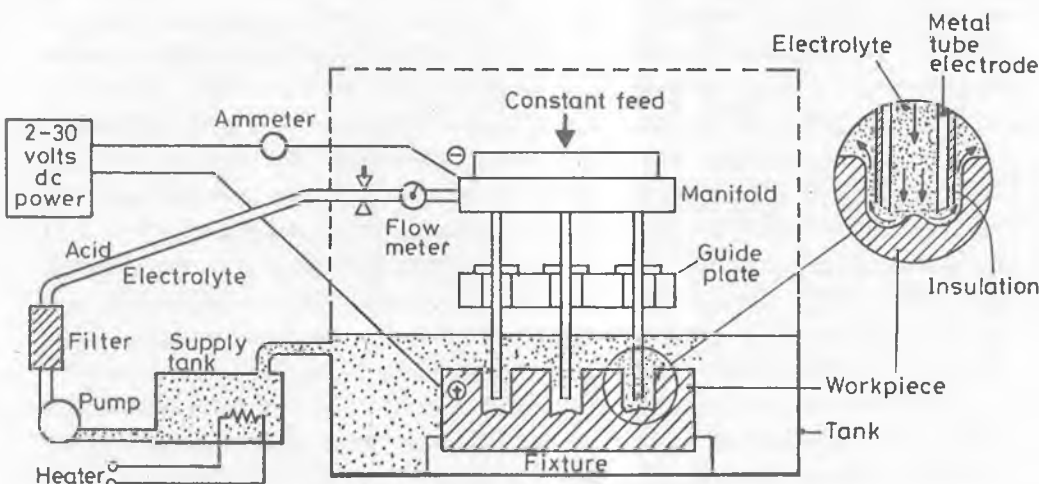


Fig. 15.1 Schematic diagram of a shaped-tube electrolytic machining system.

ACRONYMS

DC Direct current

M/C Machine

STEM Shaped-tube electrolytic machining

CHAPTER 15
AT-A-GLANCE
SHAPED - TUBE ELECTROLYTIC MACHINING
(STEM)

- SMALL DIAMETER DEEP HOLES IN ELECTRICALLY CONDUCTIVE MATERIALS
- HIGH ASPECT RATIO \Rightarrow ROUND & SHAPED HOLES
- SUPERALLOY MACHINING
- ACID-BASED ELECTROLYTE
- REACTION PRODUCTS \Rightarrow DISSOLVED
- SHAPED TUBE COATED ON EXTERIOR SURFACE EXCEPT TIP
- LOW VOLTAGE \Rightarrow 5 - 15 V
- AT HIGHER VOLTAGE \Rightarrow HIGHER MRR, DAMAGE TO ELECTRODE COATING, AND BOILING OF THE ELECTROLYTE.
- OVERCUT CONTROL \Rightarrow APPLIED VOLTAGE & ELECTROLYTE FLOW VELOCITY
- TAPER OBTAINED \rightarrow 0.015 mm/cm AND SURFACE FINISH \Rightarrow 0.8 - 3.1 μm



WORKPIECE & MACHINING PARAMETERS

- ELECTROLYTE \Rightarrow 10% H_2SO_4 + WATER.
 TEMPERATURE : 37 - 49 °C.
- COATED TUBE (TOOL) \Rightarrow ELIMINATES STRAY CUTTING



PIN HOLES, SCRATCHES & DELAMINATION OF COATING

- MULTIPLE ELECTRODES \Rightarrow 100 HOLES SIMULTANEOUSLY
- PROPER EXHAUST SYSTEM \Rightarrow EXTRACT CORROSIVE ELECTROLYTE MIST & H_2 GAS
- TIP REMOVES MATERIAL \Rightarrow CHANGE ITS SHAPE RATHER THAN FULL TUBE

CHEMICAL MACHINING (ChM)

INTRODUCTION

In ancient days, this process was used by artists for engraving the metals. However, they were unaware of how the process worked. Chemical machining (ChM) is a process used to remove material by dissolution in a controlled manner, from the workpiece by application of acidic or alkaline solution (i.e. *etchant*). *Maskants* (chemically resistant coatings) are used to cover the surfaces which are not to be machined. Maskants are the materials which do not allow etchants to penetrate through to reach the work material to dissolve. This technique is quite useful for producing complex configurations in delicate parts that otherwise would get damaged by the application of forces in case of the conventional machining processes. This process is used in many industries, viz. aviation industries for making aircraft wing panels, printed circuit boards (PCB), jewelery, etc.

It is also used for the manufacture of very thin laminations without burrs. Other applications include large turbine engine containment rings [Benedict, 1987], milling of spun aluminium pressure vessel bulkheads, and also shuttle components. It is also an useful process for finishing of parts to close tolerances and to achieve precision fits. Some sheet metal components are manufactured by ChM in place of welding or riveting.

Chemical milling and chemical blanking are the two most common versions of ChM. During *chemical milling*, the material is removed to produce “blind” details (pockets, channels, etc) or to reduce the weight. During *chemical blanking*, the details that usually penetrate the material entirely (holes, slots etc) are produced. This is also the process of blanking complete parts from the sheet by chemically etching the periphery of the desired shape. Fig. 16.1 shows a set-up used in chemical machining which involves various steps listed in the following.

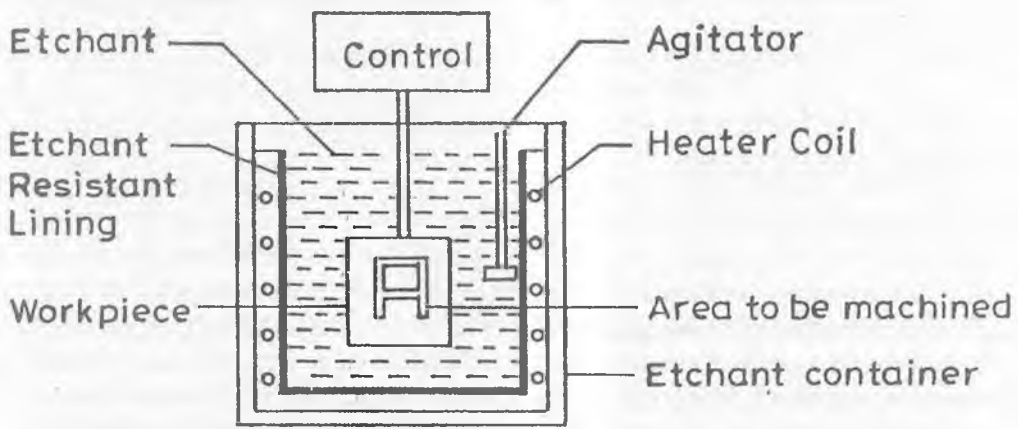


Fig. 16.1 Schematic of chemical milling/machining.

- Clean the workpiece with alkaline solution and then wash with fresh water.
- Apply a thin coating of maskant by 'cut and peel' method, screen method, or by photoresist method (details are given elsewhere).
- Dip the workpiece in the etchant bath and let it be there for the desired duration of time.
- Take the workpiece out from the etchant bath and remove the maskant layer, if any.
- Wash the workpiece thoroughly under fresh water.

Chemical **cleaning** is necessary to ensure proper adhesion of the masking material to workpiece. In case of debonding of maskant, stray etching would occur. The type of the cleaning (vapour degreasing, alkaline etching, etc) to be used depends upon the kind of maskant, kind of work material, and required machined depth. However, *cleaning of porous workpiece* material is rather difficult.

To avoid uneven removal of material from the workpiece, the fresh etchant is either continuously sprayed or the component is submerged in the etchant tank. To increase material removal rate, the etchant is agitated and, if necessary, heated as well.

The **strength of the etchant** contaminated with the reaction products can be maintained by proper filtration, addition of new chemicals as well as by periodically replacing a certain percentage of the used etchant by the fresh one. Material removal during ChM takes place both downward and laterally from the exposed surface (Fig. 16.2). First one is known as *depth of cut (or machined depth)* while the latter is called *undercut*. The extent of undercut depends upon the factors like depth of cut, the type and strength of the etchant, and the workpiece material. From process design point of view, the quantification of undercut is quite important. This is done by what is known as "*etch factor*" (Fig. 16.3).

$$\text{Etch Factor} = \text{undercut}/\text{machined depth}$$

...(16.1)

Total machined depth and extent of undercut are controlled by controlling the immersion time in the etchant. To avoid non-uniform machining, gas bubbles being evolved during the process should not be allowed to get trapped. When etching is over, the parts are cleaned either mechanically (in case of thicker and more durable mask), or chemically (more appropriate for thinner mask and sophisticated parts).

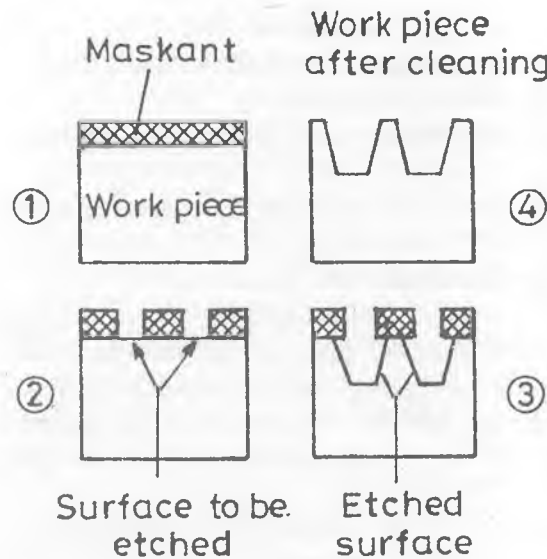


Fig. 16.2 Downward and lateral material removal

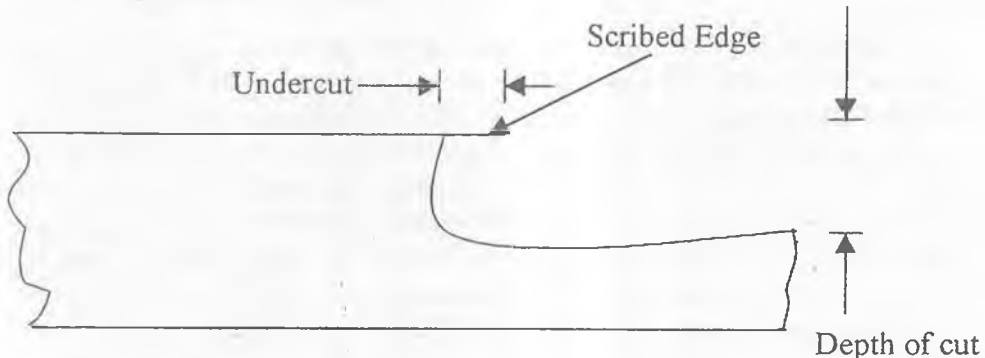


Fig. 16.3 Chemical machining: undercut and machined depth during ChM.

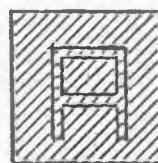
Performance of ChM process is influenced by many **process parameters**, viz type of etchant, temperature of etchant, type of maskant, method of applying the maskant, and method of circulating the etchant. The surface finish produced during ChM is about $0.75\text{--}3.75 \mu\text{m}$.

MASKANTS

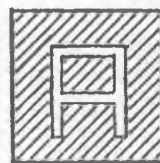
Maskants are the substances used in ChM for protecting surfaces from chemical etching by etchants. They are basically of three types, viz cut and peel, screen print, and photoresist.

Cut and Peel

Cut and peel maskants are neoprene, butyl, or vinyl based materials, which are applied by either dipping the component in the tank, spraying the mask on the part, or flow coating. The thickness of the coating usually ranges from 0.025-0.13 mm. This maskant is first applied to the entire surface then it is cut and peeled off from the selected areas to be exposed to the etchant (Fig. 16.4). Scribing and peeling off of the maskant is easily done by hand using a template as a guide. Because of large thickness of the layer of maskant, etching can be done as deep as 13 mm but accuracy is not high (usually ± 0.13 to ± 0.75 mm), and it usually depends upon the size and type of the component being produced. Time of etching controls the depth to which material removal takes place. This characteristic has been used to produce a taper on the workpiece. In case of '*cut and peel*' maskant, re-scribing is possible. This characteristic has been used to produce a stepped component. The general applications of this technique are: large sized workpieces used in chemical industries, aircraft industries, missile industries, etc. The technique is good for batch size production, for products with large depth (>1.5 mm) to be etched, etc.



Maskant coated
area marked



Maskant peeled off
from marked area,
for etchant reaction

Fig. 16.4 "Cut and peel off" method of chemical machining.

Screen Printing

This technique is good for high volume production with low accuracy, comparatively low etching depth (< 1.5 mm), and for parts sized normally not more than 1.2 m × 1.2 m. In this method, a screen (usually stainless steel) is used. The screen has the areas blocked off that are to be selectively etched. Press the screen against the surface of the part and roll up the maskant. Now, remove the screen and dry the part by baking. The exposed (unmasked) area is the one from which material is to be etched.

Photoresist Maskant

This technique has become very common and is called “**photochemical machining (PCM)**”. This method is used to produce complicated but accurate shapes. In this method, the following successive operations are carried out:

- (i) Prepare the enlarged drawing of the part accounting for the effects of undercut.
- (ii) Photograph the artwork and produce the reduced, highly accurate, photographic master transparency. An alternative to this procedure is to use a laser pattern-generator which receives design data from a CAD system and images (or produces) the features directly onto the photo master film.
- (iii) The part to be chemically machined is thoroughly cleaned to remove the dirt and oxides.
- (iv) Now, apply a thin coating of photoresist (light activated etchant resistant material) and dry by baking.
- (v) Hold the photo master and workpiece together in intimate contact. Throw the strong ultraviolet light through the photo master on the workpiece so that after development, the coating is removed from all areas where etching is to take place.
- (vi) The parts are now chemically etched, stripped off residual photo resist, and inspected. Accuracies of 0.025 mm and repeatability of 0.0005 mm are possible. The choice of maskant depends upon many factors, viz it should be resistant to the etchant, it should be easily removable after machining is over, it should not have any chemical effect on the workpiece, and it should be stable at the high temperature of the etchant bath.

ETCHANT

Etchant dissolves metal by changing it into a metallic salt that goes into solution. Some of the etchants are FeCl_3 (for Al, Cu, Ni & their alloys), FeNO_3 (for Ag), HF (for Ti), and HNO_3 (for tool steel). Other etchants used are chromic acid and ammonium persulphate. While selecting an etchant, the factors that should be considered are surface finish, material removal rate, depth of penetration, type of workpiece, type of maskant, damage to the workpiece by etchant, availability, and cost.

ADVANTAGES AND LIMITATIONS

ChM can remove material uniformly. It is also possible to make tapered sheets and structural members with close tolerances and good surface finish. Also, highly skilled operators are not required. The process has certain limitations. Only a few metals can be machined by this process because it is not possible to find appropriate etchant and maskant for other materials. Evolved gases collect under the maskant and result in uneven etching of the work. Such gases when they come out of the system, attack the surrounding equipment. Material removal rate obtained is very low. Chemicals used are corrosive in nature and may be toxic as well. As a result, it may be harmful. In case of chemical machining of alloys, differential machining rates result in poor surface finish. Further, material removal rate goes down because the etchant gets contaminated with the reaction products.

BIBLIOGRAPHY

1. Allen D. M. (1986), *The Principles and Practice of Photochemical Machining and Photo-etching*, Adam Hilger, Bristol.
2. Benedict G.F. (1987), *Nontraditional Manufacturing Processes*, Marcel Dekker Inc., New York.
3. Bhattacharyya A. (1971), *New Technology*, The Institution of Engineers (I), Calcutta.
4. DeBarr, A.E. and Oliver D.A. (1975), *Electrochemical Machining*, Macdonald and Co. Ltd., London.
5. Gunter D. (1984), Photochemical machining, *Engineering (London)*, 224(2), I-IV.

6. Pandey P.C. and Shan H.S., (1980), *Modern Machining Processes*, Tata-McGraw-Hill, New Delhi.
7. Snoeys R., Staelens F., and Dekeyser W. (1986). Current trends in non-conventional material removal processes, *Annls CIRP*, Vol. 35(2), p. 467.
8. Taniguchi N. (1983), Current trends in and future trends of ultra-precision machining and ultra-fine materials processing, *Annls CIRP*, Vol. 32(2), p. 18.

REVIEW PROBLEMS

- (1) What do you understand by “etch factor”?
- (2) Name various parameters that influence the performance of ChM process.
- (3) Write in table form, the basic differences between ChM and ECM.
- (4) Why surface finish obtained in case of ChM of alloys is poor? Explain, in brief.

ACRONYMS

ChM	Chemical machining
MR	Material removal
PCM	Photochemical machining
PCB	Printed circuit board.

CHAPTER 16
AT-A-GLANCE
CHEMICAL MACHINING
(ChM)

INTRODUCTION

- ANCIENT PROCESS \Rightarrow ENGRAVING OF METALS
- REMOVES MATERIAL IN A CONTROLLED MANNER
- APPLICATION OF MASKANT AND ETCHANT
 - ↓
- DOES NOT ALLOW ETCHANT TO REACH AND REACT WITH WORKPIECE TO DISSOLVE IT
 - ↓
- DISSOLVES WORKPIECE MATERIAL BY CHEMICAL ACTION
- APPLICATIONS
 - AVIATION INDUSTRIES
 - PRINTED CIRCUIT BOARDS
 - JEWELLERY
 - TURBINE ENGINES
 - PRESSURE VESSEL BULKHEADS
- CHEMICAL MILLING \Rightarrow PRODUCTION OF BLIND HOLES \Leftarrow POCKETS, CHANNELS, ETC
- CHEMICAL BLANKING \Rightarrow PRODUCTION OF THROUGH CAVITIES (THROUGH HOLES, SLOTS, ETC)
- STEPS TO BE FOLLOWED \Rightarrow
 - (1) CLEAN THE WORKPIECE \Rightarrow ALKALINE SOLUTION AND THEN WITH FRESH WATER
 - (2) APPLY THE MASKANT COAT \Rightarrow
 - ⊗ CUT & PEEL METHOD
 - ⊗ SCREEN METHOD
 - ⊗ PHOTORESIST METHOD
 - (3) IF CUT & PEEL METHOD \Rightarrow CUT AND PEEL OFF THE MASKANT
 - (4) DIP THE WORKPIECE IN THE ETCHANT BATH AND LET IT BE THERE FOR THE DESIRED TIME
 - (5) TAKE THE WORKPIECE OUT FROM ETCHANT BATH. REMOVE THE MASKANT LAYER IF ANY
 - (6) WASH UNDER FRESH WATER

CLEANING

TO ENSURE PROPER ADHESION OF MASKANT ON WORKPIECE



IF DEBONDING \Rightarrow STRAY ETCHING

- TYPE OF CLEANING $\rightarrow \phi$ (MASKANT, WORKPIECE MATERIAL, & MACHINED DEPTH)
- CLEANING OF POROUS MATERIAL \Rightarrow DIFFICULT
- HIGHER MRR \Rightarrow AGITATE & HEAT THE ETCHANT
- HOW TO MAINTAIN HIGH MRR \Rightarrow
 - FILTRATION OF ETCHANT
 - PERIODICAL ADDITION OF NEW ETCHANT
 - DISCARDING SOME PERCENT OF USED ETCHANT

* MR IN TWO DIRECTIONS DOWNWARD



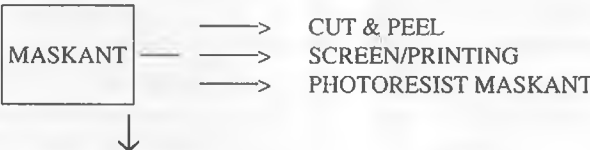
LATERAL



DEPTH OF CUT

ETCH FACTOR = UNDERCUT/DEPTH OF CUT

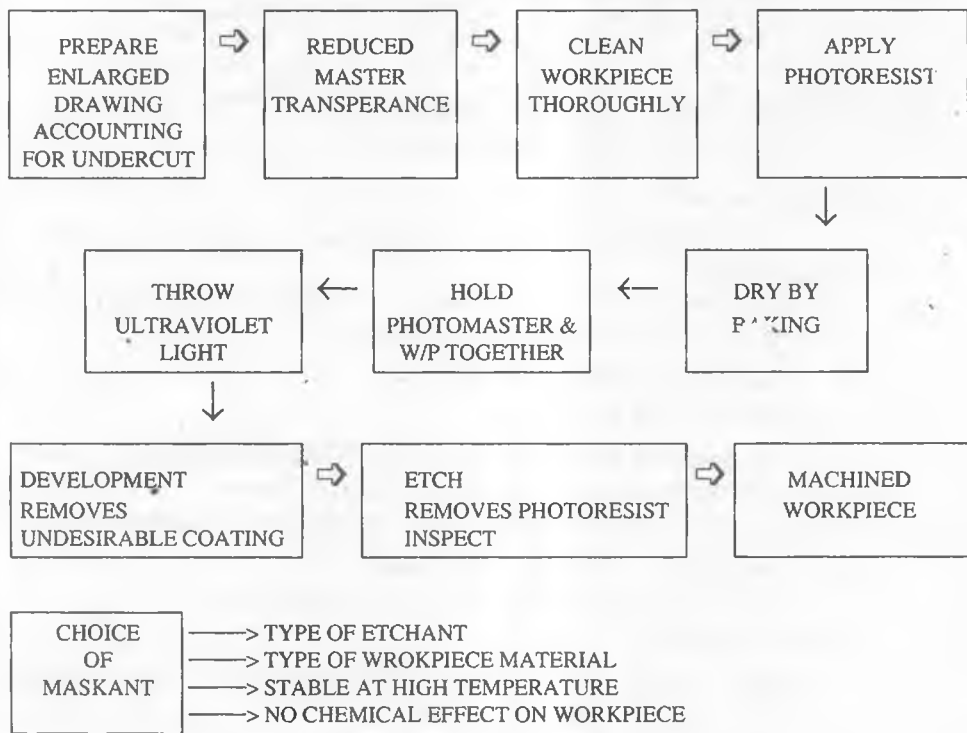
* FOR UNIFORM MACHINING DON'T ALLOW GAS TO BE TRAPPED



* PROTECTS THE WORKPIECE SURFACE FROM CHEMICAL ATTACK

- CUT AND PEEL
 - NEOPRENE, BUTYL, OR VINYL BASED MATERIAL ← MASKANTS
 - DIPPING, SPRAYING, OR FLOW COATING
 - COATING THICKNESS → 0.025-0.13 MM
 - APPLY TO ENTIRE SURFACE
 - "CUT AND PEEL OFF" FROM THE AREA TO BE EXPOSED TO ETCHANT
 - ACCURACY USUALLY OBTAINED ± 0.3 TO ± 0.75 MM
 - MACHINED DEPTH → ETCHING TIME → TAPERED WORKPIECE
 - RE-SCRIBING → STEPPED COMPONENT
 - GOOD FOR LARGE SIZED PRODUCTS, LARGE DEPTHS
- SCREEN PRINTING
 - HIGH VOLUME PRODUCTION, LOW ACCURACY, LOW ETCHING DEPTH, & PART SIZE $< 1.2 \text{ m} \times 1.2 \text{ m}$
 - SCREEN BLOCKS OFF AREAS TO BE MACHINED
 - ROLL UP THE MASKANT
 - REMOVE SCREEN & DRY BY BAKING
- PHOTORESIST MASKANT
 - FOR COMPLICATED & ACCURATE SURFACES
 - ENLARGE DRAWING ACCOUNTING FOR UNDERCUT → PRODUCED REDUCED & ACCURATE MASTER TRANSPARENCY OR PHOTOMASTER FILM (LASER)
 - CLEAN THOROUGHLY THE WORKPIECE
 - APPLY A THIN COATING OF PHOTORESIST & DRY BY BAKING
 - HOLD PHOTOMASTER & WORKPIECE TOGETHER

- THROW ULTRAVIOLET LIGHT THROUGH PHOTOMASTER ON WORKPIECE → AFTER DEVELOPEMENT → REMOVE COATING FROM AREAS WHERE ETCHING IS TO TAKE PLACE
- ETCH. STRIP OFF RESIDUAL PHOTORESIST & INSPECT



ETCHANT

- * CHANGES METAL INTO METALLIC SALT
- * FeCl_3 ; (Al, Cu, Ni), FeNO_3 (Ag), HF (Ti), HNO_3 (TOOL STEEL)

- FACTORS TO BE CONSIDERED DURING SELECTION OF ETCHANT
- SURFACE FINISH
 - DEPTH OF PENETRATION
 - TYPE OF WORKPIECE

- TYPE OF MASKANT
- DAMAGE TO WORKPIECE
- AVAILABILITY & COST

ADVANTAGES

- GOOD FINISH, CLOSE TOLERANCE
- TAPERED & STEPPED WORKPIECE
- DOES NOT REQUIRE HIGHLY SKILLED OPERATORS

LIMITATIONS

- ONLY A FEW METALS CAN BE MACHINED
- EVOLVED GASES
 - UNEVEN MATERIAL REMOVAL
 - ATTACK THE SURROUNDING EQUIPMENTS
- LOW MRR
- ETCHANTS → CORROSIVE & TOXIC → HARMFUL
- DIFFERENTIAL MACHINING OF ALLOYS → POOR SURFACE FINISH

ANODE SHAPE PREDICTION AND TOOL DESIGN FOR ECM PROCESSES

INTRODUCTION

As described in earlier chapters, ECM is the process of controlled anodic dissolution and has got wide **applications** as a manufacturing process, viz. turning [Bergsma, 1968; Hofstede *et al.* 1970; Dietz *et al.*, 1979], grinding [Kuppuswamy *et al.* 1978], fine hole drilling [Bannard, 1978], deburring [Rolsten *et al.*, 1969], etc. This process is extensively used in aeronautics, nuclear [Sorkhel *et al.*, 1972],

bio-medical, space and similar other industries. Many research data have been published about ECM but the potential of this production process has not been fully exploited due to complex nature of the process, the practical difficulties faced in the design of tools and the prediction of anode shapes.

Tool design in ECM deals basically with the computation of tool shape which under specified machining conditions would produce a workpiece having the prescribed shape and accuracy [Tipton, 1964; Tsuei et al., 1977; Dietz et al., 1973]. Since the actual tool design problems are still difficult to solve, little progress has been made in this direction. Conversely, procedures, empirical or otherwise, have been well established for the *prediction of anode (or work) shape* obtainable from a tool while operating under the specified conditions of machining. For **anode shape prediction**, different models have been developed ranging from the one based on simple ' $\cos \theta$ ' principle to those based on approximate numerical techniques (Fig. 17.1) like finite difference technique (FDT) [Tipton, 1971; Nanayakkara, 1976], finite element technique (FET) [Jain, 1980; Jain et al., 1987; Jain and Murugan, 1987], and boundary element technique (BET) [Narayanan et al., 1986].

Anode shape prediction in case of ECM with parallel electrodes is simpler than the one of electrochemical drilling of blind holes. However, different models are used to predict work profile in different zones of electrochemically drilled blind hole, viz., side, transition, front, and stagnation zones as shown in Fig. 17.2.

The classical **theory of ECM** is valid only under ideal conditions. '*Trial and error*' methods for tool profile correction have been extensively used. An alternative method for tool profile correction is to calculate the working gap and account for it during tool manufacture. With the availability of high speed computers, it has been possible to determine, by successive approximations, the tool shape that would yield a workpiece of specified geometry. Since the computing time is only a small fraction of the time required for carrying out the experiments, application of tool correction technique has proved to be time saving and economical.

A number of models for anode shape prediction and tooling design in ECM have been developed. Ability to predict variations in IEG for any given operating conditions is a prerequisite for proper design of ECM tools and anode shape prediction. Hence, the various models in practice, therefore, have been discussed in terms of the equilibrium gap.

Tooling Design in ECM

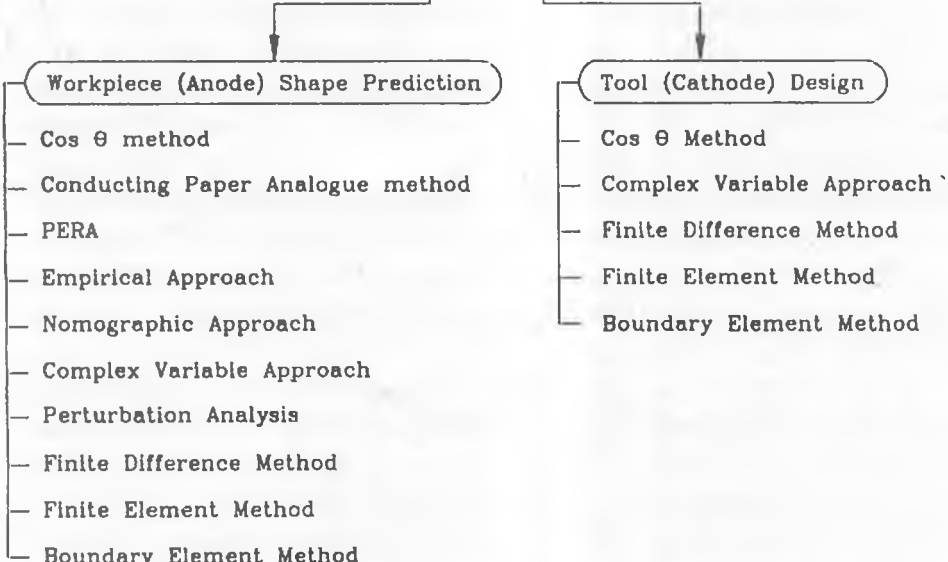


Fig. 17.1 Various models proposed for tooling design in ECM

ANODE SHAPE PREDICTION

Present day techniques require the use of high speed computers for anode shape prediction in ECM. Step by step procedure followed for anode shape prediction is as follows.

- Decide whether the analysis to be made is one-, two-, or three-dimensional.
- Collect all the initial data in the proper units and, if necessary, preliminary computation (for example, flow velocity from the volumetric flow rate) is also done.

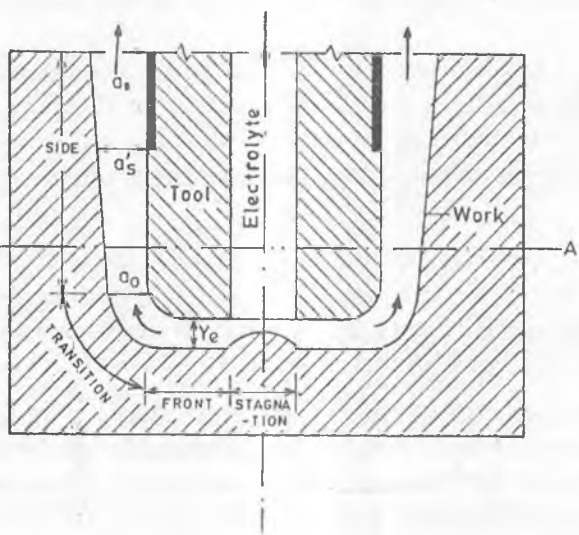
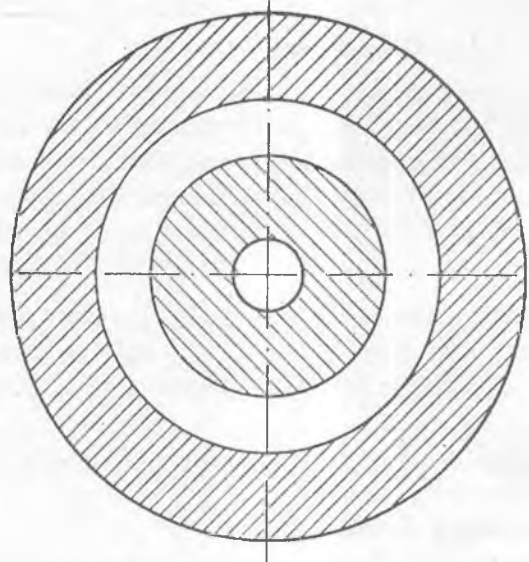


Fig. 17.2 Schematic diagram of electrochemical drilling using partially coated tool with outward mode of electrolyte flow. Zone 1 (Stagnation), Zone 2 (front), Zone 3 (transition), and Zone 4 (side).

- Now, decide whether the problem is to be solved as a temperature distribution, or electric field potential distribution problem.

There are mainly two alternatives (A) and (B), as described in what follows, for solving basic anode shape prediction problem. For this purpose, (A) either evaluate temperature distribution, or (B) evaluate the electric field potential distribution in the domain of interest. After this evaluation, intermediate computations are performed to finally arrive at the IEG at different nodal points as discussed in the following.

- (A) (i) Use appropriate differential equation to evaluate **temperature distribution** along the electrolyte flow direction. This equation can be solved by one of the approximate numerical methods (FDM, FET, or BET).
- (ii) From the above temperature distribution, calculate electrolyte conductivity (Ch. 11) at different points.
- (iii) Find out effective feed rate at different points.
- (iv) Assuming that Ohm's law is followed, compute current density (J) (Ch. 11).
- (v) Using the value of J , calculate IEG at different points along the electrolyte flow direction using a generalized equation for IEG (Ch. 11) which is applicable for both zero and finite feed rates.
- (vi) Once the IEG at different points is known the anode shape can be plotted.

However, in the above discussed approach the assumption that the Ohm's law is obeyed is not very true. Lines of electric potential are not always straight and normal to the electrode surface specially when a curved zone is analyzed. To take care of this, another approach (B) may be followed:

- (B) (i) The **electric field potential** at different points is calculated by solving Laplace equation in one-, two-, or three-dimensions as the case may be. This may be done by one of the above stated approximate numerical methods (FDM, FEM, BEM).
- (ii) Using the above electric field distribution data, current density is calculated.
- (iii) With the help of Eq. (11.22), temperature at different points is found and is used to modify the electrolyte conductivity.

- (iv) Now, IEG is computed at different points in the domain of interest so that the expected anode shape can be predicted.

However, there are certain approaches for anode shape prediction in which a few of the above steps may not be needed and some new ones may have to be added. A concise description of different approaches used for anode shape prediction in ECM will be given now.

Cos θ Method

According to the theory proposed by *Tipton [1964]*, if a tool is having its face normal to the feed direction, the equilibrium gap is given by Eq. (11.4). However, if the feed direction is inclined at an angle θ to the normal to the tool face or vice versa, the equilibrium gap would be equal to $y_e/\cos \theta$. Thus, in this method, equilibrium work shape is computed corresponding to the tool whose profile has to

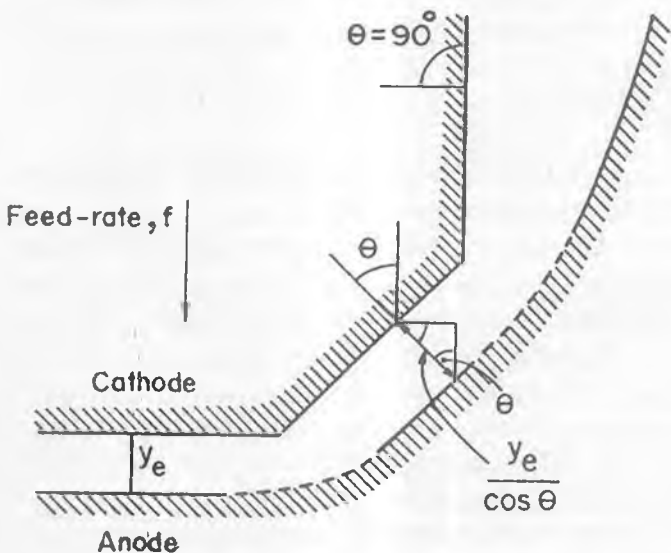


Fig. 17.3 Schematic diagram to explain the principle of tool design by 'cos θ' method [after *Tipton, 1964*].

be approximated by a large number of planar sections inclined at different angles (Fig. 17.3). Thus, this method is based on the computation of equilibrium gap for the given conditions but excludes the considerations of the mode of electrolyte flow, overvoltage, variation in electrolyte conductivity, heat transferred to the environment, etc. However, the scope of this theory is limited due to the following reasons:

- Regions with sharp corners cannot be analyzed.
- Generally applicable only if $\theta < 45^\circ$.
- It is not possible to account for the effects of the mode of electrolyte flow, void fraction, change in electrolyte temperature and conductivity, overvoltage, heat conducted away to the tool and workpiece, etc.

There are conflicting opinions about the reference surface for the measurement of angle θ . *Tsuei et al* [1977] suggested that θ should be taken as an angle between tool feed direction and normal to the anode surface, and not the cathode surface as suggested by others [*Tipton, 1968*]. However, in view of the above stated approximations involved, use of $\cos \theta$ method is not recommended, specially when complex shaped workpieces are to be analyzed [*Jain and Pandey, 1981*].

Empirical Approach

The exact path of the electric current flow lines within the IEG is difficult to determine analytically. Therefore, normally, the chordal distance between the two stations is taken as the length of current flow line. This approximation in majority of the cases is an important factor responsible for the discrepancy between the analytical and experimental results. It is easier to determine equilibrium gap in the front zone but difficult to evaluate the same in transition zone. It has also been found that the conformity of the surface radii of the tool and anode cavity decreases as the angle θ increases. Therefore, attempts have been made to derive empirical (based solely on the experimental observations rather than theory) equations for the evaluation of IEG in the transition and side zones.

Based on the analysis of experimental results, *Konig et al*, [1977] have suggested the following equation to evaluate interelectrode gap (a_o) at the start of transition zone (Fig. 17.2).

$$a_o = (r_c^{0.35}) 0.35 [(10e^*) y_e]^{0.5} \quad \text{for } 0.15 \leq y_e \leq 0.6 \text{ and } 0.5 \leq r_c \leq 5\text{mm}$$

where, e^* is Euler's number, r_c is tool corner radius, y_e is equilibrium gap and a_o is IEG in the transition zone.

For the case of tools partially or fully coated on side wall and having $1 \leq r_c \leq 5$ mm, following equations have been suggested.

$$a_o = (0.1 + y_e)(0.314r_c + 1.17) \quad \text{for } b_b = 0 \quad \text{and} \quad 0.1 < y_e < 0.7 \text{ mm.}$$

$$a_o = 2y_e + 0.1 [6.283(r_c - 1)]^{0.5} \quad \text{for } b_b \geq 1 \text{ mm,}$$

where, b_b is length of the bare part of the tool in side zone (Fig. 17.2).

The above equations are reported to yield erroneous results at low feed rates ($f \leq 0.006 \text{ mm s}^{-1}$) and large equilibrium gap ($y_e \geq 1 \text{ mm}$). Regression analysis of experimental data [Jain, Jain and Pandey, 1984] has yielded the following simple equation for the evaluation of a_o ,

$$a_o = R_{c_1} \cdot y_e + R_{c_2}. \quad \dots(17.1)$$

The values of R_{c_1} and R_{c_2} (constants) depend upon many factors like tool and work material combination, electrolyte, etc.

Following equations also have been suggested to evaluate IEG (a_s and a'_s) in the side zones under coated and bare part of the tool (Fig. 17.2).

$$a_s = [2b_b y_e + r_c^{0.7} 0.123(10e^*) y_e]^{0.5} + 0.65 y_e \quad \dots(17.2)$$

$$a'_s = (2b_b \cdot y_e + a_0^2)^{0.5} \quad \dots(17.3)$$

where, a_s is side gap in the coated part of the tool, and a'_s is side gap in the bare part of the tool (Fig. 17.2).

Test results show that the overcut in ECM is a function of machining parameters but does not depend on the tool dimensions. Further, it should be noted that above Eqs. (17.2) & (17.3) are valid only for the case of non-passivating electrolytes, specified tool-work combination, and specified machining conditions. The discrepancy between experimental and analytical results increases with an increase in the value of kEV/f .

From above discussion, it is evident that for the evaluation of side and front gaps, y_e can be used as a basic parameter. In some of the cases, side gap has been demonstrated to be independent of the machining time which, however, does not seem true. It is to be noted that in majority of the cases the effect of electrolyte

flow mode (inward, outward, and side) has been neglected. Further, empirical equations are normally valid only under specified working conditions which further limit their use.

Nomographic Approach

Nomograph is a set of scales for the variables in a problem which are so distorted and placed that a straight line connecting the known values on some scales will provide the unknown values at its intersections with other scales.

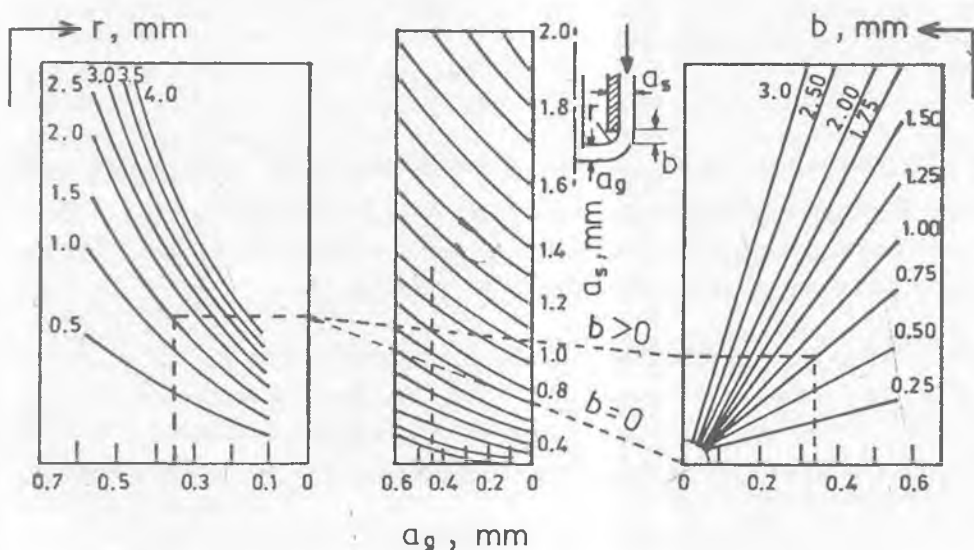


Fig. 17.4 A nomogram proposed by Konig & Pahl [1970] for the evaluation of side gap.

For the evaluation of equilibrium anode shape, a nomographic approach has also been used. Konig and Pahl [1970] have prepared a nomogram for the evaluation of side gap for the known equilibrium gap, tool radius and bare tool length. Fig. 17.4 shows one such nomograph for $b_b = 0$ and $b_b > 0$ for a given tool. Heitman [1968] has used nomograms for evaluation of electrolyte temperature

rise (ΔT) while working under specified conditions. Nomograms have proved to be useful in planning an ECM operation. However, the nomograms are very often prepared based on a number of simplified assumptions.

Numerical Methods

Conducting paper analogue method represents physical analogue of the ECM process whereas computer method is based on a mathematical analogue of the process. It is necessary to solve Laplace's equation over the domain of interest to determine the potential at a large number of points. Laplace's equation can be analytically solved only for simple shapes but in majority of the cases one comes across complicated shapes in ECM. Hence, in general, solution of the field problem must be obtained by approximate methods, based on finite difference technique (FDT), finite element technique (FET), or boundary element technique (BET) [Jain, 1980; Narayanan et al. 1986]. All these techniques require high speed computers for solving design and analysis problems of ECM. This would give the solution stated in step B(i) under the section "Anode Shape Prediction".

TOOL (CATHODE) DESIGN FOR ECM PROCESS

Tool design for ECM is considered to be a difficult but important problem. Various researchers have attempted to solve this problem by applying different approaches, viz. analytical, empirical, approximation (or numerical), etc. The analytical solutions have limited applications while numerical solutions require high speed computers for solving real life problems. The ' $\cos \theta$ ' method discussed in what follows is simple to handle and can tackle a wide range of problems to provide first approximation for tool shape. It is based on steady-state machining conditions.

'Cos θ ' Method

Fig. 17.5 shows a tool having angle θ between feed direction and normal to the tool surface. For a general case ($0^\circ < \theta < 90^\circ$), the value of equilibrium gap is given by $y_e/\cos \theta$. Note that the application of this method is based on the assumption that the electric field is normal to the surfaces of the electrodes. Further, this method is applicable only in those areas where the local radii of curvature of the anode and cathode surfaces are larger compared with the equilibrium gap. The assumption is that the surfaces are smooth with gentle variations so that the

electric current flow lines are straight and parallel to each other. However, if this assumption is not valid (say, in case of complex shaped workpieces) then the numerical solution to the electric field is desirable.

Let the workpiece surface be expressed as

$$y = f(x). \quad \dots(17.4)$$

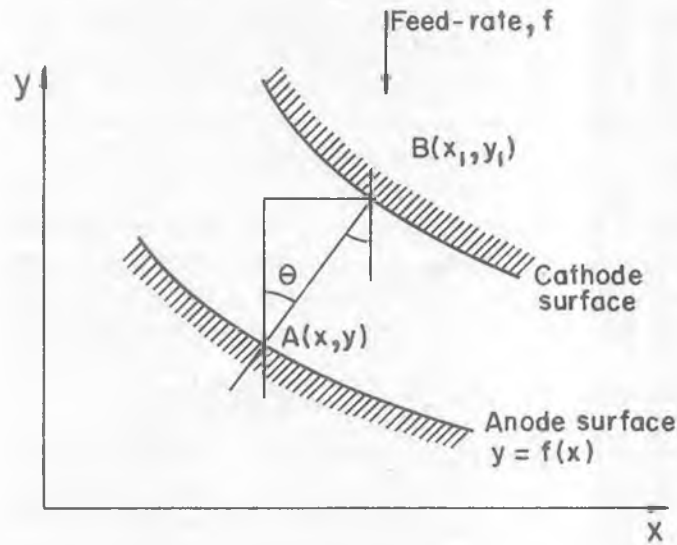


Fig. 17.5 Cathode design by 'cos θ ' method.

Let a point A (x, y) on the workpiece surface correspond to an equivalent point B (x_1, y_1) on the tool surface. From Fig. 17.5,

$$\begin{aligned} y - y_1 &= AB \cdot \cos \theta \\ &= \frac{y_e}{\cos \theta} \cdot \cos \theta \end{aligned} \quad \dots(17.5)$$

or, $y_1 + y_e = y.$

Also,

$$x_1 - x = AB \cdot \sin \theta = \frac{y_e}{\cos \theta} \cdot \sin \theta$$

$$= y_e \tan \theta$$

$$= y_e \frac{dy}{dx}$$

or,

$$x = x_1 - y_e \left(\frac{dy}{dx} \right). \quad \dots(17.6)$$

Suppose the anode surface can be expressed by the following equation:

$$y = a + bx + cx^2. \quad \dots(17.7)$$

Substitute the values from Eq. (17.5) and Eq. (17.6) in Eq. (17.7) to get

$$\begin{aligned} y_1 + y_e &= a + b \left\{ x_1 - y_e \left(\frac{dy}{dx} \right) \right\} + c \left\{ x_1 - y_e \left(\frac{dy}{dx} \right) \right\}^2 \\ &= a + bx_1 - by_e \left(\frac{dy}{dt} \right) + cx_1^2 - 2cx_1y_e \frac{dy}{dx} + cy_e^2 \left(\frac{dy}{dx} \right)^2. \end{aligned} \quad \dots(17.8)$$

From Eq. (17.7), dy/dx can be obtained as

$$\frac{dy}{dx} = b + 2cx$$

$$= b + 2c \left(x_1 - y_e \frac{dy}{dx} \right).$$

Simplifying it to get

$$\frac{dy}{dx} = \frac{b + 2cx_1}{1 + 2cy_e}. \quad \dots(17.9)$$

Now, substitute the value from Eq. (17.9) in Eq. (17.8), simplify it, and ignore the term $cy_e^2 (dy/dx)^2$ assuming it to be insignificant. Then, we get

$$y_1 = a + bx_1 + cx_1^2 - y_e - y_e \left[\frac{(b + 2cx_1)^2}{1 + 2cy_e} \right]. \quad \dots(17.10)$$

In the above Eq. (17.10), the first four terms indicate anode surface displaced by a distance equal to the equilibrium gap, y_e . The last term indicates the correction for the curvature of the anode.

Above analysis can be repeated for a surface $y = f(x, z)$ taking into account the changes in the z -direction.

$$y = a + bx + cx^2 + dz + ez^2 + gxz. \quad \dots(17.11)$$

Following the same procedure as in case of 2-D geometry, the tool shape can be represented as:

$$y_1 = \underline{a + bx_1 + cx_1^2 + dz_1 + ez_1^2 + gx_1z_1} - y_e \left[\frac{(b + 2cx_1 + gz_1)^2 (d + 2ez_1 + gx_1)^2}{1 + 2(c + e)y_e} \right] \dots(17.12)$$

Correction Factor Method

Recently, a correction factor method using the finite element technique has been proposed [Reddy *et al*, 1988; Jain *et al*, 1991] for one- and two-dimensional tool design in ECM. The correction factor concept has been applied to modify, in different stages, tool shape assumed in the first design cycle. The modification process continues until the difference between the predicted work shape and the desired work shape is within the specified tolerance. Tool design procedure involves the following five major steps:

1. Using the anode shape prediction model based on FEM (or any other method), the anode profile is estimated for an assumed (or modified) tool shape and specified machining conditions. The initial tool shape is assumed to be approximately complementary to the workpiece shape.
2. The computed and the desired work shapes are compared at every node and the difference between the two is evaluated as an error at that node.
3. If the error is more than the specified tolerance value the correction factor is calculated.
4. The tool shape is modified by applying the correction factor.
5. Steps 1-4 are repeated until the desired tool shape is achieved. This concept has been applied for designing one-and two-dimensional tools for plane par-

electrodes machining and electrochemical drilling. This concept of correction factor can also be applied to other tool design models employing finite difference or boundary element techniques for anode shape prediction.

Fig. 17.6 shows a comparison of an experimental bare tool and the bare tool designed by using the correction factor model in conjunction with FET. The difference between the experimental and the computed work shapes at the top of a drilled hole is depicted in some examples [Reddy *et al.*, 1988]. It is due to the fact that the effect of stray current attack has not been incorporated in the present model. The disagreement between the designed tool shape and the experimental tool shape has been attributed to the inaccuracy inherited in the anode shape prediction model and some built-in inaccuracy in the measurement technique used for the measurement of overcut in the transition zone.

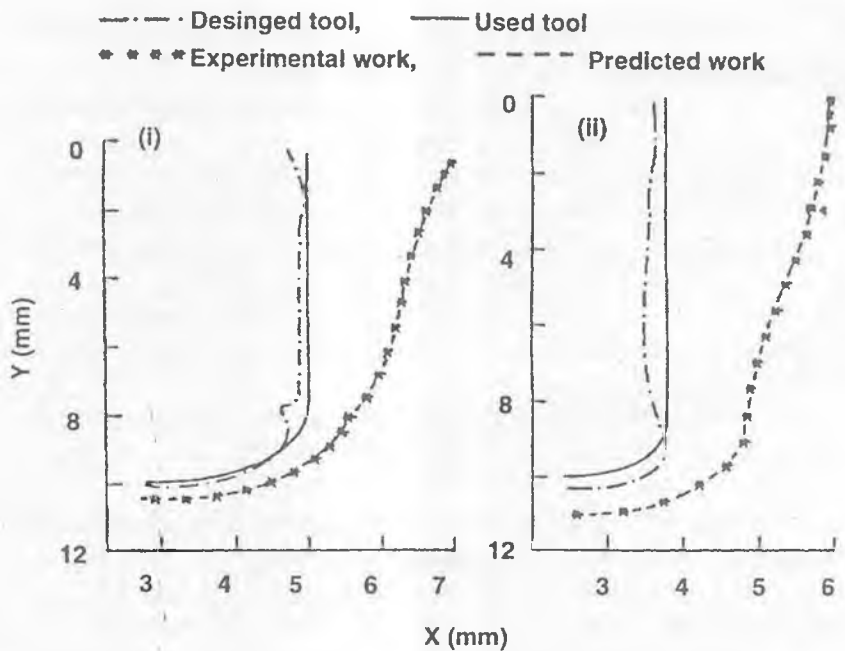


Fig. 17.6 Comparison of a bare tool used during experimentation and the one designed using correction factor Method [Reddy *et al.* 1988]. (i) and (ii) indicate two different test coditions.

BIBLIOGRAPHY

1. Bannard J. (1978), Fine hole drilling using electrochemical machining, *Proc. 19th Int. MTDR Conf.*, pp. 503-510.
2. Bergsma F. (1968), Electrochemical machining of metals, *Annls CIRP*, pp. 93-99.
3. Dietz H., Gunther K.G. and Otto K. (1973), Reproduction accuracy with electrochemical machining: Determination of side gap, *Annls CIRP*, Vol. 22/1, pp. 61-62.
4. Dietz H., Gunther K.G., Otto K. and Stark G. (1979), Electrochemical turning considerations on machining rates which can be attained, *Annls CIRP*, Vol. 28/1, pp. 93-97.
5. Heitman H. (1968), Surface roughness formation and determination of optimum working conditions in electrochemical diesinking, *Proc. 2nd AIMTDR Conf.*, pp. 41-47.
6. Hofstede A. and Berkel Van den. (1970), Some remarks on electrochemical turning, *Annls CIRP*, Vol. 18, pp. 93-106.
7. Jain V.K. (1980), *An Analysis of ECM Process for Anode Shape Prediction*, Ph.D. thesis, University of Roorkee, Roorkee, India.
8. Jain V.K. and Murugan S. (1987), Workshape prediction in electrochemical drilling and electrochemical boring operations, *Microtechnic*, pp. 42-47.
9. Jain V.K. and Pandey P.C. (1981), Tooling design for ECM: A finite element approach, *Trans. ASME, J. Engg. for Ind.*, Vol. 103, pp. 183-190.
10. Jain V.K., Raju K. Ravi, Lal G.K. and Rajurkar K.P. (1991), Investigations into tool design for electrochemical drilling, *Process. Adv. Mater.*, Vol. 1, pp. 105-121.
11. Jain V.K., Jain V.K., and Pandey P.C. (1984), On the reproduction of anode corner profile during electrochemical drilling of blind holes, *Trans. ASME, J. Engg. Ind.*, Vol. 106, No. 1, pp. 55-61.
12. Jain V.K., Yogindra P.G. and Murugan S. (1987), Prediction of anode profile in ECB and ECD, *Int. J. Mach. Tools Manuf.*, Vol. 27(1), pp. 113-134.
13. Konig W. and Pohl D., (1970), Accuracy and optimal working conditions in ECM, *Annls CIRP*, Vol. 18(2), pp. 223-230.
14. Konig W. and Humb H.J. (1977), Mathematical model for the calculation of the contour of the anode in electrochemical machining, *Annls CIRP*, Vol. 25, pp. 83-87.

15. Kuppuswamy G. (1978), Effect of Magnetic field on electrolytic grinding, *Proc. 8th AIMTDR Conf.*, pp. 546-549.
16. Nanayakkara M.B. and Larsson C.N. (1976), Computation and verification of workpiece shape in electrochemical machining, 20th *Int. Mach. Tool Des. Res. Conf.*, pp. 617-624.
17. Narayanan O.H., Hinduja S. and Noble C.F. (1986), The prediction of work-piece shape during electrochemical machining by the boundary element method, *Int. J. Mach. Tool Des. & Res.*, Vol. 26(3), pp. 323- 338.
18. Reddy M.S., Jain V.K. and Lal G.K. (1988), Tool design for ECM: Correction factor method, *Trans. ASME, J. Engg. for Ind.*, pp. 111-118.
19. Rolsten R.F. and Manning E.J. (1969), Electrochemical deburring, *Tool & Manufg. Engr.*, pp. 14-16.
20. Sorkhel S.K., et al. (1972), Electrochemical machining, *Proc. 5th AIMTDR Conf.*, pp. 651-656.
21. Tipton H. (1964), The dynamics of electrochemical machining, *Proc. 5th Int. Mach. Tool Des. & Res. Conf.*, pp. 509-522.
22. Tipton H. (1968), The determination of tool shape for electrochemical machining, *Machinery & Prod. Engg.*, pp. 325-328.
23. Tipton H. (1971), Calculation of tool shape for ECM, in *Fundamentals of Electrochemical Machining*, (Ed.) C.L. Faust, Electrochemical Society, New Jersey pp. 87-102.
24. Tsuei Y.G. and Nilson R.H. (1977), Effects of variable electrolyte conductivity on side gap geometry in ECM, *Int. J. Mach. Tool Des. Res.*, Vol. 17, pp. 169-178.

QUESTIONS

1. (a) Derive an equation to determine tool geometry when the work geometry is given by the parabolic equation.
 (b) Using the above derived equation find the equation for the tool shape for the following work shape:

$$Y = 10 + 0.3 X - 0.05 X^2 \quad (X \text{ and } Y \text{ are in cm})$$

Given: applied voltage = 15 V, over potential = 0.67 V, feed velocity = 0.75 mm/min, atomic weight = 63.57, Z = 1, density = 8.96 g/cm³, k = 0.2 S/cm.
2. Write the tool equation if the workpiece surface is approximated by a straight line given as:

$$Y = a + bX.$$

NOMENCLATURE

A, b, c, d, e, g,	Constants
a_o	Inter-electrode gap at the start of transition zone
a_s	Side gap in the coated part of the tool (Fig. 17.2)
a'_s	Side gap in the bare part of the tool (Fig. 17.2)
b, b_b	Length of the bare part of the tool
e^*	Euler's constant
E	Electrochemical equivalent
f	Feed rate
J	Current density
k	Electrolyte's electrical conductivity
r, r_c	Tool corner radius
Rc_1, Rc_2	Constants
ΔT	Rise in electrolyte temperature
V	Applied voltage
x	Distance along x-coordinate
y	Interelectrode gap
y_e	Equilibrium gap
θ	Angle between feed direction and a normal to the tool face under consideration.

ACRONYMS

BET	Boundary element technique
ECD	Electrochemical drilling
ECM	Electrochemical machining
FDM	Finite difference method
FEM	Finite element method
IEG	Inter-electrode gap
PERA	Production engineering research association
W/P	Workpiece

CHAPTER 17
AT-A-GLANCE
ANODE SHAPE PREDICTION
&
TOOL DESIGN FOR ECM PROCESSES

- ECM PROCESS CAPABILITIES ARE NOT FULLY EXPLOITED →
 - COMPLEX NATURE OF THE PROCESS
 - TOOL DESIGN PROBLEMS
 - ANODE SHAPE PREDICTION PROBLEMS
- TOOL DESIGN IN ECM → COMPUTES TOOL SHAPE WHICH UNDER SPECIFIED MACHINING CONDITIONS, PRODUCES DESIRED ANODE (W/P) SHAPE, A DIFFICULT PROBLEM
- ANODE SHAPE PREDICTION IN ECM → PREDICTION OF OBTAINABLE W/P SHAPE & SIZE FROM GIVEN TOOL AND SPECIFIED MACHINING CONDITIONS
- MANY METHODS AVAILABLE FOR TOOL DESIGN AND ANODE SHAPE PREDICTION → COS θ , NOMOGRAPHIC, EMPIRICAL, ETC
- TRIAL & ERROR METHOD OF TOOL PROFILE CORRECTION → STILL WIDELY USED
- APPLICATION OF HIGH SPEED COMPUTERS → SAVES TIME

ANODE SHAPE PREDICTION

* GENERAL PROCEDURE

- DECIDE ABOUT THE TYPE OF ANALYSIS (1-D, 2-D, OR 3-D)
- DATA COLLECTION & PRELIMINARY CALCULATIONS
- TYPE OF PROBLEM TO BE SOLVED (TEMPERATURE OR FIELD POTENTIAL CALCULATION)
- SOLVE TEMPERATURE DISTRIBUTION PROBLEM USING NUMERICAL / APPROXIMATE METHOD, CALCULATE k , f_{eff} , AND J . EVALUATE 'IEG' TO PLOT ANODE SHAPE

OR

- SOLVED LAPLACE EQ BY NUMERICAL METHOD AND CALCULATE 'J' AND USE IT TO FIND 'T' TO MODIFY k COMPUTE 'IEG' TO PREDICT ANODE PROFILE

COS θ METHOD

- THIS METHOD IS NOT APPLICABLE FOR THE REGIONS WITH SHARP CORNERS
- COMPUTE EQUILIBRIUM GAPS AT DIFFERENT PLANAR SECTIONS INCLINED AT DIFFERENT ANGLES
- PLOT ANODE PROFILE USING COMPUTED EQUILIBRIUM GAPS

EMPIRICAL APPROACH

DISCREPANCY BETWEEN THE ANALYTICAL AND EXPERIMENTAL RESULTS →
EMPIRICAL EQS. DERIVED TO EVALUATE IEG IN THE TRANSITION & SIDE ZONES

NOMOGRAPHIC APPROACH

WITHOUT CALCULATIONS, IT PROVIDES DESIRED UNKNOWN VALUES OF PARAMETERS LIKE SIDE GAP, ELECTROLYTE TEMPERATURE, ETC, USEFUL IN PLANNING AN ECM OPERATION

NUMERICAL METHODS

USED TO SOLVE LAPLACE EQN. FOR DETERMINING POTENTIAL OR TEMPERATURE DISTRIBUTION IN IEG. THEN EQUILIBRIUM SHAPE IS DETERMINED AS DISCUSSED EARLIER

CATHODE DESIGN FOR ECM PROCESS

COS 'θ' METHOD

- θ ANGLE BETWEEN FEED DIRN. AND NORMAL TO THE TOOL SURFACE
- NOT FOR SHARP CORNERS
- DETERMINE TOOL SHAPE FOR THE GIVEN WORKPIECE SHAPE

CORRECTION FACTOR METHOD

MODIFY ASSUMED TOOL SHAPE IN DIFFERENT STAGES UNTIL THE DIFFERENCE BETWEEN THE PREDICTED W/P SHAPE AND DESIRED W/P SHAPE IS WITHIN SPECIFIED TOLERANCES

The book

Many of the non-traditional machining processes have already moved out of research laboratories. These are higher-level processes being frequently used in medium and large-scale industries.

The technology developed in research laboratories cannot be brought to the shop floor unless its applications are realized by user industries. Diversified industrial applications of different AMPs discussed in the book help readers in evolving new areas of applications to make the fullest possible use of the capabilities of AMPs.

At the end of each chapter there is a section titled AT-A-GLANCE which will definitely help students in quick revision of a chapter, for teachers in preparing transparencies as teaching aids, and practicing engineers in making quick decisions about the specific process to be used for machining a particular product.

Some of the recently developed machining processes (AFM, MAF, AWJM, STEM, etc) other than the processes usually discussed (AJM, USM, EDM, EBM, ECM, etc) in available books on this subject have been incorporated.

The author

Vijay K. Jain obtained his B. E. (Mechanical) from Vikram University, and M. E. (Production) and Ph. D. from the University of Roorkee (now I.I.T., Roorkee). He has about 30 years of teaching and research experience and served as a Visiting Professor at the University of Nebraska at Lincoln (USA) and University of California at Berkeley (USA). Presently he is a Professor at Indian Institute of Technology Kanpur (India).

In recognition of the research work done by him, Dr. V.K. Jain has been opted as a member of the editorial board of five INTERNATIONAL JOURNALS, namely Processing of Advanced Materials, Machining Science & Technology, Advanced Manufacturing Systems, Int J. Industrial Engineering, and Product and Process Development. He has around 160 publications to his credit and has published about 100 research papers in Journals, and authored 2 books. His areas of interest include advanced machining techniques (ECM, EDM, AFM, and MAF), machining of advanced engineering materials, shear strain acceleration phenomenon in metal cutting, and computer aided manufacturing.

"We are the single largest book suppliers in Andhra Pradesh covering all subjects/ all syllabi for colleges, universities, corporates, schools, Inter, Degree, P.G., Engineering, MBA, MCA, B.Ed., CA, ICWA, Medicine, Pharma. Contact us for bulk and immediate supplies".

SARACARDENS, VISAKHAPATNAM-20
PHONES : 0891-6671365
FAX : 0891-6671309
E-MAIL : redindia@rediffmail.com

ISBN-81-7764-294-4

Allied Publishers Pvt. Limited